UNIVERSITAT DE
BARCELONA

New antimicrobial strategies against bacterial infections

Aida Baelo Álvarez

Aquesta tesi doctoral està subjecta a la llicència ***Reconeixement- NoComercial – SenseObraDerivada 4.0. Espanya de Creative Commons***.

Esta tesis doctoral está sujeta a la licencia ***Reconocimiento - NoComercial – SinObraDerivada 4.0. España de Creative*** **Commons.**

This doctoral thesis is licensed under the ***Creative Commons Attribution-NonCommercial-NoDerivs 4.0. Spain License***.

UNIVERSITAT DE BARCELONA

New antimicrobial strategies against bacterial infections

Aida Baelo Álvarez

Doctoral thesis

Barcelona, 2020

UNIVERSITAT DE BARCELONA

IBEC
Institute for Bioengineering of Catalonia

EXCELENCIA
SEVERO
OCHOA

BIAT
Bacterial Infections &
Antimicrobial Therapies

UNIVERSITAT DE BARCELONA
PROGRAMA DE DOCTORAT EN BIOMEDICINA

New antimicrobial strategies against bacterial infections

Memòria presentada per Aida Baelo Álvarez per a optar
al títol de Doctora per la Universitat de Barcelona

Treball experimental realitzat a l'Institut de Bioenginyeria de Catalunya (IBEC)
al grup de recerca "Bacterial Infections and Antimicrobial Therapies"

Barcelona, 2020

Eduard

BAELO ALVAREZ AIDA - 47624893N

Firmado digitalmente por BAELO ALVAREZ AIDA - 47624893N
Fecha: 2020.11.02 20:17:53 +01'00'

Doctoranda:
Aida Baelo Álvarez

Director i tutor de la tesi:
Dr. Eduard Torrents Serra
Institut de Bioenginyeria de Catalunya (IBEC)
Facultat de Biologia
(Univeristat de Barcelona)

CONTENTS

CONTENTS I

LIST OF FIGURES V

LIST OF TABLES VII

ABBREVIATIONS AND ACRONYMS IX

I. INTRODUCTION ....¡ERROR! MARCADOR NO DEFINIDO.

1. The problem of antibiotic-resistant bacteria 1

2. *Pseudomonas aeruginosa* 3

2.1. *P. aeruginosa* antimicrobial resistance mechanisms and virulence factors ... 4

3. *Staphylococcus aureus* 7

3.1. *S. aureus* virulence factors and pathogenicity 8

4. Biofilms 10

4.1. Biofilm formation and structure: *P. aeruginosa* as a model 11

4.2. Biofilm matrix 13

4.2.1. *P. aeruginosa* EPS 14

4.2.1.1. Extracellular polysaccharides 14

2.1.1.1. eDNA 16

2.1.1.1. Extracellular proteins and other components 16

2.1.1. *S. aureus* EPS 17

2.1.1.1. Polysaccharides 17

2.1.1.2. eDNA 17

2.1.1.3. Proteins 19

2.1.1.1. Other components 19

3. Ribonucleotide reductases 20

3.1. General RNR reaction mechanism 21

3.2. External electron donors 22

3.3. RNR current classification 23

3.3.1. Class I RNRs 25

3.3.2. Class II RNRs 28

3.3.3. Class III 28

3.4. RNR regulation 29

3.4.1. RNR allosteric regulation 29

3.4.1.1. Allosteric regulation by the activity site 29

3.4.1.2. Allosteric regulation by the specificity site 31

3.4.2. RNR gene regulation in bacteria 31

3.5. RNR inhibitors 32

3.5.1. Enzymatic inhibitors 34

3.5.1.1. Substrate and effector analogues 34

3.5.1.2. Inactivators of sulfhydryl groups 36

3.5.1.3. Radical scavengers 36

3.5.1.4. Metal chelators 38

3.5.1.5. Other enzymatic inhibitors 39

3.5.2. Oligomerization inhibitors 39

3.5.3. Gene expression or antisense inhibitors 40

II. OBJECTIVES 43

III. RESULTS 47

Chapter 1: Radical scavengers as RNR inhibitors with antimicrobial properties 51

PUBLICATION 1: Methyl-Hydroxylamine as an Efficacious Antibacterial Agent That Targets the Ribonucleotide Reductase Enzyme 51

PUBLICATION 2: Hydroxylamine Derivatives as a New Paradigm in the Search of Antibacterial Agents..73

Chapter 2: Improving the treatment of biofilm infections 105

PUBLICATION 3: Disassembling bacterial extracellular matrix with DNase-coated nanoparticles to enhance antibiotic delivery in biofilm infections 105

IV. ABSTRACT OF THE RESULTS AND DISCUSSION 117

Chapter 1: Radical scavengers as RNR inhibitors with antimicrobial properties 119

PUBLICATION 1 119

PUBLICATION 2 125

Chapter 2: Improving the treatment of biofilm infections 133

PUBLICATION 3 133

V. CONCLUSIONS 139

REFERENCES 143

ANNEXES 161

Report of the impact factor of the presented scientific papers..... 161

Report of participation in the presented scientific papers 162

LIST OF FIGURES

Figure 1. *P. aeruginosa* antibiotic resistance mechanisms. 5

Figure 2. *P. aeruginosa* virulence factors. 6

Figure 3. *S. aureus* virulence factors. 9

Figure 4. *P. aeruginosa* biofilm formation cycle. 12

Figure 5. Biofilm matrix. 14

Figure 6. RNR catalyzes the synthesis dNTPs. 20

Figure 7. Structure representation of the three diferent RNR classes. 21

Figure 8. General RNR reaction mechanism. 22

Figure 9. External electron supply systems in RNRs. 23

Figure 10. RNR radical generation mechanisms. 26

Figure 11. Specificty-site and activity-site allosteric regulation in RNRs. 31

Figure 12. RNR inhibitors families. 33

Figure 13. Chemical structures of the radical scavangers HA, HU and M-HA. 119

Figure 14. M-HA displays intracellular antimycobacterial activity in macrophages culture. 123

Figure 15. Reduction of *P. aeruginosa* biofilm by the radical scavengers HU, HA, and M-HA. 124

Figure 16. Chemical structures of the N-hydroxylamines library molecules from Publication 2. 126

Figure 17. Free radical scavenging activities (FRS) of the *N*-hydroxylamine molecules. 127

Figure 18. Effect of N-HA molecules on RNR. 129

Figure 19. Antibiofilm properties of N-HA radical scavengers. 130

Figure 20. PLGA NPs characterization. 134

Figure 21. Eradication of mature biofilms by soluble ciprofloxacin and different formulations of PLGA NPs loaded with ciprofloxacin. 137

LIST OF TABLES

Table 1. *P. aeruginosa* biofilm matrix components. 15

Table 2. *S. aureus* biofilm matrix components. 18

Table 3. Biochemical characteristics of the different RNR classes. 24

Table 5. RNR inhibitors of the catalytic subunit. 35

Table 6. RNR inhibitors of the activator subunit. 37

Table 7. RNR dimerization inhibitors. 40

Table 8. Minimal Inhibitory Concentrations of soluble ciprofloxacin and PLGA NPs loaded with ciprofloxacin. 135

ABBREVIATIONS AND ACRONYMS

2-Cda	Cladribine (2-Chloro-2'-deoxyadenosine)
2-F-ara-A	Fludarabine (9-beta-D-Arabinofuranosyl-2-fluoroadenine)
3AP	Triapine (3-Aminopyridine-2-carboxaldehyde thiosemicarbazone)
ADP	Adenosine diphosphate
AMP	Adenosine monophosphate
Ara-C	Cytarabine (cytosine arabinoside)
ATP	Adenosine triphosphate
ATPase	Adenosine triphosphatase
c-di-GMP	3',5'-cyclic diguanylic acid
CDP	Cytidine monophosphate
CF	Cystic Fibrosis
Cl-F-ara-A	Clofarabine (2-chloro-2'-fluoroarabino-2'-deoxyadenosine)
CPX	Ciprofloxacin
CTP	Cytidine triphosphate
dAMP	Deoxyadenosine monophosphate
dATP	Deoxyadenosine triphosphate
dCMP	Deoxycytidine monophosphate
dF-dC	Gemcitabine (2',2'-Difluorodeoxycytidine)
dGTP	Deoxyguanosine triphosphate
DNA	Deoxyribonucleic acid
DNase	Deoxyribonuclease
DNaseI	Deoxyribonuclease I
dNTP	Deoxyribonucleotide triphosphate
DX	Didox (3,4-Dihydroxybenzohydroxamic acid)
eDNA	Extracellular DNA
EPS	Extracellular polymeric substance
FRS	Free Radical Scavenging
GDP	Guanidine diphosphate
HA	Hydroxylamine
HU	Hydroxyurea (hydroxycarbamide)
LPS	Lipopolysaccharide
mRNA	Messenger RNA

MRSA	Methicillin-resistant *Staphylococcus aureus*
M-HA	*N*-methyl-hydroxylamine
NADPH	Nicotinamide adenine dinucleotide phosphate (reduced)
N-HA	*N*-substituted hydroxylamines
NTP	Nucleoside triphosphate
O_2	Molecular oxygen
PIA	Polysaccharide intercellular adhesin
PL	Poly(lysine)
PLGA	Poly(lactic-co-glycolic acid)
QS	*Quorum sensing*
R1	RNR catalytic subunit
R2	RNR activator subunit
RNA	Ribonucleic acid
RNR	Ribonucleotide reductase
TX	Trimidox (3,2,5-Trihydroxybenzamidoxamic acid)
UDP	Uridine diphosphate
UTP	Uridine triphosphate

I. INTRODUCTION

1. The problem of antibiotic-resistant bacteria

The discovery and the use of antimicrobials – and particularly antibiotics – completely transformed the treatment of bacterial infections, reducing the lethality levels and becoming an essential tool in different medicine areas, such as surgeries, transplants, and cancer therapies [7]. However, bacteria rapidly evolve and adapt to the presence of antibiotics, leading to the appearance of antibiotic-resistant strains, which limits the treatment options [8, 9].

Antibiotic-resistance has been a reality since the first use of antibiotics since it is a widespread phenomenon in nature, and genetic determinants that confer resistance even appeared long time ago before humans discovered antibiotics [10]. Though, it's been in the recent years that dangerous multidrug and extensively drug resistant strains (MDRs and XDRs, respectively) have emerged due to antibiotics overuse and misuse both in the clinics and in agriculture, which causes an increase in resistance rates and the spreading of antibiotic-resistant bacteria into the environment [11, 12]. As a consequence, multidrug resistance has become one of the main global public health threats [13].

In contrast, **research and investment** on new antimicrobial drugs has diminished recently as a consequence of economic and regulatory issues. The lack of antibiotics seriously endangers public health systems worldwide, putting the situation in a serious global emergency, as stated by health authorities [13-15].

Besides the appearance of **genetically-acquired antibiotic-resistance mechanisms**, many infections that are difficult to treat are caused by **innate bacterial persistence mechanisms**, which include community-associated bacterial growth modes, such as biofilms [16].

Biofilms are the predominant bacterial growth-mode in nature [17] and highly specialized microbial communities with selective advantage in different environments since they tolerate many antibiotics and resist to the host immune system defense mechanisms. Most biofilms exist as a stable consortium of several bacterial and other microbial species, developing specialized **multi-species communities** that are extremely difficult to eradicate. Under such circumstances, microorganisms are prone to establish synergistic and cooperative relationships that improve the overall community survival under harsh conditions, including the host-pathogen interactions [18-23]. Such bacterial communities constitute the prevalent form of infections – between 65% and 80% of the total infections are caused by biofilms [24] – being associated to high rates of recalcitrance and chronicity [19, 25]. In addition, they are the main cause of healthcare-associated infections, which have high rates of morbidity and mortality, entailing a huge healthcare and economic burden [12].

Different Gram-negative and Gram-positive bacterial pathogens are in **critical priority** for which antibiotics are urgently needed, as published in a list by the World Health Organization (WHO) that aims to establish the guides for research and development of antibiotic treatments [26]. This list includes as critical pathogens some Gram-negative **multidrug-resistant bacteria**, such as carbapenem-resistant strains of *Acinetobacter baumannii* and *Pseudomonas aeruginosa;* and various carbapenem- and third-generation cephalosporin-resistant Enterobacteriaceae (*Klebsiella pneumoniae*, *Escherichia coli*, *Enterobacter* spp., *Serratia* spp., *Proteus* spp., *Providencia* spp., and *Morganella* spp.). Other "high priority pathogens" include vancomycin-resistant strains of *Enterococcus faecium*; methicillin-resistant, vancomycin-intermediate and vancomycin-resistant strains of *Staphylococcus aureus* (MRSA, VISA and VRSA); clarithromycin-resistant *Helicobacter pylori*; fluoroquinolone-resistant *Campylobacter* and *Salmonella* species; and fluoroquinolone- and third-generation cephalosporin-resistant *Neisseria* gonorrhea. As medium priority pathogens, penicillin-non-susceptible strains of *Streptococcus pneumoniae*, ampicillin-resistant *Haemophilus influenzae*, and fluoroquinolone-resistant *Shigella* spp. are mentioned. Although *Mycobacteria* pathogens (including *Mycobacterium tuberculosis*) are not listed, they have been prioritized since a long time ago by the WHO, as the causative agent of tuberculosis is one of the top 10 death causes worldwide [27].

The acronym ESKAPE is being employed to name six of these priority pathogens (*Enterococcus faecium*, *S. aureus*, *K. pneumoniae*, *A. baumannii*, *P. aeruginosa*, and *Enterobacter* species) that are the cause of most **nosocomial or healthcare-associated infections** [28]. Due to the increasing multidrug resistance and virulence traits that they express, they are able to "escape" from the action of antimicrobial agents and the host immune system [28, 29].

Overall, the lack of new antibiotics development together with the increasing resistance mechanisms, either genetically-acquired or as a result of adaptation into biofilms, put in risk the global population. Therefore, the discovery and development of **novel antibiotics and antimicrobial therapies** to face multidrug-resistant and biofilm-related infections is a global health urgency.

The work here presented is mainly centered in the discovery of novel antimicrobial and antibiofilm therapies, focusing on different bacterial pathogens, specially *P.*

aeruginosa and *S. aureus*. Both have received attention for their virulence and antibiotic resistance mechanisms, being the cause of many biofilm-related infections, including some of the most prevalent nosocomial infections. Thus, critical aspects of both pathogens are described below.

2. *Pseudomonas aeruginosa*

P. aeruginosa is a Gram-negative, rod-shape, polar-monoflagellated free-living bacterium that belongs to the *Proteobacteria* phylum. As a **ubiquitous organism**, It commonly inhabits a wide range of environmental niches, such as aquatic habitats [30] and soils [31], but also **infects various vegetal and animal species** [32]. Compared with other species of the *Pseudomonas* genus, *P. aeruginosa* particularly causes both acute and chronic infections in human and other mammals, as a consequence of both inherent and acquired antibiotic resistant mechanisms [33].

Being considered one of the **main opportunistic** pathogens, it produces serious **acute infections** in individuals with underlying conditions, or with a compromised immune system, such as cancer patients or with viral infections (like AIDS patients) [34]. *P. aeruginosa* further causes nosocomial (**healthcare-associated infections** (HAIs)), causing bacteremia, pneumonia, and ventilator-associated pneumonia [35, 36].

P. aeruginosa produces lethal **airway infections** in cystic fibrosis (CF) or chronic obstructive pulmonary disease (COPD) patients [37]; infects bones and joints, the urinary-tract, and implanted clinical devices; and causes infections in burn wounds and skin (developing into ulcers, keratitis, and folliculitis); all of them with significant costs for the healthcare systems [38].

P. aeruginosa genome size is large – from 5.5 to 7 Mb, depending on the strain [39] –, complex, and with a variable number of plasmids. These features enable the bacterium to have great **genetic adaptability and metabolic versatility** through complex genetic regulatory networks that allow it to develop in a high diversity of hosts and environments [40]. Metabolically, it is an aerobic facultative bacterium that can use a wide range of substrates as carbon source and can be cultured in low-nutrient content media, as it contains a high number of genes involved in energy metabolism, being able to metabolize toxic compounds of recalcitrant wastes, such as heavy metals [41] and petroleum [42]. *P. aeruginosa* additionally owns a catabolite repression control pathway that optimizes the use of carbon substrates when various substrates are available [43, 44].

As an **aerobic facultative**, *P. aeruginosa* uses as main catabolism the aerobic respiration, which is a complex and flexible electron transfer pathway with respiratory hydrogenases and terminal oxidases [45]. Alternatively, it can grow, although slowly, in anaerobic conditions, either using nitrate or nitrite as a terminal acceptor in respiration instead of O_2 by using different denitrification enzymes [46], or by fermenting arginine [47] or pyruvate [48] when nitrate or nitrite are not present. Anaerobic metabolism plays a role during pathogenesis, as biofilms formed in different infective diseases such as in CF patients are oxygen-limited [49, 50].

2.1. *P. aeruginosa* antimicrobial resistance mechanisms and virulence factors

P. aeruginosa can tolerate many antimicrobial drugs and disinfectants that improve its pathogenesis, including aminoglycosides, quinolones, and β-lactams. This is because it encodes in its chromosome several **intrinsic antibiotic-resistance mechanisms**, including efflux pumps (MexAB-OprM, MexCD-OprJ, MexEF-OprN and MexXY-OprM), high restrictive porins (OprF), antibiotic-inactivating enzymes such as β-lactamases (AmpC cephalosporinase and extended-spectrum-β-lactamase OXA), and other aminoglycoside-modifying enzymes (APH, AAC, and ANT) [2, 51]. Additional non-inherent resistance mechanisms can turn the strains into multi-resistant, including the acquisition of **exogenous resistance genes** in mobile elements such as plasmids and the appearance of **mutations** [52]. Some multi-drug resistant (MDR) *P. aeruginosa* strains have acquired a variety of antibiotic-resistance genes by horizontal gene transfer, such as β-lactamases, *K. pneumoniae* carbapenemase (KPC), and metallo-β-lactamases (MBLs). Other strains acquire antibiotic resistance through **mutations on the antibiotic targets** or by deregulation of the expression of efflux pumps systems, porins, and antibiotic-modifying enzymes [2] (**Figure 1**).

The ability of *P. aeruginosa* to grow forming a **biofilm** can be considered an **adaptive antibiotic-resistance mechanism**: cells in biofilms differentially express a set of genes that involve complex phenotypic changes, contributing to increased antibiotic tolerance [53] and resistance against phagocytosis and oxidative stress generated by the host immune system [54]. For instance, a subgroup of cells inside biofilm – the **persister**

cells, are highly tolerant to antibiotics and associated to recalcitrant infections since have low metabolic rates [55, 56].

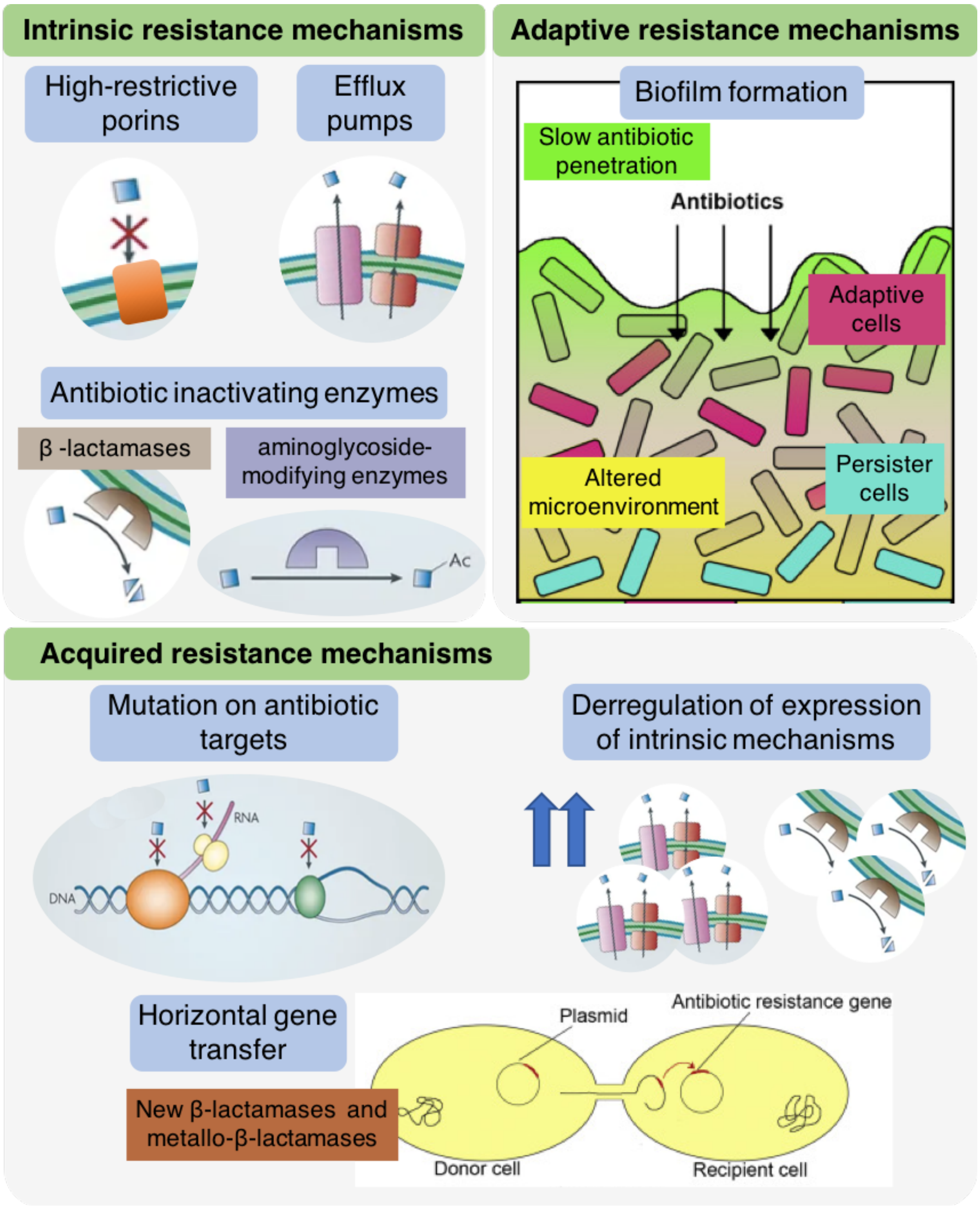
Intrinsic resistance mechanisms
High-restrictive porins
Efflux pumps
Antibiotic inactivating enzymes
β -lactamases
aminoglycoside-modifying enzymes
Ac
Adaptive resistance mechanisms
Biofilm formation
Slow antibiotic penetration
Antibiotics
Adaptive cells
Altered microenvironment
Persister cells
Acquired resistance mechanisms
Mutation on antibiotic targets
RNA
DNA
Derregulation of expression of intrinsic mechanisms
Horizontal gene transfer
New β-lactamases and metallo-β-lactamases
Plasmid
Antibiotic resistance gene
Donor cell
Recipient cell

Figure 1. ***P. aeruginosa* antibiotic resistance mechanisms.**

P. aeruginosa resists antibiotics through different mechanisms: **intrinsic mechanisms** comprise efflux pumps and high-restrictive porins, which reduce cell permeability, and antibiotic modifying enzymes; **acquired mechanisms** include mutations on antibiotic targets or in other chromosome locations that deregulate intrinsic mechanisms, and horizontal gene transfer of new antibiotic resistance mechanisms; and **adaptive mechanisms** include biofilm formation and the appearance of persister cells. Source: Modified from [2] and [6].

P. aeruginosa displays a wide repertoire of **virulence factors** (**Figure 2**) that allow the bacteria to colonize, invade the host tissues, cause cellular damage, and evade the immune system. Some of the *P. aeruginosa* virulence factors include **LPS, single polar flagellum, and type IV pili**, with key roles in colonization and adherence to host cells, biofilm formation, and motility; **secreted enzymes** (proteases, elastases, phospholipases) that destroy the extracellular matrix, interfere with signaling, or promote immune evasion; **exotoxins** that promote host cell death; and type I, type II, type III, type V and type VI **secretion systems** that directly extrude the host cells toxins or secrete enzymes that favor the infection. Other secreted molecules promote the infection, such as **phenazines** (like pyocyanin), **siderophores** (pyoverdine and pyochelin), **surfactants** (rhamnolipids), **lectins**, and **exopolysaccharides** (alginate, Pel and Psl) [34].

***P. aeruginosa quorum sensing* (QS) system**, one of the most complex bacterial signaling systems, is considered a virulence factor since it regulates virulence factors expression, biofilm formation, and motility. *P. aeruginosa* codifies for four known QS systems based on the signaling molecules las, rhl, *Pseudomonas* quinolone signal (pqs), and iqs [57].

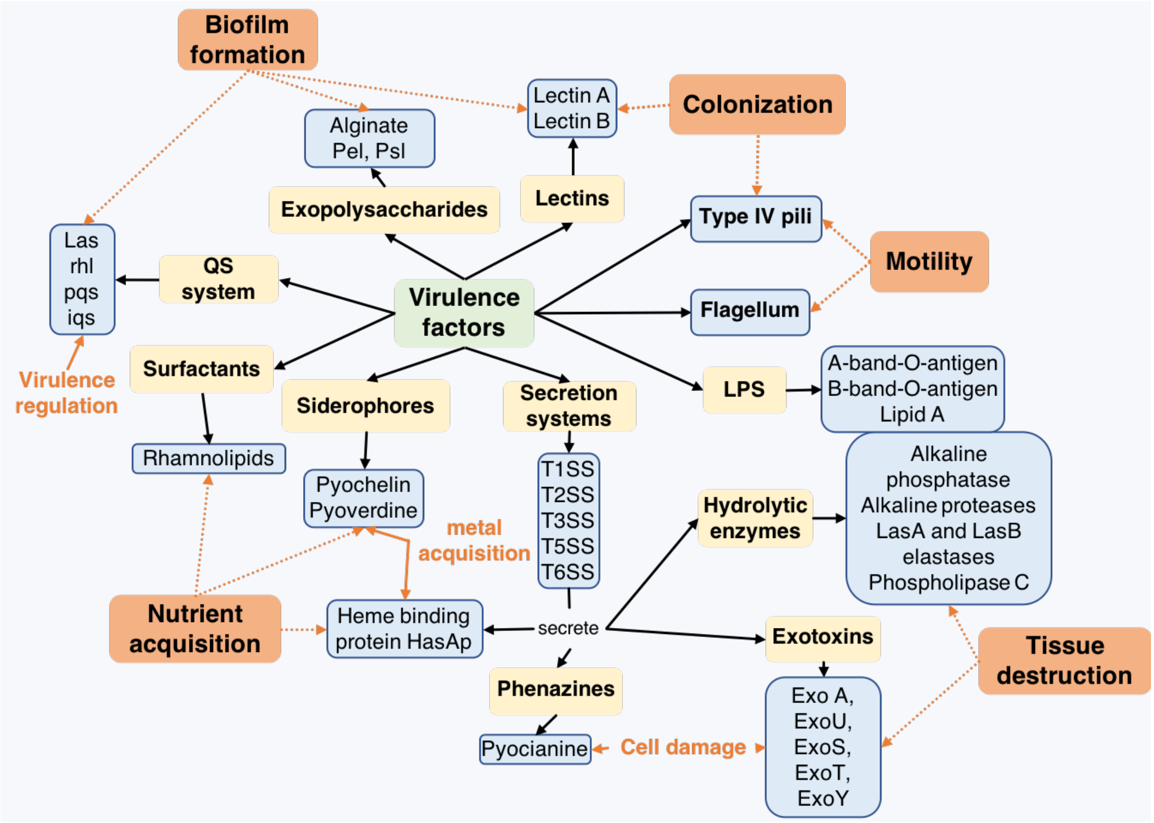
Biofilm formation
Alginate Pel, Psl
Lectin A Lectin B
Colonization
Exopolysaccharides
Lectins
Type IV pili
Motility
Las rhl pqs iqs
QS system
Virulence factors
Flagellum
Surfactants
Virulence regulation
Siderophores
Secretion systems
LPS
A-band-O-antigen B-band-O-antigen Lipid A
Rhamnolipids
Pyochelin Pyoverdine
T1SS T2SS T3SS T5SS T6SS
Hydrolytic enzymes
Alkaline phosphatase Alkaline proteases LasA and LasB elastases Phospholipase C
metal acquisition
Nutrient acquisition
Heme binding protein HasAp
secrete
Exotoxins
Tissue destruction
Phenazines
Exo A, ExoU, ExoS, ExoT, ExoY
Pyocianine
Cell damage

Figure 2. *P. aeruginosa* **virulence factors.**

3. *Staphylococcus aureus*

S. aureus is a Gram-positive, facultative anaerobe, non-motile, spherical-shaped bacterium from the *Firmicutes* phylum that grows forming grape-like clusters. It lives as a commensal in the skin, mucosal membranes, and gastrointestinal tract of healthy human and other animals, being found permanently in 20% of the nasal mucosa of the global population [58, 59]. However, as a **major human pathogen**, *S. aureus* produces a broad range of virulent **chronic and acute infections** [60], being the first cause of bacteremia and infective endocarditis, with high rates of mortality [61, 62].

S. aureus causes some **community-acquired infections,** such as superficial skin and soft tissue infections (impetigo, folliculitis, and wound infections) [63]; deep and invasive infections (bacteremia, endocarditis [61], osteomyelitis [64] septic arthritis [65], pneumonia [66], UTIs [67]); and toxin-mediated diseases (food poisoning [68], scalded skin syndrome, and toxic shock syndrome (TSS) [69]). *S. aureus* usually infects immunocompromised patients and is a major cause of **healthcare-associated infections**, causing chronic infection in sutures, prosthetic devices, catheters, and joint implants [61, 70], where it grows forming **biofilms** [71, 72]. In animals, this bacterial pathogen causes skin infections, severe septicemias, and mastitis in ruminants, acting as a transmission source to humans. As a consequence, *S. aureus* is of significance for both agriculture and public health [73].

The infections caused by *S. aureus* are difficult to eradicate because it can grow in a wide variety of host tissues and abiotic devices, it disseminates through the bloodstream, displays lots of **virulence factors**, and easily develops **antibiotic-resistant mechanisms** [74]. For instance, penicillin-resistant strains appeared early in the 1940s and the highly virulent MRSA strains in the 1960s after the use of the first β-lactam antibiotics [75]. MRSA have acquired a mobile genetic element that contain the *mecA* gene [76], encoding a low affinity penicillin-binding protein (PBP) that protects bacteria from β-lactam antibiotics effects. Infections caused by MRSA are very frequent, both in the community (community acquired-MRSA, CA-MRSA) and in the hospital (hospital acquired-MRSA, HA-MRSA). Both CA-MRSA and HA-MRSA infections fail in the treatment since the strain rapidly develops resistance to other antibiotics, with recurrent appearance of multi-resistant strains, such as vancomycin-intermediate and vancomycin-resistant *S. aureus* strains (VISA and VRSA, respectively).

3.1. *S. aureus* virulence factors and pathogenicity

S. aureus is a highly pathogenic bacteria, well-provided of virulence factors that are mainly acquired by horizontal gene transfer events, mainly by prophages [77]. *S. aureus* virulence factors enable it to **colonize host tissues**, **evade the host immune system** [78], and **disseminate the infection** through the bloodstream (**Figure 3**). Virulence actors include surface adhesins colonize host tissue and form biofilm, extracellular enzymes to both acquire nutrients and destruct host tissue, and toxins to evade the immune system.

It is fitted with a wide number of **surface proteins**, including IsdABCH proteins for heme uptake; the Staphylococcal protein A (SpA); and some implicated in biofilm formation, like SasC and SasG. Some relevant surface proteins are **adhesins**: fibronectin (FnBP-A, FnBP-B) and fibrinogen (ClfA, ClfB) binding proteins; collagen binding protein Can; and serine-rich adhesion platelets SraP. Adhesins, together with the extracellular matrix-binding proteins EbhA and EbhB and teichoic acids (WTA and LTA), perform functions in colonization [79].

S. aureus secretes a high diversity of **exoenzymes**: some produced **proteases** play roles in immune evasion, like in aureolysin metalloprotease, the staphopains cysteine proteases (ScpA and ScpB), the staphylococcal serine protease A (SspA), and other serine proteases (SplA to SplF); other **degrading enzymes** destroy tissues, like hyaluronidase, lipases, phospholipases, and nucleases [80].

Besides, *S. aureus* sequesters the host coagulation system to protect itself and help to spread the infection. For this, it secretes two protein cofactors or activator zymogens, the **coagulases** Coa and von-Willebrand factor binding protein (vWbp), which promote the host fibrinogen to polymerize into fibrin, forming blood clots [81]. Polymerized fibrin enshells bacteria in a network that the immune cells are unable to clear, producing abscesses, tissue damage, and bacterial dissemination. Paradoxically, *S. aureus* can also interfere in the fibrinolysis process by secreting **staphylokinase** (Sak), which binds plasminogen and converts it to plasmin, preventing coagulation and favoring bacterial dissemination [61].

S. aureus produces 40 **toxins**, with similar structures and functions [80]. Some of them act as **superantigens (SAgs)** that trigger massive cytokine production: Staphylococcal protein A (SpA) triggers B lymphocytes expansion, and both staphylococcal endotoxins (SEs) (SEA to SEE, SEG to SEJ, SEL to SEQ, and SER to SET) and toxic shock syndrome toxin-1 (TSST-1) trigger T lymphocytes expansion; **cytolytic toxins** lyse host cells and comprise α-hemolysins (Hla), β-hemolysins (Hlb), and pore-forming toxins (PFTs) (these last including leukocidins (LukAB/GH, LukDE, Luk-PV), γ-hemolysins (HlgAB and HlgCB), and phenol-soluble modulins (PSMs)); and **cytotoxic toxins** damage the host tissue without lysis and include the exfoliative toxins (ET) (ETA, ETB, ETC, ETD), serine proteases that produce staphylococcal scalded skin syndrome (SSSS) [82].

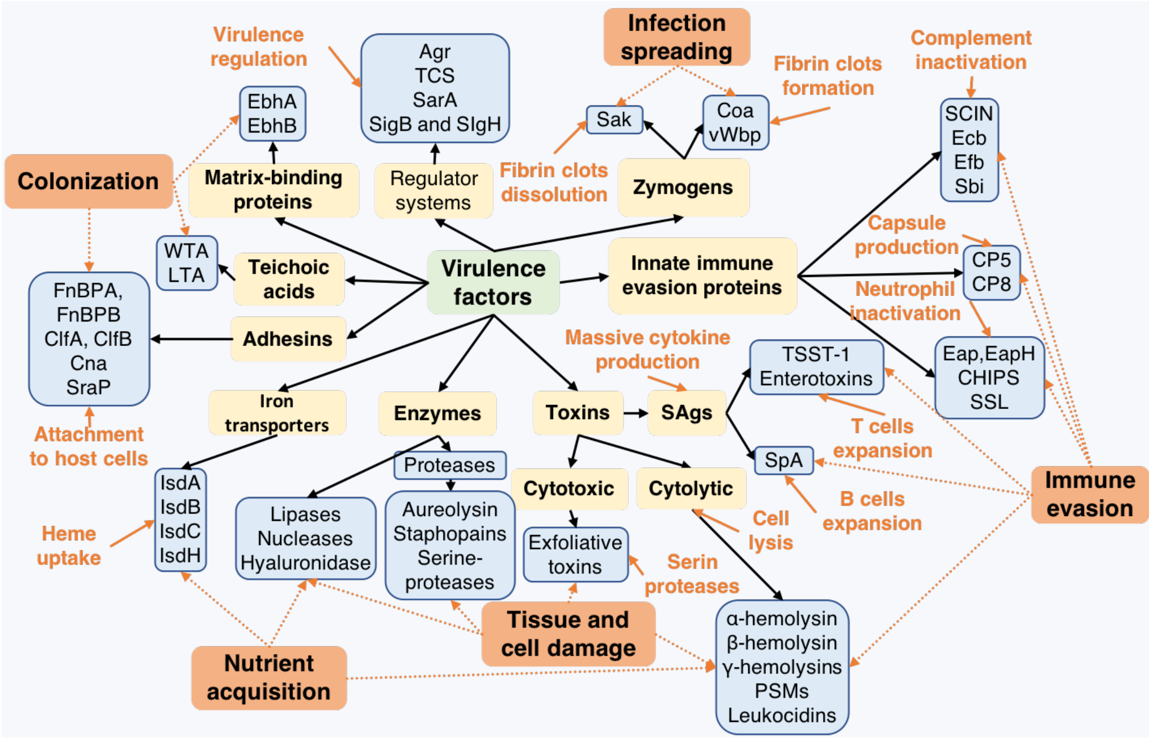
Virulence regulation
Agr
TCS
SarA
SigB and SlgH
Infection spreading
Complement inactivation
Fibrin clots formation
EbhA
EbhB
Sak
Coa
vWbp
SCIN
Ecb
Efb
Sbi
Colonization
Matrix-binding proteins
Regulator systems
Fibrin clots dissolution
Zymogens
Capsule production
WTA
LTA
Teichoic acids
Virulence factors
Innate immune evasion proteins
CP5
CP8
FnBPA, FnBPB
ClfA, ClfB
Cna
SraP
Neutrophil inactivation
Adhesins
Massive cytokine production
TSST-1
Enterotoxins
Eap,EapH
CHIPS
SSL
Attachment to host cells
Iron transporters
Enzymes
Toxins
SAgs
T cells expansion
SpA
IsdA
IsdB
IsdC
IsdH
Proteases
Cytotoxic
Cytolytic
Immune evasion
Heme uptake
Lipases
Nucleases
Hyaluronidase
Aureolysin
Staphopains
Serine-proteases
Exfoliative toxins
Cell lysis
B cells expansion
Serin proteases
Tissue and cell damage
α-hemolysin
β-hemolysin
γ-hemolysins
PSMs
Leukocidins
Nutrient acquisition

Figure 3. ***S. aureus*** **virulence factors.**

CHIPS: Chemotaxis inhibitory protein of Staphylococcus, *ClfA and ClfB: Clumping factors A and B, Can: collagen adhesion protein, Eap and EapH: Extracellular adherence proteins, Ecb: Extracellular complement-binding protein, Efb: Extracellular fibrinogen binding protein, FnBPA and FnBPB: Fibronectin binding proteins A and B, LTA: Lipid-anchored teichoic acids, PSMs: Phenol-soluble modulins, SAgs: Superantigens, Sbi: Staphylococcal binding of IgG, SCIN: Staphylococcal complement inhibitor, SpA: Staphylococcal protein A, SraP: Serine-rich adhesin of platelets; SSL: Staphylococcal superantigen-like, TCS: Two-component systems, TSST-1: Toxic shock syndrome toxin, WTA: Wall teichoic acids.*

Some non-catalytic proteins favor the **innate immune evasion**: they target neutrophil functions (staphylococcal superantigen-like proteins (SSL1 to SSL13), extracellular adherence proteins (Eap and EapH), and chemotaxis inhibitory protein of *Staphylococcus* (CHIPS); block the activation of complement (staphylococcal complement inhibitor (SCIN), extracellular complement-binding protein (Ecb), extracellular fibrinogen-binding protein (Efb); and produce capsule (CP5 and CP8) [78].

To provide a tight control of the optimal virulence factors expression under each particular host condition, *S. aureus* express **specific regulatory systems** that coordinate the local environment with the host signals: the master virulence quorum-sensing regulatory system *agr*; the two-component systems SaeRS, SrrAB, abd ArlRS; the cytoplasmic SarA-family regulators; and the alternative sigma factors SigB and SigH [83].

4. Biofilms

Biofilms are complex aggregated microbial communities, frequently polymicrobial, that grow either on biological or inert surfaces, or as floating aggregates, in an air-liquid interface [84, 85]. In these communities, bacteria grow together encased in a dense hydrated and sticky self-produced extracellular matrix – the extracellular polymeric substance (EPS), which protects bacterial cells from antimicrobials and other toxic chemicals, from physical stresses, and from the host immune clearance.

Biofilm growth is an adaptation mechanism to overcome stress conditions in which bacterial survival is threatened. Its formation comprise mainly phenotypic but also genetic changes that allow improved resistance against external agents [86]. Several factors are involved in **biofilm-mediated resistance**: **restricted penetration** of toxic compounds through the matrix, **reduced growth and metabolic rates**, induction of specific **tolerance mechanisms** (as multidrug efflux pumps and stress-response regulons), and **induction of dormant or persister subpopulations** proliferation, including small-colony variants (SCVs) [87]. Persisters are a small subgroup of biofilm population cells that have acquired temporary antibiotic resistance due to either a metabolic quiescent state or other phenotypic changes, and are responsible for repopulating biofilm after an antibiotic treatment [56, 88].

Biofilms inhabit a large number of environments, including natural and industrial, but also medical environments, where they cause a large number of **difficult-to-treat and long-lasting infections** [16]. For instance, colitis, urethritis, vaginitis, conjunctivitis and otitis are quite common [84]. Biofilms play a role in **healthcare associated infections** as colonizers of medical devices (like catheters, heart valves, and prosthetic joints), in surgical site infections, and in pneumonia and ventilator-associated pneumonia [16, 89]. Likewise, biofilms frequently appear in wounds (as in diabetic and venous leg ulcers infections) [90, 91], and in the lung of CF and COPD patients, where they prevent correct gas exchange and cause severe symptoms [37, 92].

4.1. Biofilm formation and structure: *P. aeruginosa* as a model

Physical and chemical microenvironment conditions – pH, nutrients, oxygen, and flow conditions – that depend on the environment and the bacterial species taking part define biofilm global architecture [93]. Bacteria in mature or differentiated biofilms organize themselves in **microcolonies**, which are compact bacterial clusters surrounded by EPS. Structured **liquid channels** interconnect microcolonies to deliver both nutrients and oxygen and to remove waste metabolic products [85]. Bacteria inside microcolonies exhibit **phenotypic heterogeneity**: they possess spatial and temporally different metabolic and gene expression profiles as a consequence of microenvironments formation (concentration gradients of metabolites, signal, and waste compounds) and stochastic gene switching (mutation and recombination) [84, 94, 95]. The presence of this physiologically-differentiated subpopulations serves as a mechanism to provide the entire biofilm community protection against harsh conditions [96].

Bacterial cells within a biofilm **communicate** to each other through complex interactions by exchanging different molecules, including metabolites, signaling molecules, genetic material, and defensive compounds [85]. These **cooperative or competitive relations** ultimately affect the biofilm formation and its structure and, consequently, how the biofilm interacts towards the environment and host factors [97, 98].

Because *P. aeruginosa* biofilm has been for long a model for biofilm research, it has been well characterized. Its **formation** is complex, tightly regulated, and needs the expression of various factors, such as adhesins, aggregation proteins, EPS, cell motility appendages, and cell-to-cell communication mediated by *quorum sensing* systems. It occurs in a **five-stage cycle** that includes **i) the initial reversible attachment** of free-living bacteria to a biotic or abiotic surface, mediated by biological specific interactions and/or hydrophobic and electrostatic forces; **ii) the irreversible attachment** mediated by EPS production; **iii) the formation of microcolonies** with strong surface adherence; **iv) the maturation** of differentiated matrix-embedded microcolonies through the formation of interconnecting channels; and **v) cell death and bacterial dispersion** events to continue the cycle with the establishment of new biofilms (**Figure 4**).

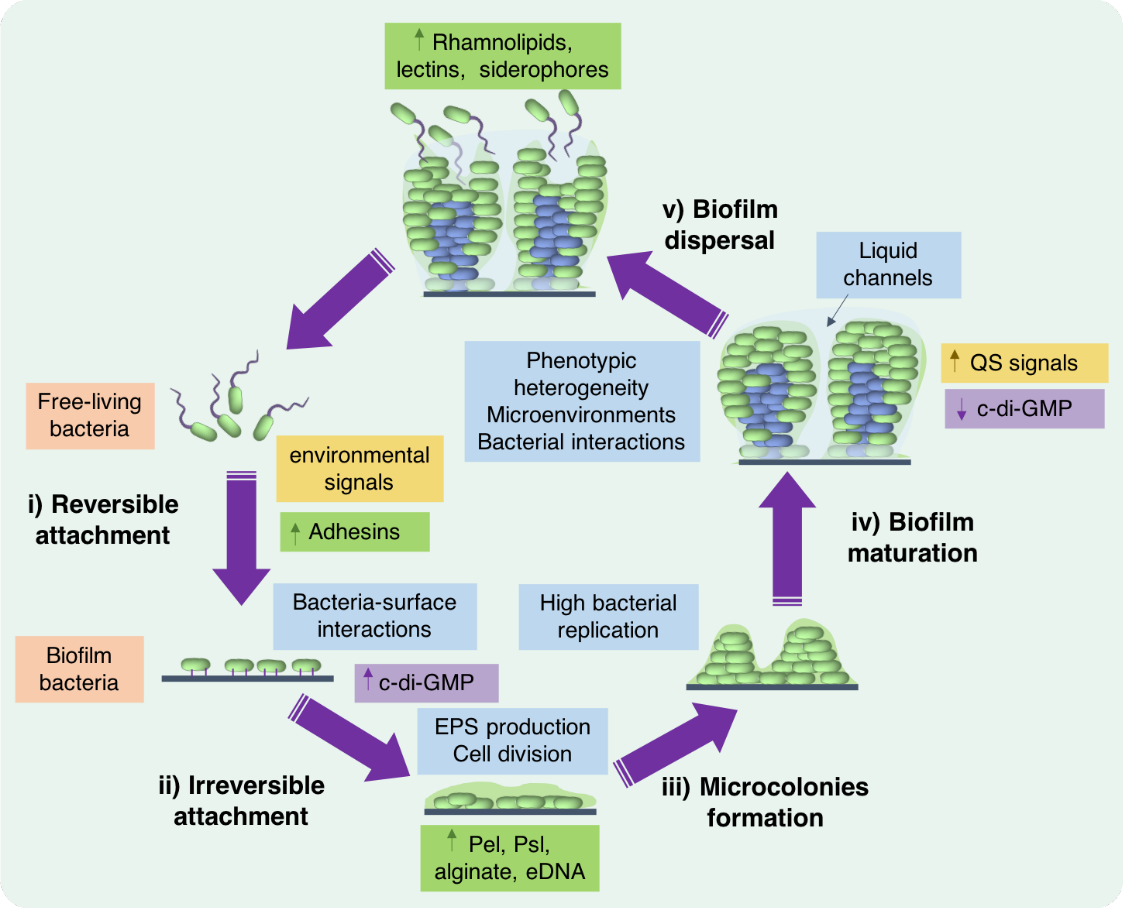
↑ Rhamnolipids, lectins, siderophores
v) Biofilm dispersal
Liquid channels
Phenotypic heterogeneity Microenvironments Bacterial interactions
↑ QS signals
↓ c-di-GMP
Free-living bacteria
environmental signals
i) Reversible attachment
↑ Adhesins
iv) Biofilm maturation
Bacteria-surface interactions
High bacterial replication
Biofilm bacteria
↑ c-di-GMP
EPS production Cell division
ii) Irreversible attachment
iii) Microcolonies formation
↑ Pel, Psl, alginate, eDNA

Figure 4. ***P. aeruginosa*** **biofilm formation cycle.**

P. aeruginosa biofilm formation follows a 5-stage cycle: **i)** the **reversible attachment** of planktonic or free-floating bacteria to a surface mediated by adhesins and electrostatic interactions, **ii)** the **irreversible attachment**, in which a matrix constituted by Pel, Psl, alginate and eDNA is formed, **iii) microcolonies formation** as a consequence of an elevated bacterial replication, **iv)** a **maturation** of biofilm with the appearance of metabolic gradients and phenotypic heterogeneity, and **v) dispersal events** that leads to free-living bacteria that can start new biofilm formation.

All the steps of biofilm formation take place through complex phenotypic changes that are controlled through **3',5'-cyclic diguanylic acid (c-di-GMP)**. C-di-GMP acts as second messenger, regulating multiple cellular functions through interactions with **kinase-response two-component regulators** [99, 100]. For instance, c-di-GMP regulate cell cycle, virulence, antibiotic resistance mechanisms, and the switching from motile to sessile cells. In biofilms, high levels of c-di-GMP are involved in the initial formation stages, whereas low levels are linked to further biofilm maturation stages and dispersal events. In first biofilm formation stages, c-di-GMP regulates flagellum swimming motility, which is inhibited after interacting with a surface [101]; type IV pili twitching motility, which is also downregulated to mediate attachment [102]; the synthesis of the exopolysaccharides Pel, Psl, and alginate [103, 104]; and the aggregation protein CdrA [105], which induces irreversible attachment and contributes to biofilm maturation. In dispersal events, di-GMP modulates swimming and swarming motility [99, 106].

The **QS cell-density dependent regulation** plays a role in in the maintenance of microcolonies and void channels during biofilm maturation since it induces the synthesis of some EPS components, like the extracellular DNA (eDNA) [107] and the extracellular polysaccharide Pel [108]. Low c-di-GMP levels during maturation and dispersal events activate the QS system, increasing the production of rhamnolipids, lectins, pyoverdine, and pyochelin production [109].

Small non-coding regulatory RNAs (sRNA), such as RsmY, RsmZ, and RsmW, also regulate biofilm attachment and further formation as a response to diverse environmental signals [110].

4.2. Biofilm matrix

The production of EPS matrix in which bacteria are embedded is an essential process in biofilm formation and maintenance, and its presence is what defines a bacterial community as a biofilm. EPS directly participates in the processes of attachment, cell-to-cell interaction, nutrient acquisition, tolerance to physicochemical stresses and to host defense, and genetic exchange [111]. EPS serves as a physical connection between bacterial cells themselves and the substrate to which they are adhered, providing mechanical stability and compartmentalized microenvironments. Consequently, the **EPS composition** of a particular biofilm – and the structural scaffold that it constitutes – determines the **physical and physiological properties** of biofilms [112, 113].

Usually, EPS is a highly hydrated matrix comprising soluble polymeric molecules, such as polysaccharides, nucleic acids, and soluble and cell-surface proteins, all of them forming a mesh structure in which bacteria are interconnected (**Figure 5**). Depending on bacterial species and environmental conditions (properties of the surface where they atteach, nutrients availability, temperature, oxygen diffusion, hydrodynamics, and host factors), biofilms synthesize different matrix components in different amounts, adopting different morphologies [111]. Moreover, EPS composition is not fixed to a given biofilm, yet is under continuous remodeling phenomena to adapt its properties to changing situations [85, 114, 115]. This plasticity trait allows the bacteria to adapt to different niches and, of course, confers resistance to stresses.

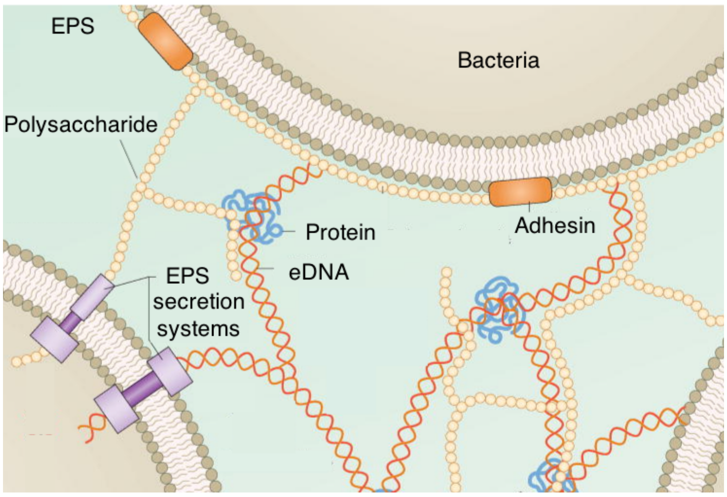

Figure 5. Biofilm matrix.

Different EPS components in the biofilm matrix interconnect bacterial cells. Polysaccharides, soluble and cell-surface proteins (like adhesins), and nucleic acids (mainly eDNA) are the main components. Modified from [1].

4.2.1. *P. aeruginosa* EPS

Soluble polymeric substances – polysaccharides, proteins, and nucleic acids – mainly constitute *P. aeruginosa* biofilm EPS. Other bacterial components, such as lipids, fimbriae, pili, flagella, and extracellular membrane vesicles, contribute to cell to cell interconnection and matrix functionality [112] (see **Table 1).**

4.2.1.1. Extracellular polysaccharides

Polysaccharides constitute the main part of biofilm EPS and provide moisture, surface adhesion, and cell-aggregation. Three different known exopolysaccharides contribute to the matrix composition in *P. aeruginosa* biofilms: Psl, Pel, and alginate. The global polysaccharide composition in *P. aeruginosa* biofilms strongly depends on the strain, and some strains tend to produce EPS enriched with a specific polysaccharide.

Alginate, which is formed by residues of mannuronic and guluronic acid, is not an essential but a relevant component of the EPS matrix in biofilms of strains that overproduce alginate. Alginate overproducer strains – called mucoid strains – frequently produce chronic and recalcitrant biofilms in the CF patients airways [37] because alginate acts as a protective layer that increases bacterial tolerance against antibiotics and host defenses [112]. Alginate affects biofilm architecture, being involved in microcolonies formation and mechanical stability in mature biofilms [116].

Table 1. ***P. aeruginosa*** **biofilm matrix components.**

		Composition/Types	**Functions**	**Other characteristics**
Exopolysaccharides	**Alginate**	O-acetylated 1,4-linked β-D-mannuronic and α-L-guluronic acids	Antibiotic tolerance Mechanical stability Microcolonies formation	Main component in mucoid strains Negatively-charged
	Psl	1,3-linked and 1,2-linked β-D-mannose, α-L-rhamnose, and β-D-glucose	Surface attachment Cell-to-cell aggregation	Important in early biofilms Neutral charge
	Pel	Partly deacetylated 1,4-linked *N*-acetylgalactosamine and *N*-acetylglucosamine	Cell-to-cell aggregation eDNA crosslinker Antibiotic tolerance	Important in mature biofilms Positively-charged
eDNA		Chromosomic DNA	Cell-to-cell agreggation (initial biofilm formation) Antibiotic tolerance Genetic exchange	Most abundant component in non-mucoid strains Negatively charged
Proteins	**Adhesins**	CdrA	Psl crosslinker Cell-to-cell aggregation	Cell-associated or secreted
	Lectins	LecA, LecB	Polysaccharide binding Adhesion Biofilm formation and stability	Virulence factors
	Extracellular enzymes	Alkaline phosphatase, LipA, chitinase, Protease IV, DNase	Nutrient uptake Biofilm detachment	Secreted
Cell appendages		Pili, fimbriae, flagella	Surface attachment Cell-to-cell aggregation	Pili acts as an eDNA crosslinker
Other components		LPS	Adherence	Virulence factor
		Rhamnolipids	Adherence Microcolonies formation Dispersal events Nutrient uptake	Surfactant properties Virulence factors
		OMVs (outer membrane vesicles)	Interaction with eDNA	Release of enzymes, eDNA, and virulence factors

Psl and Pel play key roles in biofilm stability in nonmucoid phenotypes. Both Psl and Pel are branched heteropolysaccharides composed of mannose, rhamnose and glucose, and partly deacetylated *N*-acetylgalactosamine and *N*-acetylglucosamine, respectively [117]. Whereas Psl participates in the initial surface attachment in biofilm formation and facilitates cell-to-cell interactions [118], Pel functions as an eDNA crosslinker, promoting cellular interactions in mature biofilms [117]. The presence of Pel is also associated to a reduced antibiotic efficiency [119].

2.1.1.1. eDNA

Extracellular DNA (eDNA) is a key component of the EPS matrix in *P. aeruginosa*, being the most abundant component in mature biofilms, excluding the mucoid strains. eDNA acts as an intercellular linker that stabilizes biofilm by forming a grid-like structure [107], and physically interacting with Psl [120]. eDNA plays a key role in the early stages of biofilm formation since the presence of the DNA-degrading DNase I prevents its formation, although DNase I also disperses established biofilms [121]. eDNA enhances tolerance against antibiotics, including aminoglycosides [122], by inducing the expression of drug-resistance systems such as Type VI Secretion System (T6SS) [123]. Like in some other biofilm-forming bacteria, the eDNA in *P. aeruginosa* originates from autolysis of a biofilm subpopulation [107], which is a process under the control of the QS system. Alternatively, eDNA releases from DNA-containing vesicles, which randomly encapsulate chromosomal DNA [124].

2.1.1.1. Extracellular proteins and other components

Different proteinaceous compose *P. aeruginosa* EPS, including structural proteins, extracellular enzymes, and cellular appendages. **Structural proteins** can mediate surface adhesion and interact with other matrix components to favor matrix stability. Some structural proteins include **adhesins** and **carbohydrate-binding proteins**. For instance, the matrix adhesin CdrA creates cell-to-cell interconnections by itself or by binding and crosslinking Psl [105, 125]. Some virulence factors with carbohydrate-binding activities, as lectins LecA and LecB, perform roles during cell adhesion and biofilm formation and stabilization [126-128]. **Extracellular enzymes**, which are retained within the EPS through interactions with polysaccharides, can provide particular functions such as nutrient uptake, biofilm detachment in dispersal events, or either serve as virulence factors [111]. *P. aeruginosa* secretes several enzymes within biofilm, including alkaline phosphatase, the LipA lipase, chitinase, protease IV, and a putative magnesium-dependent DNase [129].

Cell appendages – pili, fimbriae, and flagella – play structural roles on biofilm, interacting with other matrix components and favoring cell-to-cell interactions [130]. For instance, Type IV Pili crosslinks eDNA [131].

EPS is composed of accessory components, like **LPS**, the surfactants **rhamnolipids**, and **Outer membrane vesicles (OMVs)**. LPS mediates adherence and biofilm formation; rhamnolipids mediate surface adherence, colonization, bacterial motility during biofilm dispersal, and nutrients uptake [112]; and OMVs – produced as a consequence of bacterial outer membrane blebbing – incorporate a high diversity of cytoplasmic compounds, including enzymes and virulence factors. These last also interact with eDNA, contributing to EPS cohesion [132].

2.1.1. *S. aureus* EPS

EPS produced in *S. aureus* biofilms is constituted by polysaccharides, eDNA, and soluble and surface-associated proteins. The polysaccharide intercellular adhesin (PIA) and eDNA constitute the major EPS components in a high number of strains [133]. Other relevant components contribute globally in less amount to the matrix but with relevant roles, such as some surface-associated adhesins, cytoplasmic and extracellular proteins, and degrading enzymes (see **Table 2**).

2.1.1.1. Polysaccharides

PIA (or **poly-*N*-acetylglucosamine (PNAG)**) is the main cell-to-cell adherent substance in numerous *S. aureus* strains, contributing to biofilm stability and participating in early biofilm formation [134]. PIA – synthesized by the enzymes encoded in the *icaADBC* locus – is composed of several positively-charged deacetylated units of *N*-acetylglucosamine that mediate the binding to negatively charged bacterial surface and probably to the negatively charged eDNA [133, 135]. However, the production of this matrix component is strain- or condition-specific because certain number of *S. aureus* strains establish protein-enriched, PIA-independent biofilms. Surface-attached or cytoplasmic proteins with moonlighting functions can serve as cell-to-cell aggregation components in such circumstances [136-139].

2.1.1.2. eDNA

Extracellular DNA, together with surface associated adhesins, mediates initial attachment to a surface. It is the most common matrix component in *S. aureus* biofilms

[140] and creates intercellular connections by binding to positively-charged matrix components. In *S. aureus*, *cidA* and *lrgAB* operons mediate the autolysis process by which eDNA is released [141, 142]. As in *P. aeruginosa*, *S. aureus* biofilm treated with DNase shows decreased mass, and DNase also prevents the initial attachment [141, 143].

Table 2. *S. aureus* biofilm matrix components.

		Composition/ Types	Functions	Other characteristics
PIA/PNAG		β-1,6-linked *N*-acetylglucosamine with some deacetylated residues	Cell-to-cell aggregation Biofilm stability Interaction with eDNA	Main matrix component in PIA-dependent strains Positively charged
eDNA		Chromosomic DNA	Initial attachment Interaction with PIA	Most common matrix component Produced by cell autolysis Negatively charged
Proteins	**Cationic proteins**	Cytoplasmic proteins	Cell-to-cell aggregation	Release mediated by autolysins Aggregation due to acidic environment
	Extracellular enzymes and toxins	Hemolysins, leukotoxins, lipases, proteases	Host tissue destruction Dispersion events Nutrient uptake	Virulence factors
	CWA (Cell-wall anchored) proteins	ClfAB, FnBP-AB, SdrCDE, SasCG, SpA IsdABCH Bap SraP	Adherence to host cells Cell-to-cell aggregation	Surface-associated proteins Some can form amyloid aggregates that contribute to stability (like Bap)
Other components	**Teichoic acids (TA)**	WTA LTA	Cell-to-cell aggregation Abiotic surface adherence	Negatively charged Attached to cell surface
	α-PSMs	Small surfactant peptides	Liquid channels formation Dispersal events	Can form amyloid aggregates that contribute to stability
	Fibrin	Host-derived protein	Cell-to-cell aggregation	Accumulation mediated by CoA and vWbp coagulases in certain biofilms

PIA: Polysaccharide intercellular adhesin; PNAG: Poly-N-acetylglucosamine; WTA: Wall Teichoic acids; LTA: Lipid-anchored Teichoic acids; α-PSMs: α-phenol soluble modulins.

2.1.1.3. Proteins

Despite initial investigations in *S. aureus* EPS revealed PIA as the main component, proteins – mainly cytoplasmic – constitute the major part of EPS in *S. aureus* PIA-independent biofilms. **Cytoplasmic cationic proteins** accumulate in the matrix due to the autolysis of some *S. aureus* cells mediated by bacterial autolysins [139]. These proteins abound in the EPS and promote cell-to-cell aggregation since the acidic environment created by *S. aureus* fermentation provides the proteins with positive charge that interacts with negatively-charged *S. aureus* cells [135, 139].

Secreted extracellular proteins also abound in the biofilm matrix, including virulence factors like hemolysins, leukotoxins, lipases, and extracellular adherence proteins [139]. Some secreted extracellular enzymes degrade matrix components that promote dispersion events, including **proteases** and **nucleases** [144-146]. Specifically, nucleases mediate early cell dispersal – in a process named exodus – that promote biofilm restructuring by degrading eDNA [147].

Surface-associated proteins like **sortase-mediated cell-wall anchored (CWA) proteins** promote adhesion to host cells and interconnect cells in biofilms [146, 148]. CWA proteins include the clumping factors ClfA and ClfB [149]; the fibronectin-binding proteins FnBP-A and FnBP-B [137]; the serine-aspartate repeat family proteins SdrC, SdrD, and SdrE [150]; the *S. aureus* surface proteins SasC and SasG [151, 152]; the protein A (SpA) [153]; the iron-regulated surface determinants IsdA, IsdB, IsdC, and IsdH [154]; the carbohydrate binding proteins like SraP [155]; and the biofilm associated protein (Bap) [156]. Bap – found in bovine mastitis isolates – forms amyloid aggregates that contribute to the matrix biofilm forming a scaffold [157]. The surface-associated major autolysin AtlA mediates attachment on abiotic surfaces and is important for initial biofilm development [158, 159].

2.1.1.1. Other components

Teichoic acids locate in the surface of Gram-positive bacteria in two different forms: they can directly attach to cell wall (wall teichoic acids, WTA) or to cell membrane via a lipid anchor (lipid teichoic acids, LTA). Teichoic acids provide bacterial cells negatively-charge surface, favoring cell-to-cell aggregation by binding to positively-charged matrix components [133] and attachment to abiotic surfaces [160].

The virulence factors **α-phenol soluble modulins** (α-PSMs) – small amphipathic surfactant peptides – shape liquid channels and disaggregate cells during dispersal events [161, 162]. Under certain conditions, α-PSMs can form amyloid fibers located on bacterial surface that contribute to structural stability in biofilms [163, 164].

Fibrin is present in *S. aureus* biofilms formed by the presence of host blood. Fibrin fibers are host-derived, and their accumulation is mediated by bacterial secreted coagulases Coa and vWbp. Remarkably, fibrin presence plays a role in physiological conditions such as in wound infections, abscesses, and in device-related infections [165, 166].

3. Ribonucleotide reductases

The synthesis of the four different deoxyribonucleotides (dNTPs), the monomeric precursors of DNA, is an indispensable process for any cellular organism. **Ribonucleotide reductases (RNRs)** are essential enzymes that participate in a critical step of the synthesis of all dNTPs present in DNA: they catalyze the unique reaction in *de novo* biosynthesis pathway by which ribonucleotides (NTPs) are converted into dNTPs [4]. Thus, RNRs are key enzymes in **DNA synthesis and repair**, being indispensable for the maintenance of all replicating cells [3] (**Figure 6**).

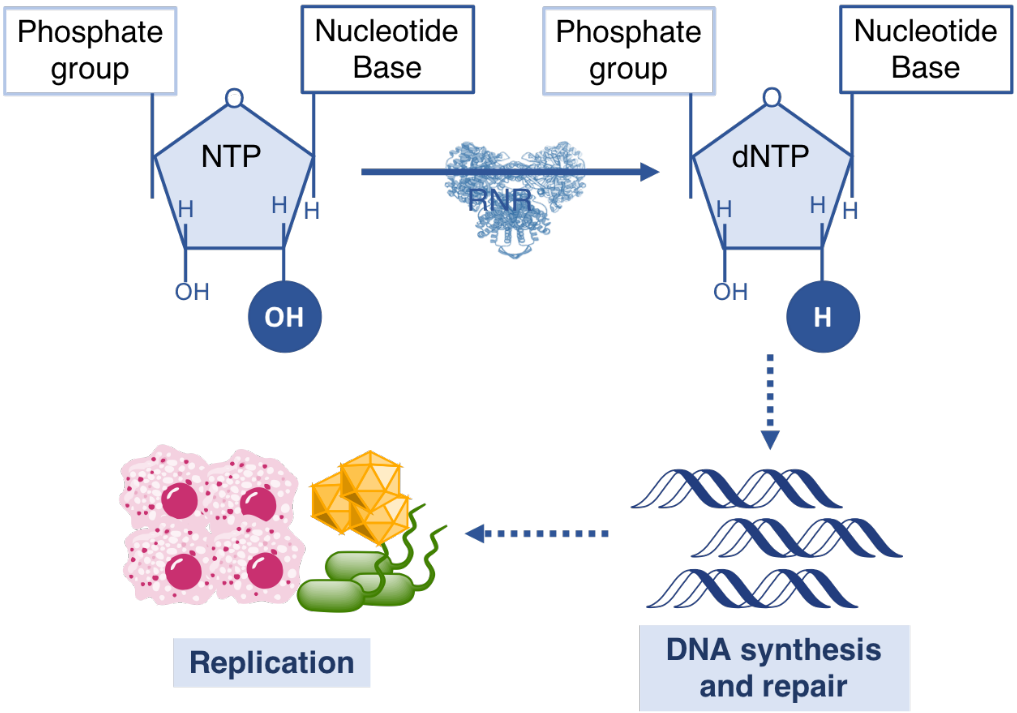

Figure 6. RNR catalyzes the synthesis dNTPs.

RNR catalyzes the synthesis of the DNA monomers by reducing NTPs to dNTPs, which are essential for DNA synthesis, and so, for the replication process of any líving cell.

The reaction catalyzed by RNR is conserved and based on **radical chemistry**. It requires the coordination of three main processes: **i) the generation of a protein radical** that is transferred to the active center, **ii) the reduction of a ribonucleotide** in the active center, and **iii) the re-reduction of the active center** by an external electron donor.

RNR enzymes have been divided in **three main classes** (class I, class II and class III), which differ in their cofactor requirements and so, in the environmental conditions in which they are active [3, 167, 168] (**Figure 7**). Despite some remarkable differences regarding the radical generation mechanisms and the reduction by external electron donors, all of the RNR classes share a common reaction mechanism, with small differences.

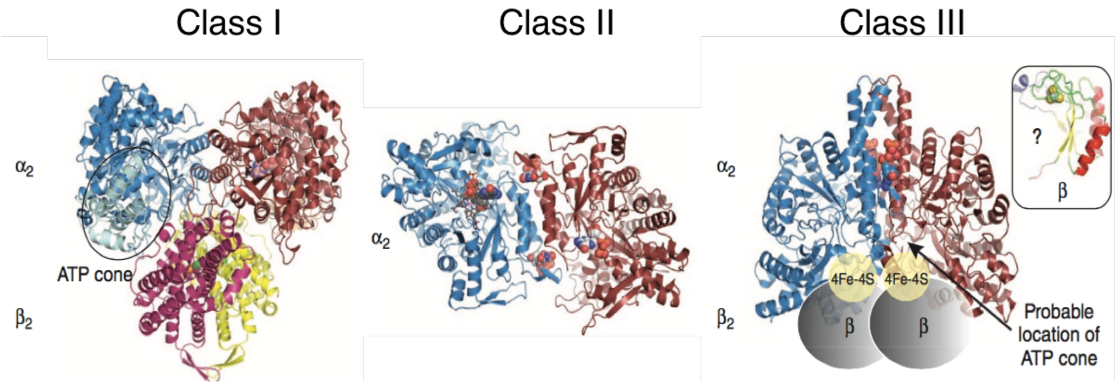

Figure 7. Structure representation of the three diferent RNR classes.

Three-dimensional models of the different RNR classes (class I (specifically class Ia,), class II, and class III). Source: [5].

3.1. General RNR reaction mechanism

In the reaction catalyzed by RNRs, the C2’ hydroxyl group of a ribonucleotide (di- or triphosphate (NDP or NTP)) is reduced to a hydrogen giving a deoxyribonucleotide (di- or triphosphate (dNDP or dNTP)) by using radical chemistry that requires electron donors. The reaction is accomplished in a **unique active center** for all the different nucleotides (ADP or ATP, CDP or CTP, GDP or GTP, UDP or UTP).

To initiate the catalysis, a **thiyl radical in a conserved cysteine** (cysteinyl radical) in the active site of the enzyme must be generated. Afterwards, the reduction takes place in a **four-step reaction**: i) first, the cysteinyl free radical in the active center activates the ribonucleotide substrate by oxidizing the hydroxyl moiety in the 3’ carbon of the ribose, forming a 3’ carbon radical; ii) the hydroxyl group at the 2’ carbon leaves forming a water molecule; iii) the 2’ carbon of the substrate is reduced with the addition of two electrons that come from two conserved reduced cysteines in class I and II enzymes, or directly by formate in class III; and iv) a final reduction takes place in the 2' carbon, thus introducing the initially abstracted hydrogen by cysteinyl radical. (**Figure 8**) [4, 169, 170].

During catalysis, the RNR enzyme interact with the substrate through hydrogen bonds, suffering a series of conformational changes that promote i) the reduction of the active cysteines, ii) the opening and adaptation of the substrate binding site, iii) the formation of a channeling system to allow the electron transfer between subunits, and iv) spatial movements to favor the expulsion of the reduced dNTPs.

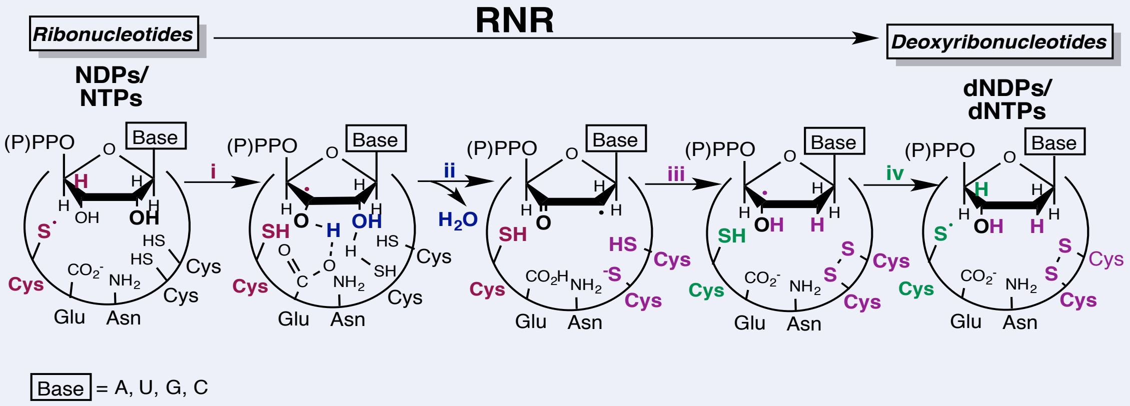

Figure 8. General RNR reaction mechanism.

Representation of the reaction mechanism of RNRs in the catalytic site. The four different di- or triphosphateribonucleotides (NDPs or NTPs) are reduced to di- or tri-phosphatedeoxyribonucleotides (dNDPs or dNTPs) via a mechanism that requires the formation of a transient thyil radical in a conserved cystein in the catalytic center of the enzyme. An additional reduced cystein pair is needed each turnover to directly reduce the hydroxyl in the C2'. The scheme shown is completely representative for both class I and II RNRs. Class III RNR enzyme lacks one of the reduced cysteines and uses formate as an electron donor. Source: adapted from [4].

3.2. External electron donors

To carry out the reduction reaction, RNRs need the supply of external reduction power. Class I and II RNRs need two reduced cysteine residues in the active site every reaction cycle to reduce the substrate (**Figure 11)**. After each catalytic cycle, the cysteine pair form a disulfide bridge that is reduced before performing another catalytic cycle by **external electron donors**. The external electron donors are small proteins with redox-active thiols, such as **thioredoxins and glutaredoxins**, that are reduced via either specific thioredoxin and glutaredoxin reductases [167], which, in turn, are reduced by glutathione or $FADH_2$. Ultimately, the reducing power comes from **NADPH** (**Figure 9**).

Class I enzymes use thioredoxin or glutaredoxin, but also the specific RNR reductant glutaredoxin-like protein **NrdH-redoxin** [171], (see **Table 3**) and class II enzymes employ thioredoxin. However, class III uses formate as external reductant instead of redoxin proteins [172], which acts directly in RNR reaction by replacing the action of one of the cysteines that lacks the enzyme.

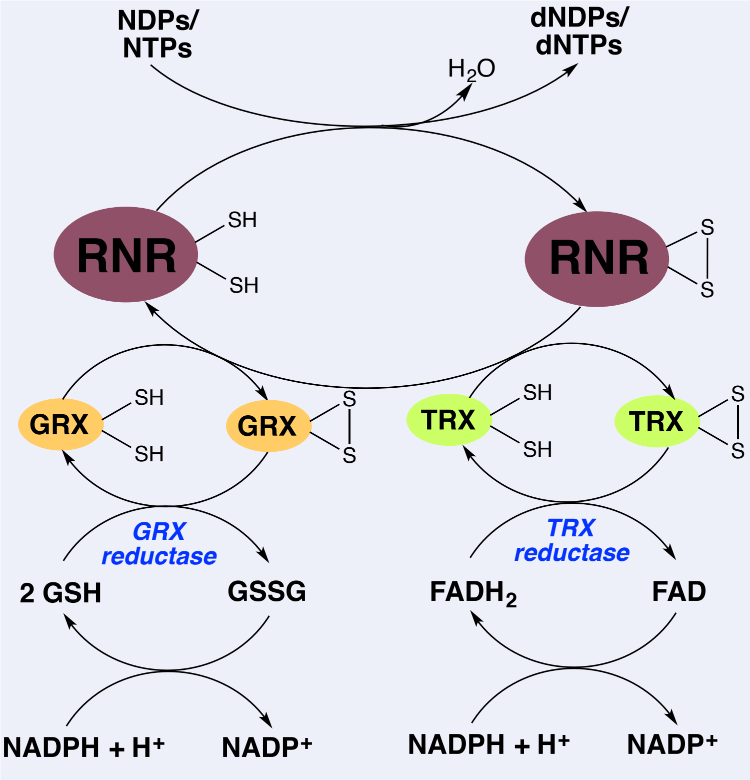

Figure 9. External electron supply systems in RNRs.

RNRs need to be reduced by external redox proteins, such as glutaredoxins (GRX) and thioredoxins (TRX), to perform the catalysis. In turn, these proteins are reduced by specific reductases (GRX or TRX reductases), which are also reduced by either glutathione (GRX) or $FADH_2$ (TRX). Finally, NADPH cofactor is responsible for reducing both glutathione and $FADH_2$. This electron supply system is characteristic of some RNRs. However, some class I RNRs use a specific redoxin, NrdH, and class III RNRs usually use formate as electron donor.

GSSG: oxidized glutathione; GSH: reduced glutathione.

3.3. RNR current classification

RNRs currently known are arranged into three main classes: **class I, class II and class III**. All three RNR classes perform the catalysis by using unpaired electrons through the formation of stable or transient protein radicals in the enzyme. RNR classes fundamentally differ in how they generate the radical and thus, in the **metal and cofactors requirements** (see **Figure 10**) [3, 4]: class I RNRs use a ferritin-like protein – the activator subunit – that requires a divalent metal center and either O_2 or peroxide to produce a stable radical that is transferred to the catalytic subunit; class II RNRs employ 5’-deoxyadenosylcobalamin (vitamin B_{12}) coenzyme to generate a transient 5’-deoxyadenosyl radical; and class III RNRs require an independent activase protein with an iron-sulfur (Fe-S) center to form of a stable glycyl radical through S-adenosylmethionine action in the absence of O_2 (see **Table 3**).

The type of substrate used also differs among the three classes: class I uses ribonucleotides diphosphates (NDPs) as substrates; class II can reduce ribonucleotides diphosphates (NDPs) or triphosphates (NTPs), depending on the organism; and class III exclusively reduces ribonucleotides triphosphates (NTPs).

Table 3. Biochemical characteristics of the different RNR classes.

	Class I **O_2-dep. (aerobic)**					**Class II** **O_2-indep.**	**Class III** **O_2-sensitive**
Genes	***nrdAB***			***nrd(HI)EF***		***nrdJ***	***nrdDG***
Subclass	**Class Ia**	**Class Ic**	**Class Id**	**Class Ib**	**Class Ie**		
Catalytic subunit	NrdA (α)			NrdE (α)		NrdJ (α)	NrdD (α)
Activator subunit	NrdB (β)			NrdF (β)			
Active structure	$\alpha_2\beta_2$/ $\alpha_6\beta_6$			$\alpha_2\beta_2$		α/ α_2	α_2 (activated by β_2)
Activator protein	none			NrdI		none	NrdG (β_2)
Radical generation	Tyr·… **Cys·**	Mn^{IV}-O-Fe^{II} …**Cys·** Mn^{IV}·…**Cys·**	Mn^{III}-O-Mn^{IV} … **Cys·** Mn^{IV}·…**Cys·**	Tyr·… **Cys·**	DOPA· **…Cys·**	dAdo·… **Cys·**	dAdo·… **Cys·**
Metal cofactor	Fe^{III}/Fe^{III}	Mn^{II}/Fe^{III}	Mn^{III}/Mn^{IV}	Fe^{III}/Fe^{III} Mn^{III}/Mn^{III}	none	AdoCbl (Co)	AdoMet (Fe^{IV}-S^{IV})
Oxidant	O_2	O_2	O_2-	O_2-	O_2		
Substrate	NDPs					NDPs NTPs	NTPs
Final reductant	Thioredoxin/ glutaredoxin			NrdH-redoxin		Thioredoxin	Formate

O_2-dep.: O_2-dependent; O_2-indep.: O_2-independent; AdoCbl: Adenosylcobalamin; AdoMet: Adenosylmethionin; Tyr·: Tyrosyl radical; Cys·: Cysteinyl radical; dAdo·: 5'-deoxyadenosyl radical.

Even the differences, the distinct RNR classes have a **common evolutionary origin** [170]. They possess a common active site tertiary structure, formed by a 10-stranded α/β barrel, which is only described in RNR family and radical enzymes related to class III RNR [173]. This **structural homology** explains their common reaction mechanism and the similar allosteric regulation systems.

The differences among RNR classes are believed to be a consequence of the oxygenation event that appeared during evolution, adapting completely the chemistry of the radical-based catalytic reactions to the new environmental conditions. It is currently believed that different RNR classes evolved from a **common ancestor** that worked in the ancient anaerobic conditions, and during the **transition from an RNA to a DNA world**. Whereas it is unclear whether the first RNR was more similar to class II or class III, class I is obviously the most recent RNR [174].

The nowadays diversification of RNR in enzymes with different cofactors and oxygen requirements allows the growth in a wide range of environments. The ability for an organism to encode different RNR classes, consequently, will determine its **adaptability to different oxygen and cofactor conditions**. This is especially important for bacteria and other microorganisms because it has an impact on the ecological niches that any microorganism can occupy.

Whereas eukaryotes encode for one RNR (class Ia), with little exceptions in some unicellular organisms related to prokaryotes (such as *Euglena*, *Dictyostelium*, *Gibberella*, *Phytophthora* species), all three classes can be found in prokaryotes, and one organism frequently encodes more than one class, finding any possible combination of classes. More than a third part of prokaryotes encode for at least two RNR classes, with extra operons probably acquired via horizontal gene transfer [4], which enable them to grow on both aerobic and anaerobic environments. RNR genes can also be codified in some double-stranded DNA viruses (usually class Ia) and bacteriophages (where all RNR classes genes can be found), highlighting RNRs as essential enzymes for replication processes.

A detailed explanation of the different RNRs classes is given below.

3.3.1. Class I RNRs

The discovery of RNRs dates back in the 1960's when one of the RNRs codified by *E. coli* was described [167, 175]. It was the first radical protein discovered and such RNR belongs to the class I. Class I are known as the **aerobic RNRs** since oxygen conditions are indispensable to generate the stable free radical for the catalysis. They are structurally composed of **two homodimeric subunits**: the major subunit **α (R1)**, which is the **catalytic subunit,** and the small subunit **β (R2)**, which is the radical generator or **activator subunit.** The catalytic subunit (α) contains both the active site of the enzyme with the three conserved cysteines, where binding and reduction of the substrate takes place (see **Section 3.1.**), and also two allosteric regulation sites (explained in **Section 3.4.1**). The activator subunit (β) is essential to activate the substrate, and usually harbors a dimetal cluster that allows the formation of the initial free radical, mainly a stable tyrosyl radical (Y·) [176], that is transferred every catalytic cycle to one of the conserved cysteines in the active site in the catalytic subunit. This transfer occurs through a mechanism that involves a proton coupled electron transfer (PCET) chain – over a distance of 35 Å – in which certain conserved aromatic residues of both α and β are involved [177]. Although the general active quaternary structure is proposed as $\alpha_2\beta_2$, like in *E. coli* class Ia [178], other class I RNRs may have different oligomeric active quaternary structures bed ($\alpha_6\beta_6$ in the mammalian class Ia [179]).

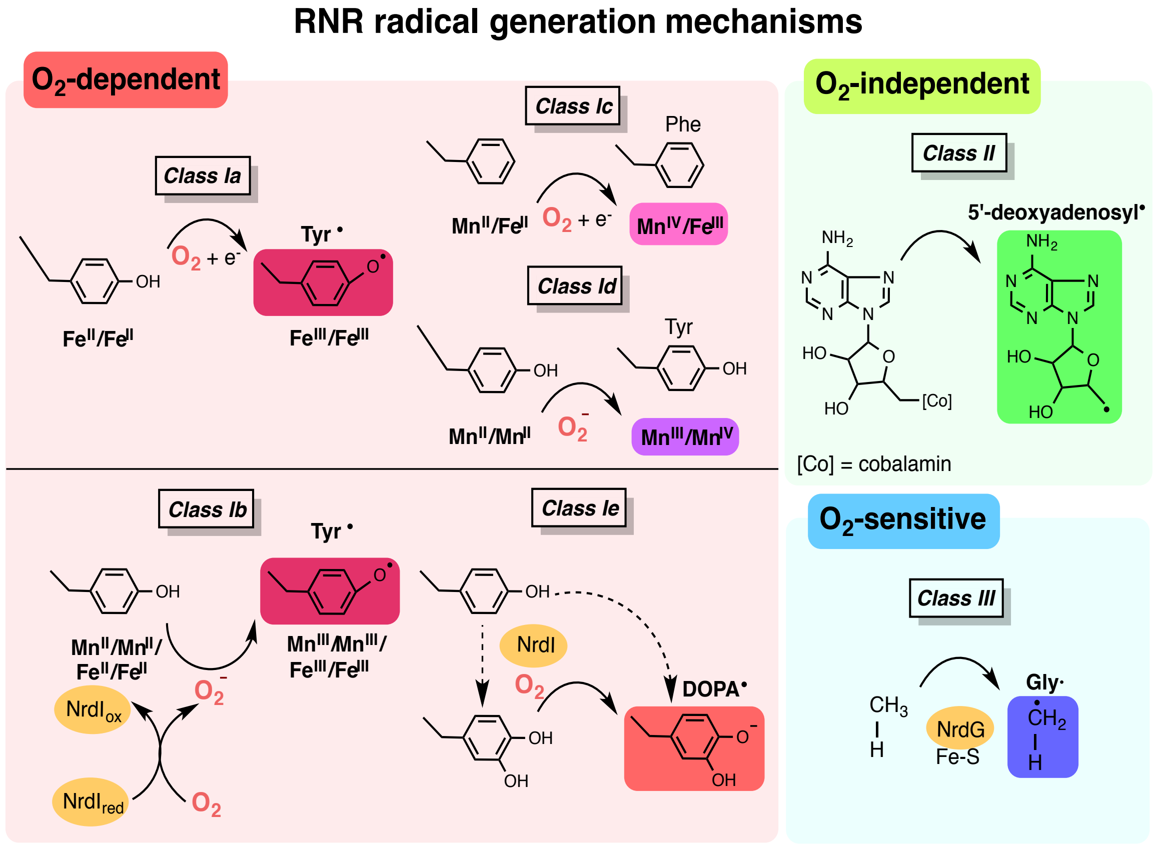
RNR radical generation mechanisms
O2-dependent
Class Ia
OH
Fe^II/Fe^II
O2 + e-
Tyr•
O•
Fe^III/Fe^III
Class Ic
Phe
Mn^II/Fe^II
O2 + e-
Mn^IV/Fe^III
Class Id
OH
Tyr
OH
Mn^II/Mn^II
O2-
Mn^III/Mn^IV
Class Ib
Tyr•
OH
O•
Mn^II/Mn^II/
Fe^II/Fe^II
Mn^III/Mn^III/
Fe^III/Fe^III
NrdI_ox
O2-
NrdI_red
O2
Class Ie
OH
NrdI
O2
DOPA•
OH
OH
O-
OH
O2-independent
Class II
5'-deoxyadenosyl•
NH2
N
N
N
N
HO
O
HO
[Co]
[Co] = cobalamin
O2-sensitive
Class III
CH3
H
NrdG
Fe-S
Gly·
CH2
H

Figure 10. RNR radical generation mechanisms.

RNRs classes use different pathways to activate the enzyme by forming a radical. **Class I** generates the free radical in a reaction that needs O_2 or O_2-activated species: subclasses Ia, Ib, Ic and Id use divalent metal centers (composed of iron, manganese or both), whereas subclass Ie is metal-independent; subclasses Ia and Ib generate a tyrosyl radical, alone (class Ia) or by using the activase protein NrdI (class Ib); subclasses Ic and Id generate the radical directly in the dimetal cluster; and subclass Ie generates the radical by hydroxylation and activation of a tyrosine residue generating a dihydroxyphenylalanine (DOPA) radical. **Class II** generates a transient radical in a reaction that does not require O_2 by promoting the homolytic cleavage of the cofactor 5'-desoxyadenosylcobalamin to form a 5'deoxyadenosyl radical. **Class III** requires an activase NrdG protein containing an iron-sulfur center to generate a stable glycyl radical in a reaction that is sensitive to O_2.

Since class I is the enzyme that specifically requires oxygen for its activity, it is the most spread class across the different domains of life: it is found in eukaryotes, in aerobic and facultative bacteria and archaea, in eukaryote viruses, and in some bacteriophages.

Class I is further subdivided in the subclasses Ia, Ib, and Ic [3] and in the recently proposed Id [180, 181] and Ie [182, 183]. All class I subclasses harbor a dimetal center in the activator subunit to generate the initial radical, except in the novel class Ie, where no metal is required (see **Figure 10).**

Subclass Ia is normally encoded by a continuous *nrdAB* operon that codifies for the α (NrdA) and β (NrdB) polypeptides; it corresponds to the first RNR described in *E. coli* [167, 175]. Subclass Ia enzymes contain a diferric cluster (Fe^{II}/Fe^{II}) in the activator subunit (NrdB) that is oxidized in the presence of molecular oxygen (O_2) to Fe^{III}/Fe^{III} to allow the formation of an initial stable tyrosyl radical.

Subclass Ib, firstly described in *Salmonella typhimurium* [184], is encoded by *nrdE* (the α polypeptide, NrdE) and *nrdF* (the β polypeptide, NrdF) with the additional *nrdH* and *nrdI* genes, in a *nrdHIEF* operon [185]. Subclass Ib enzymes contain a dimanganese (Mn^{II}/Mn^{II}) center in the activator subunit (NrdF), but some may contain a diferric center (Fe^{II}/Fe^{II}) instead [186-188]. Subclass Ib uses the flavodoxin protein NrdI to produce superoxide (O_2^-) from O_2 that oxidizes the dimetal center in NrdF to either Mn^{III}/Mn^{III} or Fe^{III}/Fe^{III} [189, 190]. Like subclass Ia, the oxidation is needed to produce a stable tyrosyl radical. As a reductant, subclass Ib uses the independent glutaredoxin-like protein NrdH instead of redoxin/glutaredoxin systems [171, 191, 192].

Subclass Ic (firstly described in *Chlamydia trachomatis* [193]) and new **subclass Id** (up to date described in *Flavobacterium johnsoniae* [180] and *Actinobacillus ureae* [181]) do not generate a tyrosyl radical. Instead, subclasses Ic and Id use the oxidized form of the dimetal cluster itself to generate the cysteinyl radical in the catalytic subunit. In subclass Ic, a phenylalanine residue replaces the essential tyrosine residue present in subclasses Ia and Ib [194]. Whereas **subclass Ic**, encoded by the *nrdAB* genes, contains an ironmanganese center (Mn^{II}/Fe^{II}) in the activator subunit (NrdB) that is directly oxidized by O_2 to the Mn^{IV}/Fe^{III} active state [194, 195], novel **subclass Id**, encoded by the *nrdAB* genes, harbors a dimanganese center (Mn^{II}/Mn^{II}) that is oxidized by free superoxide (O_2^-) captured from the medium to get a $Mn^{III}Mn^{IV}$ active state [180].

In all the above-described class I RNR subclasses, the enzymes generate a stable protein radical by using a dimetal center. However, some bacterial pathogens encode a metal-independent active class I RNR [182, 183, 196]. Novel **subclass Ie**, analogous to the known subclass Ib and encoded by the *nrdHIEF* genes, contains a modified β subunit that lacks the essential residues that shelter the metal center. To generate the free radical, the activator subunit oxidizes a posttranslationally-modified tyrosine to the 3,4-dihydroxyphenylalanine (DOPA) radical in the presence of O_2. This subclass is present in *Streptococcus pyogenes* and *Aerococcus urinae* [182] and in some Firmicutes, Chlamydiae, Fusobacteria, and Tenericutes, including some pathogenic *Mycoplasma* species [183]. The capability to provide dNTPs in a metal starvation environment seems an advantageous trait in infections because the host limits the availability of metals as a strategy to combat pathogens in what is known as "nutritional immunity". Thus, this new RNR probably evolved to allow bacteria survive in metal-restricted environments [183].

3.3.2. Class II RNRs

Class II RNRs, first discovered in *Lactobacillus leichmannii* [197], do not depend on O_2 presence but require adenosylcobalamin to generate the protein radical essential for the catalysis. Class II is encoded by *nrdJ* gene that may be split in two different genes in the same operon (*nrdJa* and *nrdJb*) [198] and is constituted by one α polypeptide (NrdJ) that contains the active site and one allosteric site [199]. Class II can be found in the active structures α or α_2. The metallocofactor 5'-deoxyadenosylcobalamin locates near the active site and undergoes a hemolytic cleavage to generate the 5'-deoxyadenosyl radical that afterwards generates the thyil radical at the cysteine in the active site, at approximately 6 Å from the cofactor [200-202]. As the enzyme activity is independent from O_2, it can be found in facultative bacteria, in strict anaerobic archaea, and in unicellular eukaryote organisms.

3.3.3. Class III

Class III RNRs were first identified in *E. coli* anaerobic cultures as oxygen-sensitive RNRs that could be active during strict anaerobic conditions [203]. Class III RNRs are encoded by the *nrdDG* operon, sometimes split in separated *nrdD* and *nrdG* genes. The catalytic protein, NrdD, which generally contains two allosteric regulation sites like most class I enzymes, is an α-polypeptide with an active α_2 quaternary structure that requires the independent activase protein NrdG for its activation [204]. The activase NrdG contains a Fe^{II}-S^{II} center mediates the cleavage of S-adenosylmethionine (SAM) cofactor into 5'-deoxyadenosyl radical [204-208]. Once the 5'-deoxyadenosyl is formed, the radical is then transferred at an approximate tridimensional distance of 5 Å to the cysteine in the active site of NrdD, forming a cysteinyl radical required to perform the catalysis. Class III slightly differs in the reaction mechanism from classes I and II, containing one of the two disulfide-forming cysteines involved in substrate reduction during catalysis in class I and II [209] (see Section 4.1), directly oxidizing a formate molecule in the active center that provides the reduction power [172]. However, some class III RNRs use thioredoxins with a similar reaction mechanism to class I; thus, some authors have proposed a class III subtype [210]. As glycyl radical is highly labile in aerobic conditions, the enzyme is limited to strict anaerobic conditions and thus, class III is found in facultative and strict anaerobic bacteria and archaebacteria, but also in bacteriophages and some eukaryotic parasites [4].

3.4. RNR regulation

The synthesis of the four different dNTPs requires a tight regulation of all the reactions that take place – such as the reaction catalyzed by RNRs – to allow a balanced dNTPs pool for every cell situation. Many regulation mechanisms at different levels interact to adjust RNR and establish the required amounts and proportions of dNTPs that sustain the cellular growth. RNR regulation mechanisms include transcriptional regulation, protein and mRNA degradation, posttranscriptional regulation, the presence of specific inhibitors, compartmentalization, and allosteric activity regulation mechanisms.

3.4.1. RNR allosteric regulation

Two different allosteric sites – different enzyme locations than the active site – mediate RNR activity modulation to adapt the cells to current dNTPs requirements [3, 4, 168]. Different nucleotide effector molecules bind to the allosteric sites and cause conformational changes to modify RNR enzymatic activity. RNR allosteric regulation mechanisms are essential to avoid problems associated to unbalanced dNTPs, including high mutation rates, chromosomal anomalies, genome instability, and cell death [3, 167, 211-215].

3.4.1.1. Allosteric regulation by the activity site

The overall activity of the enzyme is regulated in the **“activity site” (a-site)**, which acts as a master switch that senses and responds to dNTP levels through the binding of ATP or dATP: ATP activates the enzyme by increasing its activity and dATP decreases the enzyme activity [216]. This is a general activity regulation mechanism that controls the global dNTP pool by direct sensing of dATP concentrations as an indicator of total dNTPs. Its functionality relies on the presence of an ATP-cone, a domain composed of a four α-helix bundle and three-stranded β-sheet cap in the N-terminal region of the catalytic subunit where the ATP/dATP effectors bind to either activate or inactivate the enzyme. In the transition from the active to the inactive state, the binding of the negative effector dATP triggers the formation of high-number oligomeric structures in which the electron transfer is blocked [179, 217-220].

The a-site, and so the ATP-cone domain, is present in some class I (47%), some class II (7%), and most class III (76%) RNRs [170]. In class I, ATP-cone is commonly found in the catalytic subunit (NrdA or NrdE), but most NrdE lack the ATP-cone [170, 219]. In some class I catalytic subunits lacking ATP-cone, the domain is present in the activator subunit (NrdB or NrdF), thus compensating the absent a-site activity in the catalytic subunit [219, 221]. Though, there are some class Ib RNRs that completely lack a functional ATP-cone in which the overall regulation takes place transcriptionally [170]. Other class I completely lacking an ATP-cone, such as in *Bacillus subtilis* class Ib, the a-site regulation is conserved and dATP inhibits the enzymatic activity in an ATP-cone independent manner [222, 223]. The existence of multiple (two or three) ATP-cones in a single RNR occurs frequently in RNRs from all three classes. For instance, *Chlamydia trachomatis* NrdA and *P. aeruginosa* NrdA contain three and two ATP-cone domains, respectively [193, 224], but some of them lack functionality in terms of allosteric regulation.

ATP-cone domains are mobile elements, independent from the catalytic domains, that are frequently lost, acquired or degenerated throughout the RNR evolution [220, 225]. As a consequence, the modularity of the a-site is broadly variable and so are the mechanisms of ATP/dATP binding, oligomerization, and transitions from the active to the inactive states of the enzyme. The ATP-cone driven allosteric modulation has been classically studied in well-known class I enzymes, including some eukaryotic class Ia (human [226-229], mouse [179, 217], and *Saccharomyces cerevisiae*), *E. coli* class Ia [178, 216, 218], and *P. aeruginosa* class Ia RNRs [219, 220, 224]. Several mechanisms by which class Ia enzymes are inhibited through dATP binding exist: in *E. coli*, the active form is $\alpha_2\beta_2$ and the inactive form is an $\alpha_4\beta_4$ octamer where the ATP-cones sequester the β subunits [178]; in the eukaryotic enzyme, α_2 dimers assemble into an α_6 oligomer where β_2 subunits can bind, forming either inactive ($\alpha_6\beta_2$) or active ($\alpha_6\beta_6$) complexes [229]; and in *P. aeruginosa* with one of two ATP-cone binding nucleotides, the active form is $\alpha_2\beta_2$ whereas the inactive form is an α_4 ring that interacts through the exterior ATP-cones, binding β_2 and forming an inactive $\alpha_4\beta_2$ complex [219, 220]. In class Id of the marine bacteria *Leeuwenhoekiella blandensis*, with the ATP-cone present in the activator subunit (β), the β subunits form tetramers (β_4) through ATP-cone interactions that lead to an inactive $\alpha_4\beta_4$ complex and the active state is formed by an $\alpha_2\beta_2$ complex [221]. Whereas the exact allosteric mechanisms have been more extensively studied in class I RNRs, in which different protein complexes between activator and catalytic subunits must be formed to get an active enzyme, in class II and class III these interactions do not occur, and it is presumed that the mechanisms are appreciably different [220].

3.4.1.2. Allosteric regulation by the specificity site

An additional allosteric site, the **"specificity site" (s-site)**, binds to different nucleotides ((d)ATP, dGTP, and dTTP) to adapt the active center to reduce a specific substrate, ensuring that the amount of each different dNTP supports the cellular needs. The s-site is placed in the interphase of the catalytic subunits and in all the RNR classes the binding of ATP in the s-site causes the reduction reaction of CDP or CTP and UDP or UTP. Likewise, the binding of dGTP induces the reduction of ADP or ATP, and dTTP induces the reduction reaction of GDP or GTP [230]. The s-site allosteric regulation system and its mechanism is conserved in all RNR classes, except in the Herpesviridiae virus family RNRs [167].

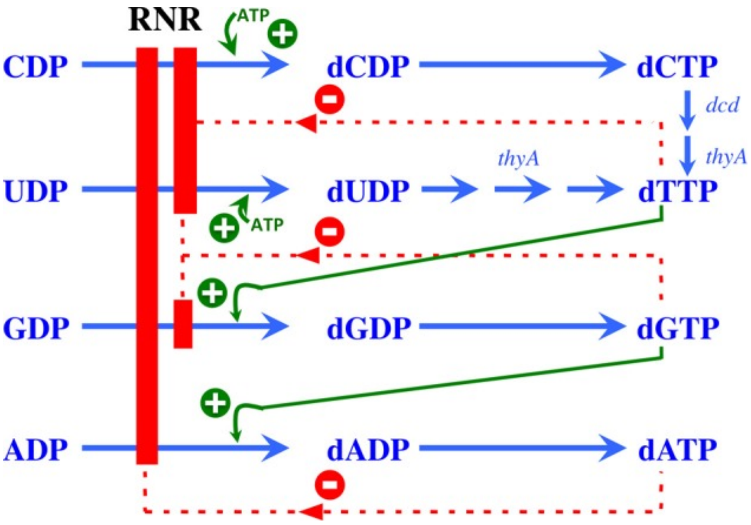

Figure 11. Specificty-site and activity-site allosteric regulation in RNRs.

Scheme of the allosteric mechanisms that regulate RNR activity at the specificity and activity (s-site and a-site, respectively). Source: [3]

3.4.2. RNR gene regulation in bacteria

Despite allosteric regulation is the most well-known and studied RNR regulatory mechanism, RNR gene expression regulation also contributes to provide cells with a balanced dNTP pool. Both microorganisms and eukaryotes regulate RNRs according to the cell-cycle since a large dNTP supply is needed during the first stages of cell division. As a consequence, the inhibition of DNA synthesis and DNA damage induce RNRs expression [231]. In addition, during metabolic changes, RNR regulation adapts the cells for a particular growth condition, such as the presence or absence of specific metabolites.

Specifically, bacterial RNR gene regulation is complex because most bacteria encode for more than one RNR class and they must provide a proper concentration of the different RNR enzymes to get a balanced dNTP pool at any situation. Under a specific condition or environment, bacteria encoding several RNRs express a predominant RNR that mainly supports bacterial growth, despite they must coordinate the expression of all the RNRs. To understand the role that each RNR play under different conditions, therefore, we need to study which are the factors that drive the differential RNR expression.

Bacterial RNRs have been described to be transcriptionally regulated by i) cell-cycle regulators, being associated to DNA replication initiation, ii) stress conditions, such as oxidative and nitrosative damage, iii) oxygen levels through anaerobic transcriptional regulators, and iv) by the master RNR regulator NrdR, which responds to nucleotides levels. In addition, some RNRs are regulated post-transcriptionally, through B_{12}-riboswicthes placed in the 5'-untranslated region (5'-UTR) of mRNA, which bind and respond to vitamin B_{12} (adenosylcobolamin) levels.

3.5. RNR inhibitors

Due to the critical role RNR has on cellular division and repair processes, RNR has been considered for long as an attractive target for the treatment of a wide repertoire of diseases in which the inhibition of cell proliferation is desirable: cancer diseases [232] and viral [233], protozoan [234, 235], and bacterial infections [3].

During the last decades, hundreds of inhibitors targeting RNR have been studied for the treatment of cancer [236-239] and infectious diseases [240-244], and even some have been used as antiproliferative drugs for cancer [245-247]. However, certain difficulties have arisen during the development of RNR inhibitors as anti-infection therapy: the low specificity, as some interfere and block RNR from cells other than the target, resulting in toxicity; and the frequent appearance of drug-resistance [4].

Different aspects of RNR – comprising both the structure and function of the enzyme, but also its regulation at many levels – can be targeted to design inhibitors. Inhibitors acting on RNR can be classified according to the mode of action: **enzymatic inhibitors** targeting the enzyme to block its activity, **oligomerization inhibitors** hindering the formation of a functional quaternary structure of the enzyme, and **gene expression inhibitors** acting on the transcriptional and translational level by blocking mRNA and protein synthesis (**Figure 12**). A description of the different RNR inhibitors families and subfamilies is given below.

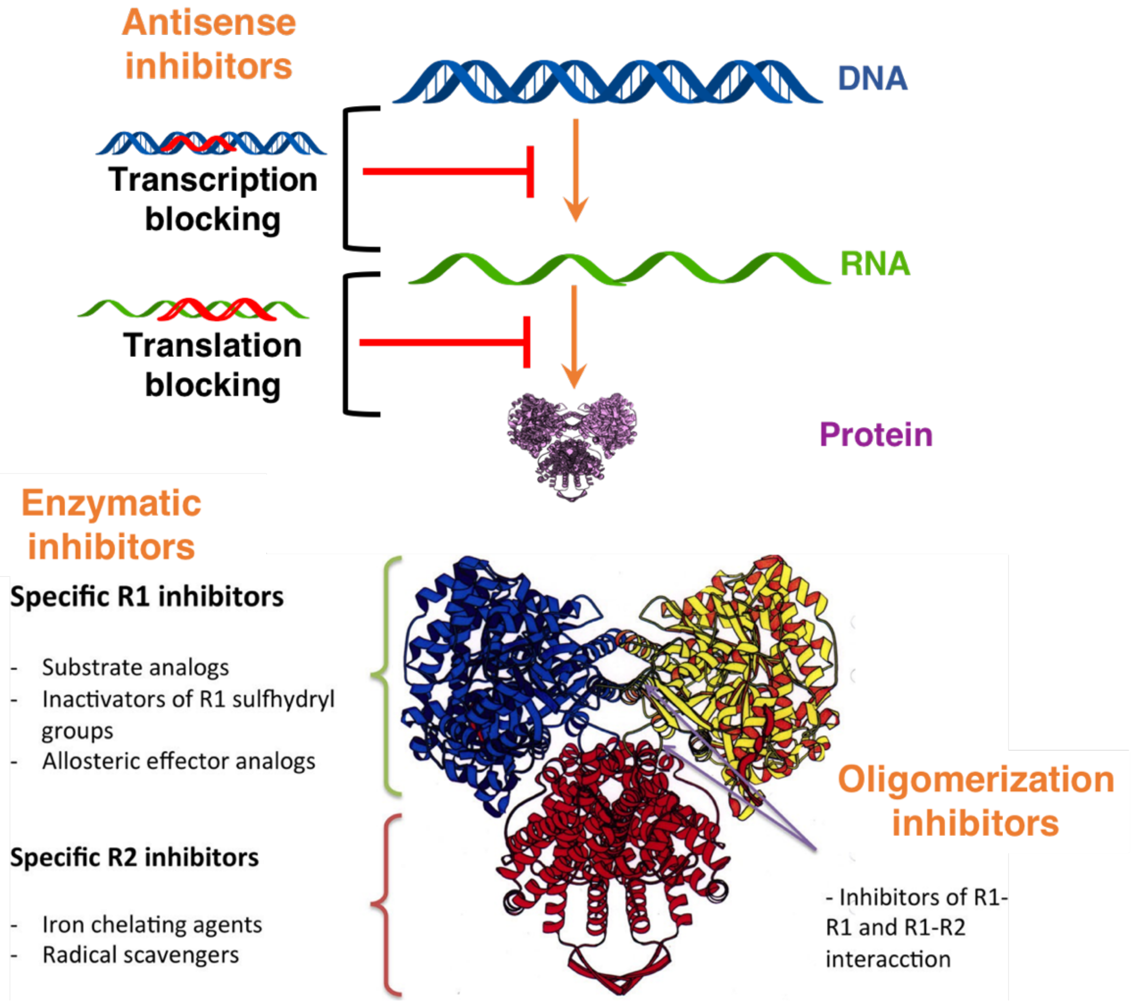
Antisense inhibitors
DNA
Transcription blocking
RNA
Translation blocking
Protein
Enzymatic inhibitors
Specific R1 inhibitors
- Substrate analogs
- Inactivators of R1 sulfhydryl groups
- Allosteric effector analogs
Specific R2 inhibitors
- Iron chelating agents
- Radical scavengers
Oligomerization inhibitors
- Inhibitors of R1-R1 and R1-R2 interacction

Figure 12. **RNR inhibitors families.**

RNR inhibitors are mainly classified based on the mode of action: **enzymatic inhibitors** that act on either R1 or R2 subunits or both, gene expression or **antisense inhibitors** that block mRNA or/and protein synthesis, and **oligomerization inhibitors** that prevent the formation of the active quaternary structure. Source: modified from [3].

3.5.1. Enzymatic inhibitors

Enzymatic inhibitors can target i) the catalytic subunit (R1) or ii) the activator subunit (R2). Whereas inhibitors of the catalytic subunit block the active site (**substrate analogues** and **inactivators of sulfhydryl groups**) or bind to the allosteric sites (**effector analogues**), inhibitors of the activator subunit hinder the radical generation by either sequestering the metal cofactors indispensable for radical generation (**metal chelators**) or quenching the already formed radical (**radical scavengers**).

3.5.1.1. Substrate and effector analogues

Substrate or effector analogues are modified (di- or tri-) nucleotides that bind to either the active or the allosteric sites of the enzyme, respectively, by disturbing the radical reaction and preventing cysteinyl radical regeneration (see **Section 3.1.**). Substrate and effector analogues are usually synthesized as prodrugs in a non-phosphorylated form (as nucleoside analogues), needing further processing in the cytosol by kinases to be active as di- or tri- phosphate nucleotides [232]. Most nucleoside analogues are modified at the 2' position of the ribose, and commonly with halogenated groups in the case of substrate analogues.

Relevant substrate analogues include the deoxycytidine analogues **gemcitabine (dF-dC)**, **tezacitabine (FM-dC)**, **DMCD (2'-deoxy-2'-methylidenecytidine)**, and **cytarabine (ara-C)** (**Table 4**). Despite the fact that some of them are currently used for cancer chemotherapy [246], resistance to these analogues occurs frequently at several levels, including cell uptake, phosphorylation, increase in phosphatase and deaminase activities, and RNR overexpression [248-250].

dF-dC is a well-known modified deoxycytidine analog that irreversibly inhibits RNR in both the catalytic (R1) and activator (R2) subunits [251]. It is clinically approved and used for long alone or in combination with other drugs in pancreas, bladder, breast, ovarian, and lung cancers, as it has a broad range of anti-tumor activity [252]. FM-dC is a deoxycytidine analog similar to dF-dC with potent inhibitory activity [253], approved for esophagus and stomach adenocarcinomas. DMDC is a modified deoxycytidine nucleoside that acts by inhibiting both RNR and DNA polymerase, showing a broad anti-cancer activity.

ara-C acts mainly by inhibiting DNA polymerase after being incorporated in DNA, but there are doubts about its inhibitory effect against RNR. It was used for long to treat both acute and chronic myeloid leukemia (AML and CML).

Table 4. RNR inhibitors of the catalytic subunit.

	Characteristics	Examples	
		Inhibitor	Structure
Substrate analogues	Deoxycytidine analogues Active site binding General irreversible inhibition	Gemcitabine (dF-dC)	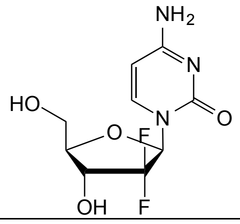
		2'-deoxy-2'-methylidene-cytidine (DMDC)	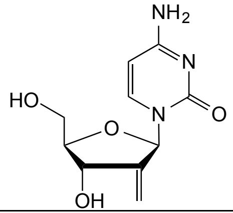
		Tezacitabine (FM-dC)	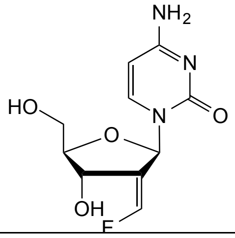
Effector analogues	Deoxyadenosine analogues Allosteric site binding General reversible inhibition	Cladribine (2-CdA)	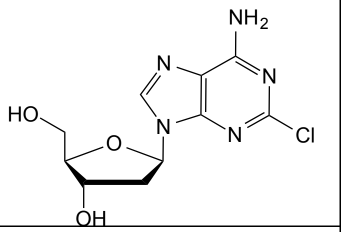
		Fludarabine (2-F-ara-A)	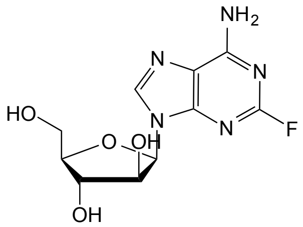
		Clofarabine (Cl-F-ara-A)	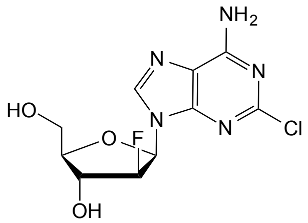
Inactivators of sulfhydryl groups	Inactivate sulfhydryl groups of the active site cysteines	Cisplatin	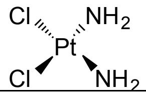
		Caracemide	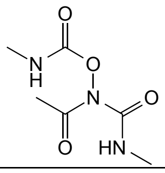

Other nucleoside analogues reversibly inhibit RNR as allosteric effectors by mimicking the role that dATP has as allosteric inhibitor. These include the deoxyadenosine nucleosides **cladribine (2-CdA)** and **fludarabine (2-F-ara-A)** and the second-generation purine nucleoside analog **clofarabine (Cl-F-ara-A)** (**Table 4**). 2-F-ara-A and 2-CdA are used for different types of leukemia, acting both as substrate and effector analogues that inactivate the enzyme by altering the RNR oligomeric structure [254]. Cl-F-ara-A – used to treat hematological malignancies, like acute lymphoblastic leukemia in children [255, 256] – also inhibits DNA polymerase, ribosomal reductase and deoxycytidine kinase [257].

As nucleosides and nucleotides are metabolites involved in several cellular processes related to DNA and RNA, most of substrate and effector analogues that act on RNR lack specificity and affect other enzymes and processes, specially related to DNA synthesis [245]. It is thus frequent for them to inhibit other enzymes, including DNA polymerase, DNA gyrase, DNA primase, deoxycytidine deaminase (dCMP deaminase), thymidylate synthase, CTP synthase, and topoisomerase I.

3.5.1.2. Inactivators of sulfhydryl groups

Since reduced cysteines in the active center of RNRs play a critical role on reducing the NTPs, the inactivation of cysteines sulfhydryl groups can inhibit the catalytic activity.

Cisplatin is one of the most potent inactivator of sulfhydryl groups inhibitor and is widely used in cancer therapies. Apart from its RNR inhibitory role [258], it is an alkylating agent that causes DNA damage and cell toxicity [259].

Caracemide is a hydroxamic acid derivative that irreversibly inhibits the catalytic subunit by covalently binding to the cysteine residues in the active center of the enzyme [260], but it is not clinically approved due to toxicity side effects [246].

3.5.1.3. Radical scavengers

Radical scavengers are RNR inhibitors that directly block the tyrosyl radical in the activator subunit (R2) or either interfere with transient radical residues in the electron transfer pathway created between the activator and the catalytic subunits (see **Section 3.3.1**.) (**Table 5**).

Table 5. RNR inhibitors of the activator subunit.

	Mechanism of action	Examples	
		Inhibitor	Structure
Radical scavengers	Radical tyrosyl quenching in the activator subunit	Hydroxyurea (HU)	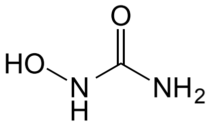
		Didox (DX)	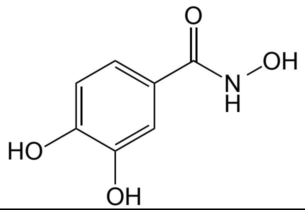
		Trimidox (TX)	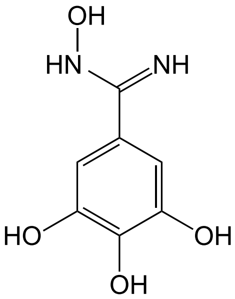
Metal chelators	Prevent metal center formation in the activator subunit by metal chelation Produce reactive oxygen species (ROS)	Triapine (3AP)	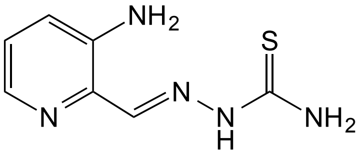
		Deferoxamine (DFO)	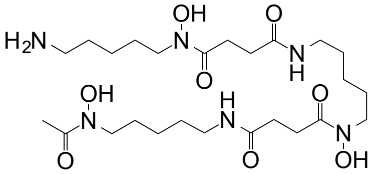
		Quercetin	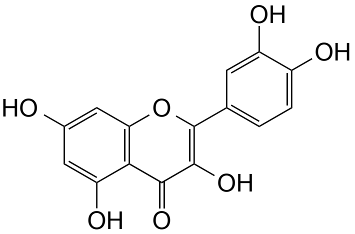
Others	Prevent metal center formation by iron mimicking	Gallium nitrate	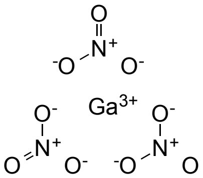

Hydroxyurea (HU) (or hydroxycarbamide) is one of the first anticancer agents developed in the 1960s [261] and acts as a radical scavenger inhibiting RNR [262]. HU has also metal chelator activity and creates cytotoxic reactive oxygen species (ROS) and reactive nitrogen species (RNS)nitric oxide [263]. HU is clinically used in Chronic Myeloid Leukemia (CML), Acute Myeloid Leukemia (AML), and glioblastoma [232, 264]. However, several drawbacks are associated to HU use in cancer, including the frequent development of resistance and the lack of specificity – since HU inhibits other enzymes like DNA primase [265].

HU and derivative compounds have also been studied for long as a treatment of many infectious diseases, such as the bacterial infections caused by *C. trachomatis* [266], *S. epidermidis* and *Micrococcus lysodeikticus* [267], and *P. aeruginosa* [268]; viral infections like HIV infections [269]; and protozoan infections, including the sleeping disease caused by *Trypanosoma brucei* [270]. HU and compounds from the same family (hydroxamic acid derivatives) also show antimalarial acivity [271].

Other important radical scavenger drugs similar to HU are hydroxybenzohydroxamic derivatives, including **didox (DX)** and **trimidox (TX)**, which also work as iron-forming complexes with chelating properties [272]. Didox and trimidox have more effective radical scavenging capacity *in vitro* than HU [273]. Despite didox has been extensively evaluated in clinical trials for cancer therapies, it shows low efficacy [246]. Together with hydroxyurea, didox and trimidox successfully inhibit the human cytomegalovirus (HCMV) [274] and supress retrovirus-induced immunodeficiency disease in mice [275].

Other relevant radical scavenger compounds are the **alcoxyphenols**, a family of compounds that also act by stopping the radical transfer from the activator to the catalytic subunit [276]. **Nitric oxide (NO)**, which is an intrinsic immune system mechanism, can diffuse inside RNR and reduce the protein radical in the active site, thus inhibiting RNR and inhibiting tumor cell replication [277]. **Thionitrites**, as nitric oxide donors, also inhibit RNR [278]. The polyphenolic compound **resveratrol** and derivatives, also inhibit RNR as radical scavengers in tumoral cells [279].

3.5.1.4. Metal chelators

Since reducing iron – or other RNR metal cofactors – availability is a way to prevent the formation of the diferric center of the activator subunit needed for radical formation, some iron chelators are RNR inhibitors. Some of them have redox activity and also act as radical scavengers by trapping the radical formed in the activator subunit.

Triapine (3AP), a heterocyclic carboxaldehyde thiosemicarbazone, is a well-known iron chelator with potent anticancer activity alone or in combination with other drugs [280]. Triapine may inhibit RNR through different mechanisms: i) by chelating intracellular iron and preventing cofactor assembly, by directly chelating iron from the R2 cofactor, ii) by quenching the tyrosyl radical by reactive oxygen species (ROS) produced by the binding of iron to triapine, and iv) by forming a complex between triapine and Fe(II) that directly reduce the tyrosyl radical, inhibiting RNR activity faster than by chelating iron [281]. Apart from its action in RNR, free radicals that may be generated through its binding to iron can lead to direct DNA damage [259]. Several clinical trials are evaluating its use for cancer chemotherapy [282, 283].

Other explored iron chelating agents in antiproliferative chemotherapies include **deferoxamine (DFO)**, a potent iron chelator agent that acts by binding Fe(III). To evaluate its use for the treatment *T. brucei* infections, deferoxamine has been tried together with **pyridoxal isonicotinoyl hydrazine (PIH)** derivatives, phenolic compounds with iron-chelating properties [284, 285]. These last chelate iron with high affinity and have been evaluated against both malaria and cancer [245]. **Quercetin** is another iron chelator that targets RNR with anti-leishmanial activity [286].

3.5.1.5. Other enzymatic inhibitors

Motexafin gadolinium (MGd), an expanded porphyrin with anticancer properties, oxidizes reducing molecules. During RNR inhibition, it precludes subunits oligomerization and also directly inhibits the catalytic subunit [287]. It is currently evaluated in several clinical trials for cancer therapies [246].

Other RNR enzymatic inhibitors act by mimicking iron, such as gallium, and are incorporated in the activator subunit as a cofactor instead but producing a non-functional enzyme [288]. Gallium can be administered as gallium maltolate or gallium nitrate, which is clinically approved for hypercalcemia and bladder cancer.

3.5.2. Oligomerization inhibitors

RNRs are enzymes with complex quaternary structures that can be intrinsically activated or inactivated through changes in the oligomerization state, mainly mediated by the ATP-cone present in several RNRs allosteric a-site (see **Section 4.4.1.1.**). Thus, molecules that interfere with the formation of an active oligomerization state or that lead to the transition from an active to an inactive state can serve as RNR inhibitors.

Dimerization inhibitors prevent the complexation of the catalytic (R1) and the activator (R2) subunits in class I RNRs [289] (**Table 6**). Most well-known dimerization inhibitors are peptides and **peptidomimetics** with aminoacidic sequences similar to the C-terminal region of the R2 subunit, which is responsible of the interaction with R1, and compete with R2 to form a protein complex with R1 [290]. Compared with other RNR inhibitors, peptidomimetics are more species-specific and, for thus, its use has been explored in infectious diseases, such as in *Herpes simplex* Virus (HSV) [291-293], *Mycobacterium tuberculosis* infections [294-296], and *Plasmodium falciparum* infections [245]. Some peptidomimetics are also designed to target mammalian RNR for cancer treatment [297, 298]. However, drug delivery and protease degradation events are a handicap for their clinical use.

Table 6. RNR dimerization inhibitors.

	Mechanism of action	**Examples**	
		Targeted species	**Peptide sequence**
Dimerization inhibitors	Prevent complexation between R1 and R2 subunits through interaction with R1	*Herpes simplex* virus (HSV)	STSYAGAVVNDLYVVNDL (BILD 1357)
		Mycobacterium tuberculosis	N-Ac-DDDWDF EDDDWDF N-Ac-VTEDDDWDF
		Mammalian	N-Ac-NSFTLDADF N-Ac-FTLDADF N-Ac-AGAFTFNEDF N-Ac-FTFNEDF

Some **nucleoside analogues**, such as Cl-F-ara-A, 2-Cda, and 2-F-ara-A, and novel non-nucleoside inhibitors like **phthalimide** affect the oligomerization state of RNR because they bind to the R1 α_6 complex, making it unable to form a functional complex with the R2 subunit [228, 236, 254, 255, 299]. The reversible **NSC73735** inhibitor acts as an oligomerization inhibitor by preventing the formation of an α_6 oligomerization state in R1, needed for a functional enzyme [239].

3.5.3. Gene expression or antisense inhibitors

Antisense inhibitors, the most recently explored RNR inhibitors, are based on the natural antisense systems occurring in life. They consist on the targeting of a specific gene

– mRNA or DNA sequences – using oligonucleotides that block its transcription, translation or splicing processes.

RNR antisense inhibitors were first explored for cancer with an **inducible antisense cDNA** [300]. Later, **antisense oligonucleotides** for *Herpes simplex* Virus (HSV) infection [301] and for the malaria causative agent *P. falciparum* [302] were designed.

An antisense 20-mer modified **phosphonothioate oligonucleotide**, GTI-2040, targeting R2 human gene expression, has shown RNR downregulation and anticancer activity [303, 304]. The oligonucleotide binds to R2 mRNA blocking its interaction with regulatory protein complexes involved in translation and causing a decrease in both mRNA and protein levels. It is currently being tested in clinical trials in combination with other drugs [238, 305] and its use is intended for several solid tumors. Other antisense nucleotides based on **small interfering RNA (siRNA)** combined with nanoparticles have been used to knockdown R2 subunit in human tumors [306-309].

In *T. brucei*, **inducible RNA-interference (RNAi)** constructs against both R1 and R2 RNR subunits have recently been able to decrease parasite growth due to a reduction in RNR expression [270].

II. OBJECTIVES

The current lack of effective antibiotics and the increasing emergence of recalcitrant infections have encouraged the scientific community to find new ways to fight multidrug-resistant strains and biofilm-forming bacteria.

In this context, this thesis aims to develop new antibacterial strategies by using different approaches: **i)** by inhibiting RNR enzymatic activity with radical scavenger molecules and **ii)** by combining antibiotics action with biofilm matrix-degrading enzymes. Specifically, the objectives of the current thesis are:

1. **To evaluate the antibacterial activity of the RNR radical scavenger inhibitor *N*-methyl-hydroxylamine**, as compared with the two well-known and cytotoxic radical scavengers, hydroxyurea and hydroxylamine. Determination of the antibacterial activity in planktonic cultures of several Gram-positive and Gram-negative bacterial pathogens. Evaluation of the cytotoxicity in murine macrophages *in vitro* cultures. Study of the antibiofilm activity on *P. aeruginosa in vitro* biofilm models alone, or as adjunctive therapy with an antibiotic. Evaluation of the antibacterial activity on *Mycobacterium bovis* BCG infecting macrophages.

2. **To develop new radical scavengers that inhibit the bacterial RNR enzyme based on the *N*-hydroxylamine moiety to use them as antibacterial agents**. Chemical synthesis of a *N*-hydroxylamine molecules library to improve radical scavenging activity in RNR. Evaluation of the antibacterial activity of the newly synthesized radical scavenger molecules on different relevant pathogenic bacteria. Determination of the *in vitro* minimum inhibitory concentration (MIC) in planktonic cultures, the *in vitro* antibiofilm activity, and the eukaryotic cytotoxicity. Evaluation of the *in vitro* radical scavenger activities. Study of the inhibitory effect on bacterial RNR, by determining dNTPs levels and the effect on RNR expression.

3. **To design a drug delivery system based on nanoparticles to target *P. aeruginosa* biofilm infections.** Synthesis of biodegradable PLGA nanoparticles that combine the antibiotic ciprofloxacin with the extracellular DNA-degrading enzyme DNase I to improve antibiotic delivery on biofilm cells. Physical characterization of the nanoparticles and drug-release kinetics. Evaluation of the antibacterial activity, the antibiofilm activity on *P. aeruginosa* biodilms and eukaryotic cytotoxicity.

III. RESULTS

The current doctoral thesis is presented as a compendium of several publications. It is divided in the following chapters:

CHAPTER 1. Radical scavengers as RNR inhibitors with antimicrobial properties

Publication 1:

Methyl-Hydroxylamine as an Efficacious Antibacterial Agent That Targets the Ribonucleotide Reductase Enzyme

Esther Julián, **Aida Baelo**, Joan Gavaldà, Eduard torrents

Published in: *PLoS ONE*, 2015; 10(3): e0122049. DOI: 10.1371/journal.pone.0122049

Publication 2:

Hydroxylamine Derivatives as a New Paradigm in the Search of Antibacterial Agents

Laia Miret-Casals,[1] **Aida Baelo,**[1] Esther Julián, Josep Astola, Ariadna Lobo-Ruiz, Fernando Albericio, and Eduard Torrents

[1] These authors contributed equally to this work

Published in: *ACS Omega*, 2018; 3, 17057-17069. DOI: 10.1021/acsomega.8b01384

CHAPTER 2. Improving the treatment of biofilm infections

Publication 3:

Disassembling bacterial extracellular matrix with Dnase-coated nanoparticles to enhance antibiotic delivery in biofilm infections

Aida Baelo[1], Riccardo Levato[1], Esther Julián, Anna Crespo, José Astola, Joan Gavaldà, Elisabeth Engel, Miguel Angel Mateos-Timoneda, and Eduard Torrents

[1] These authors contributed equally to this work

Published in: *Journal of Controlled Release*, 2015; 209, 150-158. DOI: 10.1016/j.jconrel.2015.04.028

Chapter 1: Radical scavengers as RNR inhibitors with antimicrobial properties

PUBLICATION 1: Methyl-Hydroxylamine as an Efficacious Antibacterial Agent That Targets the Ribonucleotide Reductase Enzyme

ABSTRACT: The emergence of multidrug-resistant bacteria has encouraged vigorous efforts to develop antimicrobial agents with new mechanisms of action. Ribonucleotide reductase (RNR) is a key enzyme in DNA replication that acts by converting ribonucleotides into the corresponding deoxyribonucleotides, which are the building blocks of DNA replication and repair. RNR has been extensively studied as an ideal target for DNA inhibition, and several drugs that are already available on the market are used for anticancer and antiviral activity. However, the high toxicity of these current drugs to eukaryotic cells does not permit their use as antibacterial agents. Here, we present a radical scavenger compound that inhibited bacterial RNR, and the compound's activity as an antibacterial agent together with its toxicity in eukaryotic cells were evaluated. First, the efficacy of N-methyl-hydroxylamine (M-HA) in inhibiting the growth of different Gram-positive and Gram-negative bacteria was demonstrated, and no effect on eukaryotic cells was observed. M-HA showed remarkable efficacy against *Mycobacterium bovis* BCG and *Pseudomonas aeruginosa*. Thus, given the M-HA activity against these two bacteria, our results showed that M-HA has intracellular antimycobacterial activity against BCG-infected macrophages, and it is efficacious in partially disassembling and inhibiting the further formation of *P. aeruginosa* biofilms. Furthermore, M-HA and ciprofloxacin showed a synergistic effect that caused a massive reduction in a *P. aeruginosa* biofilm. Overall, our results suggest the vast potential of M-HA as an antibacterial agent, which acts by specifically targeting a bacterial RNR enzyme.

PLOS ONE

RESEARCH ARTICLE

Methyl-Hydroxylamine as an Efficacious Antibacterial Agent That Targets the Ribonucleotide Reductase Enzyme

Esther Julián[1], Aida Baelo[2], Joan Gavaldà[3], Eduard Torrents[2]*

1 Departament de Genètica i de Microbiologia, Facultat de Biociències, Universitat Autònoma de Barcelona, Bellaterra, Spain, **2** Institute for Bioengineering of Catalonia (IBEC), Bacterial infections and antimicrobial therapies; Baldiri Reixac 15-21, Barcelona, Spain, **3** Infectious Diseases Research Laboratory, Infectious Diseases Department, Vall d'Hebron Research Institute, Hospital Universitari Vall d'Hebron, Barcelona, Spain

* etorrents@ibecbarcelona.eu

Abstract

The emergence of multidrug-resistant bacteria has encouraged vigorous efforts to develop antimicrobial agents with new mechanisms of action. Ribonucleotide reductase (RNR) is a key enzyme in DNA replication that acts by converting ribonucleotides into the corresponding deoxyribonucleotides, which are the building blocks of DNA replication and repair. RNR has been extensively studied as an ideal target for DNA inhibition, and several drugs that are already available on the market are used for anticancer and antiviral activity. However, the high toxicity of these current drugs to eukaryotic cells does not permit their use as antibacterial agents. Here, we present a radical scavenger compound that inhibited bacterial RNR, and the compound's activity as an antibacterial agent together with its toxicity in eukaryotic cells were evaluated. First, the efficacy of N-methyl-hydroxylamine (M-HA) in inhibiting the growth of different Gram-positive and Gram-negative bacteria was demonstrated, and no effect on eukaryotic cells was observed. M-HA showed remarkable efficacy against *Mycobacterium bovis* BCG and *Pseudomonas aeruginosa*. Thus, given the M-HA activity against these two bacteria, our results showed that M-HA has intracellular antimycobacterial activity against BCG-infected macrophages, and it is efficacious in partially disassembling and inhibiting the further formation of *P. aeruginosa* biofilms. Furthermore, M-HA and ciprofloxacin showed a synergistic effect that caused a massive reduction in a *P. aeruginosa* biofilm. Overall, our results suggest the vast potential of M-HA as an antibacterial agent, which acts by specifically targeting a bacterial RNR enzyme.

OPEN ACCESS

Citation: Julián E, Baelo A, Gavaldà J, Torrents E (2015) Methyl-Hydroxylamine as an Efficacious Antibacterial Agent That Targets the Ribonucleotide Reductase Enzyme. PLoS ONE 10(3): e0122049. doi:10.1371/journal.pone.0122049

Academic Editor: José A. Bengoechea, Queen's University Belfast, UNITED KINGDOM

Received: September 15, 2014

Accepted: February 6, 2015

Published: March 17, 2015

Copyright: © 2015 Julián et al. This is an open access article distributed under the terms of the Creative Commons Attribution License, which permits unrestricted use, distribution, and reproduction in any medium, provided the original author and source are credited.

Data Availability Statement: All relevant data are within the paper and its Supporting Information files.

Funding: Funding provided by BFU2011-24066. Ministerio de Economia y Competitividad. Principal investigator: Dr. Eduard Torrents. 2009SGR66 and 2014SGR1442 from the Generalitat de Catalunya to Eduard Torrents. 2009SGR-108 from the Generalitat de Catalunya to Dr. Esther Julián. IIIPI10/01438 from the Instituto de Ivestigación Carlos III. Principal Investigator Dr. Esther Julián. ERA-Net pathogenomics from the Ministerio de Economia y Competitividad. Principal investigator: Dr. Eduard Torrents. Catalan and Spanish cystic foundation

Introduction

Infectious diseases constitute a tenacious and major public health problem worldwide. For many years, antibiotic-resistant pathogens have been recognized as one of the primary threats to human survival, and some experts predict a return to the pre-antibiotic era. The emergence

federations. The funders had no role in study design, data collection and analysis, decision to publish, or preparation of the manuscript.

Competing Interests: The authors have declared that no competing interests exist.

and increasing prevalence of bacterial strains that are resistant to available antibiotics urge the discovery of new therapeutic approaches [1]. An equally alarming decline has occurred in the research and development of new antibiotics to address the threat. Certain virulence factors have been shown to be potential targets for drug design and therapeutic intervention, and new insights are crucial for exploiting others [2, 3].

Bacterial DNA synthesis represents an attractive field for the discovery of new antibacterial targets because of remarkable differences from the eukaryotic system. During the course of infection, bacteria need to multiply inside the body, and they require active DNA synthesis to multiply. The key enzyme that provides the nucleotide precursors for DNA replication and repair are RiboNucleotide Reductases (RNRs). Three major classes of this enzyme are known (class I, II and III). Class I RNRs (subclasses Ia (*nrdAB*) and Ib (*nrdEF*)) carry a stable tyrosyl radical and are oxygen-dependent and thus, they only work under aerobic conditions; class II RNRs (*nrdJ*) require the vitamin B_{12} cofactor 5'-deoxyadenosylcobalamin and are oxygen-independent. Class III RNRs (*nrdD*, with their cognate *nrdG* activase) carry a stable glycyl radical, are oxygen-sensitive and only work under strict anaerobic conditions [4–8]. Eukaryotes only encode for one RNR class (Ia), but microorganisms have the ability to encode all possible RNR combinations [9, 10]. For this reason, RNRs could be considered a good antimicrobial target candidate to inhibit bacterial growth because they present substantial differences relative to their eukaryote counterparts [11, 12].

Several potential RNR inhibitors were reported, which included the following: free radical scavengers, iron chelators and substrate analogs [13–16]. Radical scavenger agents main mechanism of action is elicited through the inhibition of the RNR enzymes by scavenging the tyrosyl free radical (on the small class I subunits; NrdB and NrdF) that is required for the catalytic process [17]. These compounds have been shown to be useful for cancer treatment [18, 19]. One known family of radical scavenger compounds are derivatives from the hydroxylamine (HA) moiety, specifically hydroxyurea (HU), which is most commonly used for cancer treatment [18]. In fact, these compounds effectively inhibit the RNR of eukaryotic cells [19], reducing the possibility of using these drugs to treat bacterial infections without interfering in human RNR.

The modes by which different radical scavenger compounds interact in response to purified RNR enzyme were studied in our previous works [11, 12]. One compound, namely N-methyl-hydroxylamine (M-HA), was a highly active inhibitor of purified *Bacillus anthracis* RNR enzyme without interfering with the murine RNR enzyme. Although M-HA is promising as an antibacterial agent, its potential antimicrobial activity has not been evaluated.

In the present work, we aimed to explore the capacity of M-HA to inhibit the growth of clinically interesting Gram-positive (*Staphylococcus aureus*, *Streptococcus sanguinis*, *Streptococcus mutans* and *Mycobacterium*) and Gram-negative (*Pseudomonas aeruginosa* and *Burkholderia cenocepacia*) bacteria. Next, we investigated the effects of M-HA antibacterial activity on intracellular bacterial growth and biofilm-forming bacteria. Finally, the possible synergic activity of M-HA and other antimicrobials was evaluated.

Materials and Methods

Bacterial strains and mammalian cell line

Streptococcus mutans (ATCC 25175) and *Streptococcus sanguinis* (ATCC 10556) were grown in Todd-Hewitt broth (Oxoid) at 37°C. *Staphylococcus aureus* (ATCC 12600), *Pseudomonas aeruginosa* PAO1 (ATCC 15692) and *Burkholderia cenocepacia* J2315 (ATCC BAA-245) were grown in trypticase soy broth (TSB) or trypticase soy agar (TSA) (Sharlab, Barcelona, Spain) at 37°C. *Mycobacterium bovis* Bacillus Calmette-Guérin (BCG) substrain Connaught (ATCC

35745) was grown on Middlebrook 7H10 agar (Difco Laboratories, Surrey, UK) supplemented with 10% oleic-albumin-dextrose-catalase enrichment medium at 37°C for 2 weeks.

A murine macrophage J774A.1 cell line (DSMZ ACC 170) was maintained in Dulbecco's Modified Eagle's medium (DMEM) with L-glutamine (Gibco BRL, Grand Island, NY) supplemented with 10% heat-inactivated fetal bovine serum (FBS, Lonza Ltd., Switzerland) containing 100 U/ml penicillin G (Lab ERN, Barcelona, Spain) and 100 μg/ml streptomycin (Lab Reig Jofre, Barcelona, Spain) (complete medium) at 37°C in a humidified atmosphere with 5% CO_2.

Radical scavenger compounds

The hydroxylamine-bearing compounds used in this work were hydroxyurea (HU; M = 76.05 g/mol) (Sigma-Aldrich), hydroxylamine (HA; M = 33.03 g/mol) (Sigma Aldrich) and N-methyl-hydroxylamine (M-HA; M = 83.52 g/mol) (Acros Organics). Solutions were freshly prepared in PBS and filtered through a 0.22-μm pore-size filter (Millipore) before each experiment.

Antibacterial susceptibility testing

To determine the survival of the different strains in the presence of different radical scavengers, each bacterial strain was grown in its specific medium to mid-log phase ($A_{550} \approx 0.5$) and plated on solid plates supplemented with different concentrations of each compound.

In the case of BCG, colonies were scraped from Middlebrook 7H10 plates, resuspended in phosphate-buffered saline (PBS), slightly vortexed with glass beads to dissolve clumps, and allowed to settle for 30 minutes. The supernatant was diluted in PBS and adjusted to 1.0 McFarland standard. Serial dilutions were then plated on solid plates containing freshly prepared compounds at the indicated concentrations. Colony-forming units (cfu) were counted after growing.

Inhibitory concentration 50% (MIC_{50}) was defined as the compound concentration that reduced bacterial growth (cfu) by 50%, and MIC_{100} was defined as the lowest concentration of drug that visibly inhibited bacterial growth by 100%.

Determining mammalian cytotoxicity

Murine J774 macrophages ($6x10^4$ per well) were seeded onto 48-well tissue culture plates in complete medium without antibiotics in the presence of different doses of HU, HA and M-HA, or left untreated. After 24, 72 and 120 h of exposure to the different compounds, culture supernatants were removed and cell viability was assessed by using a 3-[4,5-dimethylthiazol-2-yl]-2,5-diphenyltetrazolium bromide (MTT) colorimetric assay (Sigma Aldrich) (20). Absorbance was measured at 550 nm with an ELISA reader (Infinite M200 Microplate Reader, Tecan). The results were expressed as a percentage of cell survival relative to untreated cells. Each experiment was repeated at least three times.

In another set of experiments, cells were washed at 24 hours after adding the compounds for the first time, and new, freshly made compounds were added. Cell viability was measured each 24 hours as described above.

The 50% cytotoxicity inhibitory concentration (CC_{50}) of each drug was determined from dose-response curves by using Graph Pad Prism v6. The selectivity index (SI) ($SI = CC_{50}/MIC_{50}$) was calculated on the basis of the CC_{50} and MIC_{50} values as determined after 24 h of exposure.

washed gently with water and the pegs were dried in air for 5 min. The dye that was bound to the cells was dissolved with 150 µl of ethanol 95%, centrifuged at 2000 rpm for 10 min, and read at 570 nm with a microplate reader (Infinite M200).

Biofilm culture in flow cell system and confocal microscopy analysis

To prepare biofilms developed under continuous flow, *P. aeruginosa* cells ($5x10^5$ cfu/ml) were cultured in LB medium at 25°C in flow chambers with channel dimension of 1x4x40 mm as described previously [22]. After 96 h of culture, formed biofilms were treated with 40 µg/ml of HA, HU or M-HA, and LB medium was used alone in the control sample. After 24 h of treatment at 25°C, biofilms were stained with 5 µM SYTO 9 at room temperature in the dark for 30 min, according to the specifications of the LIVE/DEAD BacLight Bacterial Viability kit (Molecular Probes, Invitrogen).

Confocal scanning laser microscopy of the biofilms was performed with a Leica TCS-SP5 confocal scanning laser microscope (Leica Microsystems, Wetzlar, Germany), with an excitation wavelength of 477 for SYTO9. To measure biofilm thickness, sections were scanned and Z-stacks were acquired at z step-size of 0.388 µm. Field size was 456 µm x 456 µm at 20X magnification. Microscope images were further processed with ImageJ analysis software (National Institute of Health, USA) and COMSTAT 2 software, specific for biofilm quantitative analysis [23].

Statistical analyses

Data were presented as the means ± standard deviation (SD). The statistical significance of differences between cytokine levels and BCG growth inhibition using the different radical scavenger compounds was assessed by using Student's t-tests (SigmaStat, SPSS, Chicago, IL). Differences were considered significant when $P < 0.05$. All statistical procedures were performed with SPSS 15.0 software (SPSS Inc., Chicago, IL).

Results

M-HA showed greater antibacterial activity than HU and HA radical scavengers

The antibacterial activity of three radical scavengers (HU, HA and M-HA) was evaluated against four Gram-positive bacteria (*S. aureus*, *S. mutans*, *S. sanguinis* and *M. bovis* BCG) and two Gram-negative bacteria (*P. aeruginosa* and *B. cenocepacia)*. As shown in Table 1, the HU compound exhibited moderate activity against *S. aureus*, *S. mutans* and *S. sanguinis* (200–330 µg/mL) and high growth inhibitory activity against *P. aeruginosa*, *M. bovis* and *B. cenocepacia* (7.6 to 13 µg/mL). HA showed better growth inhibitory activity relative to HU in all tested bacteria (2 to 52 µg/mL). M-HA was highly active in *M. bovis* BCG and *P. aeruginosa* cultures, with a 1.5 to 4.5-fold lower MIC_{50} than HU and HA. In BCG cultures, 7.5 to 43 times lower concentrations of M-HA (MIC_{50} = 1.9 µg/mL) were needed to obtain the same results as the other bacteria cultures (from 14.2 µg/mL for *B. cenocepacia* to 81.9 µg/mL for *S. sanguinis*) (Table 1).

To investigate the mechanisms through which M-HA inhibits bacteria growth, we specifically stained bacteria with the Live/Dead BactLight bacterial viability assay (Invitrogen). As shown in Fig. 1, the different radical scavengers (at a MIC_{50} concentration) did not apparently modify the bacterial membrane integrity after 3 hours of treatment because all of them were stained green. After 24 h of treatment, the proportion of non-viable cells (red cells) increased, especially when treated with M-HA.

Table 1. The antibacterial activity of HU, HA and M-HA against Gram-positive and Gram-negative bacteria.

	HU μg/ml				HA μg/ml				M-HA μg/ml			
	MIC_{50}	MIC_{100}	CC_{50}	SI	MIC_{50}	MIC_{100}	CC_{50}	SI	MIC_{50}	MIC_{100}	CC_{50}	SI
S. aureus	279.9	>380	25.9	0.09	28.4	<132.2	12.9	0.45	58.5	<334.1	350.8	6
S. mutans	205.3	>1140	25.9	0.13	16.5	<231.4	12.9	0.78	77.7	<584.7	350.8	4.5
S. sanguinis	336.9	>1140	25.9	0.08	51.5	<231.4	12.9	0.25	81.9	<417.6	350.8	4.3
***M. bovis* BCG**	8.36	>380	25.9	3.1	2.6	<16.5	12.9	4.96	1.9	<41.8	350.8	184.6
P. aeruginosa	7.6	<41.8	25.9	3.4	8.3	<66.1	12.9	1.55	6.7	<108.6	350.8	52.4
B. cenocepacia	12.9	>129.3	25.9	2	2.6	>66.1	12.9	4.96	14.2	>142	350.8	24.7

The growth inhibition of different bacteria after culturing them in HU-, HA-, or M-HA-supplemented media. The data are representative of one of at least three independent experiments. HU, hydroxyurea; HA, hydroxylamine; M-HA, methyl-hydroxylamine; MIC_{50}, 50% inhibitory concentration; MIC_{100}, 100% inhibitory concentration; CC_{50}, 50% cytotoxicity inhibitory concentration; and SI, selectivity index ($SI = CC_{50}/MIC_{50}$).

doi:10.1371/journal.pone.0122049.t001

M-HA does not affect eukaryotic cell growth

The antiproliferative activity of the three radical scavengers was evaluated against murine J744 macrophages by MTT staining. As expected, HU and HA interfere with macrophage proliferation even when low concentrations are used (Fig. 2). Only the lowest dose of HA (10 μg/ml) permits macrophage growth. By contrast, concentrations of up to 250 μg/ml M-HA do not inhibit macrophage proliferation (Fig. 2). The same results were obtained when culture medium plus radical scavenger compounds were renewed every 24 hours (data not shown), and even if the cells were treated for up to 120 hours (data not shown). As shown in Table 1, a cytotoxic concentration (CC_{50}) is observed for M-HA when doses higher than 250 μg/mL were used.

The selectivity index (SI) was calculated on the basis of the MIC_{50} and CC_{50} values that were determined after 24 h of exposure (Table 1). High SI values were obtained for M-HA in *Mycobacterium* and *Pseudomonas* growth inhibition (SI = 182.6 for *M. bovis* and 52.5 for *P.*

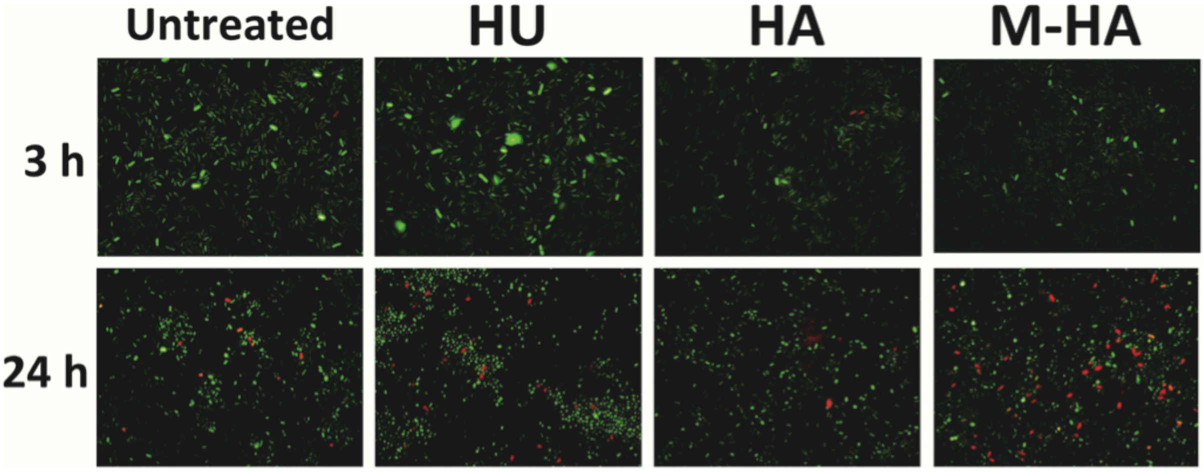

Fig 1. *P. aeruginosa* viability according to the LIVE/DEAD assay after treating with HU, HA, and M-HA. The bacteria were grown with HU (7.6 μg/ml), HA (8.3 μg/ml), or M-HA (6.7 μg/ml) for 3 and 24 hours and stained with LIVE/DEAD assay. Live cells were green (SYTO 9 dye) and dead cells were red (propidium iodide dye) under a fluorescent microscope. Magnification, x 1000. HU, hydroxyurea; HA, hydroxylamine; and M-HA, methyl-hydroxylamine.

doi:10.1371/journal.pone.0122049.g001

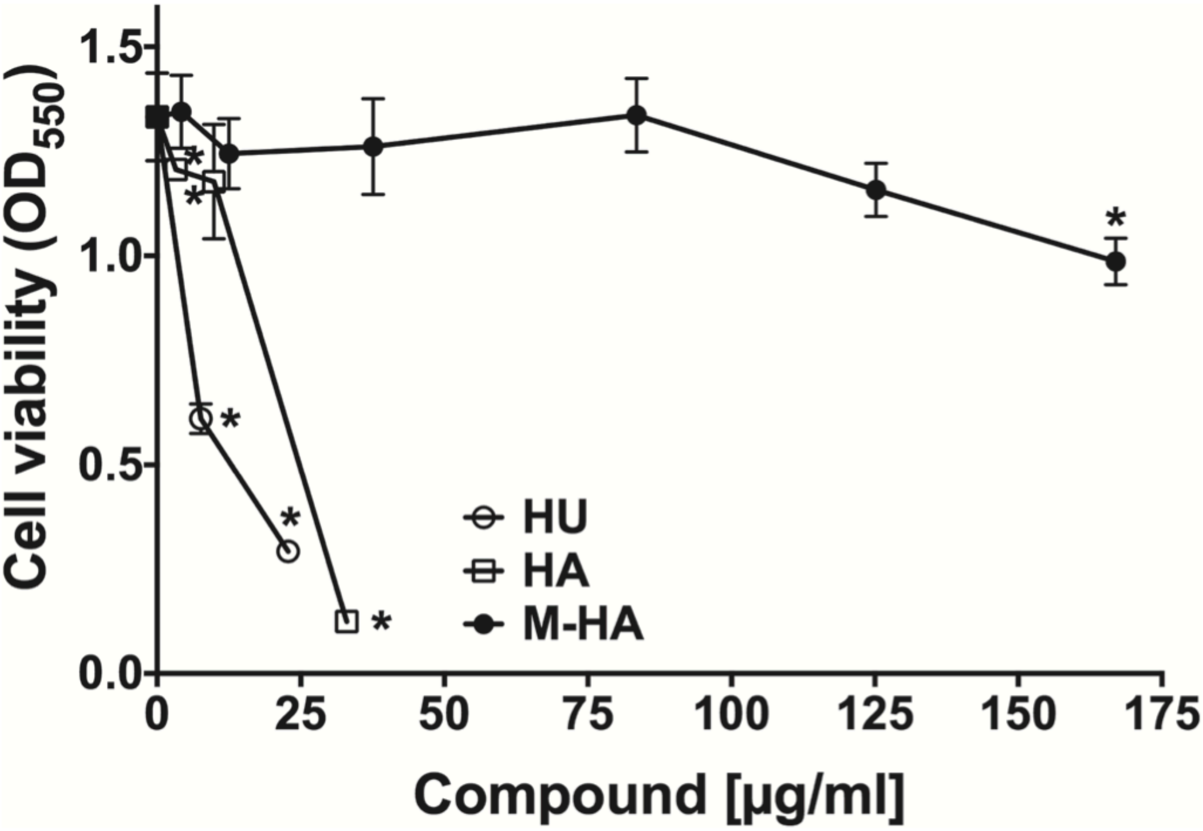

Fig 2. Dose-response curves for HU, HA and M-HA treatments of murine macrophages. The level of growth alteration for J774 macrophages that were treated with different doses of radical scavenger compounds at 72 hours post-treatment. Cell viability was measured by using an MTT assay. Values represent the means ± standard deviation (SD) of triplicate cultures. The data are representative of one of at least three independent experiments. (*, $P < 0.05$ *vs*. non-treated cells). HU, hydroxyurea; HA, hydroxylamine; and M-HA, methyl-hydroxylamine.

doi:10.1371/journal.pone.0122049.g002

aeruginosa), which were much higher than the SI obtained with HA or HU (SI from 0.08 to 4.9).

M-HA shows intracellular antimycobacterial activity

In view of the results shown in Table 1, M-HA seems to be a promising antimycobacterial candidate because mycobacteria are the intracellular pathogens for which we aimed to demonstrate activity in infected macrophages. As shown in Fig. 3A, *M. bovis* BCG viability was diminished when infected macrophages were incubated in the presence of the different radical scavenger compounds related to untreated wells. At 72 hours post-infection, HU triggers a BCG growth inhibition of approximately 50%, but only HA treatments exhibited better inhibition values when the dose was greater than 35 µg/ml. As explained before, this finding also corresponds to a concomitantly drastic reduction in macrophage viability (see Table 1, CC and Fig. 2). By contrast, M-HA showed enhanced intracellular *M. bovis* BCG growth inhibition in comparison with that of HU or HA at a range of concentrations that were not toxic for eukaryotic cells between 74.6% BCG survival at 8 mg/ml and 42.6% at 125 mg/ml (Fig. 3A). Moreover, the M-HA intracellular antimycobacterial activity improved when the culture medium was

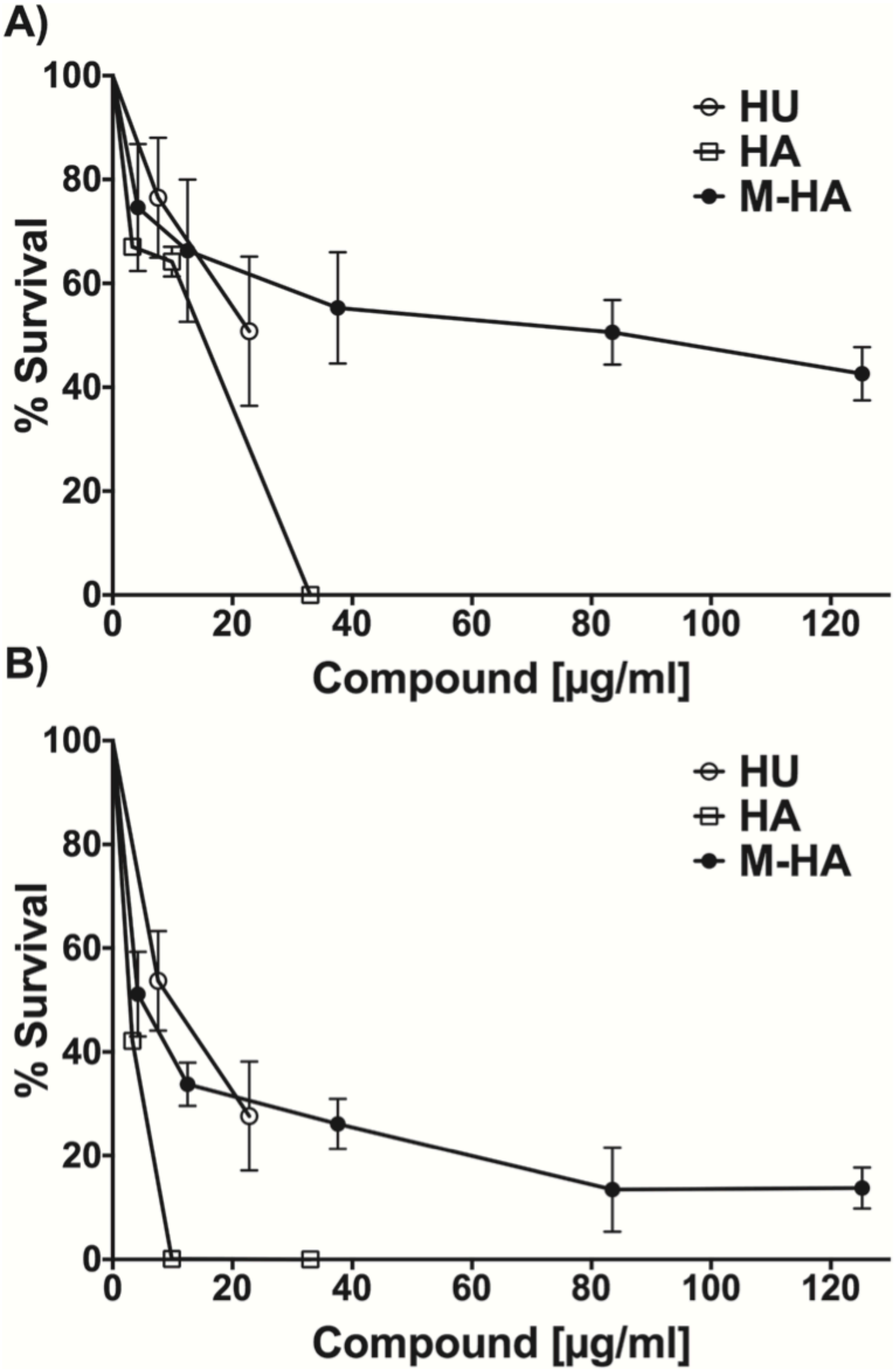

Fig 3. The intracellular BCG growth inhibition of macrophages treated with different doses of HU, HA and M-HA. The effects of different doses of radical scavenger compounds on the intracellular viability of BCG at 72 hours post-infection. A) Compounds were added 3 hours after infection B) Compounds were renewed every 24 hours after infection. The results are expressed as the means ± standard deviation (SD) of triplicate wells in percentages of inhibition with respect to non-treated cells. The data are representative of one of at least two independent experiments where statistically significant

differences between treated and untreated cells ($P < 0.05$) for all compounds and concentrations. HU, hydroxyurea; HA, hydroxylamine; and M-HA, methyl-hydroxylamine.

doi:10.1371/journal.pone.0122049.g003

changed every 24 hours by adding freshly prepared compounds, and values of up to 13% BCG survival were reached (Fig. 3B). In absolute numbers, this finding represents up to a one log reduction, i.e., at 72 hours post-infection, an M-HA concentration of 82 mg/ml was reduced from $6.3\text{x}10^4$ (untreated wells) to $8.4\text{x}10^3$ viable BCG cells (cfu). Similar values were observed in both cases (replacing or not replacing the compounds every 24 hours) at 120 hours post-infection (data not shown).

Increased TNF production by M-HA

We investigated the production of two bactericidal products that are able to kill intracellular BCG, namely TNF-α and NO [24], when the macrophages were infected with BCG and treated with the different radical scavenger compounds. As shown in Fig. 4, M-HA-treated macrophages produce higher TNF-α values at 24 hours post-infection than untreated cells (Fig. 4A). The highest amount of cytokine production was observed when cells were treated with high concentrations of M-HA (Fig. 4A). The amount of cytokine production did not increase after longer periods of incubation (72 or 120 hours after infection) (data not shown). When TNF-α production was evaluated in non-infected cultures, similar values were obtained in radical scavenger-treated and non-treated macrophages (data not shown).

Low but detectable amounts of NO production between 1 and 3 μM of NO were found in both BCG-infected radical scavenger-treated and untreated macrophages. No significant differences were observed between HA, HU and M-HA-treated macrophages. These data are consistent with previous data from [25].

When the production of IL-10 and IL-12 was studied in BCG-infected macrophages treated with the different radical scavengers, the results differ between cytokines and treatments. While IL-10 production was not detected in any case (data not shown), IL-12 production was significantly increased in HA-treated macrophages in a dose-dependent manner (Fig. 4B). At the highest HA concentration, however, IL-12 production dramatically diminished, probably due to the reduced presence of viable macrophages (Fig. 2).

M-HA inhibits *P. aeruginosa* biofilm formation

As explained previously, good M-HA antibacterial activity was also observed against *P. aeruginosa* (SI = 52.4). Thus, we further investigated the capacity of M-HA in reducing *P. aeruginosa* biofilms because it is one of the most important forms of persistent bacteria and is a characteristic of chronic *P. aeruginosa* infections. We used the quantitative microtiter plate method to determine the effect of the different hydroxylamine derivative compounds on biofilm formation. A dose-effect concentration was observed for each compound (Fig. 5). At 20.6 μg/ml HA and 82.5 μg/mL HU and M-HA, *P. aeruginosa* growth was completely arrested and no biofilm was formed (Fig. 5).

The M-HA effect on a preformed *P. aeruginosa* biofilm

Once a biofilm has been established, the cells are extremely resistant against all types of antibiotics and detergents and it is often challenging to remove. The effects of the different radical scavengers on existing *P. aeruginosa* biofilms were initially assessed using crystal violet-based biomass staining assay. As Fig. 6 shows, all compounds reduce the amount of biofilm formed, reaching values of approximately 55%, 90% and 70% reduction from HU, HA, and M-HA,

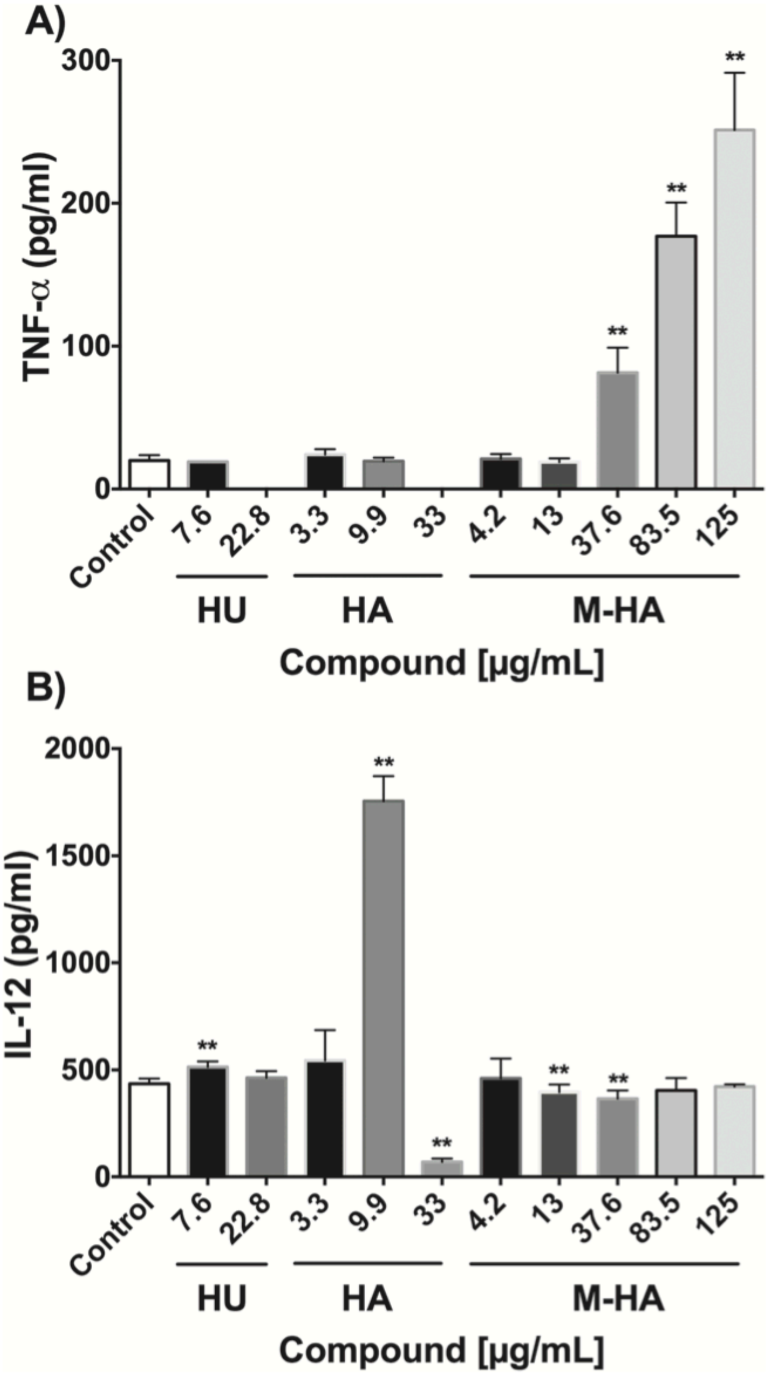

Fig 4. TNF-α and IL-12 production as triggered by BCG-infected macrophages that were treated with different doses of HU, HA and M-HA. J774 macrophages were infected with BCG and treated with different concentrations of radical scavenger compounds, and TNF-α and IL-12 levels were measured 24 hours post-infection. The results represent the means ± SD of triplicate preparations with one representative of two

independent experiments. A Mann-Whitney test was performed (*, $P < 0.01$; versus non-treated macrophages (control)). HU, hydroxyurea; HA, hydroxylamine; and M-HA, methyl-hydroxylamine.

doi:10.1371/journal.pone.0122049.g004

respectively, at the highest tested concentrations and three days of treatment. When employing M-HA concentrations that did not affect eukaryotic cell viability (up to 165 mg/ml), increasing amounts of compound diminished the established biofilms, indicating that the cells in an

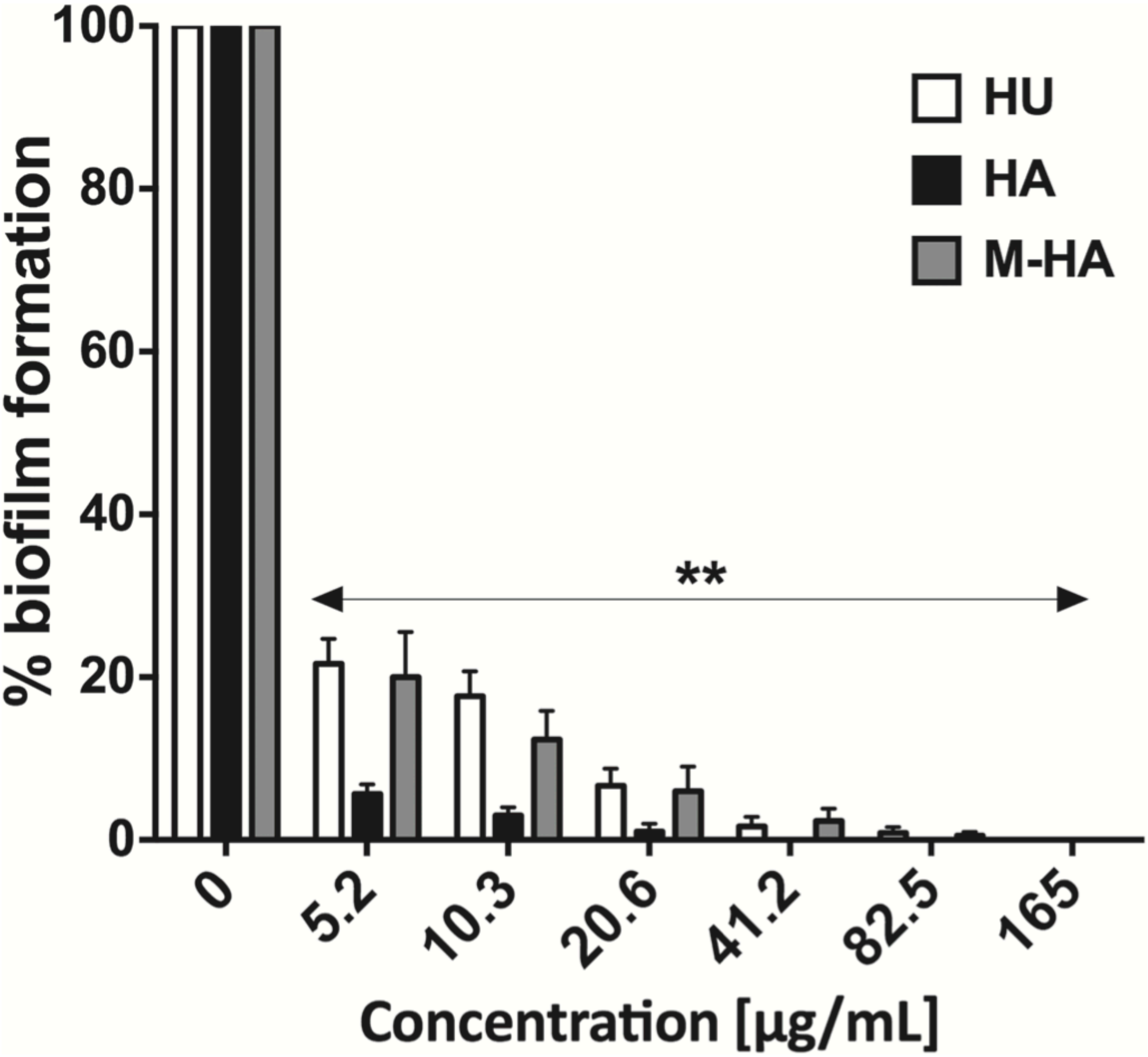

Fig 5. The inhibition of biofilm formation by different doses of HU, HA and M-HA. The biofilm formation of *P. aeruginosa* PAO1 was quantified as the absorbance of crystal violet stain (A_{570} nm) after being cultured for 24 h in 96-well plates in the presence and absence of the radical scavenger compounds. The values represent the percentages of biofilm biomass production. The results are expressed as the means ± SD of five replicates from one representative of three independent experiments. A Student's t-test was performed (**, $P < 0.01$; versus non-treated biofilms). HU, hydroxyurea; HA, hydroxylamine; and M-HA, methyl-hydroxylamine.

doi:10.1371/journal.pone.0122049.g005

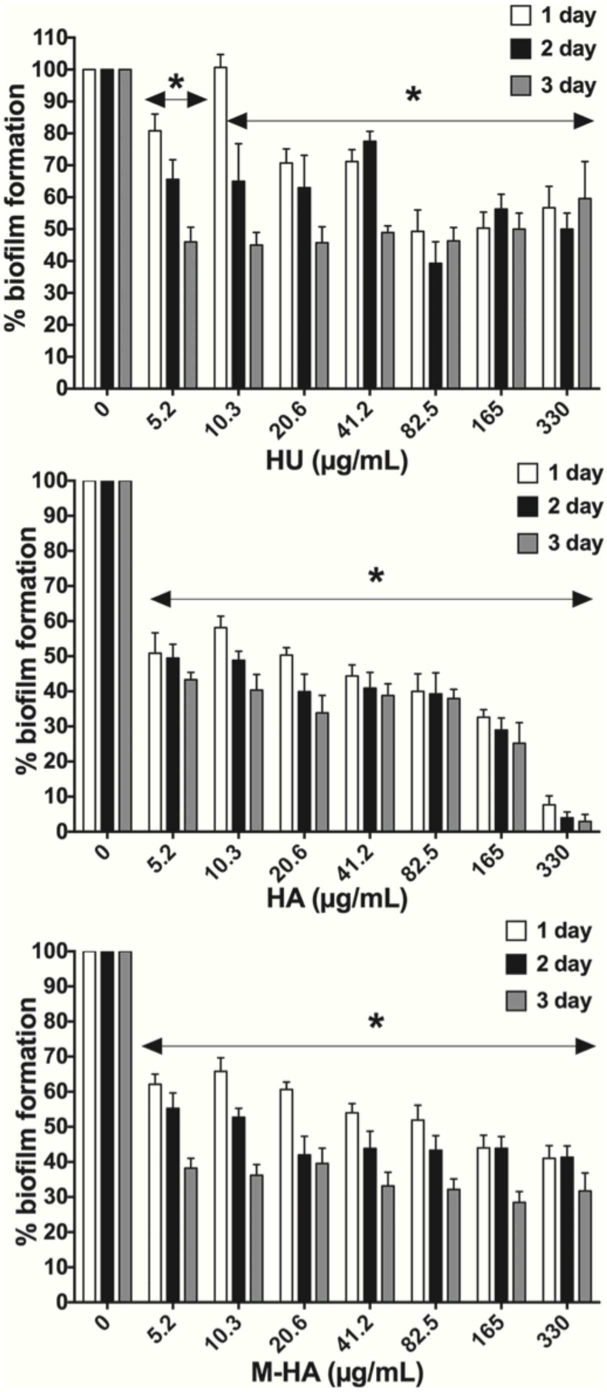

Fig 6. Disassembling the existing *P. aeruginosa* biofilms by adding HU, HA and M-HA. *P. aeruginosa* bacteria were allowed to form biofilms in peg plates for 24 h, the medium was removed and fresh medium with different concentrations of radical scavenger compounds were changed every 24 hours over three days (Days 1, 2 and 3). The percentage of biofilm biomass production is represented for each day. The results are

the means ± SD of three-five replicates from one representative of two independent experiments. A Student's t-test was performed (*, $P < 0.05$; versus non-treated biofilms). HU, hydroxyurea; HA, hydroxylamine; and M-HA, methyl- hydroxylamine.

doi:10.1371/journal.pone.0122049.g006

existing biofilm can be removed or disaggregated. Moreover, the highest biofilm reductions under M-HA treatment were found after three days of treatment, with 20% less remaining biofilm compared with the first day of treatment (Fig. 6). Further, confocal scanning laser microscopy of a biofilm grown in a flow cell chamber in the presence of the different radical scavengers showed significantly reduced biomass and average thickness of the treated samples (HA, HU and M-HA) compared to the untreated sample (Table 2 and Fig. 7).

Synergic effects on biofilm reduction by ciprofloxacin plus M-HA

The capacity to remove a pre-existing biofilm was evaluated when treating with ciprofloxacin in combination with M-HA. Ciprofloxacin alone showed a dose-dependent effect on *P. aeruginosa* biofilm reduction (Fig. 8). However, in comparison with treatments that employed ciprofloxacin alone, the combined use of ciprofloxacin and M-HA was more efficient for removing pre-existing biofilm, yielding 50% reduction values at ciprofloxacin concentrations of 0.016 or 0.008 μg/ml, and 6.6 or 86 μg/m of M-HA, respectively, was added. (for 5 to 8 times lower concentration than ciprofloxacin alone to have the same effect) (Fig. 8).

Discussion

The clinical use of RNR inhibitors has a history of several decades, and this history has demonstrated that RNR inhibitors have antitumor activity alone or in combination with other drugs [13, 18, 19]. Among RNR inhibitors, some radical scavenger compounds derived from hydroxylamines such as HU have been used for some types of cancer treatment [18]. Both HA and HU dramatically affect eukaryotic viability, and thus little interest has been aroused in studying these compounds as antimicrobial agents. It remains an important goal to develop a novel HA derivative with low toxicity and improved cytostatic action especially for treating bacterial infections. We previously demonstrated the capacity of the HA derivative M-HA in inhibiting RNR enzymatic activity in *B. anthracis* [11], although its potential as an antimicrobial drug has not been investigated. When exploring the role of M-HA in inhibiting the growth of a wide range of pathogenic Gram-positive or Gram-negative bacteria during a comparison of HA and HU, the intracellular bacterial growth and the formation of biofilms was evaluated.

Table 2. Biofilm parameters of wild-type *P. aeruginosa* treated with 40 μg/ml HA, HU and M-HA.

	Live cells (green)	
	Biomass ($\mu m^3/\mu m^2$)	**Averange thickness (μm)**
Untreated	28.9 ±4.7	40.2±3.5
HU (40 μg/ml)	11.9±4.5*	24.2±8.2*
HA (40 μg/ml)	10.7±3.2*	19.4±2.5*
M-HA (40 μg/ml)	20.5±5.9*	30.6±2.9*

Biomass values indicate the amount of living cells inside the biofilm. Values represent the mean ± SD of three independent experiments. Asterisk denotes significant differences compared to non-treated biofilm ($p<0.05$, Student's *t*-test).

doi:10.1371/journal.pone.0122049.t002

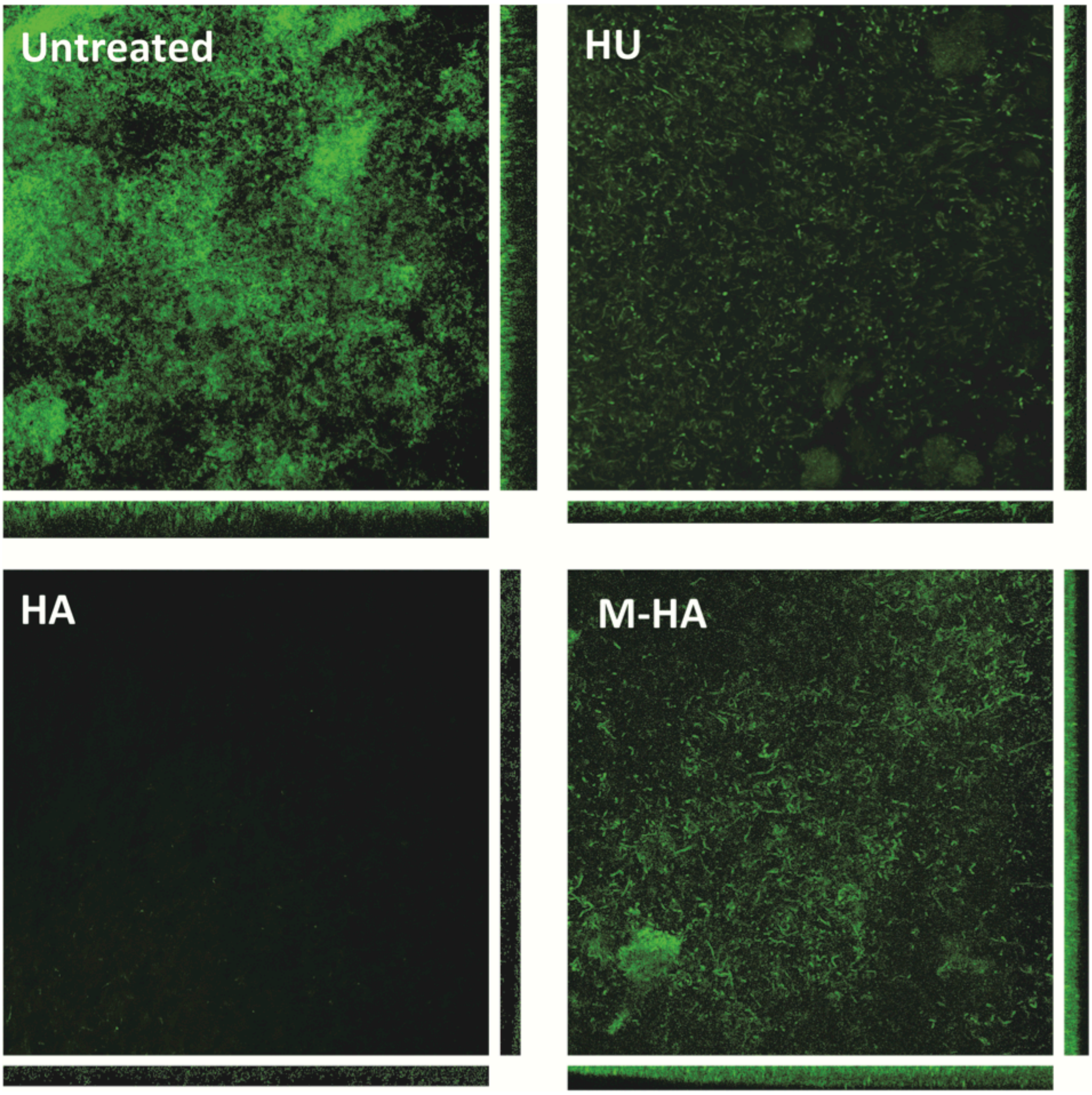

Fig 7. Confocal microscopy of *P. aeruginosa* biofilms grown on flow cell. The formed biofilms were treated for 24 h with HU, HA and M-HA at 40 μg/ml final concentration. Each panel shows the maximum Z-projection and the orthogonal views for each stack.

doi:10.1371/journal.pone.0122049.g007

Our results show that HA and M-HA are more efficacious that HU as antimicrobial agents for both Gram-positive and Gram-negative bacteria (Table 1). For instance, *P. aeruginosa* and *M. tuberculosis* use an iron containing class I RNR (class Ib) [26, 27] while *B. anthracis* clearly uses a manganese class I RNR (Class Ib) [28]. Our results suggest that M-HA is an active inhibitor for both iron and manganese forms of RNR.

When eukaryotic cytotoxicity was evaluated, HU and HA exerted high toxicity in murine macrophage cells (CC_{50} of 25.8 and 12.9 μg/ml, respectively) as expected (Fig. 2). Our results are consistent with previous results in which HU and resveratrol (a radical scavenger aromatic

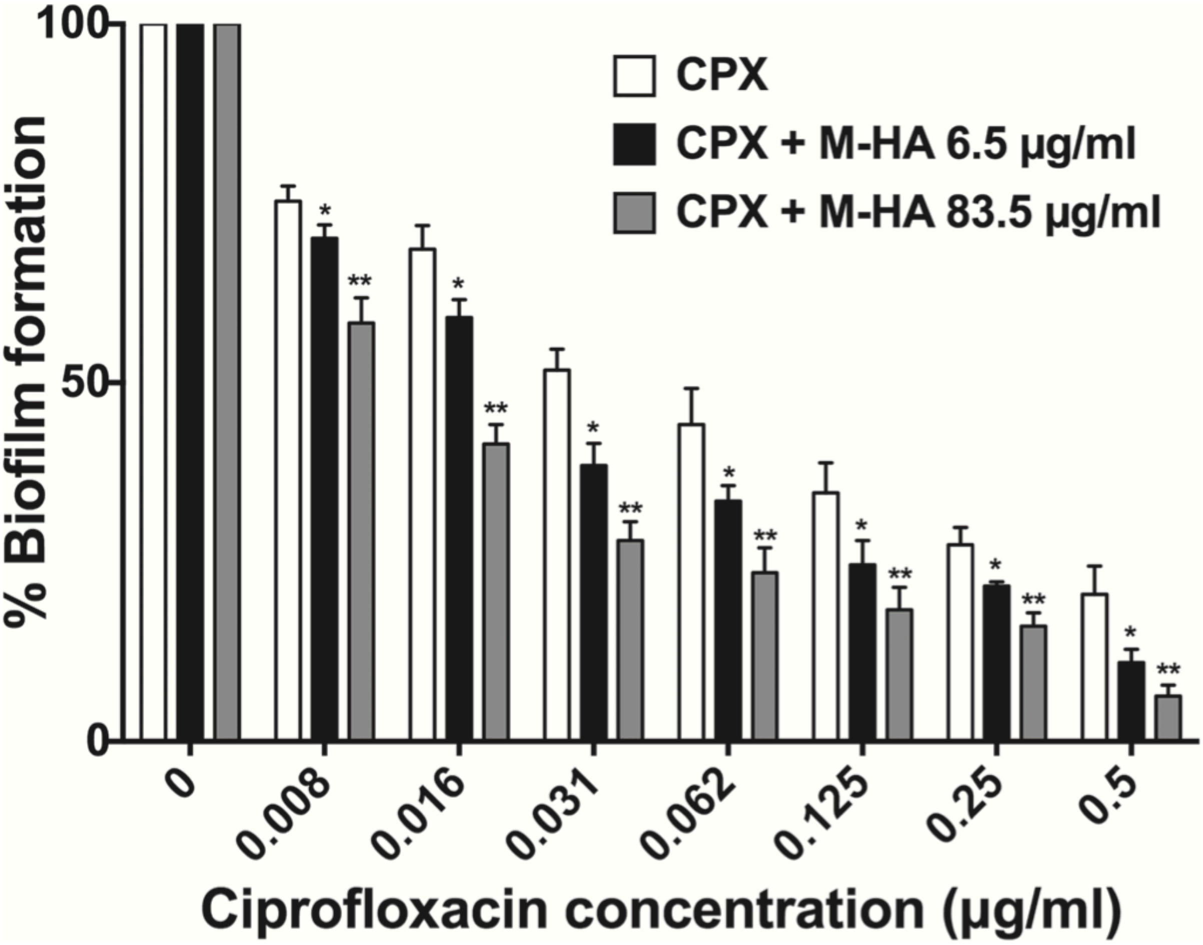

Fig 8. The synergistic effect of ciprofloxacin and M-HA on the reduction in *P. aeruginosa* biofilm formation. *P. aeruginosa* bacteria were allowed to form biofilms in peg plates for 24 h, the medium was removed and fresh medium with different concentrations of ciprofloxacin with/without M-HA were added. Biofilm formation (crystal violet stain) was evaluated 24 hours later. The biofilm biomass production percentage is represented here. The results are the means ± SD of three-five replicates from one representative of two independent experiments. A Student's t-test was performed (*, $P < 0.05$; **, $P < 0.005$ versus ciprofloxacin treated biofilms). CPX, ciprofloxacin; and M-HA, methyl-hydroxylamine.

doi:10.1371/journal.pone.0122049.g008

compound that is not derived from HA) were efficacious against pathogenic bacteria (*P. aeruginosa*, *Propionibacterium acnes*, *S. aureus*, and *Enterococcus faecalis*) but had high toxicity in eukaryotic cells as well [29, 30]. However, M-HA showed a highly reduced toxic effect on macrophage culture (CC_{50} of 351 µg/mL), corroborating the low toxicity of M-HA that was also found against human lung fibroblasts [31]. Thus, our first results confirm the promising role of M-HA as an antimicrobial agent.

Because of their small sizes, these compounds would easily cross the cell wall and membrane and exert their antimicrobial activity directly through RNR enzyme inhibition. In previous works, we determined that M-HA specifically inactivates the bacterial enzymatic activity of the essential RNR enzyme by quenching the tyrosyl radical that is necessary for enzymatic activation, thus making it unable to form dNTPs and blocking DNA synthesis [11]. The exact mode of M-HA is not completely understood, but some authors hypothesize that this molecule can interact directly in the places where the tyrosyl radical is formed because of its small size [32]. In terms of HU, which is a bigger molecule than M-HA, it seems that the interaction does not occur directly where the tyrosyl radical is generated but is more directed at interrupting the catalytic electron transfer pathway of the small subunit at the interface between the interaction between the small (α) and large RNR (β) subunits [33–35]. This finding could explain why M-HA was approximately several orders of magnitude more effective at inhibiting bacterial RNR than HU. Confirmation was established with the use of HA, the smallest HA, with the highest antimicrobial activity that also presents the highest toxicity because this molecule surely interacts with and can reach the tyrosyl radical site easily in both prokaryotic and eukaryotic RNR. Another issue is to understand the precise mechanism of action for the bacterial killing of radical scavengers after blocking the RNR enzyme. In *E. coli* [36] HU has been recently shown to cause increased superoxide production, and together with increased iron uptake, this increase fuels the formation of hydroxyl radicals that contribute to HU-induced cell death. Based on the HU analogy, we believe that the M-HA mode of action or bacterial killing might be similar.

Interestingly, M-HA has the highest therapeutic index for cytotoxicity (SI) for its inhibition of *M. bovis* BCG (182.6 μg/ml), which is 3.5 times that of *P. aeruginosa* (52.5 μg/ml). Because of the global relevance of these two agents, we should search for the possible role of M-HA in treating these agents.

To measure the potential growth inhibitory capacity of these compounds against mycobacteria, we selected BCG as a model in murine macrophages. Although there are significant differences between *M. tuberculosis* and BCG, they are closer genetically, and previous studies have demonstrated the validity of BCG for the in vitro evaluation of drug candidates against tuberculosis [37, 38]. In our case, a comparison of the BCG RNR primary protein structure showed 100% shared identity with that of the *M. tuberculosis* RNR protein, the causative agent of tuberculosis (see S1 Fig.). This finding indicates a possible identical mode of action for M-HA on the *M. tuberculosis* RNR. BCG intracellular kinetics in J774 macrophages has been very well characterized [25, 39]. Initially, J774 macrophages ingest mycobacteria and internalize BCG cells into phagosomes. An initial killing is observed during the first three days of infection, and then a stable level of viable BCG can be observed in J774 macrophages. Despite the fact that BCG does not grow as exponentially inside macrophages as *M. tuberculosis* does, BCG is continuously growing and being killed by macrophages [25]. This finding permits the use of this model for evaluating new drug candidates with the capacity to interfere in mycobacterial DNA synthesis.

Our results showed that up to 85% of mycobacterial growth inhibition by M-HA occurs at 72 hours post-infection (Fig. 3). In view of the impressive results obtained here, we aimed to go further in understanding the mechanism. As expected [40], our results showed that BCG-infected macrophages do not induce NO production. Treatment with HA-derivatives did not significantly modify these results. However, enhanced TNF-α production, which is another killing mechanism of macrophages, is observed in M-HA-treated macrophages. The increased production of TNF-α in BCG-infected M-HA-treated macrophages could be explained by different reasons. On the one hand, BCG-infected J774 macrophages release exosomes that contain mycobacterial antigens such as a 19 kDa antigen or phosphatidyl inositol mannosides known to induce pro-inflammatory cytokines such as TFN-α by exerting bystander effects on other cells [41]. The M-HA treatment could induce a higher production of these exosomes than non-treated macrophages. On the other hand, M-HA could directly induce TNF-α production in BCG-infected macrophages. Two reasons led us to support this last option. First, TNF-α production is observed as early as 24 hours post-infection (Fig. 4), whereas the exosome released from BCG-infected J774 macrophages is primarily detected between 48 and 72 hours post-infection [41]. Second, an M-HA dose-dependent response is observed in TNF-α production, leading us to favor the second hypothesis. The fact that TNF production levels in non-infected M-HA-treated macrophages were lower than those detected in M-HA-treated BCG-infected macrophages indicates that a BCG-infection must be related to the capacity of M-HA to induce TNF-α production, as was previously described for other drugs [42, 43]. Nevertheless, we cannot rule out other possible mechanisms, such as the influence of such radical scavengers in other routes related to cytokine production. Supporting this idea, significant IL-12 levels were only detected in BCG-infected HA-treated macrophages. Although in vitro and in vivo data indicated that HU or HA treatment triggers chemokines and/or cytokines production [44–48], the mechanism by which these compounds interfere with cytokine-mediated signaling is also unclear. TNF-α and IL-12 are critical cytokines in the control of mycobacterial infections [49]. Synergically with IFN-γ, the compounds activate naive macrophages, which in turn help to control mycobacteria growth. Previous studies demonstrated that TNF-α and IL-12 production is differently regulated in mycobacteria infected macrophages [50]. Thus, our results provide an initial step to further understand the possible role of cytokines production in BCG cell growth inhibition as mediated by these radical scavengers.

To our knowledge, this is the first report describing the use of a radical scavenger and more specifically the first to observe the M-HA effect on mycobacterial inhibition. Among infectious diseases, tuberculosis (TB) is the leading killer with over two million casualties annually worldwide. The WHO considers tuberculosis to the most dangerous chronic disease in the world. In recent years, the emergence and spread of resistant *M. tuberculosis* strains has fuelled the TB epidemic by making it more difficult to treat. These results make the M-HA a potentially valuable agent, and further analyses must be performed to test it in a combination therapy with existing, well-known antimycobacterial drugs.

Regarding *P. aeruginosa*, the primary point of interest is an evaluation of the capacity to reduce biofilm formation. Considering that biofilm formation protects bacteria during infections, such as in chronic wounds, hospital-related pneumonia and bacterial chronic lung infections [51], the inhibition of biofilm formation by M-HA is a critically important quality as a potential therapeutic, possibly more so than its anti-microbial activity. Bacterial biofilms generally become 10–1000 times more resistant to the effects of antimicrobial agents than planktonic cells [52].

We were able to demonstrate that M-HA is capable of inhibiting *P. aeruginosa* biofilm formation (for an approximately 60% reduction at 5.2 μg/mL on the third day of continuous treatment); this study compared favorably with other studies that employed different anti-biofilm strategies [53]. These results were corroborated by growing *P. aeruginosa* cells to form a continuous biofilm in flow cells and imaging by laser scanning confocal microscopy (Table 2 and Fig. 7). Moreover, the combination of M-HA with the well-known antibiotic ciprofloxacin increased the ability to reduce an existing biofilm 10–20 times better than ciprofloxacin or M-HA alone. Using new and existing antimicrobials may provide a new strategy for bacterial therapy. Drug combinations would decrease the likelihood of resistance [54]. This finding demonstrates the feasibility of combined chemotherapy with known antibiotics for combating multi-resistant bacteria infections.

The global emergence of antibiotic-resistant strains continues unabated, along with an overall increase in the number of infections worldwide, highlighting the urgent need for new agents to treat *Mycobacterium* and *Pseudomonas* infections. Non-conventional anti-infective approaches must be explored. Our findings may provide a new basis for the discovery of new and potent radical scavenger inhibitors and improved clinical applications of these compounds in antimicrobial therapy.

Supporting Information

S1 Fig. A sequence alignment of NrdFs from *M. tuberculosis* (Mtub NrdF2), *M. bovis* subs *bovis* (Mbbo), *M. bovis* BCG strain Pasteur (MboP), *Salmonella typhimurium* (Styp), *E. coli* (Ecol) and *B. anthracis* (Bant). Iron ligands (ligated iron ion) and tyrosyl radical-harboring residues are shown.
(TIF)

Author Contributions

Conceived and designed the experiments: EJ AB JG ET. Performed the experiments: EJ AB ET. Analyzed the data: EJ AB JG ET. Contributed reagents/materials/analysis tools: EJ AB ET. Wrote the paper: EJ AB JG ET.

References

1. Spellberg B, Guidos R, Gilbert D, Bradley J, Boucher HW, Scheld WM, et al. The epidemic of antibiotic-resistant infections: a call to action for the medical community from the Infectious Diseases Society of America. Clin Infect Dis. 2008; 46(2):155–64. doi: 10.1086/524891 PMID: 18171244
2. Payne DJ. Microbiology. Desperately seeking new antibiotics. Science. 2008; 321(5896):1644–5. doi: 10.1126/science.1164586 PMID: 18801989
3. May M. Drug development: Time for teamwork. Nature. 2014; 509(7498):S4–5. doi: 10.1038/509S4a PMID: 24784427
4. Torrents E, Sahlin M, Sjöberg B-M. The Ribonucleotide Reductase Family- Genetics and Genomics. In: Ribonucleotide Reductases (ed Andersson KK) Nova Science Publishers. 2008:pp. 17–77.
5. Nordlund P, Reichard P. Ribonucleotide reductases. Annu Rev Biochem. 2006; 75:681–706. PMID: 16756507
6. Hofer A, Crona M, Logan DT, Sjoberg BM. DNA building blocks: keeping control of manufacture. Crit Rev Biochem Mol Biol. 2012; 47(1):50–63. doi: 10.3109/10409238.2011.630372 PMID: 22050358
7. Cotruvo JA, Stubbe J. Class I ribonucleotide reductases: metallocofactor assembly and repair in vitro and in vivo. Annu Rev Biochem. 2011; 80:733–67. doi: 10.1146/annurev-biochem-061408-095817 PMID: 21456967
8. Torrents E. Ribonucleotide reductases: Essential Enzymes for bacterial life. Front Cell Infect Microbiol. 2014; 4:52. doi: 10.3389/fcimb.2014.00052 PMID: 24809024
9. Lundin D, Gribaldo S, Torrents E, Sjoberg BM, Poole AM. Ribonucleotide reduction—horizontal transfer of a required function spans all three domains. BMC Evol Biol. 2010; 10:383. doi: 10.1186/1471-2148-10-383 PMID: 21143941
10. Lundin D, Torrents E, Poole AM, Sjoberg BM. RNRdb, a curated database of the universal enzyme family ribonucleotide reductase, reveals a high level of misannotation in sequences deposited to Genbank. BMC Genomics. 2009; 10:589. doi: 10.1186/1471-2164-10-589 PMID: 19995434
11. Torrents E, Sahlin M, Biglino D, Graslund A, Sjoberg BM. Efficient growth inhibition of *Bacillus anthracis* by knocking out the ribonucleotide reductase tyrosyl radical. Proc Natl Acad Sci U S A. 2005; 102(50):17946–51. PMID: 16322104
12. Torrents E, Sjoberg BM. Antibacterial activity of radical scavengers against class Ib ribonucleotide reductase from *Bacillus anthracis*. Biol Chem. 2010; 391(2–3):229–34.
13. Cerqueira NM, Fernandes PA, Ramos MJ. Ribonucleotide reductase: a critical enzyme for cancer chemotherapy and antiviral agents. Recent patents on anti-cancer drug discovery. 2007; 2(1):11–29. PMID: 18221051
14. Shao J, Zhou B, Chu B, Yen Y. Ribonucleotide reductase inhibitors and future drug design. Current cancer drug targets. 2006; 6(5):409–31. PMID: 16918309.
15. Moorthy NS, Cerqueira NM, Ramos MJ, Fernandes PA. Development of ribonucleotide reductase inhibitors: a review on structure activity relationships. Mini reviews in medicinal chemistry. 2013; 13(13):1862–72. PMID: 24032510
16. Aye Y, Li M, Long MJ, Weiss RS. Ribonucleotide reductase and cancer: biological mechanisms and targeted therapies. Oncogene. 2014:In Press.

17. Lassmann G, Thelander L, Graslund A. EPR stopped-flow studies of the reaction of the tyrosyl radical of protein R2 from ribonucleotide reductase with hydroxyurea. Biochem Biophys Res Commun. 1992; 188(2):879–87. PMID: 1332707
18. Saban N, Bujak M. Hydroxyurea and hydroxamic acid derivatives as antitumor drugs. Cancer Chemother Pharmacol. 2009; 64(2):213–21. doi: 10.1007/s00280-009-0991-z PMID: 19350240
19. Basu A, Sinha BN. Radical scavengers as ribonucleotide reductase inhibitors. Curr Top Med Chem. 2012; 12(24):2827–42. PMID: 23368105
20. Secanella-Fandos S, Luquin M, Julian E. Connaught and Russian strains showed the highest direct antitumor effects of different Bacillus Calmette-Guerin substrains. The Journal of urology. 2013; 189 (2):711–8. doi: 10.1016/j.juro.2012.09.049 PMID: 22982433
21. Stepanovic S, Vukovic D, Hola V, Di Bonaventura G, Djukic S, Cirkovic I, et al. Quantification of biofilm in microtiter plates: overview of testing conditions and practical recommendations for assessment of biofilm production by *staphylococci*. APMIS. 2007; 115(8):891–9. PMID: 17696944
22. Tolker-Nielsen T, Sternberg C. Growing and analyzing biofilms in flow chambers. Current protocols in microbiology. 2011;Chapter 1:Unit 1B 2.
23. Heydorn A, Nielsen AT, Hentzer M, Sternberg C, Givskov M, Ersboll BK, et al. Quantification of biofilm structures by the novel computer program COMSTAT. Microbiology. 2000; 146 (Pt 10):2395–407. PMID: 11021916
24. Arko-Mensah J, Julian E, Singh M, Fernandez C. TLR2 but not TLR4 signalling is critically involved in the inhibition of IFN-gamma-induced killing of *mycobacteria* by murine macrophages. Scandinavian journal of immunology. 2007; 65(2):148–57. PMID: 17257219
25. Jordao L, Bleck CK, Mayorga L, Griffiths G, Anes E. On the killing of *mycobacteria* by macrophages. Cellular microbiology. 2008; 10(2):529–48. PMID: 17986264
26. Torrents E, Westman M, Sahlin M, Sjoberg BM. Ribonucleotide reductase modularity: Atypical duplication of the ATP-cone domain in *Pseudomonas aeruginosa*. J Biol Chem. 2006; 281(35):25287–96. PMID: 16829681
27. Hammerstad M, Rohr AK, Andersen NH, Graslund A, Hogbom M, Andersson KK. The class Ib ribonucleotide reductase from *Mycobacterium tuberculosis* has two active R2F subunits. Journal of biological inorganic chemistry: JBIC: a publication of the Society of Biological Inorganic Chemistry. 2014; 19 (6):893–902.
28. Crona M, Torrents E, Rohr AK, Hofer A, Furrer E, Tomter AB, et al. NrdH-redoxin protein mediates high enzyme activity in manganese-reconstituted ribonucleotide reductase from *Bacillus anthracis*. J Biol Chem. 2011; 286(38):33053–60. doi: 10.1074/jbc.M111.278119 PMID: 21832039
29. Docherty JJ, McEwen HA, Sweet TJ, Bailey E, Booth TD. Resveratrol inhibition of *Propionibacterium acnes*. J Antimicrob Chemother. 2007; 59(6):1182–4. PMID: 17449884
30. Chan MM. Antimicrobial effect of resveratrol on dermatophytes and bacterial pathogens of the skin. Biochem Pharmacol. 2002; 63(2):99–104. PMID: 11841782
31. Atamna H, Paler-Martinez A, Ames BN. N-t-butyl hydroxylamine, a hydrolysis product of alpha-phenyl-N-t-butyl nitrone, is more potent in delaying senescence in human lung fibroblasts. J Biol Chem. 2000; 275(10):6741–8. PMID: 10702229
32. Gerez C, Fontecave M. Reduction of the small subunit of *Escherichia coli* ribonucleotide reductase by hydrazines and hydroxylamines. Biochemistry. 1992; 31(3):780–6. PMID: 1310046
33. Luo J, Graslund A. Ribonucleotide reductase inhibition by p-alkoxyphenols studied by molecular docking and molecular dynamics simulations. Archives of biochemistry and biophysics. 2011; 516(1):29–34. doi: 10.1016/j.abb.2011.09.003 PMID: 21951815
34. Ekberg M, Sahlin M, Eriksson M, Sjoberg BM. Two conserved tyrosine residues in protein R1 participate in an intermolecular electron transfer in ribonucleotide reductase. J Biol Chem. 1996; 271 (34):20655–9. PMID: 8702814
35. Stubbe J, Nocera DG, Yee CS, Chang MC. Radical initiation in the class I ribonucleotide reductase: long-range proton-coupled electron transfer? Chemical reviews. 2003; 103(6):2167–201. PMID: 12797828
36. Davies BW, Kohanski MA, Simmons LA, Winkler JA, Collins JJ, Walker GC. Hydroxyurea induces hydroxyl radical-mediated cell death in *Escherichia coli*. Mol Cell. 2009; 36(5):845–60. doi: 10.1016/j.molcel.2009.11.024 PMID: 20005847
37. Altaf M, Miller CH, Bellows DS, O'Toole R. Evaluation of the *Mycobacterium smegmatis* and BCG models for the discovery of *Mycobacterium tuberculosis* inhibitors. Tuberculosis. 2010; 90(6):333–7. doi: 10.1016/j.tube.2010.09.002 PMID: 20933470

38. Stanley SA, Barczak AK, Silvis MR, Luo SS, Sogi K, Vokes M, et al. Identification of host-targeted small molecules that restrict intracellular *Mycobacterium tuberculosis* growth. PLoS Pathog. 2014; 10(2): e1003946. doi: 10.1371/journal.ppat.1003946 PMID: 24586159
39. Anes E, Peyron P, Staali L, Jordao L, Gutierrez MG, Kress H, et al. Dynamic life and death interactions between *Mycobacterium smegmatis* and J774 macrophages. Cellular microbiology. 2006; 8(6):939–60. PMID: 16681836
40. Peteroy-Kelly M, Venketaraman V, Connell ND. Effects of *Mycobacterium bovis* BCG infection on regulation of L-arginine uptake and synthesis of reactive nitrogen intermediates in J774.1 murine macrophages. Infect Immun. 2001; 69(9):5823–31. PMID: 11500460
41. Bhatnagar S, Shinagawa K, Castellino FJ, Schorey JS. Exosomes released from macrophages infected with intracellular pathogens stimulate a proinflammatory response in vitro and in vivo. Blood. 2007; 110(9):3234–44. PMID: 17666571
42. Mendez S, Traslavina R, Hinchman M, Huang L, Green P, Cynamon MH, et al. The antituberculosis drug pyrazinamide affects the course of cutaneous leishmaniasis in vivo and increases activation of macrophages and dendritic cells. Antimicrob Agents Chemother. 2009; 53(12):5114–21. doi: 10.1128/AAC.01146-09 PMID: 19770283
43. Cui W, Lei MG, Silverstein R, Morrison DC. Differential modulation of the induction of inflammatory mediators by antibiotics in mouse macrophages in response to viable Gram-positive and Gram-negative bacteria. Journal of endotoxin research. 2003; 9(4):225–36. PMID: 12935353
44. Trifilieff A, Fujitani Y, Mentz F, Dugas B, Fuentes M, Bertrand C. Inducible nitric oxide synthase inhibitors suppress airway inflammation in mice through down-regulation of chemokine expression. J Immunol. 2000; 165(3):1526–33. PMID: 10903760
45. Lanaro C, Franco-Penteado CF, Albuqueque DM, Saad ST, Conran N, Costa FF. Altered levels of cytokines and inflammatory mediators in plasma and leukocytes of sickle cell anemia patients and effects of hydroxyurea therapy. Journal of leukocyte biology. 2009; 85(2):235–42. doi: 10.1189/jlb.0708445 PMID: 19004988
46. Navarra P, Grohmann U, Nocentini G, Tringali G, Puccetti P, Riccardi C, et al. Hydroxyurea induces the gene expression and synthesis of proinflammatory cytokines in vivo. The Journal of pharmacology and experimental therapeutics. 1997; 280(1):477–82. PMID: 8996231
47. Navarra P, Tringali G, Fabricio AS, Proietti A, Vairano M, Pozzoli G, et al. Hydroxyurea induces vasopressin release and cytokine gene expression in the rat hypothalamus. Journal of neuroimmunology. 2006; 179(1–2):94–100. PMID: 16934875
48. Weinberg A. In vitro hydroxyurea decreases Th1 cell-mediated immunity. Clinical and diagnostic laboratory immunology. 2001; 8(4):702–5. PMID: 11427414
49. Dorhoi A, Kaufmann SH. Tumor necrosis factor alpha in mycobacterial infection. Seminars in immunology. 2014; 26(3):203–9. doi: 10.1016/j.smim.2014.04.003 PMID: 24819298
50. Wang J, Wakeham J, Harkness R, Xing Z. Macrophages are a significant source of type 1 cytokines during mycobacterial infection. The Journal of clinical investigation. 1999; 103(7):1023–9. PMID: 10194475
51. Hassett DJ, Korfhagen TR, Irvin RT, Schurr MJ, Sauer K, Lau GW, et al. *Pseudomonas aeruginosa* biofilm infections in cystic fibrosis: insights into pathogenic processes and treatment strategies. Expert opinion on therapeutic targets. 2010; 14(2):117–30. doi: 10.1517/14728220903454988 PMID: 20055712
52. Smith AW. Biofilms and antibiotic therapy: is there a role for combating bacterial resistance by the use of novel drug delivery systems? Advanced drug delivery reviews. 2005; 57(10):1539–50. PMID: 15950314
53. Overhage J, Campisano A, Bains M, Torfs EC, Rehm BH, Hancock RE. Human host defense peptide LL-37 prevents bacterial biofilm formation. Infect Immun. 2008; 76(9):4176–82. doi: 10.1128/IAI.00318-08 PMID: 18591225
54. Tamma PD, Cosgrove SE, Maragakis LL. Combination therapy for treatment of infections with gram-negative bacteria. Clinical microbiology reviews. 2012; 25(3):450–70. doi: 10.1128/CMR.05041-11 PMID: 22763634

Supporting Information

S1 FIg. Sequence alignment of NrdFs from *Mycobacterium tuberculosis* (Mtub), *M. bovis* supsp. *bovis* (Mbb), *M. bovis* BCG strain Pasteur (MBCG), *Salmonella typhimurium* (Styp), *E. coli* (Ecol), *S. mutans* (Smut), *S. sanguinis* (Ssan), *S. aureus* (Saur), and *B. anthracis* (Bant).

Iron liga

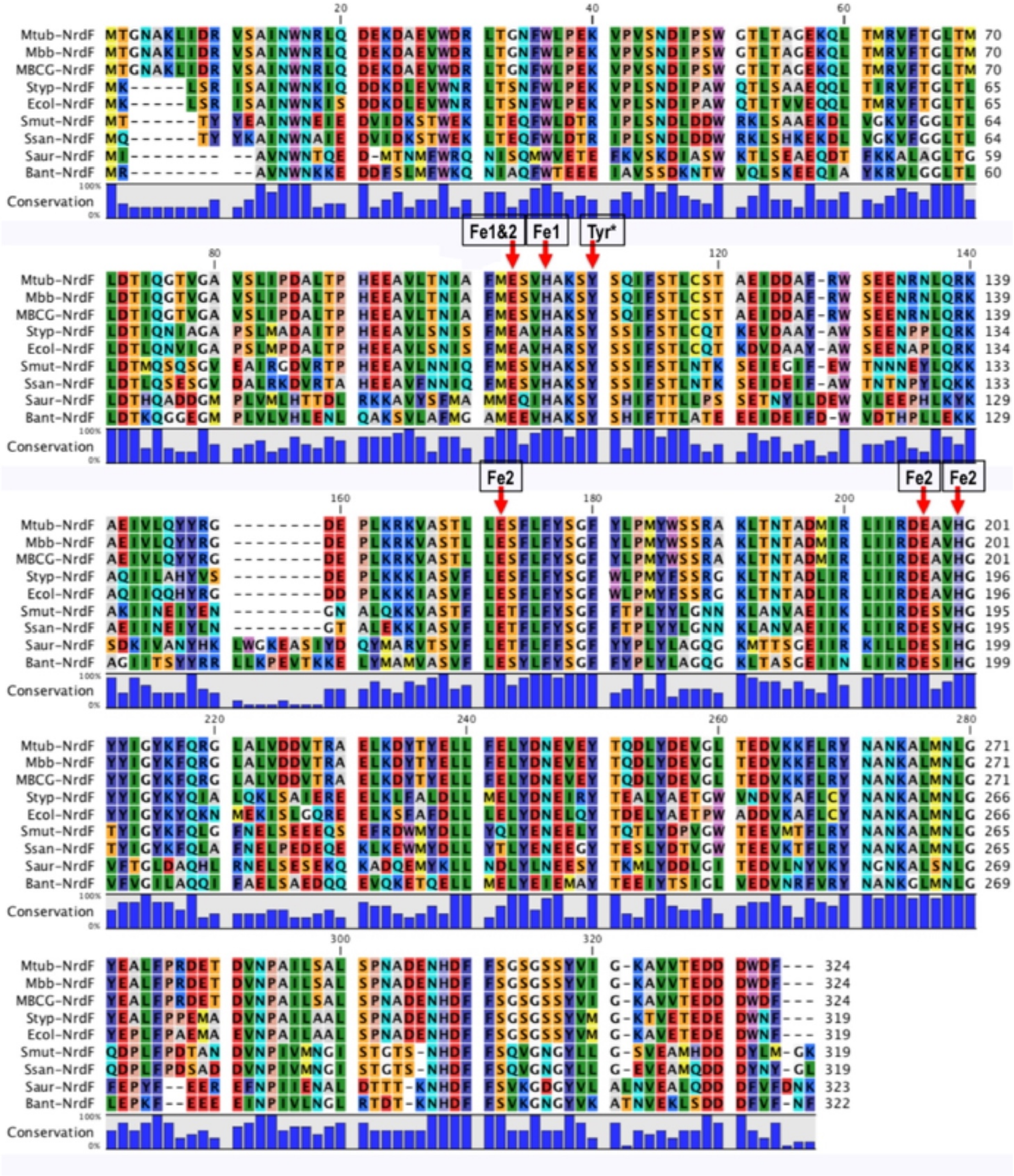
Mtub-NrdF
Mbb-NrdF
MBCG-NrdF
Styp-NrdF
Ecol-NrdF
Smut-NrdF
Ssan-NrdF
Saur-NrdF
Bant-NrdF
Conservation
100%
0%
Fe1&2
Fe1
Tyr*
Fe2
Fe2
Fe2

PUBLICATION 2: Hydroxylamine Derivatives as a New Paradigm in the Search of Antibacterial Agents

ABSTRACT: Serious infections caused by bacteria that are resistant to commonly used antibiotics have become a major global healthcare problem in the 21st century. Multidrug-resistant bacteria causing severe infections mainly grow in complex bacterial communities known as biofilms, in which bacterial resistance to antibacterial agents and to the host immune system is strengthened. As drug resistance is becoming a threatening problem, it is necessary to develop new antimicrobial agents with novel mechanisms of action. Here, we designed and synthesized a small library of *N*-substituted hydroxylamine (N-HA) compounds with antibacterial activity. These compounds, acting as radical scavengers, inhibit the bacterial ribonucleotide reductase (RNR) enzyme. RNR enzyme is essential for bacterial proliferation during infection, as it provides the building blocks for DNA synthesis and repair. We demonstrate the broad antimicrobial effect of several drug candidates against a variety of Gram-positive and Gram-negative bacteria, together with low toxicity toward eukaryotic cells. Furthermore, the most promising compounds can reduce the biomass of an established biofilm on *Pseudomonas aeruginosa*, *Staphylococcus aureus*, and *Escherichia coli*. This study settles the starting point to develop new *N*-hydroxylamine compounds as potential effective antibacterial agents to fight against drug-resistant pathogenic bacteria.

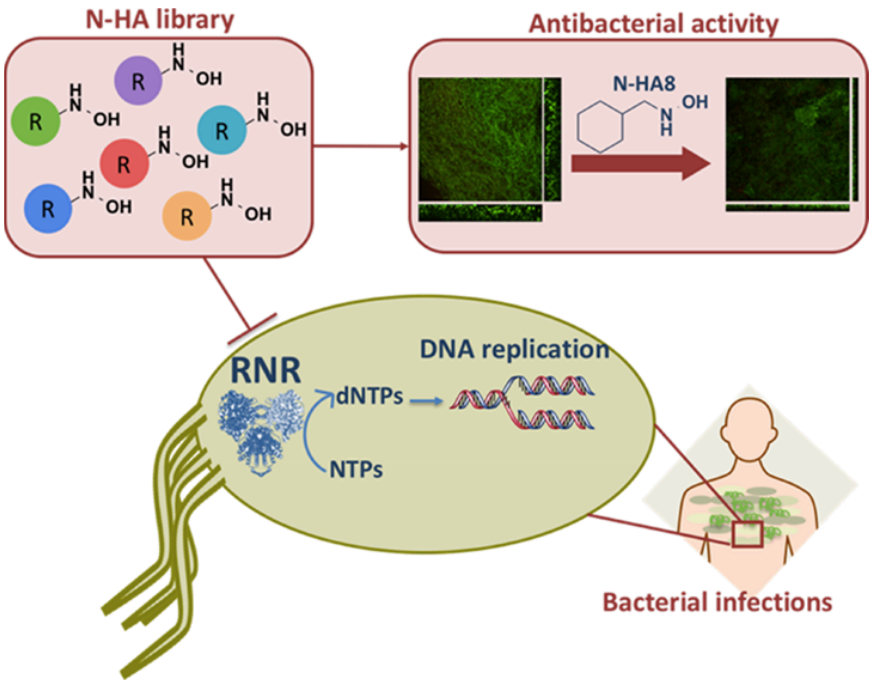

This is an open access article published under an ACS AuthorChoice License, which permits copying and redistribution of the article or any adaptations for non-commercial purposes.

ACS OMEGA
Article
Cite This: ACS Omega 2018, 3, 17057−17069
http://pubs.acs.org/journal/acsodf

Downloaded via 84.88.200.54 on January 20, 2020 at 11:39:32 (UTC).
See https://pubs.acs.org/sharingguidelines for options on how to legitimately share published articles.

Hydroxylamine Derivatives as a New Paradigm in the Search of Antibacterial Agents

Laia Miret-Casals,[†,#] Aida Baelo,[‡,#] Esther Julián,[§] Josep Astola,[‡] Ariadna Lobo-Ruiz,[†]
Fernando Albericio,*[,†,∥,⊥] and Eduard Torrents*[,‡]

[†]Department of Organic Chemistry, University of Barcelona, C/ Martí i Franquès, 1-11, 08028 Barcelona, Spain
[‡]Bacterial Infections: Antimicrobial Therapies, Institute for Bioengineering of Catalonia (IBEC), The Barcelona Institute of Science and Technology, Baldiri Reixac, 15-21, 08028 Barcelona, Spain
[§]Group of Mycobacteriology, Department of Genetics and Microbiology, Facultat de Biociències Universitat Autònoma de Barcelona, Building C, 08193 Bellaterra, Barcelona, Spain
[∥]CIBER-BBN, Networking Centre on Bioengineering, Biomaterials and Nanomedicine, C/ Martí i Franquès, 1-11, 08028 Barcelona, Spain
[⊥]School of Chemistry & Physics, University of Kwazulu-Natal, Private Bag X01, Scottsville, Pietermaritzburg 3209, South Africa

S *Supporting Information*

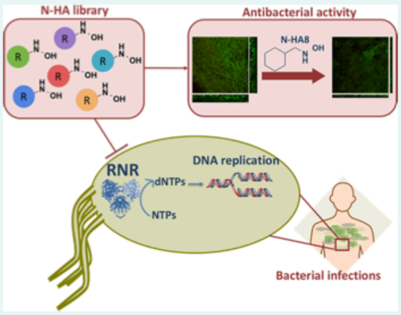

ABSTRACT: Serious infections caused by bacteria that are resistant to commonly used antibiotics have become a major global healthcare problem in the 21st century. Multidrug-resistant bacteria causing severe infections mainly grow in complex bacterial communities known as biofilms, in which bacterial resistance to antibacterial agents and to the host immune system is strengthened. As drug resistance is becoming a threatening problem, it is necessary to develop new antimicrobial agents with novel mechanisms of action. Here, we designed and synthesized a small library of *N*-substituted hydroxylamine (N-HA) compounds with antibacterial activity. These compounds, acting as radical scavengers, inhibit the bacterial ribonucleotide reductase (RNR) enzyme. RNR enzyme is essential for bacterial proliferation during infection, as it provides the building blocks for DNA synthesis and repair. We demonstrate the broad antimicrobial effect of several drug candidates against a variety of Gram-positive and Gram-negative bacteria, together with low toxicity toward eukaryotic cells. Furthermore, the most promising compounds can reduce the biomass of an established biofilm on *Pseudomonas aeruginosa*, *Staphylococcus aureus*, and *Escherichia coli*. This study settles the starting point to develop new *N*-hydroxylamine compounds as potential effective antibacterial agents to fight against drug-resistant pathogenic bacteria.

■ INTRODUCTION

Ever since antibiotics were introduced worldwide, bacterial pathogens have been developing resistance, which reduces drastically or eliminates their effectiveness. The emergence of drug-resistant bacteria is a growing challenge to anti-infective therapy. Worldwide bacteria species that have acquired multiple drug resistance and escaped the effects from our current antimicrobial drugs include different important bacterial pathogens.[1] Several bacterial pathogens such as methicillin- and vancomycin-resistant *Staphylococcus aureus* (MRSA and VRSA) or multidrug resistant *Pseudomonas aeruginosa* are resistant to almost all clinically available antibacterial drugs.[2] Moreover, recent estimates suggest that bacterial biofilms account for over 80% of microbial infections in the human body.[3,4] Bacterial biofilms are dense aggregates of cell−cell surface-attached microorganisms encased in a self-synthesized hydrated extracellular polymeric substances matrix.[5] Bacterial pathogens living in biofilms are hard to eradicate because of different strategies that involve restricted penetration of antimicrobials, resistance to the immune system, differential physiological activity with slow metabolism, the presence of phenotypic variants and persisters, efflux systems, and enhanced repair systems.[6,7]

The lack of new antibiotics in the drug development pipeline, especially those with new modes of action and active against bacteria, worsens the situation. In this context, the search of new antimicrobials acting on new targets is a critical challenge. Searching for new compounds or strategies to decrease bacterial biofilm formation and avoid antibiotic resistance is a critical stage essential for the treatment of biofilm-associated diseases.[8]

Received: June 19, 2018
Accepted: November 28, 2018
Published: December 11, 2018

ACS Publications © 2018 American Chemical Society

DOI: 10.1021/acsomega.8b01384
ACS Omega 2018, 3, 17057−17069

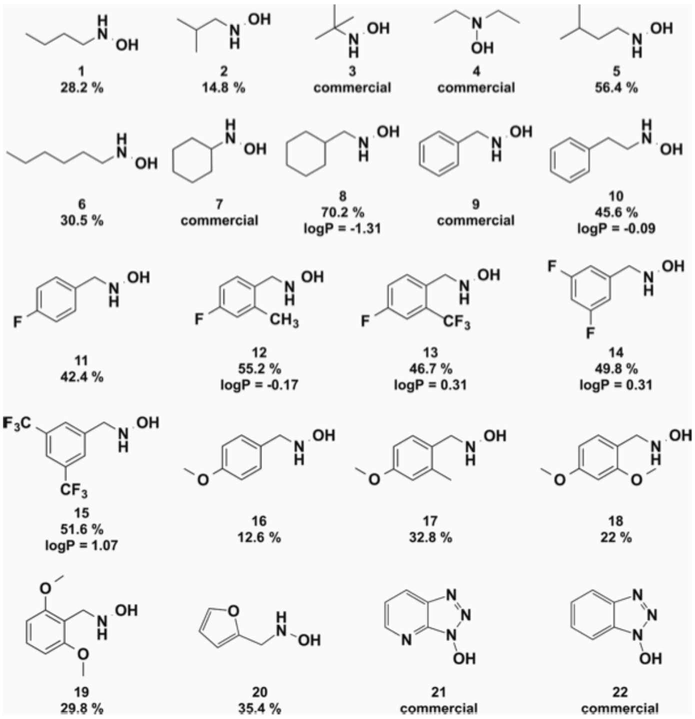

Figure 1. Library of N-HAs. Chemical structures of the N-HA compounds, designed to target the bacterial RNR enzyme, are shown. The synthesis yield obtained for each compound is shown in %, with the exception of the compounds acquired commercially. Log *P* values of representative candidates are indicated.

Ribonucleotide reductase (RNR) enzyme has shown to be an antimicrobial drug target for the treatment of several infections.[9] RNR exclusively supplies the nucleotide precursors for DNA synthesis and repair by catalyzing the reduction of ribonucleotides (NTPs) to their corresponding deoxyribonucleotides (dNTPs) via radical chemistry. Modulation of RNR activity is a rate-limiting step in DNA synthesis. Therefore, inactivation of RNR activity ceases DNA synthesis and, consequently, inhibits cell proliferation. Thus, RNR is essential for all bacteria causing both acute and biofilm infection, as they need to multiply and replicate its genome within the host and, therefore, need a constant supply of the four different dNTPs for the synthesis of the new DNA.

Up to date, three different main RNR classes are described (class I, II, and III), differing in their cofactor requirements and quaternary structures.[9−12] Class I RNR is additionally subdivided into class Ia, class Ib, and class Ic, depending on the metal type of the metallocofactor of the enzyme. Class I RNRs are tetrameric ($\alpha_2\beta_2$) enzymes, composed of two homodimeric proteins: R1 (α_2), which contains the catalytic domain (active site) and the complex allosteric domain (responsible for the regulation of the enzyme), and R2 (β_2), which carries a stable tyrosyl radical and an oxygen-linked diiron center required for free-radical production. Once the radical has been generated, an electron transfer takes place between β_2 and α_2 subunits to catalyze the reduction of NTPs to their corresponding dNTPs.

Although both bacteria and eukaryotic cells codify for RNR, there are remarkable differences between them, as the sequence similarity between them is quite low,[13] and hence, specific inhibitors can potentially be designed to differentially target bacterial RNRs. In addition, eukaryotic cells only encode for one RNR class (class Ia), whereas bacterial species can encode simultaneously for different RNR classes, thus making bacterial RNR system an attractive target for antibacterial therapies.

Numerous and diverse RNR inhibitors have been described during the last decades, including different inhibitor families such as free-radical scavengers, iron chelators, and substrate analogues, among others.[14−18] Radical scavenger compounds are well known to inhibit RNR by quenching an essential tyrosyl free radical, located in the small class I subunit,[19,20] which is required to generate the reduction power in the catalytic subunit of the enzyme. Several radical scavenger molecules, such as hydroxyurea (HU), didox, trimidox, and hydroxyguanidine, have been shown to be useful for the treatment of different cancer diseases.[16] One of these compounds, hydroxyurea, was used for general cancer treatment and is commonly used nowadays for the treatment of some specific ones.[21,22] Although these compounds inhibit bacterial replication inhibiting bacterial RNR, they cannot be used to treat bacterial infections because of the high toxicity toward eukaryotic cells. Recently, we have identified "NH−OH" moiety as an important radical scavenger family by itself. *N*-Methylhydroxylamine (M-HA) is a compound with a high capacity to specifically inhibit the *Bacillus anthracis* RNR without interfering the activity of eukaryotic RNR, thus being nontoxic.[19,20] We have also proven the antibacterial capacity of this radical scavenger on *Pseudomonas* and *Mycobacterium* infections.[23] This discovery opens new horizons in the development, identification, and investigation of the use of *N*-substituted hydroxylamine (N-HA) compounds as specific antimicrobial RNR inhibitors.

RESULTS

Design and Synthesis of the N-HA Library. We previously described the antibacterial activity of M-HA, a radical scavenger compound that specifically targets bacterial RNR without interfering the host enzyme.[19,23] It is known that low-molecular-weight compounds, such as M-HA, might have effects on structurally unrelated proteins. For this reason, we designed and synthesized a small library of N-HA compounds with different structures to better cover the chemical space and gain more selectivity (Figure 1) to directly target the bacterial class I RNR enzyme (class Ia and class Ib), acting as an antibacterial agent.

The N-HA library was generated to identify novel drugs with high free-radical scavenging (FRS) activity against RNR enzymes. As the FRS activity is based on the ability of the molecule to donate a hydrogen ion to a free radical, FRS activity of N-HAs will depend on the homolytic bond dissociation enthalpies (BDEs) of the O−H bond of hydroxylamines. It has been predicted by computational methods that the resonance and the inductive effects are important in the BDEs of the O−H bond of *N*-monosubstituted hydroxylamines. Thus, the design of N-HA with electron-donating inductive effects and resonance effects makes the corresponding *N*-oxyl species more electron-rich and more stable radicals, leading to a BDE decrease[24,25] and thus resulting in a higher FRS activity. Otherwise, the presence of electron-withdrawing groups or no resonance effects will generate an opposite effect, destabilizing the produced radicals, increasing BDE, and consequently, decreasing FRS activity.

The synthesis of N-HA products was accomplished by reductive amination of aldehydes, as described before[26] with some variations, by a general one-pot synthesis that involves the conversion of a carbonyl group to the hydroxylamine via the corresponding *N*-hydroxyimine (Scheme 1).

Scheme 1. General Synthetic Scheme for the Synthesis of the *N*-Hydroxylamine Compounds

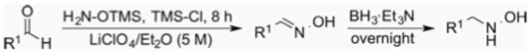

Initially, *N*-alkyl hydroxylamine isomers of four carbon atoms, including a secondary hydroxylamine and additional analogues, increasing the alkyl chain length to increase the electron-donating inductive effect to stabilize the generated radical, were synthesized or purchased (**1**−**6**). Moreover, *N*-cycloalkyl hydroxylamine derivatives were incorporated to the library (**7** and **8**) to elucidate the importance of linear and cyclic aliphatic structures in the stabilization of hydroxylamine's radicals. Replacement of the aliphatic moiety in *N*-hydroxylamine compounds by an aromatic ring, such as benzyl or homobenzyl group, was also explored to increase FRS activity due to delocalization of the free radical throughout the aromatic ring structure (**9** and **10**). To further study if radical stabilization by resonance effects can be affected by inductive effects, *N*-hydroxylamine compounds with electron-withdrawing substituents in the aromatic ring, such as fluorine and trifluoromethyl (**11**−**15**), were synthesized. In addition, the library was further extended with a series of *N*-hydroxylamine compounds with electron-donating substituents in the aromatic ring, such as methyl and methoxy (**16**−**19**). Finally, *N*-hydroxylamines containing a heteroaryl group or being part of the heterocycle as secondary hydroxylamines were also synthesized or purchased, respectively (**20**−**22**), to study the ability of heteroaromatics in stabilizing *N*-oxyl species.

Identification of New *N*-Hydroxylamines (N-HAs) with Antimicrobial Activity against Both Gram-Positive and Gram-Negative Bacteria. In the antibacterial activity screening of the newly synthesized N-HAs, compounds were tested against four Gram-positive (*B. anthracis*, *Staph. aureus*, *Staphylococcus epidermidis*, and *Enterococcus faecalis*) and two Gram-negative (*P. aeruginosa* and *Escherichia coli*) clinically relevant bacterial strains, and their minimum inhibitory concentrations (MICs) were determined (Table 1). As a reference, an importantly used antibiotic, ciprofloxacin (CIP), was also tested. As shown in Table 1, we also included the M-HA and HU antibacterial and cytotoxicity values to compare them with the new data.

Some of the compounds (**1**−**5**, **7**, **9**, **13**, **16**, and **19**−**22**) showed no antibacterial activity in any bacteria tested (MIC_{50} > 1000 μg/mL) (data not shown). In general, Gram-positive bacteria species (encoding class Ib RNR) were more sensitive to **6**, **8**, **10**, **11**, **15**, **17**, and **18**. In particular, compounds **11** and **17** with an MIC_{50} value of <15 μg/mL showed higher activity compared to M-HA against *B. anthracis*. Compounds **11** and **15** showed also high antimicrobial activity against both *Staph. aureus* and *Staph. epidermidis* with an MIC_{50} value of <60 μg/mL compared to M-HA and HU. Compound **18** also showed antibacterial activity against *Staph. epidermidis* with an MIC_{50} value of <40 μg/mL. Compounds **14** and **17** showed antimicrobial activity against *E. faecalis* with an MIC_{50} value of <80 μg/mL.

Gram-negative bacterial species exhibited high resistance to most of the compounds. Compound **8**, showing values similar to M-HA, was the most active, highly inhibiting the growth of *P. aeruginosa* with an MIC_{50} value lower than 17 μg/mL and that of *E. coli* with an MIC_{50} value lower than 60 μg/mL. Compound **12** also resulted in high antimicrobial activity against *P. aeruginosa* (MIC_{50} < 70 μg/mL), and compound **15** was also effective against *E. coli* (MIC_{50} < 60 μg/mL).

None of the *N*-hydroxylamine derivatives containing linear alkyl groups with less than six carbon atoms were active against any bacterial species tested, despite the fact that M-HA is active with one carbon atom.

These results indicate that inductive effects generated by linear alkyl groups with less than six carbon atoms are insufficient to stabilize *N*-oxyl species, except for the case of M-HA. Compound **6**, a linear aliphatic *N*-hydroxylamine with six carbon atoms, and compound **8**, a cyclic aliphatic hydroxylamine with seven atom carbons, exhibited antimicrobial activity against Gram-positive and Gram-negative bacteria, respectively. *N*-Homobenzylhydroxylamine (**10**) and some *N*-benzylhydroxylamine analogues with substituents in the aromatic ring (**11**, **12**, **14**, **15**, **17**, and **18**) exhibited higher antimicrobial activity compared to the aliphatic *N*-hydroxylamines. These results might indicate that conjugate rings lead to stable spin delocalized systems, providing stabilizing effects for *N*-oxyl species radicals generated by reduction of the tyrosyl radical of the RNR enzyme. This fact highlights the importance of the resonance effects compared to the inductive effects in the stabilization of radicals. Furthermore, the effect of the delocalization of the free radical throughout the aromatic

DOI: 10.1021/acsomega.8b01384
ACS Omega 2018, 3, 17057−17069

Table 1. Antibacterial and Cytotoxic Activities of the N-HA Compounds

	MIC_{50} (μg/mL)[a]						
	Gram-positive[b]				Gram-negative[c]		
compound	*Bant*	*Saur*	*Sepi*	*Efae*	*Paer*	*Ecol*	CC_{50} (μg/mL)
6	55 (**8.5**)	(-)	(-)	(-)	(-)	(-)	468 ± 7.64
8	60 (3)	60 (3)	60 (3)	120 (1.5)	17 (**10.5**)	60 (3)	178 ± 12.4
10	65 (4)	65 (4)	65 (4)	(-)	125 (2)	125 (2)	259 ± 9.50
11	15 (**21.3**)	60 (**5.3**)	30 (**10.6**)	125 (2.6)	(-)	(-)	320 ± 5.03
12	(-)	(-)	70 (1.9)	(-)	70 (1.9)	(-)	131 ± 21.9
14	(-)	150 (1.2)	(-)	70 (2.4)	150 (1.2)	(-)	168 ± 13.5
15	32 (**21.2**)	60 (**11.4**)	60 (**11.4**)	(-)	(-)	60 (**11.4**)	686 ± 45.4
17	8 (**45.2**)	(-)	80 (4.5)	80 (4.5)	(-)	(-)	362 ± 20.4
18	40 (**45**)	175 (2.4)	40 (**10.4**)	175 (2.4)	(-)	(-)	415 ± 29.5
HU	(-)	280 (0.1)	295 (0.1)	90 (0.33)	15 (2)	240 (0.1)	30 ± 3.4
M-HA	22 (**14.5**)	70 (4.6)	75 (4.2)	45 (**7.1**)	20 (**16**)	40 (**8**)	320 ± 20.4
CIP	0.5 (**2600**)	0.5 (**2600**)	0.5 (**2600**)	0.5 (**2600**)	0.25 (**5100**)	0.25 (**5100**)	1324 ± 49.3

[a] The MIC_{50} values (μg/mL) measured after 8 h of N-HA compounds compared to HU, M-HA, and CIP (used as the positive control) are shown. Data is representative of three independent experiments. [b] *B. anthracis* Sterne 7700 pXO1⁻/pXO2⁻ (*Bant*), *Staph. aureus* ATCC 12600 (*Saur*), *Staph. epidermidis* ATCC 1798 (*Sepi*), and *E. faecalis* ATCC 19433 (*Efae*). [c] *P. aeruginosa* ATCC 15692 (*Paer*) and *E. coli* O157:H7 (*Ecol*). (-), no antibacterial activity (MIC_{50} > 250). Cytotoxicity values in murine macrophages measured after 24 h are indicated (CC_{50}) as well as their SI (in parenthesis next to the MIC_{50} value). Selectivity indexes of ≥5 are in bold. Compounds with MIC_{50} values over 1000 μg/mL in all the strains are not shown (**1**, **2**, **3**, **4**, **5**, 7, **9**, 13, **16**, **19**, **20**, **21**, and **22**).

ring structure overlaps the inductive effect generated by substituents in the aromatic ring. *N*-Hydroxylamine derivatives with electron-withdrawing substituents and/or electron-donating substituents in the aromatic ring were active against several bacterial species with no distinction. *N*-Hydroxylamines containing a heteroaryl group or being part of the heterocycle as secondary hydroxylamines showed no antibacterial activity in any bacteria tested. However, *N*-benzylhydroxylamine analogues (**9**, **13**, **16**, and **19**) showed no antibacterial activity and clearly demonstrate a challenge to capture a structure–activity relationship. We believe that radical scavenger molecules could interact in different places along the protein electron chain transfer pathway from the β_2 to the α_2 subunits, and this explains why radical scavengers without a common scaffold are active.

Selected N-HA Compounds Exhibit Low Cytotoxicity and Good Lipophilicity Indexes. To validate hydroxylamine compounds to be used as drug candidates, eukaryotic cytotoxicity of the compounds showing higher activity against bacterial species (**6**, **8**, **10**–**12**, **14**, **15**, **17**, and **18**) was determined in murine macrophages (see Experimental Section) as described in our previous work.[23] Compounds with no antibacterial activity in the initial screening were discarded.

The 50% cytotoxic inhibitory concentration (CC_{50}) values were determined from dose–response data obtained from the toxicity assay of macrophages. Therapeutic indexes (selectivity index, SI), defined as SI = CC_{50}/MIC_{50}, were calculated (see Table 1) to measure drug safety (SI > 10). Compounds with high CC_{50} and low MIC_{50} have higher therapeutic index and are safer compared to compounds with low SI values.

Compounds **11**, **15**, **17**, and **18** showed higher SI in Gram-positive bacteria: in the case of *B. anthracis*, SI values of 21.3, 21.2, 45.2, and 45, respectively, and in *Staph. aureus*, SI values of 5.3 and 11.4 for compounds **11** and **15**, respectively. Compounds **11**, **15**, and **18** showed SI values of 10.6, 11.4, and 10.4 in *Staph. epidermidis*, respectively. For Gram-negative bacteria, the best SI values were achieved with compound **8** in the case of *P. aeruginosa* (SI = 10.5) and compound **15** in the case of *E. coli* (SI = 11.4). Although compound **12** was active against *P. aeruginosa*, SI index was lower due to a lower CC_{50} value. Still, further studies were carried with this compound to have more active N-HA compounds analyzed in the case of Gram-negative bacteria. Clearly, some of the compounds improve the SI values of the HU and M-HA compounds previously analyzed, especially against Gram-positive bacteria.

To further test *N*-hydroxylamine compounds as drug candidates, the lipophilicity of representative N-HA candidates (**8**, **10**, and **12**–**15**) was measured by calculating the *n*-octanol–water partition coefficients in their logarithmic form (log *P*) (Figure 1). The majority of the *N*-hydroxylamine analogues exhibited a moderate lipophilicity (log *P* between 0 and 3), indicating a good balance between solubility and permeability, which is optimal for oral absorption and cell membrane permeation through passive transport.

N-HA Compounds Inhibit Bacterial Growth through their Radical Scavenging Activity in Bacterial RNR. To confirm that novel *N*-hydroxylamines inhibit bacterial growth by inhibiting radical formation in bacterial RNR, the FRS activities of compounds showing antibacterial activity (**6**, **8**, **10**–**12**, **14**, **15**, **17**, and **18**) were evaluated through a radical scavenging assay by trapping the DPPH· radical as previously described[27] (see Experimental Section). Ascorbic acid (AA), HU, and M-HA were used as positive radical scavenger controls (Table 2). After 8 h of incubation and using a DPPH· concentration of 70 μM, compounds **8**, **10**, **11**, **12**, **14**, **15**, **17**, and **18** were able to scavenge the DPPH· radical with IC_{50} values of 9.3, 14.3, 6.4, 4.2, 23.1, 8.1, 4.8, and 6.5 μM, respectively, showing similar scavenging activity as AA (IC_{50} =10.2 μM), HU (IC_{50} = 8.6 μM), and M-HA (IC_{50} = 20.3 μM). Similar values were obtained at 12 h incubation time. However, compounds **2**, **3**, and **6**, with linear aliphatic N-HA with antibacterial activity, displayed a low FRS activity compared to cyclic aliphatic hydroxylamine (**8**), *N*-homobenzylhydroxylamine (**10**), and *N*-benzylhydroxylamine analogues (**11**, **12**, **14**, **15**, **17**, and **18**) with IC_{50} values higher than 140 μM. This study indicates that cyclic aliphatic rings and aromatic rings make corresponding *N*-oxyl species more

DOI: 10.1021/acsomega.8b01384
ACS Omega 2018, 3, 17057–17069

Table 2. Radical Scavenging Capacity of the N-HAs

compounds	DPPH· scavenging activity (IC_{50} (μM))[a] 8 h incubation time	12 h incubation time
2	>256	>256
3	>256	>256
6	171.4 ± 23.0	141.3 ± 17.4
8	9.3 ± 0.7	8.6 ± 0.5
10	14.3 ± 0.8	13.7 ± 0.9
11	6.4 ± 0.4	5.8 ± 0.3
12	4.2 ± 0.3	3.8 ± 0.3
14	23.1 ± 0.2	20.5 ± 0.3
15	8.1 ± 0.5	7.6 ± 0.5
17	4.8 ± 0.6	4.4 ± 0.8
18	6.5 ± 0.6	5.8 ± 0.6
AA	10.2 ± 1.8	10.1 ± 1.8
HU	8.6 ± 1.2	7.5 ± 0.9
M-HA	20.3 ± 2.0	18.1 ± 1.5

[a] Radical scavenging capacity was evaluated by measuring the reduction of the free radical DPPH· spectrophotometrically after incubating each compound with the DPPH during 8 and 12 h. AA, HU, and M-HA were used as positive controls.

electron-rich and more stable radicals, leading to a BDE decrease and thus resulting in a higher FRS activity, as we previously discussed. Also, our data supports the view that these compounds exhibit a similar capacity to scavenge RNR generated radical as other well-known RNR radical inhibitors such as HU and M-HA do (see Table 2).

To evaluate the specific inhibitory effect of the N-HA compounds in bacterial RNR, *P. aeruginosa* purine deoxyribonucleotide levels were quantified at exponential phase in the presence of N-HA compounds (**8** and **12**) and HU (positive control) at 5 mM for 3 h and in the absence of or any added compound (negative control) (Figure 2A). Relative dNTP levels were quantified in the different extracts carrying out the diphenylamine (DPA) assay.[28,29] The results showed a significant decrease of dNTP levels when *P. aeruginosa* was treated with compounds **8** and **12** (7.45% and 67.50% reduction, respectively) compared to negative control. HU, used as the positive control, also showed a reduction of 65.45% in dNTP levels.

The role of the radical scavenger HU in the inhibition of RNR has been well studied. As many other enzymatic inhibitors, when using HU, there is an induction of the expression of the inhibited enzyme (RNR), as it has been previously well described for us and many other authors.[29,30]

The induction of the expression of *P. aeruginosa* PAO1 class Ia RNR (NrdA) was studied in the presence of the most active N-HA radical scavengers against *P. aeruginosa*, using HU as a positive control. A Western blot was performed using protein extracts from PAO1 cultures in which HU, **8**, or **12** was added (at initial exponential phase and left for 3 h). As shown, both **8** and **12** were able to induce NrdA expression (1.6 and 3 times more, respectively) compared to the negative control, which was left without adding any compound. Compounds **8** and **12** had similar effects on NrdA expression to the ones HU shows (nine times of induction), showing the direct effect of the newly synthesized N-HA compounds on bacterial RNR expression (Figure 2B).

N-HA Compounds Display Antibacterial Activity through a Bacteriostatic Mode of Action. To better understand how the most active *N*-hydroxylamines affect the viability of bacterial cells in terms of physiological changes, bacterial cells were imaged through fluorescence microscopy using the Live/Dead viability assay (see Experimental Section), which allows measuring bacterial viability in terms of membrane integrity. SYTO 9 green fluorescent nucleic acid dye is able to penetrate all membrane cells, labeling all bacteria, whereas propidium iodide can only enter bacteria cells with damaged membrane.

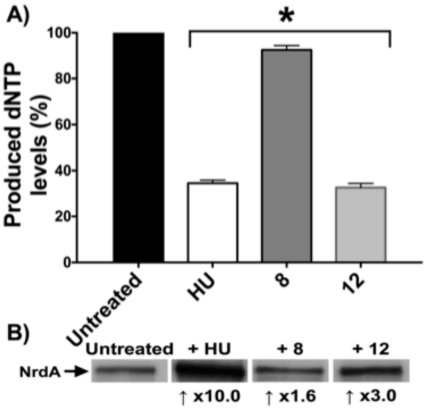

Figure 2. Inhibition of bacterial RNR by N-HA compounds. (A) In vivo inhibition of bacterial RNR in *P. aeruginosa* was determined by using DPA assay to estimate dNTP levels. Relative dNTP levels were measured in protein extracts from mid-exponential cultures incubated with or without 5 mM of the radical scavengers **8**, **12**, or HU (positive control) for 3 h. Percentage of produced dNTPs is shown for each sample using untreated culture as a reference. The results shown represent the mean ± SD of two replicates of one representative experiment. An unpaired *t* test, compared to the untreated sample, was performed to evaluate significant differences (*, $P < 0.05$). (B). Western blot analysis of class Ia RNR (NrdA) of bacteria at mid-exponential phase cultured in the presence of 5 mM of **8**, **12**, or HU for 3 h. The Western blot is representative of two independent experiments.

Staph. aureus, *P. aeruginosa*, *E. coli*, and *B. anthracis* growing cultures at early exponential phase were incubated with selected N-HA compounds showing greater antibacterial action for 2 h then subsequently stained and imaged using fluorescence microscopy (Figure 3). Images of bacteria also treated with antibiotics novobiocin (NVB) and CIP were taken to compare the effects with known antibiotics. N-HA compounds did not affect membrane integrity of the cells, as no differences were observed in the ratio of green cells (viable) and red cells (nonviable) with or without any of the treatments demonstrating a bacteriostatic property of these compounds. The same effect was previously described for other radical scavengers such as HU, hydroxylamine, and M-HA.[23]

N-HA Compounds Show Antibiofilm Activity against Different Pathogens. Because most of the bacterial infections in humans are in biofilm form,[3,31] it is crucial to study the antibacterial activity under the growth condition in which bacteria are found naturally more resistant to the action of antimicrobials.[7,31] The most promising compounds showing higher antibacterial activity, together with low cytotoxicity (highest SI values), were evaluated on *P. aeruginosa*, *Staph. aureus*, and *E. coli* static biofilms.

P. aeruginosa, *Staph. aureus*, and *E. coli* bacterial biofilms (72 h old) were established and treated with repeated admin-

DOI: 10.1021/acsomega.8b01384
ACS Omega 2018, 3, 17057−17069

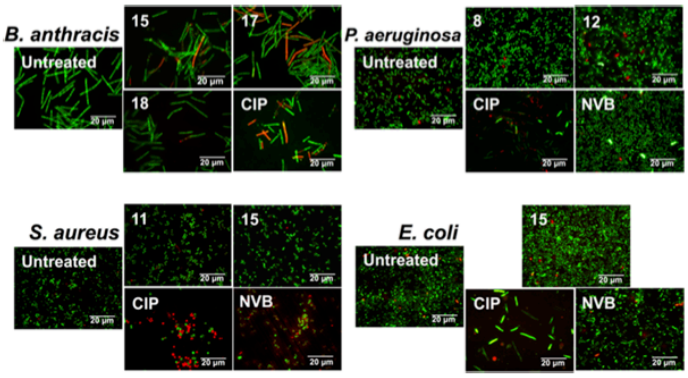

Figure 3. Bacterial viability after different compound treatments. Bacterial cultures were visualized under fluorescence microscopy after 2 h exposition with the different N-HAs at 1× MIC concentration. Images were taken at 100×. Scale bars shown represent a real distance of 20 μm. Live cells were green (SYTO 9 dye), and dead cells were red (propidium iodide dye). CIP and NVB (50 μg/mL) were used.

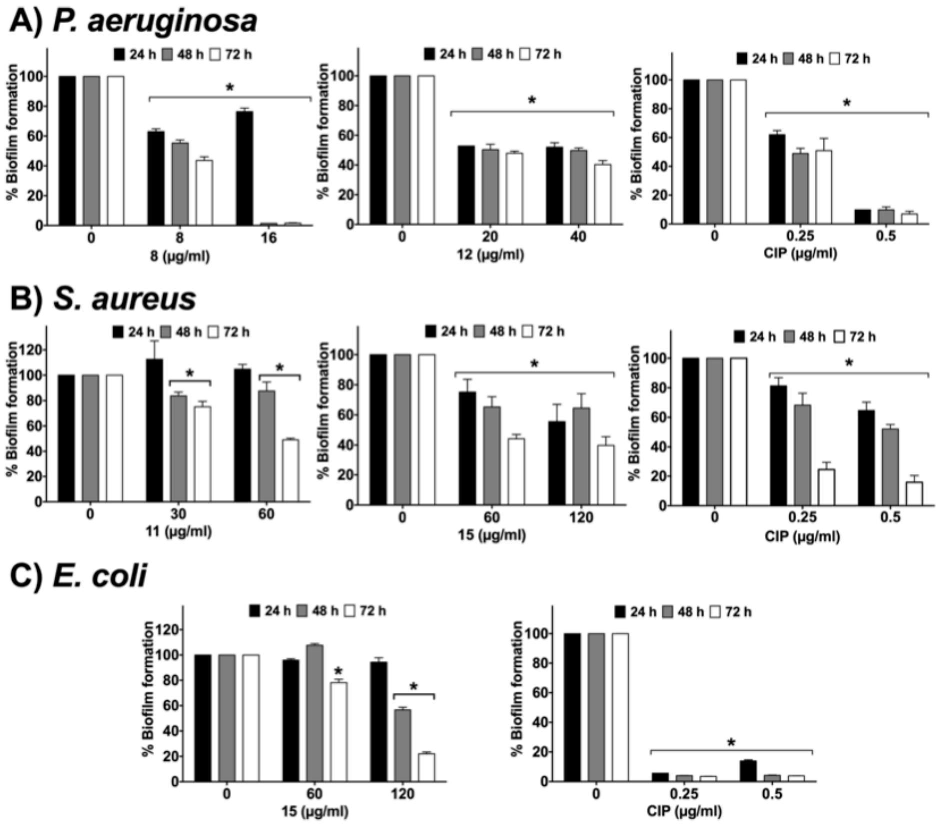

Figure 4. *P. aeruginosa*, *Staph. aureus*, and *E. coli* biofilms are inhibited by adding different concentrations of radical scavengers **8**, **11**, **12**, and **15**. Bacteria were allowed to grow as biofilms in pegs (in the case of *P. aeruginosa*) or in wells (in the case of *Staph. aureus* and *E. coli*) for 72 h using 96 well microplates (see Experimental Section). Then, the medium was removed, and fresh medium with different concentrations of radical scavenger compounds were changed every 24 h over 3 days (24 h, 48 h, and 72 h). The percentage of biofilm biomass was calculated by normalizing the data for each of the nontreated biofilms for each day. The results shown are the means ± SD of four-six replicates from one representative of two independent experiments. A Dunnett's multiple comparison test was performed to detect significant differences. A Student's *t* test was performed (*, $P < 0.05$; vs nontreated biofilms). The viable counts at control experiments without a compound were $2.1 \times 10^9 \pm 2.8 \times 10^8$ colony-forming units (cfu)/mL for PAO1, $9.8 \times 10^9 \pm 3.1 \times 10^8$ cfu/mL for *Staph. aureus*, and $3.3 \times 10^{10} \pm 1.8 \times 10^9$ cfu/mL for *E. coli*.

istration of selected compounds (one dose/24 h for three consecutive days), and biofilm biomass was evaluated (Figure 4). CIP, a commonly used and known antibiotic, was used as a positive control.

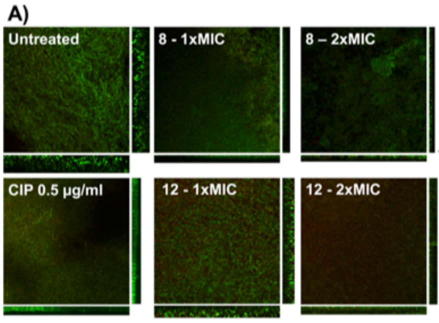

B)

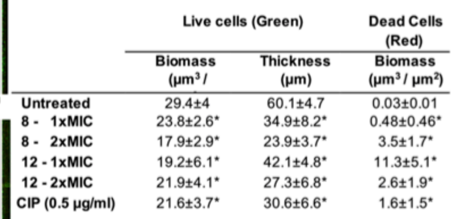

	Live cells (Green)		Dead Cells (Red)
	Biomass (µm³ /	Thickness (µm)	Biomass (µm³ / µm²)
Untreated	29.4±4	60.1±4.7	0.03±0.01
8 - 1xMIC	23.8±2.6*	34.9±8.2*	0.48±0.46*
8 - 2xMIC	17.9±2.9*	23.9±3.7*	3.5±1.7*
12 - 1xMIC	19.2±6.1*	42.1±4.8*	11.3±5.1*
12 - 2xMIC	21.9±4.1*	27.3±6.8*	2.6±1.9*
CIP (0.5 µg/ml)	21.6±3.7*	30.6±6.6*	1.6±1.5*

Figure 5. Effect of compounds **8** and **12** on a formed flow cell *P. aeruginosa* biofilm. Flow cell biofilm parameters after treatment with **8**, **12**, and CIP (positive control). *P. aeruginosa* biofilm was cultured in a flow cell system for 96 h at room temperature and subjected to a continuous supply of fresh medium at a flow rate of 3 mL/h. Different concentrations of compounds **8** and **12** and CIP were then used to treat biofilms for 24 h. Afterward, biofilms were dyed with SYTO 9 and propidium iodide, rinsed, and imaged with CLSM. (A) ImageJ-analyzed CLSM micrographs of the differently treated biofilms, showing the sum of the Z-projections and the corresponding orthogonal views of each biofilm (representative of 10 independent areas of two independent experiments). Green cells (dyed with SYTO 9) indicate viable cells, whereas red cells (dyed with propidium iodide) indicate dead cells (damaged membrane). (B) Quantitative flow cell biofilm parameters (biomass and average thickness) of the biofilms, quantified using Comstat2. A Student's *t* test was performed (*, $P < 0.05$, vs nontreated biofilms).

In the case of *P. aeruginosa* (Figure 4A), compound **8** clearly reduced drastically the preestablished biofilm in more than 95% in *P. aeruginosa* at 48 h of treatment with an MIC concentration of 16 µg/mL. Not so effective, compound **12** reduced above 55% of the established biofilm after 72 h of treatment using the highest concentrations. CIP (0.5 µg/mL), used as the positive control, reduced the preestablished biofilm in more than 85%. Compound **8** showed higher activity compared to CIP, demonstrating a good antibacterial activity to eliminate *P. aeruginosa* biofilms.

Not so notorious but also important, compounds **11** and **15**, at MIC concentration, efficiently reduced *Staph. aureus* biofilm at levels around 50% after 72 h of treatment (Figure 4B), with similar levels to those reached when treating with CIP (around 60% reduction).

In the case of *E. coli* biofilms, compound **15** also successfully removed static preestablished biofilm at more than 50% at 72 h with the highest concentration (2× MIC concentration) (Figure 4C), displaying low antibiofilm activity compared to CIP. CIP-treated biofilm control (0.25 µg/mL) showed a reduction of more than 90% formed biofilm.

To test some of the compounds under more natural conditions that better resemble the in vivo infections, *P. aeruginosa* continuous-flow biofilms were treated with two of the most effective compounds (**8** and **12**) and CIP (positive control) (Figure 5A) and observed by confocal laser scanning microscopy (CLSM) demonstrating the capacity of these compounds to decrease biofilm biomass and thickness. Note that under this grown condition, the biofilm is extremely resistant to all known antibiotics (with CIP, the formed biofilm is only reduced around 50%).[3]

P. aeruginosa flow biofilms grew in a characteristic pattern with a lawn of bacterial growth on the surface. These results showed that compounds **8** and **12** at MIC concentration clearly disrupted and inhibited *P. aeruginosa* flow biofilms. Control experiments using CIP showed that a characterized bacterial biofilm decreased, as previously described.[32] When analyzed using COMSTAT software, *P. aeruginosa* biofilms showed significant structural differences in the presence of both compounds (Figure 5B). Biomass and average thickness decreased in biofilms grown in the presence of **8** (more than 50%) and **12** (more than 30%), indicating the ability of these new radical scavengers to remove preexisting *P. aeruginosa* growing in flow biofilms with similar results as compared to the benchmarked antibiotic (CIP).

■ DISCUSSION

Because of the essential role of RNR in cellular replication, it has been studied for a long time as an antibacterial target, and different RNR inhibitors have been used as antiproliferative therapies in cancer diseases.[14,15,17] This is the case of HU, a molecule with a hydroxylamine moiety that avoids RNR activity by trapping a radical generated in the activator subunit of the enzyme that is needed to initiate the catalysis.

As there is low similarity between some pathogenic bacteria and the host RNR enzymes,[19] it is possible to specifically target bacterial enzyme without interfering eukaryotic cells and avoiding host toxicity. In this sense, methyl hydroxylamine, another radical scavenger compound with a hydroxylamine moiety, as HU, was found to show antibacterial activity against both *P. aeruginosa* and *Mycobacterium bovis* BCG without reducing eukaryotic viability.[19,20,23] This finding settled the point for the design and development of new radical scavengers with improved antibacterial activity that act against antibiotic multiresistant bacteria.

In previous studies, the direct radical scavenging of the RNR tyrosyl radical in the enzyme was demonstrated to take place when using HU, hydroxylamine, and methylhydroxylamine.[20,23]

Here, we designed and synthesized a small-molecule library of 16 N-HAs, incorporating six other molecules that were acquired commercially (Figure 1). As the design of the new N-HA chemical structures was based on a common *N*-hydroxylamine moiety as the functional group involved in the radical scavenging, we hypothesized the same mode of action for our new N-HA compounds in RNR inhibition. As expected, we could prove the radical scavenging activity of different active N-HAs by measuring the reduction of the free radical DPPH spectrophotometrically, showing the ability of these compounds to quench free radicals as positive controls, such as AA, HU, and M-HA, do (see Table 2). Moreover, we demonstrated the effect of two of the N-HAs in reducing the intracellular dNTP levels and inducing the protein expression of *P. aeruginosa* class I RNR, as HU does[29,33,34] (Figure 2), making evident the clear role of these compounds in the inhibition of bacterial RNR enzyme.

Antibacterial activity was assessed for all the library compounds. Although some of the compounds exhibited no antibacterial activity, nine of the new N-HAs were able to inhibit the growth of different bacterial pathogens, including Gram-negative and Gram-positive bacteria (see Table 1).

The library was composed of a wide diversity of structures, including aliphatic and aromatic substituents, to better cover the chemical space and gain selectivity toward the RNR enzyme. As theoretically expected, some of the molecules with cyclic aliphatic groups and aromatic groups showed better activity against bacteria than the ones with linear aliphatic groups, as it has been well described that radical scavenging activities are related to aromatic structures as phenolic compounds.[17,35] To a great extent, *N*-benzylhydroxylamines with substituents in the aromatic ring (**10**, **11**, **12**, **14**, **15**, **17**, and **18**) were the ones with higher activity against Gram-positive bacterial strains. This statement is also consistent with the fact that lower radical scavenger activity is shown in N-HAs with aliphatic substituents, such as **2**, **3**, and **6**, which displayed an IC_{50} at least 13 times higher than the other evaluated compounds (Table 2). This is probably due to the fact that electron delocalization in the aromatic ring favors the stabilization of the free radical, thus providing higher FRS activity. However, other *N*-benzylhydroxylamine analogues (**9**, **13**, **16**, and **19**) showed no antibacterial activity, highlighting a lack of structure–activity relationship. We assume that N-HA molecules could quench the free radical in different places along the protein electron chain transfer.

Overall, N-HAs resulted in higher antibacterial activity against Gram-positive species rather than Gram-negative species, excluding **8**, which showed high activity against both Gram-negative and Gram-positive bacteria. It is clear that some of the new N-HA compounds (**8**, **11**, **15**, **17**, and **18**) result in higher antimicrobial activity and SI compared to the HU and M-HA. Gram-positive bacteria studied here (*B. anthracis*, *Staph. aureus*, *Staph. epidermidis*, and *E. faecalis*) encode for a specific class Ib RNR, whereas Gram-negative (*P. aeruginosa* and *E. coli*) specifically encode for a class Ia RNR. Particularly, *E. coli* also encodes for an additional class Ib RNR, although it is not expressed under LB growing conditions.[36] This difference in RNR subclass is possibly the explanation of such preference for Gram-positive RNR enzymes. We previously described that M-HA showed better specific RNR inhibition for class Ib RNR,[19] thus demonstrating better antimicrobial activity in bacteria expressing the class Ib RNR subclass.[23]

How can such a diversity of molecule structures inhibit RNR enzymes? More specifically, where does the radical scavenging of such molecules take place? Class I RNR enzymes are made up of two homodimeric subunits ($\alpha_2\beta_2$): the large α_2 homodimeric subunit called NrdA (class Ia) or NrdE (class Ib) and the small β_2 subunit called NrdB (class Ia) or NrdF (class Ib). The large subunit (α_2) is the catalytic subunit, which harbors the substrate binding site and reduces the different nucleotides to their corresponding dNTPs, whereas the small β_2 subunit contains an oxygen-linked diferric or dimanganese metal center that generates a free tyrosyl radical. Once the radical is generated, an electron transfer takes place between β_2 and α_2 subunits from the specific radical site in the small subunit to the substrate binding site in the large subunit by a mechanism involving a long-range electron transfer pathway.[11,12]

Docking experiments with other well-known radical scavenger molecules, HU and *p*-allyloxyphenol, evidently indicate that the molecule binding site is not well defined and that in most of the cases, radical scavengers are located at the protein surface.[35] These experiments point out that the large *p*-allyloxyphenol molecule cannot access the tyrosyl radical site directly for structural reasons so that, for these inhibitors, the radical scavenging action needs to be performed during the long-range electron transfer pathway.[35] Molecules synthesized in this work have similar chemical structures and molecular weights to *p*-allyloxyphenol, so we hypothesize the same radical scavenger activity for the different N-HA molecules described in this work as compared to the *p*-allyloxyphenol. Probably, our N-HA molecules are not able to diffuse to the place where the tyrosyl radical is formed (metal center site at the small class I RNR subunit). Hence, the radical scavenging activity could take place in different places along the protein electron chain transfer. This fact could better explain why different molecular scaffolds can inhibit RNR enzymes with a similar scavenging activity.

Although some of the selected N-HAs displayed certain toxicity to eukaryotic cells, others exhibited good therapeutic index, which is a measure that takes into account both cytotoxicity and antibacterial activity values. *N*-Hydroxylamine compounds with SI > 5 are interesting and should be well studied to be used as antibiotics, as bacteria were more affected than eukaryotic cells. In addition, when analyzing the lipophilicity levels of the most promising compounds, all of them displayed moderate partition coefficients values, thus indicating good solubility under physiological conditions.

One of the current antimicrobial therapy problems we are currently facing is the use of antibiotics that are not effective to eradicate bacteria growing in biofilms. Under this growing condition, antibiotics cannot penetrate through the extracellular matrix produced by the different bacteria, or if they penetrate, they can be inactivated by some components of the matrix.[7] This is the reason why bacterial infections growing under biofilm conditions are extremely resistant to the current chemotherapy, thus preventing the infection from being eradicated. For this reason, evaluating antibacterial activity of new molecules in biofilm-growing cells becomes essential if we want to treat current infections.

When testing the ability of our new N-HA molecules to eradicate bacterial biofilms, we found that some of the compounds did reduce biofilm formation at levels similar to those found for other known antibiotics, such as CIP. In the case of *P. aeruginosa*, special attention needs to be done with compound **8** that reduced above 90% of mature biofilm at 48 h at the MIC concentration, which is similar to the levels of inhibition with the benchmarked CIP (Figure 4). Not so effective, but also important, were the results obtained with *Staph. aureus* and *E. coli* biofilms, especially with a continuous 3 day treatment.

The antibiofilm activities of compound **8** were moreover corroborated in a *P. aeruginosa* continuous-flow biofilm, which was stained and observed by CLSM. The results certainly state that compound **8** has the same effectivity as CIP to remove well-established and mature *P. aeruginosa* biofilm (with similar biomass and thickness values) (Figure 5).

P. aeruginosa is the responsible for some important chronic pulmonary infections, such as those in cystic fibrosis (CF), bronchiectasis, or chronic obstructive pulmonary disease (COPD). Our compounds could be effective for those diseases, in which once the infection is established, eradication of *P. aeruginosa* is nearly impossible due to a biofilm form of growth. As the existing therapies always fail to eradicate bacterial biofilms, the results outlined herein show that our compounds could be highly potent and effective drugs to eradicate biofilm infections and open an interesting new era of research in this field. In addition, antibiofilm candidates are ultimately explored to be used not only in clinical settings but also in eliminating contaminating biofilm growth in food and veterinary industry, processes that involve pure water systems.

■ CONCLUSIONS

In summary, we designed and synthesized a library of N-HA compounds, acting as radical scavengers, to directly target the bacterial class I RNR enzyme and inhibit bacterial proliferation. Compounds with different structures were designed to better cover the chemical space and gain more selectivity. We have demonstrated the broad antimicrobial effect of several drug candidates against a variety of Gram-positive and Gram-negative pathogenic bacteria, together with low toxicity toward eukaryotic cells. In addition, some of the compounds had the ability to eradicate bacterial biofilms at the same level of known antibiotics. This work settles the starting point to develop new radical scavenger compounds as potential antibacterial agents to fight against drug-resistant pathogenic bacteria.

■ EXPERIMENTAL SECTION

All reagents used for chemical synthesis were purchased from commercially available sources and used without further purification. Nuclear magnetic resonance (NMR) solvents were obtained from Sigma-Aldrich. ^{1}H, ^{13}C, and ^{19}F NMR spectra were recorded on a Varian MERCURY 400 spectrometer (400 MHz for ^{1}H NMR, 101 MHz for ^{13}C NMR, and 376 MHz for ^{19}F NMR). Chemical shifts (δ) are expressed in parts per million (ppm) downfield from tetramethylsilane, and deuterated solvent signal was used as reference. Coupling constants (J) are expressed in hertz (Hz). Abbreviations used are s = singlet, bs = broad singlet, d = doublet, dd = doublets of doublets, t = triplet, td = triplets of doublets, q = quartet, and m = multiplet. Mass spectra were obtained at the "Centres Científics i Tecnològics de la Universitat de Barcelona" (CCiTUB). Compounds tested in the different biological assays were previously diluted to a stock concentration of 0.5 to 1 M in H_2O to perform the experiments.

General Procedure for the Synthesis and Characterization of N-HAs. N-HAs were synthesized by reductive amination of aldehydes, as described before[26] with some variations. To a mixture of R-aldehyde (1 equiv) in a solution of 5.0 M $LiClO_4/Et_2O$ (LPDE) (10 mL), *O*-(trimethylsilyl)hydroxylamine (1.5 equiv) was added at room temperature. The mixture was stirred for 10 min, and trimethylsilyl chloride (1.5 equiv) was added. After stirring the mixture for 8 h, borane/triethylamine complex (1.5 equiv) was added, and the reaction mixture was allowed to stir at room temperature overnight. The reaction was quenched with a saturated aqueous $NaHCO_3$ solution to obtain the mono *N*-alkylhydroxylamine. The mixture was filtrated, and then the product was extracted with DCM. The organic extracts were combined, dried with $MgSO_4$, and concentrated. Finally, the crude product was flash-chromatographed (SiO_2) using a hexane−EtOAc gradient from 1:0 to 0:1.

All final compounds were confirmed by ^{1}H NMR, ^{13}C NMR, ^{19}F NMR (see Supporting Information for product characterization), and HR-ESMS. In all cases, the purity of the final product was above 95% after flash chromatography (SiO_2).

Compounds **1**, **2**, **6**, **8**, **10**, **11**, **15**, **16**, **18**, and **20** were synthesized as previously described, and their characterization agrees with the literature.

N-Hydroxy-3-methylbutan-1-amine (**5**). Isovaleraldehyde (1 g, 11.6 mmol) was dissolved in a solution of 5.0 M LPDE. Then, *O*-(trimethylsilyl)hydroxylamine (17.4 mmol), trimethylsilyl chloride (17.4 mmol), and borane/TEA complex (17.4 mmol) were added as described in the general procedure. Following purification via flash column chromatography, the product was obtained in a 56.4% yield. ^{1}H NMR shows a conformer. ^{1}H NMR (400 MHz, $CDCl_3$) δ ppm 6.48 (bs, 2H, NHOH), 2.93−2.89 (m, 2H, CH_2), 1.65−1.52 (m, 1H, CH), 1.41−1.35 (m, 2H, CH_2), 0.87 (d, J = 6.6 Hz, 6H, CH_3). Isolated signals of the conformer: 3.38 (t, J = 7.4 Hz, 2H, CH_2), 1.86−1.75 (m, 1H, CH), 0.90 (d, J = 6.9 Hz, 6H, CH_3). ^{13}C NMR (101 MHz, $(CD_3)_2CO$) δ ppm 58.9 (t), 37.7 (t), 27.5 (d), 23.6 (2q). HRMS (ESI) m/z calcd for $C_5H_{14}NO$: 104.1075 $[M + H]^+$; found, 104.1070.

N-(4-Fluoro-2-methylbenzyl)hydroxylamine (**12**). 4-Fluoro-2-methylbenzaldehyde (1 g, 7.2 mmol) was dissolved in a solution of 5.0 M LPDE. Then, *O*-(trimethylsilyl)hydroxylamine (10.9 mmol), trimethylsilyl chloride (10.9 mmol), and borane/TEA complex (10.9 mmol) were added as described in the general procedure. Following purification via flash column chromatography, the product was obtained in a 55.2% yield. ^{1}H NMR (400 MHz, D_2O) δ ppm 7.46 (dd, J = 8.44, 5.96 Hz, 1H, ArH), 7.12 (dd, J = 10.05, 2.42 Hz, 1H, ArH), 7.06 (td, J = 8.54, 2.35 Hz, 1H, ArH), 4.51 (s, 2H, CH_2), 2.43 (s, 3H, CH_3). ^{13}C NMR (101 MHz, D_2O) δ ppm 163.1 (d), 141.7 (s), 133.51 (d), 122.8 (s), 117.4 (d), 113.2 (d), 51.5(t), 18.5 (q). ^{19}F NMR (376 MHz, D_2O) δ ppm −112.40−(−112.49) (m, 1F, CF). HRMS (ESI) m/z calcd for $C_8H_{11}FNO$: 156.0819 $[M + H]^+$; found, 156.0819.

N-(4-Fluoro-2-(trifluoromethyl)benzyl))hydroxylamine (**13**). 4-Fluoro-2-(trifluoromethyl)benzaldehyde (1 g, 5.2 mmol) was dissolved in a solution of 5.0 M LPDE. Then, *O*-(trimethylsilyl)hydroxylamine (7.8 mmol), trimethylsilyl chloride (7.8 mmol), and borane/TEA complex (7.8 mmol) were added as described in the general procedure. Following purification via flash column chromatography, the product was obtained in a 46.7% yield. ^{1}H NMR (400 MHz, CD_3OD) δ ppm 7.89 (dd, J = 8.46, 5.26 Hz, 1H, ArH), 7.63 (dd, J = 8.95, 2.72 Hz, 1H, ArH), 7.55 (td, J = 8.46, 2.72 Hz, 1H, ArH), 4.93 (bs, 2H, NHOH), 4.61 (s, 2H, CH_2). ^{13}C NMR (101 MHz, CD_3OD) δ ppm 164.3 (d), 137.2 (d), 133.2 (s), 124.7 (s), 124.5 (q), 120.9 (d), 115.5 (d), 52.1 (t). ^{19}F NMR (376 MHz, CD_3OD) δ ppm −60.22 (s, 3F, CF_3), −110.52−(−110.57) (m, 1F, CF). HRMS (ESI) m/z calcd for $C_8H_8F_4NO$: 210.0537 $[M + H]^+$; found, 210.0546.

N-(3,5-Difluorobenzyl)hydroxylamine (**14**). 3,5-Difluorobenzaldehyde (1 g, 7 mmol) was dissolved in a solution of 5.0 M LPDE. Then, *O*-(trimethylsilyl)hydroxylamine (10.6 mmol), trimethylsilyl chloride (10.6 mmol), and borane/TEA complex (10.6 mmol) were added as described in the general procedure. Following purification via flash column chromatography, the product was obtained in a 49.8% yield. ^{1}H NMR

(400 MHz, D_2O) δ ppm 7.25–7.03 (m, 3H, ArH), 4.47 (s, 2H, CH_2). ^{13}C NMR (101 MHz, D_2O) δ ppm 162.8 (d), 162.7 (d), 132.0 (s), 113.7 (2d), 105.2 (d), 53.74 (t). ^{19}F NMR (376 MHz, D_2O) δ ppm −109.33-(-109.46) (m, 2F, CF). HRMS (ESI) *m/z* calcd for $C_7H_8F_2NO$: 160.0568 $[M + H]^+$; found, 160.0568.

*N-(4-Methoxy-2-methylbenzyl)hydroxylamine (**17**).* 4-Methoxy-2-methylbenzaldehyde (1 g, 6.7 mmol) was dissolved in a solution of 5.0 M LPDE. Then, *O*-(trimethylsilyl)-hydroxylamine (10 mmol), trimethylsilyl chloride (10 mmol), and borane/TEA complex (10 mmol) were added as described in the general procedure. Following purification via flash column chromatography, the product was obtained in a 32.8% yield. ^1H NMR (400 MHz, $CDCl_3$) δ ppm 7.18 (d, *J* = 8.2 Hz, 1H, ArH), 6.73 (d, *J* = 2.7 Hz, 1H, ArH), 6.70 (dd, *J* = 8.2, 2.7 Hz, 1H, ArH), 4.00 (s, 2H, CH_2), 3.78 (s, 3H, CH_3), 2.35 (s, 3H, CH_3). ^{13}C NMR (101 MHz, $CDCl_3$) δ ppm 158.9 (s), 138.4 (s), 131.3 (d), 126.6 (s), 115.8 (d), 110.8 (d), 54.9 (q), 54.9 (t), 19.1 (q). HRMS (ESI) *m/z* calcd for $C_9H_{14}NO_2$: 168.1025 $[M + H]^+$; found, 168.1027.

*N-(2,6-Dimethoxybenzyl)hydroxylamine (**19**).* 2,6-Dimethoxybenzaldehyde (1 g, 6 mmol) was dissolved in a solution of 5.0 M LPDE. Then, *O*-(trimethylsilyl)hydroxylamine (9 mmol), trimethylsilyl chloride (9 mmol), and borane/TEA complex (9 mmol) were added as described in the general procedure. Following purification via flash column chromatography, the product was obtained in a 29.8% yield. ^1H NMR (400 MHz, $CDCl_3$) δ ppm 7.19 (t, *J* = 8.4 Hz, 1H, ArH), 6.54 (d, *J* = 8.4 Hz, 2H, ArH), 3.93 (s, 2H, CH_2), 3.81 (s, 6H, CH_3). ^{13}C NMR (101 MHz, $CDCl_3$) δ ppm 159.4 (2s), 128.6 (d), 114.4 (s), 103.9 (2d), 55.8 (2q), 47.9 (t). HRMS (ESI) *m/z* calcd for $C_9H_{13}NO_3$: 184.0968 $[M + H]^+$; found, 184.0964.

Log *P* Calculations. The compounds were equilibrated in a two-phase octanol–water system in small vials, and high-performance liquid chromatography (HPLC) was used to determine the concentration of the compounds in each phase. Compound concentrations (*ci*) were calculated using the expression *ci* = *k Ii*, where *Ii* is the integral under the peak of the HPLC chromatogram and the proportionality constant *k* is called the response factor. The ratio of the integrals for the octanol and water phase gave the partition coefficient (*P*):

$$P = ci(\text{octanol})/ci(\text{water}) = k\,Ii(\text{octanol})/k\,Ii(\text{water})$$
$$= Ii(\text{octanol})/Ii(\text{water})$$

Bacterial Strains and Growth Conditions. Wild-type *P. aeruginosa* ATCC 15692 (CECT 4122), *Staph. aureus* ATCC 12600 (CECT 86), *Staph. epidermidis* ATCC 1798 (CECT 231), and *E. faecalis* ATCC 19433 (CECT 481) were obtained from the Spanish Type Culture Collection (CECT). *E. coli* O157:H7 Δ*stx* was obtained from laboratory collection, and *B. anthracis* Sterne 7700 $pXO1^-/pXO2^-$ was obtained from the Swedish Defence Research Agency. These strains were stored at −80 °C as glycerol stocks. To obtain inocula for examination, the strains were cultured overnight on trypticase soy agar (TSA) (Scharlau, Spain) or Luria agar (Scharlau, Spain) at 37 °C. Tryptic soy broth (TSB) (Sharlau, Spain) or Luria Broth (LB) was used to culture bacteria at 37 °C.

The murine macrophage J774.A1 cell line (DSMZ ACC 170) was maintained in Dulbecco's Modified Eagle's medium (DMEM) with L-glutamine (Gibco BRL, Grand Island, NY) supplemented with 10% heat-inactivated fetal bovine serum (FBS, Lonza Ltd., Switzerland), containing 100 U/mL penicillin G (Lab ERN, Barcelona, Spain) and 100 μg/mL streptomycin (Reig Jofre Laboratory, Barcelona, Spain) (complete medium), at 37 °C in a humidified atmosphere with 5% CO_2.

Antibacterial Susceptibility Testing. To determine survival of the different strains in the presence of different potential inhibitors, each bacterial strain was grown in TSB medium to initial exponential log phase (OD_{550} ≈ 0.1) and plated in a microtiter plate with different concentrations of the antimicrobial agents, following the Clinical Laboratory Standards Institute (CLSI) guidelines.[37] Growth curves were monitored for 8 h, taking the OD_{550} nm every 15 min in a microplate reader (Infinite M200 Microplate Reader, Tecan). Bacteria diluted in media with no compound were used as a positive control of bacterial growth.

The minimal inhibitory concentration 50% (MIC_{50}) was defined as the compound concentration that reduces bacterial growth, determined as the OD_{550}, by 50%.

Determination of Mammalian Cytotoxicity. Murine macrophage cells (6×10^4 per well) were seeded onto 48 well tissue culture plates in complete medium (Gibco) without antibiotics, in the presence of different doses of compounds or left untreated. After 24 h of exposure to the different compounds, culture supernatants were removed, and cell viability were measured by the addition of 10% (w/v) of 3-(4,5-dimethylthiazol-2-yl)-2,5-diphenyltetrazolium bromide (MTT) in complete medium was added and incubated for 3 h at 37 °C. Then, water-insoluble dark blue formazan was dissolved by adding acidic isopropanol. Absorbance was measured at 550 nm using a microplate reader (Infinite M200 Microplate Reader, Tecan). Results were expressed as the percent absorbance of treated versus untreated control cultures.

The 50% cytotoxicity inhibitory concentration (CC_{50}) of each drug was determined from dose–response curves. On the basis of the CC_{50} (24 h) and MIC_{50} (8 h) values, the selectivity index (SI = CC_{50}/MIC_{50}) was calculated.

Fluorescent Microscopy Viability Test Analysis. Overnight cultures of *B. anthracis*, *Staph. aureus*, *P. aeruginosa*, and *E. coli* were diluted in fresh TSB or LB medium, grown to the beginning of exponential phase (OD_{550} ≈ 0.3), and different compound concentrations were added. After 3 h of incubation at 37 °C under shaking conditions, cells were harvested and stained using the LIVE/DEAD BacLight Bacterial Viability Kit (Molecular Probes) for 30 min at room temperature under dark conditions, followed by one sterile phosphate-buffered saline (PBS) wash to remove nonspecific stain. Fluorescent bacteria were visualized by a Nikon inverted fluorescent microscope ECLIPSE Ti-S/L100 (Nikon) coupled with a DS-Qi2 Nikon camera.

Static Biofilm Formation Assay. *P. aeruginosa* PAO1 static biofilms were grown on microplates following the protocol previously described.[32,38] An overnight grown culture of *P. aeruginosa* in TSB was diluted to an OD_{550} of 0.1 in sterile TSB medium supplemented with 0.2% glucose and added to a 96 well microtiter plate with pegs (Nunc-TSP, Thermo Scientific) (200 μL per well). After 24–48 h incubation at 37 °C in a humid chamber, the culture supernatant was discarded, and the pegs were washed three times with sterile PBS to remove nonadherent cells. After rinsing, the biofilms were treated with different radical scavenger's concentrations using twofold serial dilutions in TSB medium supplemented

DOI: 10.1021/acsomega.8b01384
ACS Omega 2018, 3, 17057–17069

with 0.2% glucose. After 24 h of treatment, peg lids were transferred to a new plate and rinsed three times with PBS. Adherent bacteria were first fixed with 98% methanol for 15 min, allowed to dry for 5 min, and then stained with crystal violet (1%) for 10 min. An excess of crystal violet was washed gently with water, and pegs were dried in air for 5 min. The dye bound to the cells was dissolved with acetic acid 33%, and absorbance was read with a microplate reader (Infinite M200 Pro Multimode Microplate Reader, Tecan) at a wavelength of 570 nm.

The static biofilm formation assay for *Staph. aureus* and *E. coli* was assessed following the previous protocol but using flat-bottom 96 well polystyrene plates with lid (tissue culture-treated polystyrene, Costar 3596, Corning Inc., NY), in the case of *Staph. aureus*, and 96 well PVC plates, in the case of *E. coli*.[36]

Flow Cell Biofilm Assay. *P. aeruginosa* biofilm formed under a continuous flow was cultured in a flow cell system, as previously described[32,39] with some modifications. Channel flow cells (made of Perspex poly(methyl methacrylate)), with a channel size of 40 × 4 × 1 mm (DTU Systems Biology, Technical University of Denmark)), were used and covered with a no. 1 24 × 50 mm glass coverslip (Deltalab, ref D102450), which served as the biofilm substratum. Each flow cell channel was inoculated with 350 μL of a *P. aeruginosa* culture, diluted to an OD_{550} = 0.1, and left without medium flow for 1 h. The biofilm was then allowed to grow in LB medium supplemented with 0.04% glucose under nutrient flow conditions (3 mL/h) for 96 h at room temperature. The flow was then stopped, and different concentrations of compounds and CIP diluted in the medium were injected afterward to the formed biofilms. Medium without any added compound was injected in a channel as a control for biofilms without treatment. After 24 h, treated biofilms were dyed with 6 μM SYTO 9 and 30 μM propidium iodide (LIVE/DEAD BacLight Bacterial Viability Kit (Molecular Probes)) for 30 min under dark conditions and afterward washed with PBS. Biofilms were imaged with CLSM (Leica TCS-SP5, Leica Microsystems, Heidelberg, Germany) using excitation and emission wavelengths of 488 and 514 nm, respectively. Sections (250 × 250 μm) were scanned at a 40× magnification, and Z-stacks were obtained with a *z*-step size of 0.388 μm. The acquired images were analyzed using ImageJ software (National Institute of Health, USA) and Comstat2 software,[40] which were used to quantify biofilm biomass and thickness.

Radical Scavenging Activity Determination. The capacity of the N-HA compounds to scavenge free radicals was evaluated by determining the in vitro scavenging of the stable free radical DPPH· (Sigma-Aldrich), which has an absorption peak at 517 nm in its radical form. Twofold dilutions of the different compounds were prepared in methanol in a 96 well microplate with final concentrations ranging from 256 to 0.5 μM, and DPPH· dissolved in methanol was added to initiate the reaction with a final concentration of 70 μM. The microplate was incubated at 30 °C under dark conditions, and the absorbance was read at 517 nm after 8 and 12 h of incubation using a microplate reader (Infinite M200 Microplate Reader, Tecan). AA and HU were used as reference radical scavengers. The percentage of radical inhibition was calculated using the absorbance value of 70 μM DPPH· without any compound as a reference, and the IC_{50} value for each compound was calculated from the linear interval of the curve.

Analysis of NrdA Expression Using Western Immunoblot. *P. aeruginosa* PAO1 NrdA expression was determined in protein extracts from cultures in the presence or absence of N-HA compounds or HU. To do so, Western blot was performed, as previously described.[20] SDS–PAGE with normalized protein extracts was run, transfer was carried out in a PVDF membrane, and blotting was done using anti-NrdA rabbit polyclonal antibody (Agrisera, Sweden) at a 1/750 dilution and Goat Anti-Rabbit IgG HRP Conjugate (Bio-Rad) as a secondary antibody at a 1/500 dilution. Amersham ECL Prime Western Blotting Detection Reagent (GE Healthcare) was used for chemiluminescence detection and visualized using the LAS4000 mini system (GE Healthcare).

DPA Assay for dNTP Quantification. dNTP levels in *P. aeruginosa* PAO1 cultures were determined following the DPA assay for purine dNTP estimation, as previously described.[28,29] Bacterial pellets from PAO1 cultured in the presence or absence of N-HA compounds or HU were suspended in a lysis buffer (50 mM Tris-HCl, pH 7.4, 100 mM NaCl, 5 mM DTT, 5% glycerol), sonicated in an ultrasonic processor (Branson Sonifier SFX550) until clear, and centrifuged at 20,000*g* for 30 min. Pellet was discarded, and the protein concentration of bacterial extracts was quantified using Bradford assay (Bio-Rad). Protein concentration was then adjusted for all the samples, and 0.1 mL of each extract was mixed with 0.4 mL of 0.5 M chloroacetamide in 0.25 M potassium phosphate buffer (pH 7.3). The mixture was incubated for 10 min at 90 °C and cooled to room temperature, and 2 mL of DPA reagent (2 g of DPA dissolved in 100 mL of acetic acid and 2.75 mL of sulfuric acid) was added and incubated at 38 °C for 4 h. Absorbance values at a wavelength of 595 nm were used to determine relative dNTP levels.

Statistical Analysis. All data were statistically analyzed using GraphPad Prism version 6.00 for Mac OS X (GraphPad Software, USA).

■ ASSOCIATED CONTENT

Ⓢ Supporting Information

The Supporting Information is available free of charge on the ACS Publications website at DOI: 10.1021/acsomega.8b01384.

^{1}H NMR, ^{13}C NMR, and ^{19}F NMR spectra of all synthesized N-HA compounds (PDF)

■ AUTHOR INFORMATION

Corresponding Authors

*E-mail: albericio@ub.edu (F.A.).
*E-mail: etorrents@ibecbarcelona.eu (E.T.)

ORCID

Fernando Albericio: 0000-0002-8946-0462
Eduard Torrents: 0000-0002-3010-1609

Author Contributions

[#]These authors contributed equally to this work.

Author Contributions

The manuscript was written through contributions of all authors. All authors have given approval to the final version of the manuscript. L.M.-C. and A.B. contributed equally to this work. L.M.-C. designed and synthesized the library of *N*-hydroxylamines analogues and wrote the manuscript. A.B. and E.J. performed biological assays and wrote the manuscript. J.A. performed flow biofilm inhibition assays. A.L.-R. synthesized

N-hydroxylamines compounds. F.A. directed the research and revised the experimental data. E.T. directed the research, revised the experimental data, and wrote the manuscript.

Funding

This study was partially supported by grants from the *Ministerio de Economia y Competitividad* (BIO2015-63557-R, SAF2015-63867-R, and CTQ2015-67870-P), *AGAUR-Generalitat de Catalunya* (2017SGR-229, 2014SGR-1260, 2014SGR-137, and 2017SGR-1079), the European Regional Development Fund (FEDER), Catalan and Spanish cystic fibrosis federation, the EIT Health, and Obra Social "La Caixa" to E.T., E.J., and F.A.

Notes

The authors declare no competing financial interest.

■ ACKNOWLEDGMENTS

A.B. is thankful to the Ministerio de Educación, Cultura y Deporte for its financial support through the FPU programme (FPU13/06083).

■ ABBREVIATIONS

RNR, ribonucleotide reductase; MIC, minimum inhibitory concentration; CFU, colony-forming units; FRS, free-radical scavengers

■ REFERENCES

(1) Boucher, H. W.; Talbot, G. H.; Bradley, J. S.; Edwards, J. E.; Gilbert, D.; Rice, L. B.; Scheld, M.; Spellberg, B.; Bartlett, J. Bad bugs, No Drugs: No ESKAPE! An Update from the Infectious Diseases Society of America. *Clin. Infect. Dis.* **2009**, *48*, 1−12.

(2) Fair, R. J.; Tor, Y. Antibiotics and Bacterial Resistance in the 21st Century. *Perspect. Med. Chem.* **2014**, *6*, 25−64.

(3) Lebeaux, D.; Ghigo, J.-M.; Beloin, C. Biofilm-Related Infections: Bridging the Gap between Clinical Management and Fundamental Aspects of Recalcitrance toward Antibiotics. *Microbiol. Mol. Biol. Rev.* **2014**, *78*, 510−543.

(4) Bryers, J. D. Medical Biofilms. *Biotechnol. Bioeng.* **2008**, *100*, 1−18.

(5) Costerton, J. W.; Stewart, P. S.; Greenberg, E. P. Bacterial Biofilms: A Common Cause of Persistent Infections. *Science* **1999**, *284*, 1318−1322.

(6) Hall-Stoodley, L.; Stoodley, P. Evolving Concepts in Biofilm Infections. *Cell. Microbiol.* **2009**, *11*, 1034−1043.

(7) Høiby, N.; Bjarnsholt, T.; Givskov, M.; Molin, S.; Ciofu, O. Antibiotic Resistance of Bacterial Biofilms. *Int. J. Antimicrob. Agents* **2010**, *35*, 322−332.

(8) Sadekuzzaman, M.; Yang, S.; Mizan, M. F. R.; Ha, S. D. Current and Recent Advanced Strategies for Combating Biofilms. *Compr. Rev. Food Sci. Food Saf.* **2015**, *14*, 491−509.

(9) Torrents, E. Ribonucleotide Reductases: Essential Enzymes for Bacterial Life. *Front. Cell. Infect. Microbiol.* **2014**, *4*, 52.

(10) Lundin, D.; Berggren, G.; Logan, D. T.; Sjöberg, B.-M. The Origin and Evolution of Ribonucleotide Reduction. *Life* **2015**, *5*, 604−636.

(11) Hofer, A.; Crona, M.; Logan, D. T.; Sjöberg, B.-M. DNA Building Blocks: Keeping Control of Manufacture. *Crit. Rev. Biochem. Mol. Biol.* **2012**, *47*, 50−63.

(12) Cotruvo, J. A., Jr.; Stubbe, J. Class I Ribonucleotide Reductases: Metallocofactor Assembly and Repair in Vitro and in Vivo. *Annu. Rev. Biochem.* **2011**, *80*, 733−767.

(13) Lundin, D.; Gribaldo, S.; Torrents, E.; Sjöberg, B.-M.; Poole, A. M. Ribonucleotide Reduction - Horizontal Transfer of a Required Function Spans All Three Domains. *BMC Evol. Biol.* **2010**, *10*, 383.

(14) Cerqueira, N. M. F. S. A.; Fernandes, P. A.; Ramos, M. J. Ribonucleotide Reductase: A Critical Enzyme for Cancer Chemotherapy and Antiviral Agents. *Recent Pat. Anti-Cancer Drug Discovery* **2007**, *2*, 11−29.

(15) Aye, Y.; Li, M.; Long, M. J. C.; Weiss, R. S. Ribonucleotide Reductase and Cancer: Biological Mechanisms and Targeted Therapies. *Oncogene* **2015**, *34*, 2011−2021.

(16) Moorthy, N. S. H. N.; Cerqueira, N. M. F. S. A.; Ramos, M. J.; Fernandes, P. A. Development of Ribonucleotide Reductase Inhibitors: A Review on Structure Activity Relationships. *Mini-Rev. Med. Chem.* **2013**, *13*, 1862−1872.

(17) Saban, N.; Bujak, M. Hydroxyurea and Hydroxamic Acid Derivatives as Antitumor Drugs. *Cancer Chemother. Pharmacol.* **2009**, *64*, 213−221.

(18) Basu, A.; Sinha, B. N. Radical Scavengers as Ribonucleotide Reductase Inhibitors. *Curr. Top. Med. Chem.* **2012**, *12*, 2827−2842.

(19) Torrents, E.; Sahlin, M.; Biglino, D.; Gräslund, A.; Sjöberg, B.-M. Efficient Growth Inhibition of *Bacillus anthracis* by Knocking Out the Ribonucleotide Reductase Tyrosyl Radical. *Proc. Natl. Acad. Sci. U. S. A.* **2005**, *102*, 17946−17951.

(20) Torrents, E.; Sjöberg, B.-M. Antibacterial Activity of Radical Scavengers against Class Ib Ribonucleotide Reductase from *Bacillus anthracis*. *Biol. Chem.* **2010**, *391*, 229−234.

(21) Wang, E. S. Treating Acute Myeloid Leukemia in Older Adults. *Hematology* **2014**, *2014*, 14−20.

(22) Ferrara, F. Conventional Chemotherapy or Hypomethylating Agents for Older Patients with Acute Myeloid Leukaemia? *Hematol. Oncol.* **2014**, *32*, 1−9.

(23) Julián, E.; Baelo, A.; Gavaldà, J.; Torrents, E. Methyl-Hydroxylamine as an Efficacious Antibacterial Agent that Targets the Ribonucleotide Reductase Enzyme. *PLoS One* **2015**, *10*, e0122049.

(24) Amorati, R.; Lucarini, M.; Mugnaini, V.; Pedulli, G. F.; Minisci, F.; Recupero, F.; Fontana, F.; Astolfi, P.; Greci, L. Hydroxylamines as Oxidation Catalysts: Thermochemical and Kinetic Studies. *J. Org. Chem.* **2003**, *68*, 1747−1754.

(25) Dao, R.; Wang, X.; Chen, K.; Zhao, C.; Yao, J.; Li, H. Landscape of the Structure−O−H Bond Dissociation Energy Relationship of Oximes and Hydroxylamines. *Phys. Chem. Chem. Phys.* **2017**, *19*, 22309−22320.

(26) Heydari, A.; Tavakol, H.; Aslanzadeh, S.; Azarnia, J.; Ahmadi, N. A General One-Pot, Three-Component Mono N-Alkylation of Amines and Amine Derivatives in Lithium Perchlorate/Diethyl Ether Solution. *Synthesis* **2005**, *2005*, 627−633.

(27) Saiko, P.; Steinmann, M.-T.; Schuster, H.; Graser, G.; Bressler, S.; Giessrigl, B.; Lackner, A.; Grusch, M.; Krupitza, G.; Bago-Horvath, Z.; Jaeger, W.; Fritzer-Szekeres, M.; Szekeres, T. Epigallocatechin Gallate, Ellagic Acid, and Rosmarinic Acid Perturb dNTP Pools and Inhibit De Novo DNA Synthesis and Proliferation of Human HL-60 Promyelocytic Leukemia Cells: Synergism with Arabinofuranosylcytosine. *Phytomedicine* **2015**, *22*, 213−222.

(28) Blakley, R. L. Cobamides and Ribonucleotide Reduction. II. Estimation of the Enzymic Formation of Purine and Pyrimidine Deoxyribonucleotides by the Use of the Diphenylamine Reagent. *J. Biol. Chem.* **1966**, *241*, 176−179.

(29) Crespo, A.; Pedraz, L.; Torrents, E. Function of the *Pseudomonas aeruginosa* NrdR Transcription Factor: Global Transcriptomic Analysis and Its Role on Ribonucleotide Reductase Gene Expression. *PLoS One* **2015**, *10*, e0123571.

(30) Filpula, D.; Fuchs, J. A. Regulation of the Synthesis of Ribonucleoside Diphosphate Reductase in *Escherichia coli*: Specific Activity of the Enzyme in Relationship to Perturbations of DNA Replication. *J. Bacteriol.* **1978**, *135*, 429−435.

(31) Lebeaux, D.; Chauhan, A.; Rendueles, O.; Beloin, C. From in Vitro to in Vivo Models of Bacterial Biofilm-Related Infections. *Pathogens* **2013**, *2*, 288−356.

(32) Baelo, A.; Levato, R.; Julián, E.; Crespo, A.; Astola, J.; Gavaldà, J.; Engel, E.; Mateos-Timoneda, M. A.; Torrents, E. Disassembling Bacterial Extracellular Matrix with DNase-Coated Nanoparticles To Enhance Antibiotic Delivery in Biofilm Infections. *J. Controlled Release* **2015**, *209*, 150−158.

(33) Sjöberg, B.-M.; Torrents, E. Shift in Ribonucleotide Reductase Gene Expression in *Pseudomonas aeruginosa* during Infection. *Infect. Immun.* **2011**, *79*, 2663–2669.

(34) Torrents, E.; Poplawski, A.; Sjöberg, B.-M. Two Proteins Mediate Class II Ribonucleotide Reductase Activity in *Pseudomonas aeruginosa*: Expression and Transcriptional Analysis of the Aerobic Enzymes. *J. Biol. Chem.* **2005**, *280*, 16571–16578.

(35) Luo, J.; Graslund, A. Ribonucleotide Reductase Inhibition by *p*-Alkoxyphenols Studied by Molecular Docking and Molecular Dynamics Simulations. *Arch. Biochem. Biophys.* **2011**, *516*, 29–34.

(36) del Mar Cendra, M.; Juárez, A.; Torrents, E. Biofilm Modifies Expression of Ribonucleotide Reductase Genes in *Escherichia coli*. *PLoS One* **2012**, *7*, e46350.

(37) Clinical and Laboratory Standards Institute. *Methods for Dilution and Antimicrobial Susceptibility Test for Bacteria that Grow Aerobically: Approved Standard*, 7th ed.; CLSI Document M7-A7; Clinical and Laboratory Standards Institute: Wayne, PA, 2006.

(38) Harrison, J. J.; Stremick, C. A.; Turner, R. J.; Allan, N. D.; Olson, M. E.; Ceri, H. Microtiter Susceptibility Testing of Microbes Growing on Peg Lids: A Miniaturized Biofilm Model for High-Throughput Screening. *Nat. Protoc.* **2010**, *5*, 1236–1254.

(39) Christensen, B. B.; Sternberg, C.; Andersen, J. B.; Palmer, R. J., Jr.; Nielsen, A. T.; Givskov, M.; Molin, S. [2] Molecular Tools for Study of Biofilm Physiology. *Methods Enzymol.* **1999**, *310*, 20–42.

(40) Heydorn, A.; Nielsen, A. T.; Hentzer, M.; Sternberg, C.; Givskov, M.; Ersbøll, B. K.; Molin, S. Quantification of Biofilm Structures by the Novel Computer Program COMSTAT. *Microbiology* **2000**, *146*, 2395–2407.

Supporting Information

Hydroxylamine derivatives as a new paradigm in the search of antibacterial agents

Laia Miret-Casals$^{\alpha}$, Aida Baelo$^{\alpha}$, Esther Julián, Josep Astola, Ariadna Lobo-Ruiz, Fernando Albericio* and Eduard Torrents*

$^{\alpha}$ These authors contributed equally to this work.

*Corresponding authors:
Dr. Eduard torrents: etorrents@ibecbarcelona.eu
Prof. Fernando Albericio: albericio@ub.edu

Table of Contents:

^{1}H NMR spectrum of *N-Hydroxy-3-methylbutan-1-amine* (**5**) S2

^{13}C NMR spectrum of *N-Hydroxy-3-methylbutan-1-amine* (**5**) S3

^{1}H NMR spectrum of *N-(4-Fluoro-2-methylbenzyl)hydroxylamine* (**12**) S4

^{13}C NMR spectrum of *N-(4-Fluoro-2-methylbenzyl)hydroxylamine* (**12**) S5

^{19}F NMR spectrum of *N-(4-Fluoro-2-methylbenzyl)hydroxylamine* (**12**) S6

^{1}H NMR spectrum of *N-[4-Fluoro-2-(trifluoromethyl)benzyl)]hydroxylamine* (**13**) S7

^{13}C NMR spectrum of *N-[4-Fluoro-2-(trifluoromethyl)benzyl)]hydroxylamine* (**13**) S8

^{19}F NMR spectrum of *N-[4-Fluoro-2-(trifluoromethyl)benzyl)]hydroxylamine* (**13**) S9

^{1}H NMR spectrum of *N-[3,5-Difluorobenzyl]hydroxylamine* (**14**) S10

^{13}C NMR spectrum of *N-[3,5-Difluorobenzyl]hydroxylamine* (**14**) S11

^{19}F NMR spectrum of *N-[3,5-Difluorobenzyl]hydroxylamine* (**14**) S12

^{1}H NMR spectrum of *N-(4-Methoxy-2-methylbenzyl)hydroxylamine* (**17**) S13

^{13}C NMR spectrum of *N-(4-Methoxy-2-methylbenzyl)hydroxylamine* (**17**) S14

^{1}H NMR spectrum of *N-(2,6-Dimethoxybenzyl)hydroxylamine* (**19**) S15

^{13}C NMR spectrum of *N-(2,6-Dimethoxybenzyl)hydroxylamine* (**19**) S16

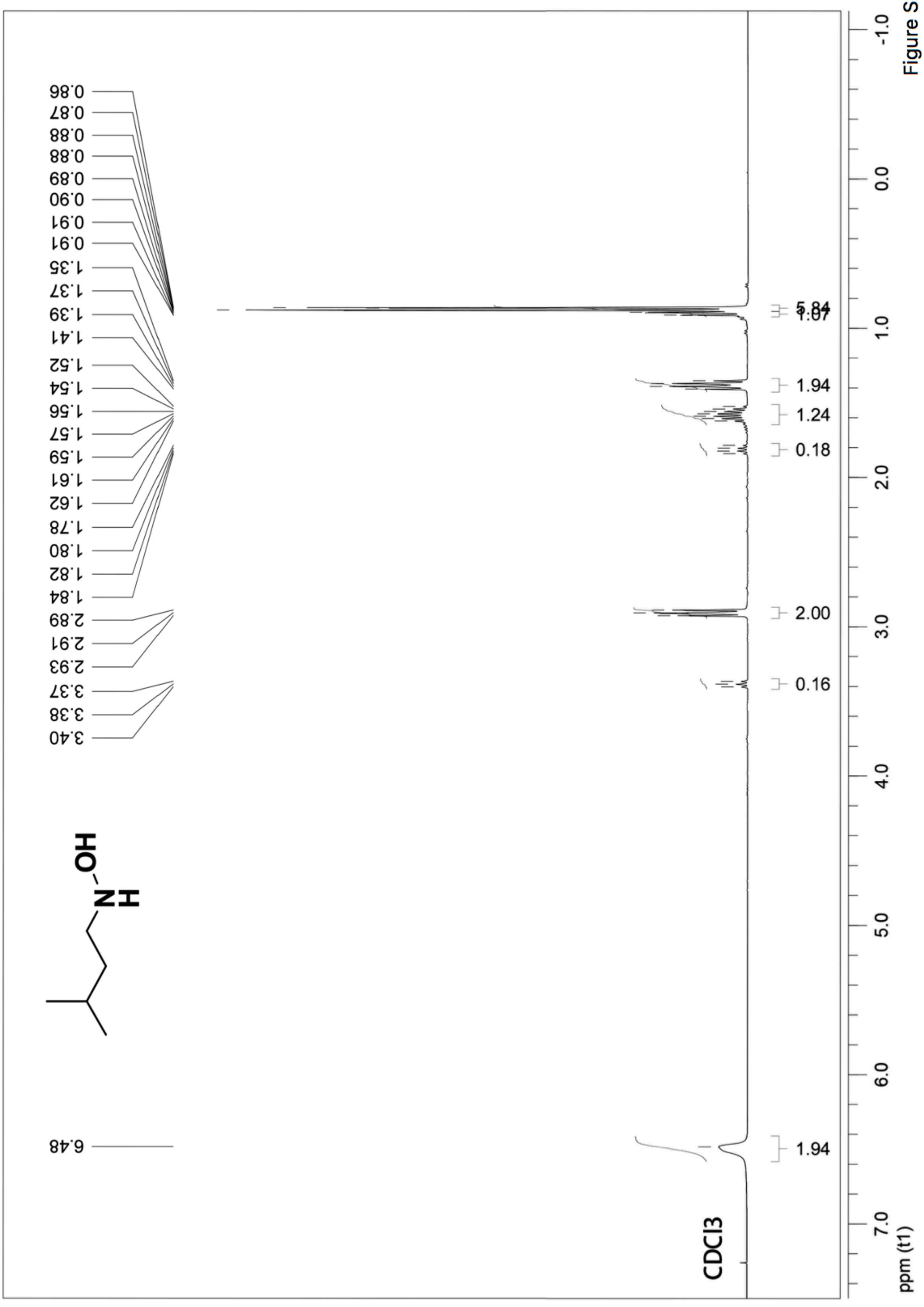
0.86
0.87
0.88
0.88
0.89
0.90
0.91
0.91
1.35
1.37
1.39
1.41
1.52
1.54
1.56
1.57
1.59
1.61
1.62
1.78
1.80
1.82
1.84
2.89
2.91
2.93
3.37
3.38
3.40
6.48
CDCl3
5.84
1.07
1.94
1.24
0.18
2.00
0.16
1.94
-1.0
0.0
1.0
2.0
3.0
4.0
5.0
6.0
7.0
ppm (t1)
OH
N
H

Figure S2

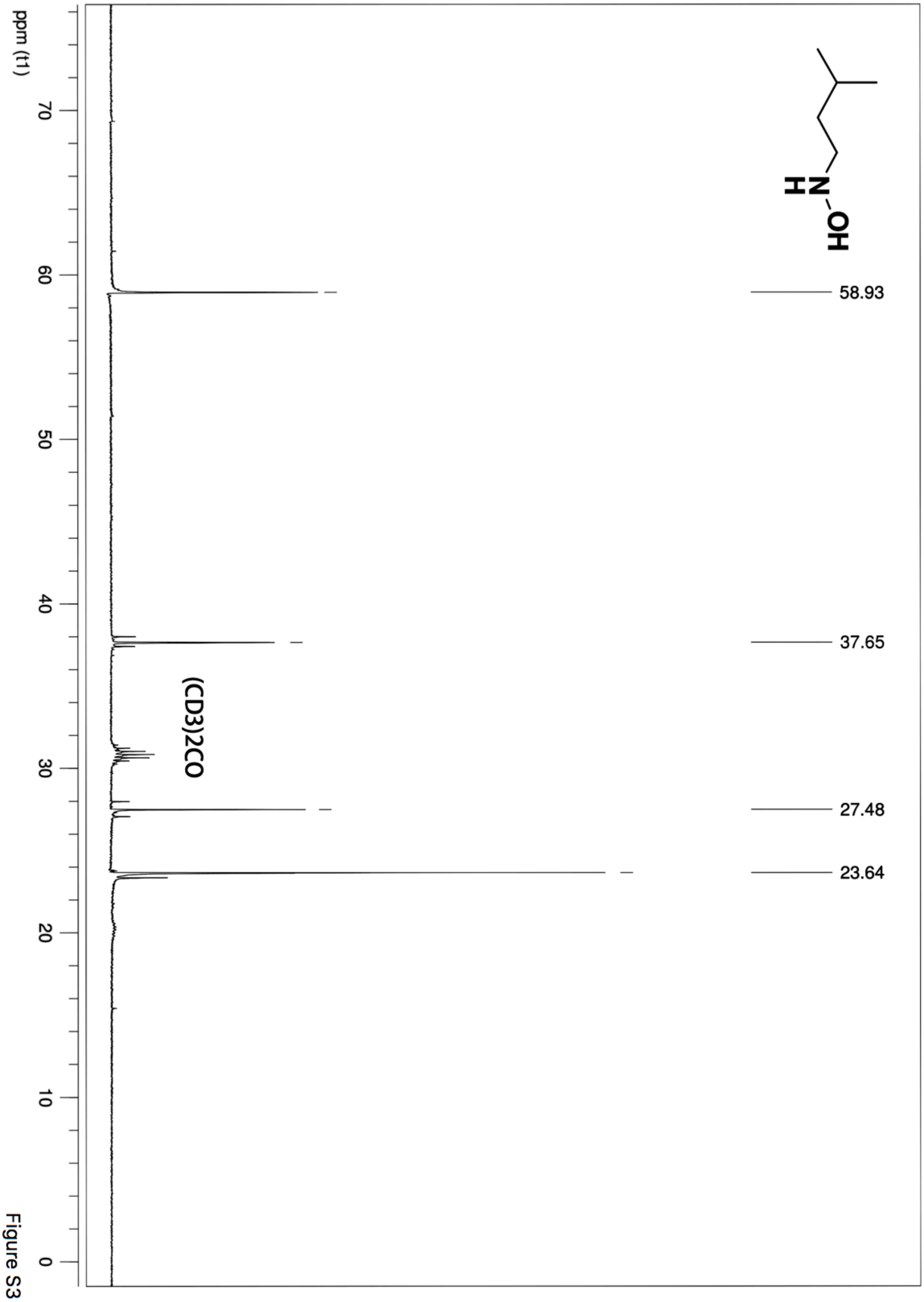

Figure S3

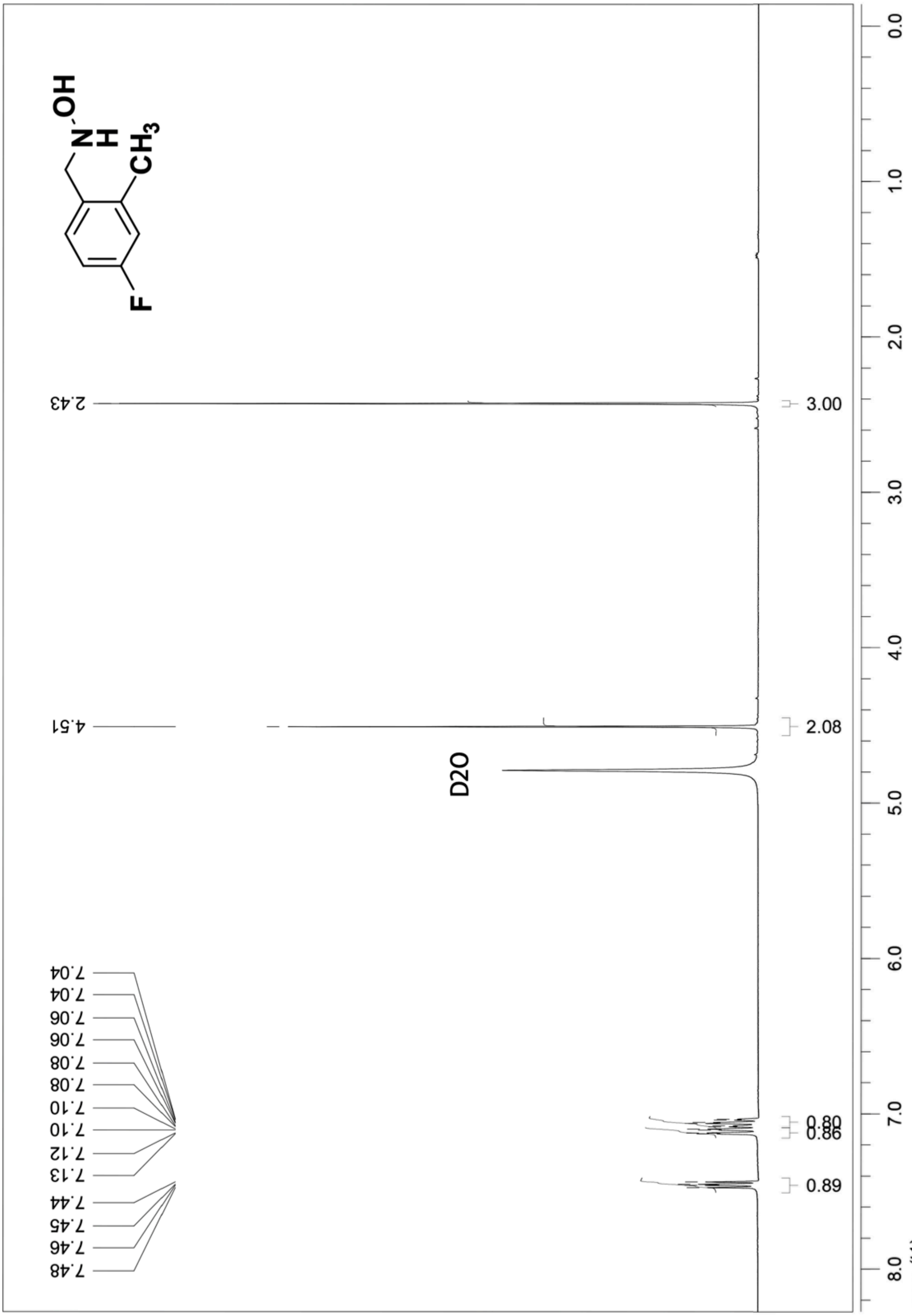
F
N
H
OH
CH3
2.43
4.51
7.04
7.04
7.06
7.06
7.08
7.08
7.10
7.10
7.12
7.13
7.44
7.45
7.46
7.48
D2O
3.00
2.08
0.80
0.86
0.89
0.0
1.0
2.0
3.0
4.0
5.0
6.0
7.0
8.0
ppm (t1)

Figure S4

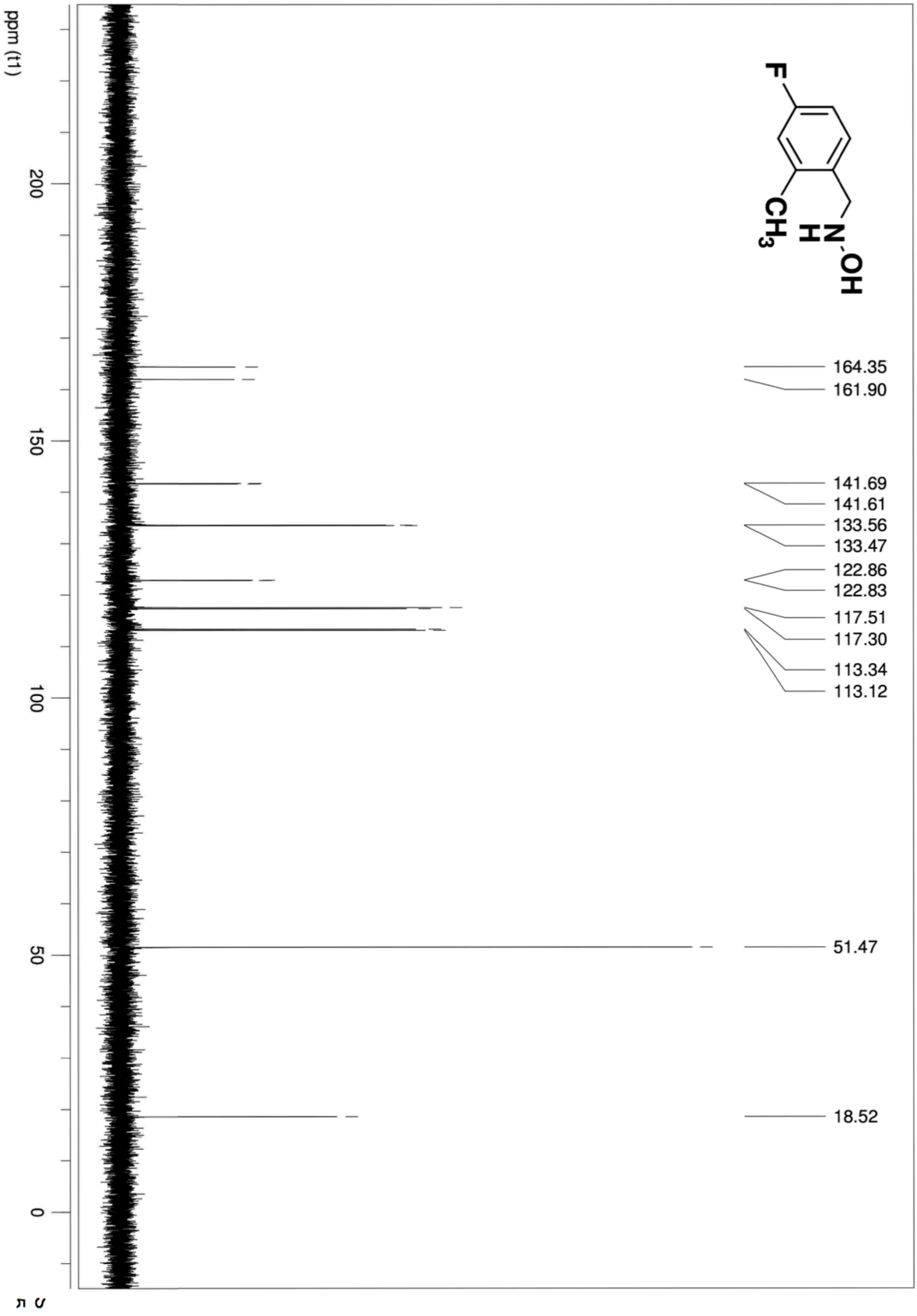
ppm (t1)
200
150
100
50
0
F
N
H
OH
CH3
164.35
161.90
141.69
141.61
133.56
133.47
122.86
122.83
117.51
117.30
113.34
113.12
51.47
18.52

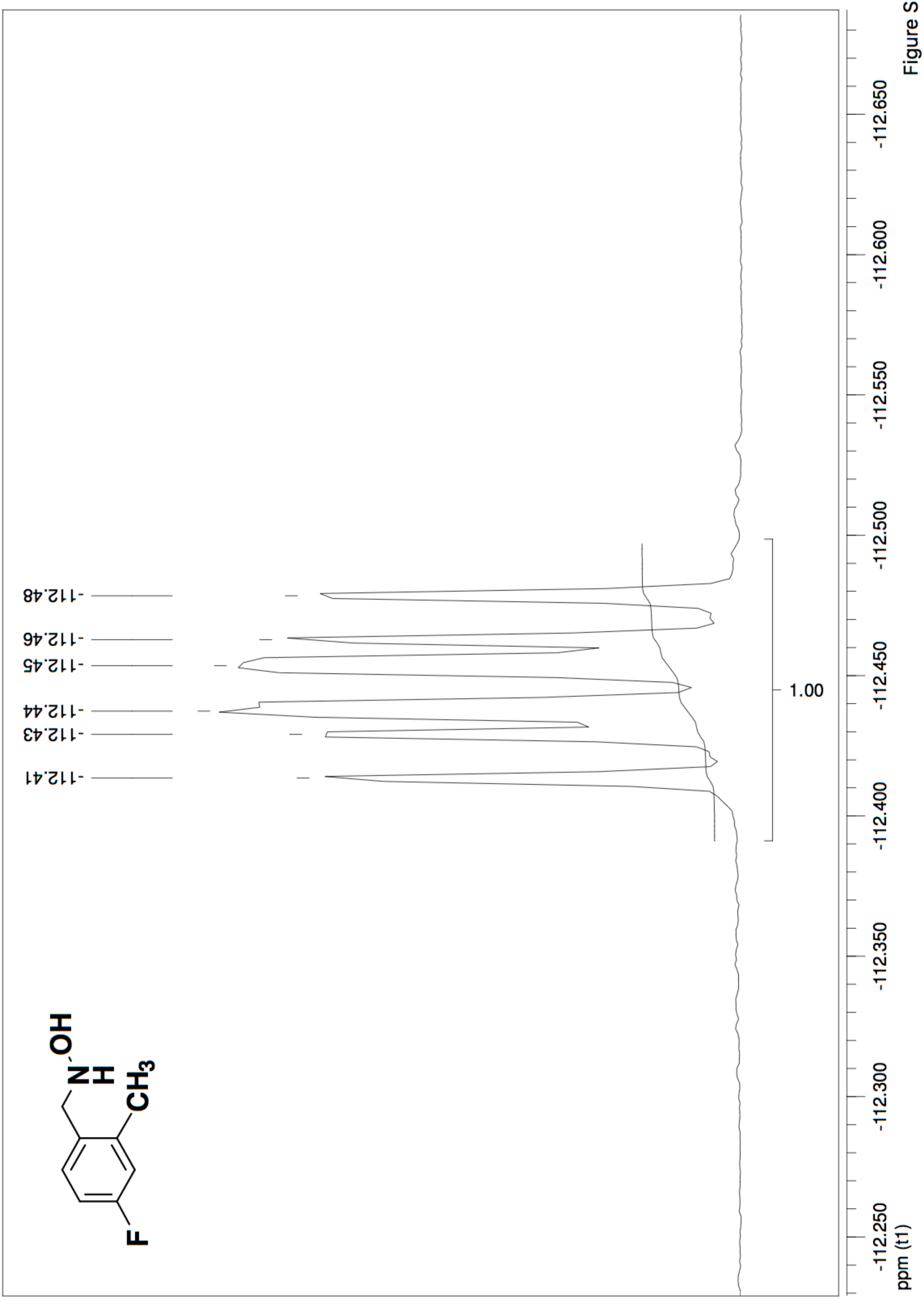
F
N
H
OH
CH3
-112.48
-112.46
-112.45
-112.44
-112.43
-112.41
1.00
-112.650
-112.600
-112.550
-112.500
-112.450
-112.400
-112.350
-112.300
-112.250
ppm (t1)

Figure S6

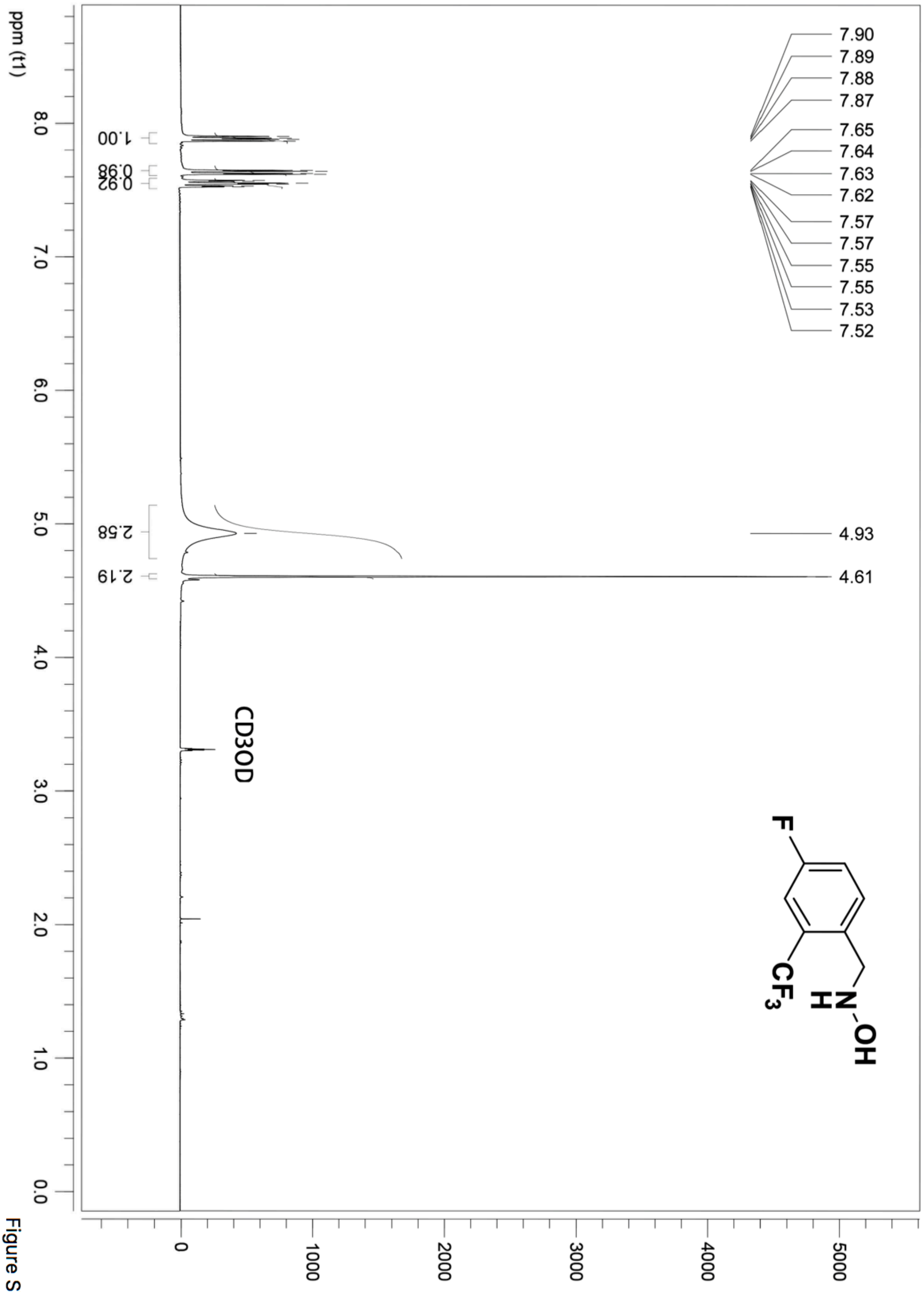
ppm (t1)
8.0
7.0
6.0
5.0
4.0
3.0
2.0
1.0
0.0
1.00
0.98
0.92
2.58
2.19
7.90
7.89
7.88
7.87
7.65
7.64
7.63
7.62
7.57
7.57
7.55
7.55
7.53
7.52
4.93
4.61
CD3OD
F
CF3
N
H
OH
0
1000
2000
3000
4000
5000

Figure S7

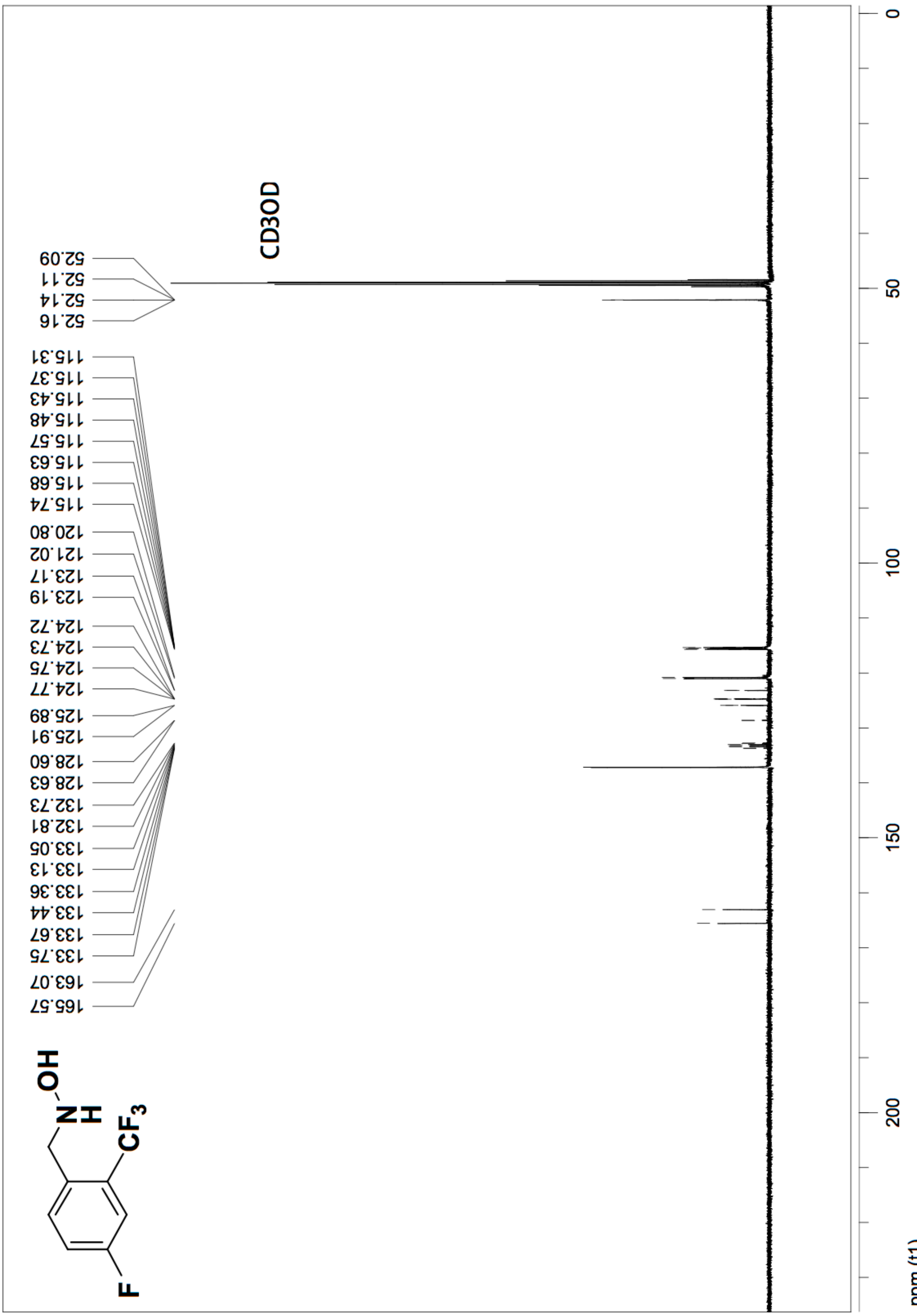
CD3OD
52.09
52.11
52.14
52.16
115.31
115.37
115.43
115.48
115.57
115.63
115.68
115.74
120.80
121.02
123.17
123.19
124.72
124.73
124.75
124.77
125.89
125.91
128.60
128.63
132.73
132.81
133.05
133.13
133.36
133.44
133.67
133.75
163.07
165.57
F
CF3
N
H
OH
0
50
100
150
200
ppm (t1)

Figure S8

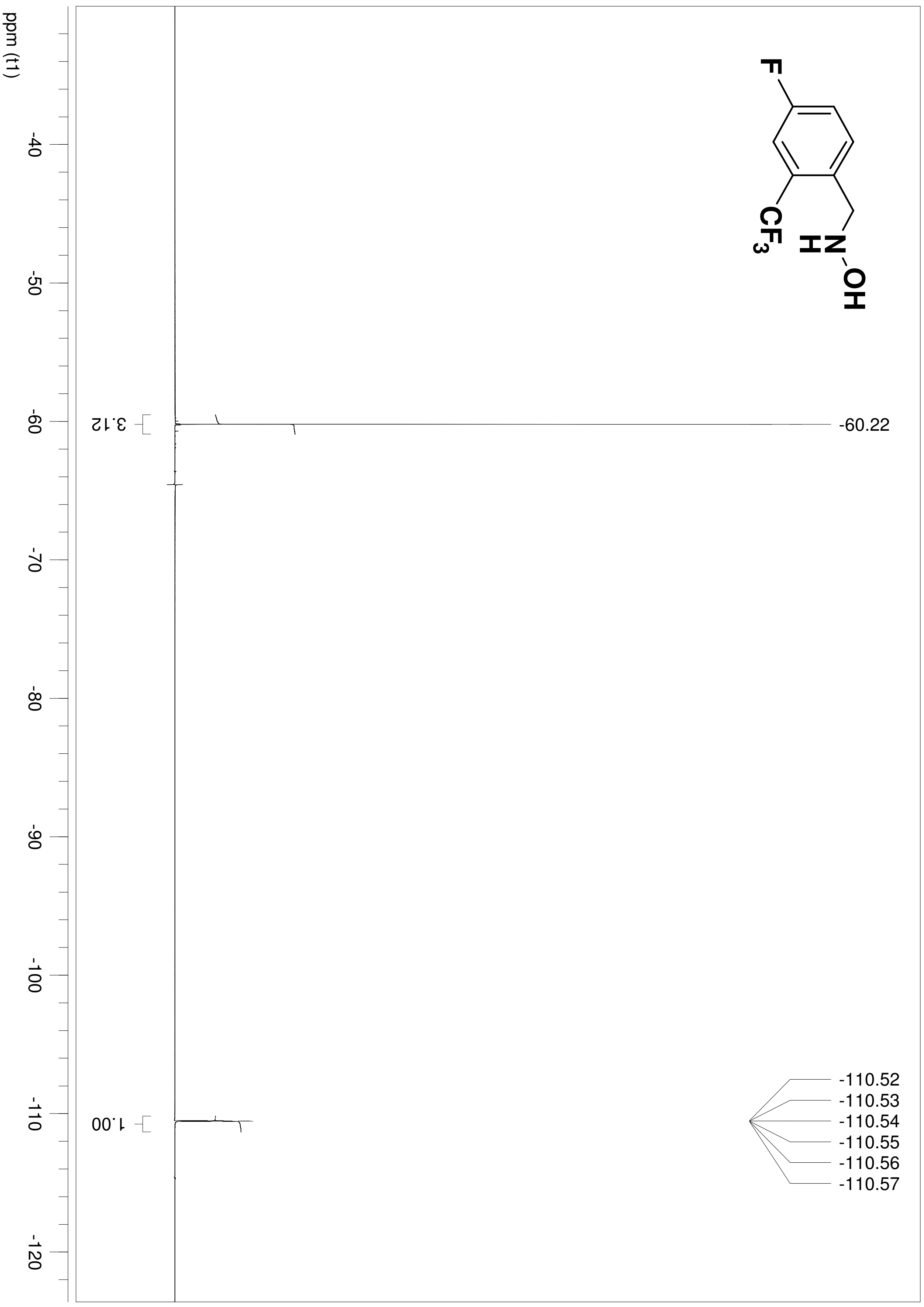
F
CF3
N
H
OH
-60.22
-110.52
-110.53
-110.54
-110.55
-110.56
-110.57
3.12
1.00
ppm (t1)
-40
-50
-60
-70
-80
-90
-100
-110
-120

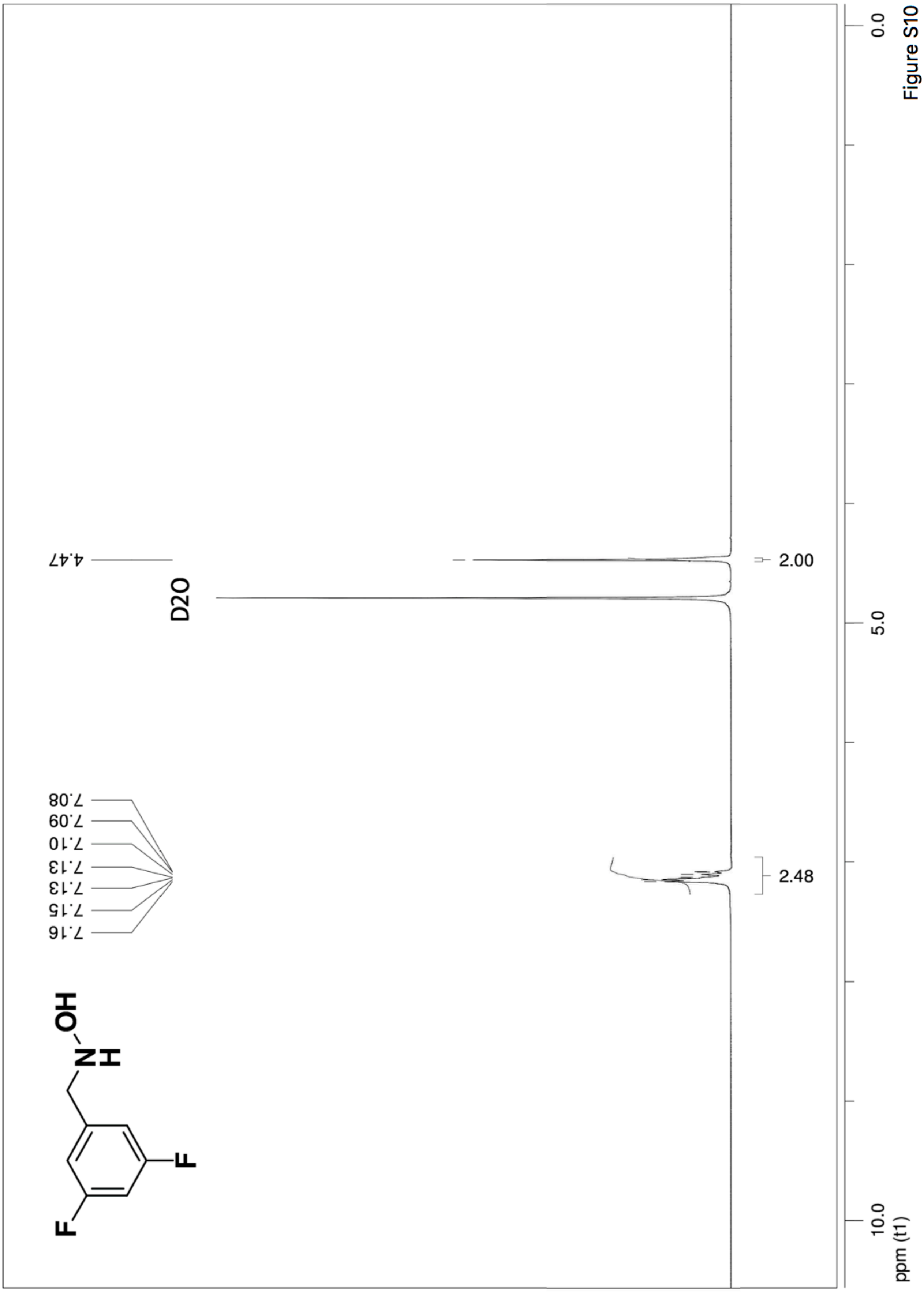
F
F
N
H
OH
7.08
7.09
7.10
7.13
7.13
7.15
7.16
4.47
D2O
2.00
2.48
0.0
5.0
10.0
ppm (t1)

Figure S10

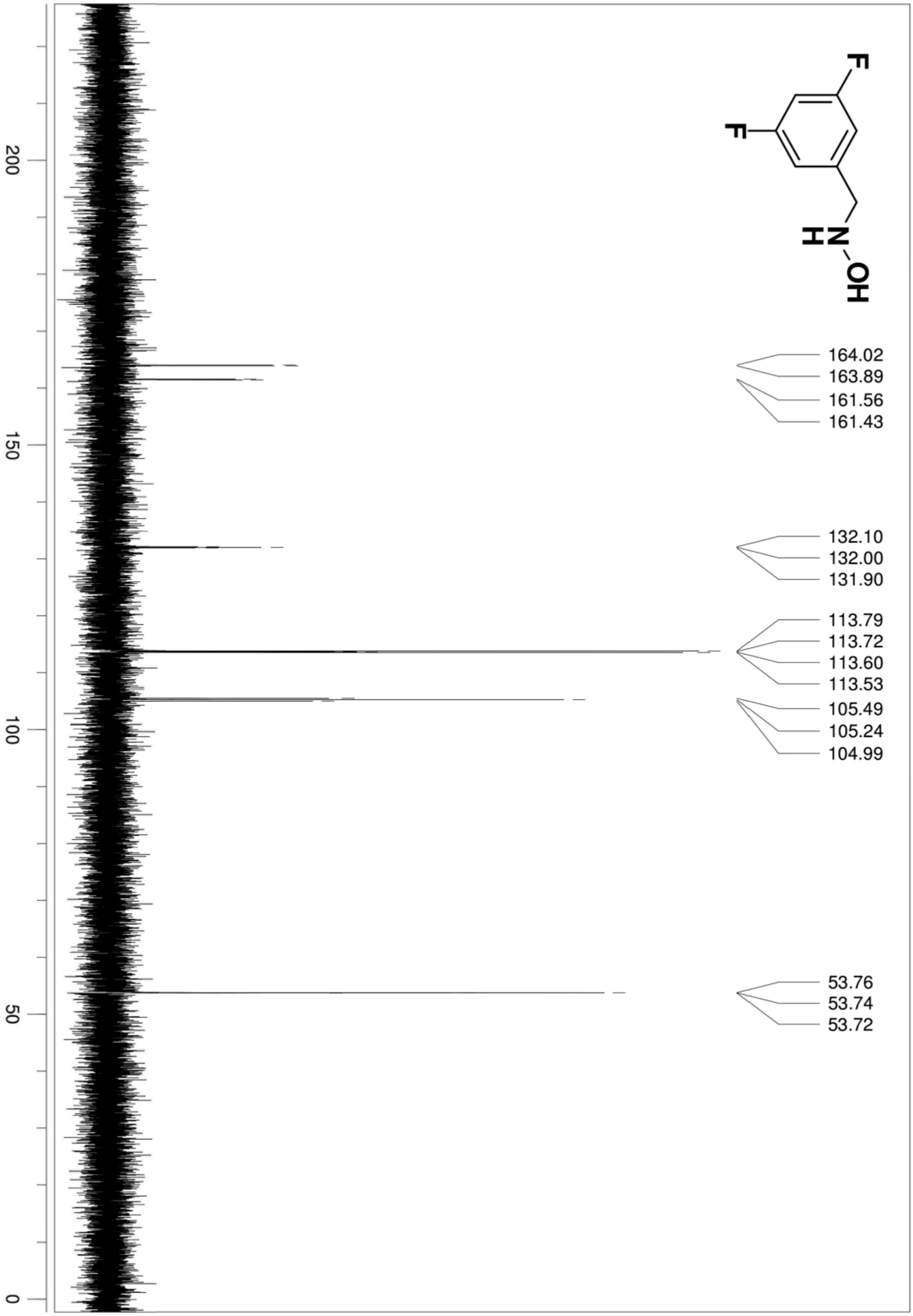
ppm (t1)
200
150
100
50
0
F
F
N
H
OH
164.02
163.89
161.56
161.43
132.10
132.00
131.90
113.79
113.72
113.60
113.53
105.49
105.24
104.99
53.76
53.74
53.72

Figure S11

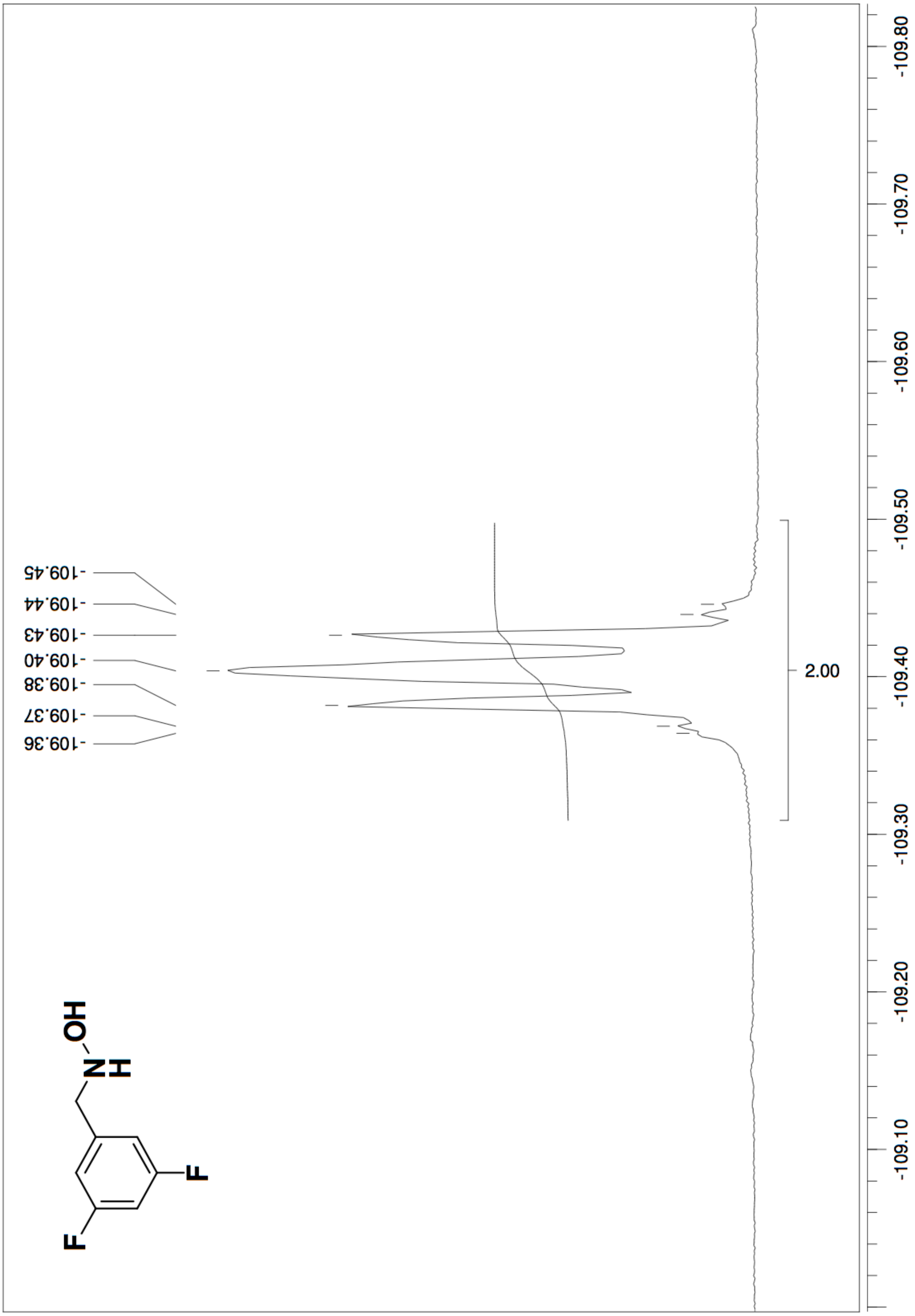
-109.45
-109.44
-109.43
-109.40
-109.38
-109.37
-109.36
2.00
F
F
N
H
OH
-109.80
-109.70
-109.60
-109.50
-109.40
-109.30
-109.20
-109.10
ppm (t1)

Figure S12

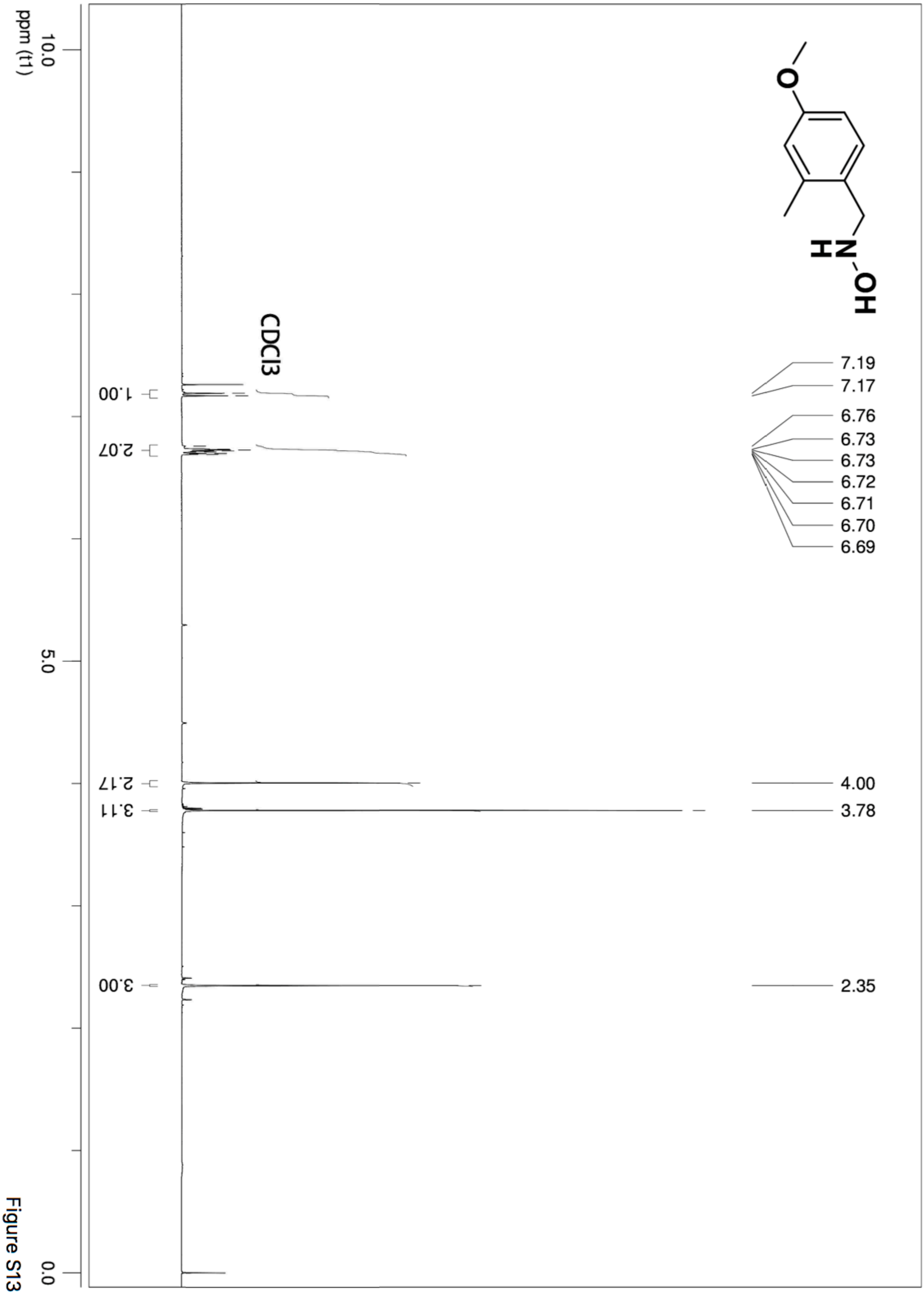
ppm (t1)
10.0
5.0
0.0
CDCl3
1.00
2.07
2.17
3.11
3.00
7.19
7.17
6.76
6.73
6.73
6.72
6.71
6.70
6.69
4.00
3.78
2.35
O
N
H
OH

Figure S13

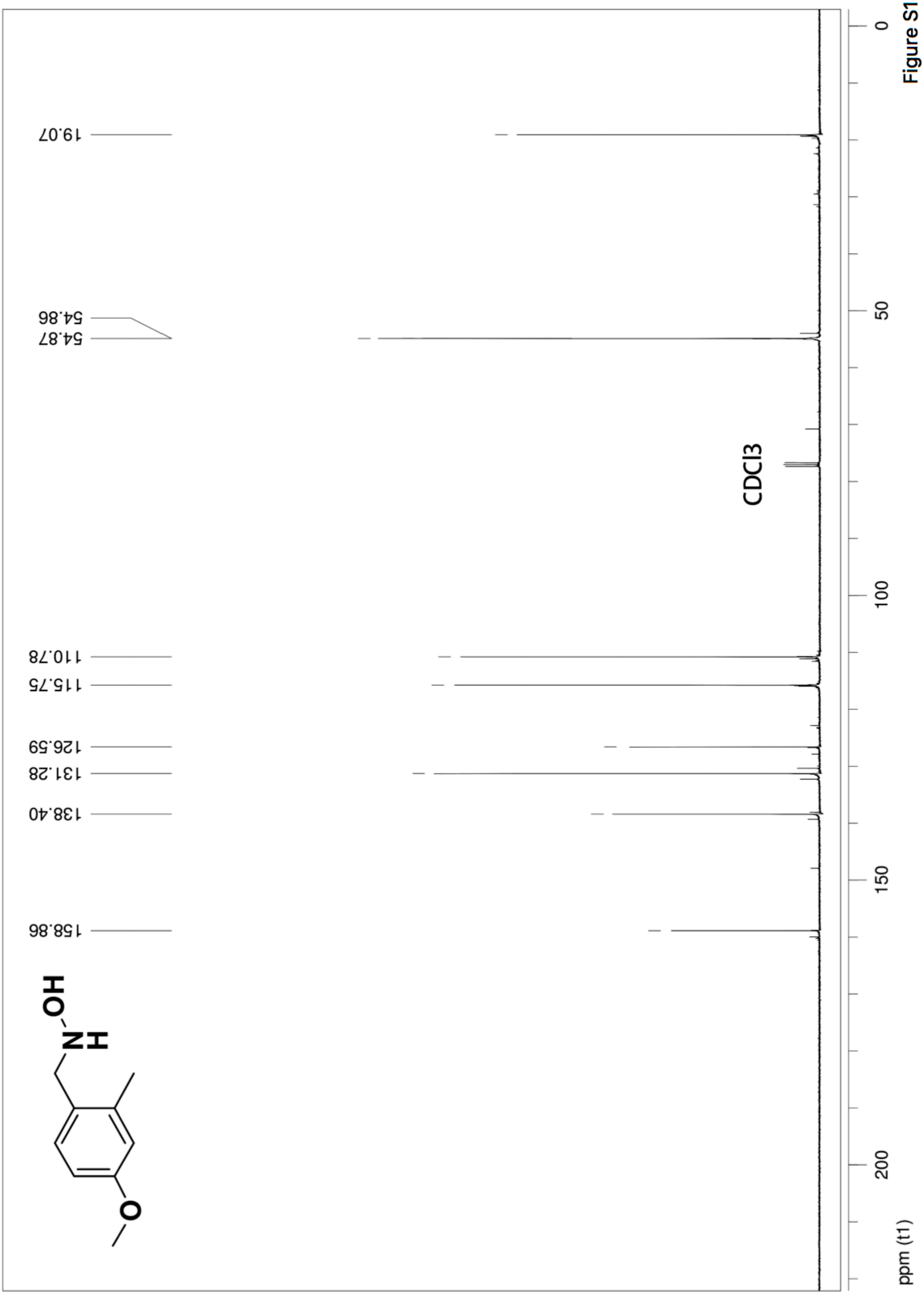
19.07
54.86
54.87
CDCl3
110.78
115.75
126.59
131.28
138.40
158.86
N
H
OH
O
0
50
100
150
200
ppm (t1)

Figure S14

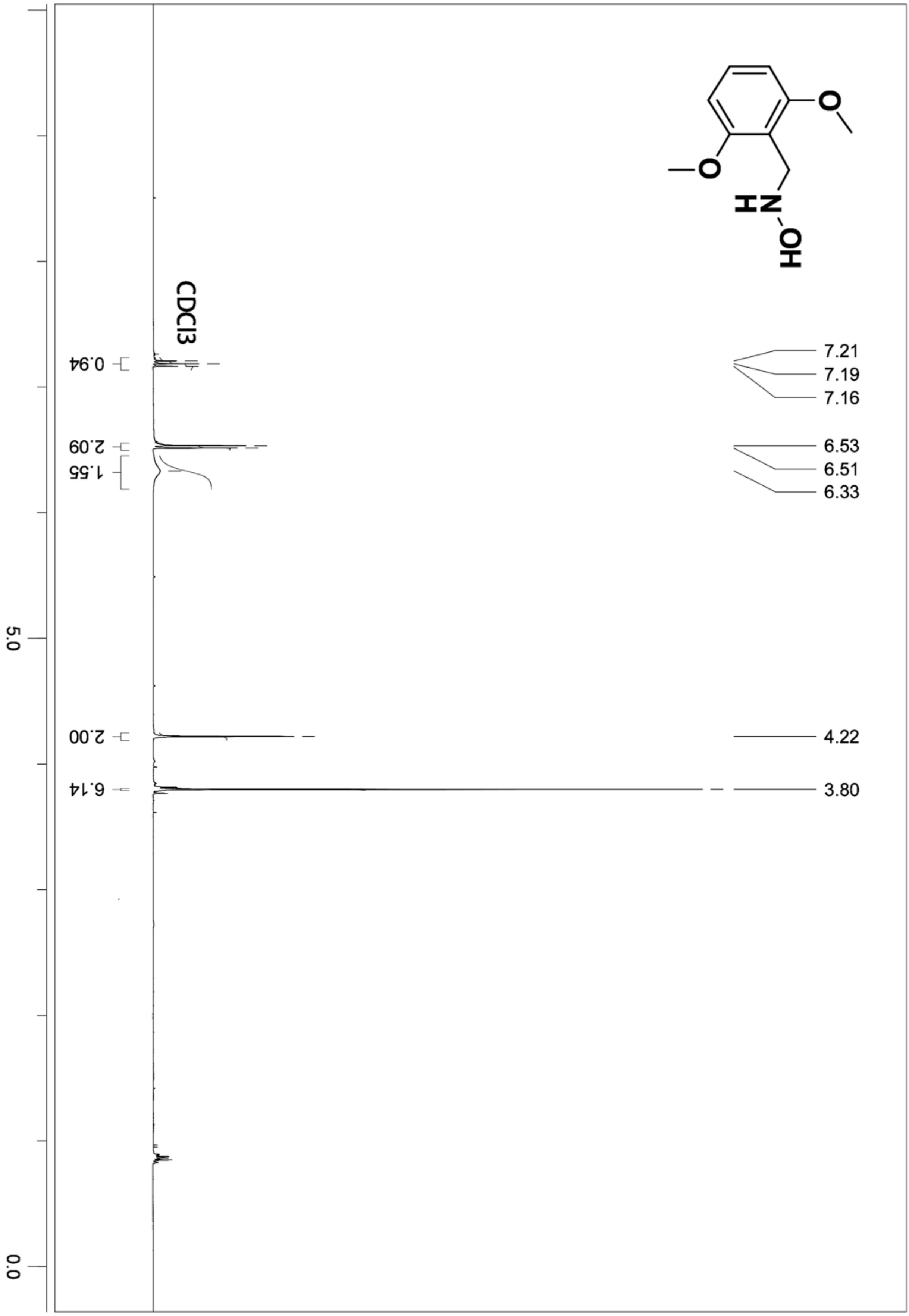
ppm (t1)
5.0
0.0
CDCl3
0.94
2.09
1.55
2.00
6.14
7.21
7.19
7.16
6.53
6.51
6.33
4.22
3.80
O
O
N
H
OH

Figure S15

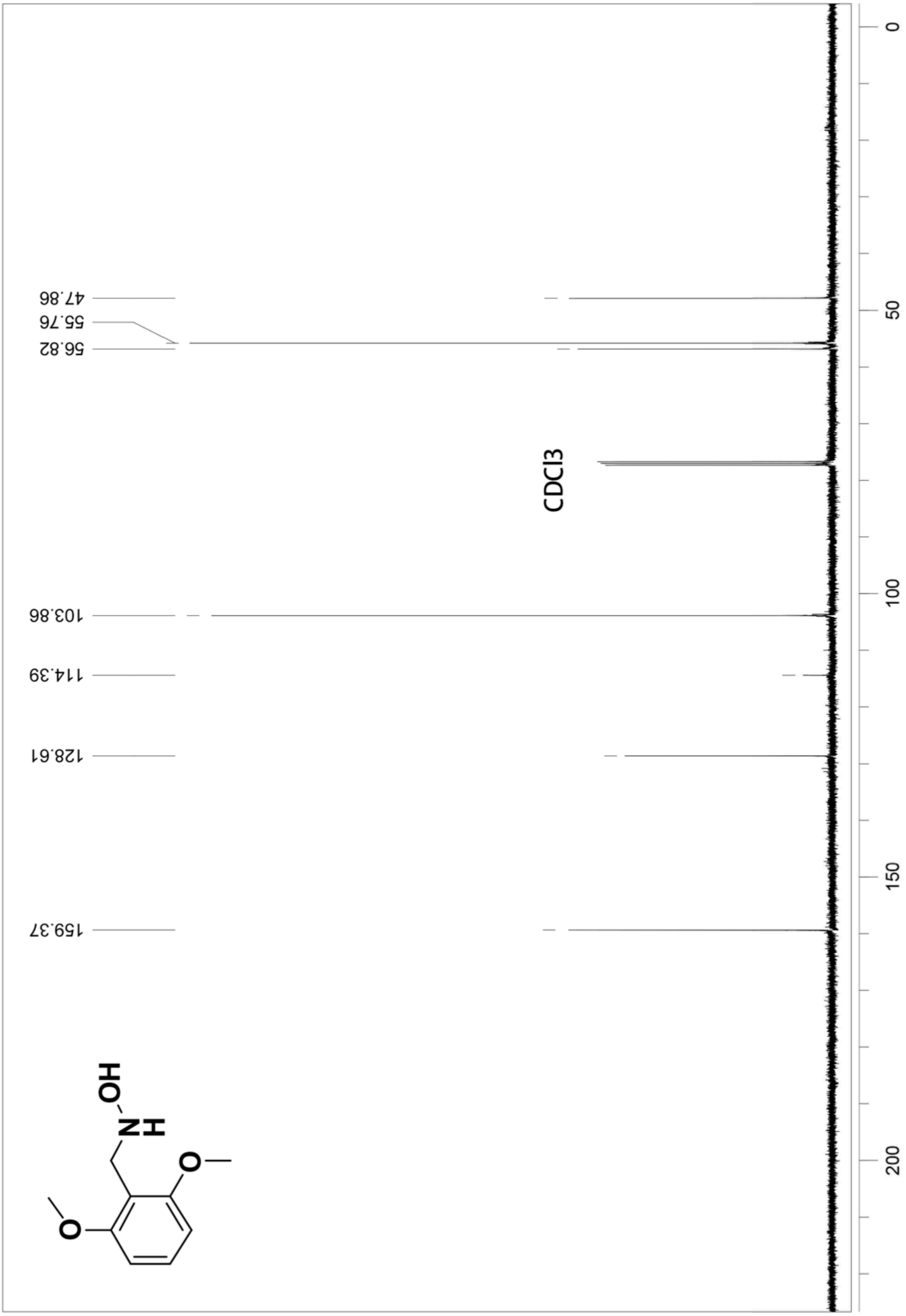
47.86
55.76
56.82
CDCl3
103.86
114.39
128.61
159.37
O
N
H
OH
O
0
50
100
150
200
ppm (t1)

Figure S16

Chapter 2: Improving the treatment of biofilm infections

PUBLICATION 3: Disassembling bacterial extracellular matrix with DNase-coated nanoparticles to enhance antibiotic delivery in biofilm infections

ABSTRACT: Infections caused by biofilm-forming bacteria are a major threat to hospitalized patients and the main cause of chronic obstructive pulmonary disease and cystic fibrosis. There is an urgent necessity for novel therapeutic approaches since current antibiotic delivery fails to eliminate biofilm-protected bacteria. In this study, ciprofloxacin-loaded poly(lactic-co-glycolic acid) nanoparticles, which were functionalized with DNase I, were fabricated using a green-solvent based method and their antibiofilm activity was assessed against *Pseudomonas aeruginosa* biofilms. Such nanoparticles constitute a paradigm shift in biofilm treatment since, besides releasing ciprofloxacin in a controlled fashion, they are able to target and disassemble the biofilm by degrading the extracellular DNA that stabilize the biofilm matrix. These carriers were compared with free-soluble ciprofloxacin, and ciprofloxacin encapsulated in untreated and poly(lysine)-coated nanoparticles. DNase I-activated nanoparticles were not only able to prevent biofilm formation from planktonic bacteria, but they also successfully reduced established biofilm mass, size and living cell density, as observed in a dynamic environment in a flow cell biofilm assay. Moreover, repeated administration over three days of DNase I-coated nanoparticles encapsulating ciprofloxacin was able to reduce by 95% and then eradicate more than 99.8% of established biofilm, outperforming all the other nanoparticle formulations and the free-drug tested in this study. These promising results, together with minimal cytotoxicity as tested on J774 macrophages, allow obtaining novel antimicrobial nanoparticles, as well as provide clues to design the next generation of drug delivery devices to treat persistent bacterial infections.

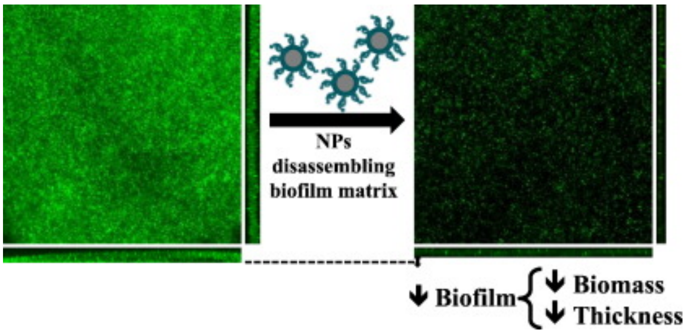

Journal of Controlled Release 209 (2015) 150–158

Contents lists available at ScienceDirect

Journal of Controlled Release

journal homepage: www.elsevier.com/locate/jconrel

Disassembling bacterial extracellular matrix with DNase-coated nanoparticles to enhance antibiotic delivery in biofilm infections

Aida Baelo [a,1], Riccardo Levato [b,c,1], Esther Julián [d], Anna Crespo [a], José Astola [a], Joan Gavaldà [e], Elisabeth Engel [b,c,f], Miguel Angel Mateos-Timoneda [b,c], Eduard Torrents [a,]*

[a] *Bacterial Infections and Antimicrobial Therapies, Institute for Bioengineering of Catalonia, Baldiri Reixac 15-21, 08028, Barcelona, Spain*
[b] *Biomaterials for Regenerative Therapies, Institute for Bioengineering of Catalonia, Baldiri Reixac 15-21, 08028, Barcelona, Spain*
[c] *CIBER en Bioingeniería, Biomateriales y Nanomedicina (CIBER-BBN), Barcelona, Spain*
[d] *Departament de Genètica i de Microbiologia, Facultat de Biociències, Universitat Autònoma de Barcelona, 08193 Bellaterra, Spain*
[e] *Infectious Diseases Research Laboratory, Infectious Diseases Department, Vall d'Hebron Research Institute VHIR, Hospital Universitari Vall d'Hebron, Barcelona, Spain*
[f] *Department of Materials Science and Metallurgy, Technical University of Catalonia (UPC), Barcelona, Spain*

ARTICLE INFO

Article history:
Received 3 February 2015
Received in revised form 20 April 2015
Accepted 21 April 2015
Available online 23 April 2015

Keywords:
Pseudomonas aeruginosa
Biofilm
Ciprofloxacin
DNase I
Nanoparticles

ABSTRACT

Infections caused by biofilm-forming bacteria are a major threat to hospitalized patients and the main cause of chronic obstructive pulmonary disease and cystic fibrosis. There is an urgent necessity for novel therapeutic approaches, since current antibiotic delivery fails to eliminate biofilm-protected bacteria. In this study, ciprofloxacin-loaded poly(lactic-co-glycolic acid) nanoparticles, which were functionalized with DNase I, were fabricated using a green-solvent based method and their antibiofilm activity was assessed against *Pseudomonas aeruginosa* biofilms. Such nanoparticles constitute a paradigm shift in biofilm treatment, since, besides releasing ciprofloxacin in a controlled fashion, they are able to target and disassemble the biofilm by degrading the extracellular DNA that stabilize the biofilm matrix. These carriers were compared with free-soluble ciprofloxacin, and ciprofloxacin encapsulated in untreated and poly(lysine)-coated nanoparticles. DNase I-activated nanoparticles were not only able to prevent biofilm formation from planktonic bacteria, but they also successfully reduced established biofilm mass, size and living cell density, as observed in a dynamic environment in a flow cell biofilm assay. Moreover, repeated administration over three days of DNase I-coated nanoparticles encapsulating ciprofloxacin was able to reduce by 95% and then eradicate more than 99.8% of established biofilm, outperforming all the other nanoparticle formulations and the free-drug tested in this study. These promising results, together with minimal cytotoxicity as tested on J774 macrophages, allow obtaining novel antimicrobial nanoparticles, as well as provide clues to design the next generation of drug delivery devices to treat persistent bacterial infections.

© 2015 Elsevier B.V. All rights reserved.

1. Introduction

Pseudomonas aeruginosa is one of the major cause of nosocomial infections in humans and is frequently associated with chronic obstructive pulmonary disease (COPD) and cystic fibrosis (CF), being the principal cause of morbidity and mortality for these patients [1,2]. The establishment of chronic *Pseudomonas* infections correlates with the formation of a biofilm, a structure with clusters of cells encapsulated in a complex extracellular polymeric matrix. In such an environment, bacteria are more likely to resist to antibiotic treatments, as most drugs do not freely diffuse into the biofilm and thus do not reach optimal therapeutic concentrations [3]. Additionally, bacteria in biofilms display a different physiology compared to planktonic cells such as a diminished metabolic rate, and improved cell to cell communication, which makes antibiotics less effective and increases the chance of development of resistances [4]. Moreover, the emergence and increasing prevalence of bacterial strains that are resistant to available antibiotics demand the discovery of new therapeutic approaches [5,6].

Micro- and nanocarriers, such as polymeric particles [7], liposomes [8] and hydrogels [9], have been studied to treat bacterial infections due to their potential to encapsulate and deliver therapeutic compounds in a sustained fashion. Among these devices, polymeric biodegradable nanoparticles (NPs) made up of the biocompatible poly(lactic-co-glycolic acid) (PLGA) have been investigated as drug delivery vehicles. A wide array of methods to fabricate such NPs is available, and most of them are easy to scale-up [10], and allow the encapsulation of several compounds having different chemical and physical properties. The degradation profile of PLGA can be tuned altering the ratio of its components (lactic and glycolic acid), which allows controlling the release kinetics of loaded drugs [11]. Additionally,

---

* Corresponding author at: Bacterial Infections and Antimicrobial Therapies Group, Institute for Bioengineering of Catalonia (IBEC), Baldiri Reixac 15-21, 08028 Barcelona, Spain.

E-mail address: etorrents@ibecbarcelona.eu (E. Torrents).

[1] These authors contributed equally to this work.

http://dx.doi.org/10.1016/j.jconrel.2015.04.028
0168-3659/© 2015 Elsevier B.V. All rights reserved.

Table 1
Composition, encapsulation efficiency and overall properties of drug loaded NPs.

	Coating	DNase I activity (μg DNA/mg NPs/1 h)	CPX content [w/w %]	Size [nm]	Size PDI	Z-potential [mV]
PLGA–CPX	–	–	0.26	213.6	0.085	−12.9 ± 11.20
PLGA–PL–CPX	Poly(lysine)	–	0.24	272.5	0.101	+33.5 ± 5.99
PLGA–PL–DNase I	Poly(lysine) DNase I	32.0	–	265.0	0.099	+30.8 ± 0.70
PLGA–PL–CPX–DNase I	Poly(lysine) DNase I	26.2	0.17	251.9	0.122	+28.9 ± 1.43

water) and NPs alone (50 μg in water) were also tested. After 30 min of incubation at 37 °C, the mixtures were loaded in a 0.8% TAE agarose gel, stained with ethidium bromide and visualized under UV light (Gel DocTM XR +, Bio-Rad Laboratories). DNase I activity was calculated by quantification of DNA degradation using Quantity One software package (Bio-Rad Laboratories).

2.5. Determination of mammalian cytotoxicity

Murine macrophage cells (J774, ATCC TIB-202, 6 × 10^4 per well) were seeded into 96-well tissue culture plates in complete medium without antibiotics, in the presence of increassing concentrations of nanoparticles, or left untreated. Cell viability was assessed by using a 3-[4,5-dimethylthiazol-2-yl]-2,5-diphenyltetrazolium bromide (MTT) colorimetric assay (Sigma-Aldrich, Spain). After 24 and 48 h of exposure to different concentrations of the compounds, culture supernatants were removed and 10% of MTT in complete medium was added to each well and incubated for 3 h at 37 °C. The water-insoluble dark blue formazan was dissolved by adding acidic isopropanol. Absorbance was measured at 550 nm using a microplate reader (Infinite M200 Microplate Reader, Tecan).

2.6. Bacterial strains and growth conditions

Wild-type *P. aeruginosa* PAO1 strain CECT 4122 (ATCC 15692) and *Staphylococcus aureus* CECT 86 (ATCC 12600) were obtained from the Spanish Type Culture Collection (CECT). To obtain inocula for examination, the strains were cultured overnight in Luria Bertani (LB) (Pronadisa, Spain) liquid medium for *P. aeruginosa* and tryptic soy broth (TSB) (Scharlab, Spain) medium for *S. aureus* at 37 °C. Cells were then harvested by centrifugation (8.000 ×g for 10 min). Bacterial growth was measured by reading absorbance at 550 nm (A_{550}).

2.7. Minimal inhibitory concentration (MIC) assays

MICs were determined by a microtiter broth dilution method as described by Cole et al. [21] and modified by Beckloff et al. [22]. In brief, 100 μl of bacteria at a density of 5 × 10^5 cfu/ml in Mueller–Hinton broth (BD Biosciences) was inoculated into the wells of 96-well assay plates (tissue culture-treated polystyrene; Costar 3595, Corning Inc., Corning, NY) at different concentrations of loaded CPX in NP used in this study (4, 2, 1, 0.5, 0.25, 0.125, 0.0625, 0.03125, 0.01562 or 0 μg/ml). The inoculated microplates were incubated at 37 °C at 150 rpm for 12 h in an Infinite 200 Pro microplate reader (Tecan) and A_{550} was read every 15 min.

2.8. Viable cell counts in biofilm inhibition after nanoparticle treatment

The anti-biofilm activity of the different NPs synthetized in this study was investigated in *P. aeruginosa* biofilms formed in peg lids, in two different assays. Firstly, the ability of the NPs to inhibit biofilm formation by planktonic bacteria was tested. In brief, the peg lids were inserted into the microplates containing a suspension of 200 μl of *P. aeruginosa* PAO1 (5 × 10^5 cfu/ml) in LB medium containing 0.2% glucose. Microplates were incubated in static conditions at 37 °C for 24 h, in the presence of CPX-loaded NPs (drug concentration from 0.0078 to 0.5 μg/ml). The peg lids with biofilm were rinsed twice with PBS 1× to remove loosely adherent planktonic cells. Cells forming biofilms were recovered in 200 μl LB by centrifugation at 2500 rpm in an Eppendorf Microcentrifuge 5430 (Eppendorf). Recovered cells were serially diluted and plated in LB agar plates, and colony-forming units were counted. Secondly, the activity of the NPs against 48 h established biofilms was also tested. Biofilms were prepared as described above and incubated in static conditions at 37 °C, this time without antibiotic agents or NPs. After 48 h, the peg lids were rinsed twice with PBS and after that were transferred to 96-well plates containing 200 μl of LB with different concentrations of loaded CPX in NP used in this study (from 0.0078 to 0.5 μg/ml). These plates were incubated at 37 °C for another 24 h. Cells were recovered and quantified as previously described. In both assays (biofilm inhibition and activity against established biofilm), free soluble CPX and a combination of CPX and DNase I (both free soluble) were used as controls.

2.9. Biofilm cultivation in flow cell chambers and microscopy

Biofilms were cultivated for 96 h at 37 °C in flow cell chambers with channel dimension of 1 × 4 × 40 mm as described previously [23]. Biofilms were stained with a mixture of 6 μM SYTO 9 and 30 μM propidium iodide at room temperature in the dark for 30 min, according to the specifications of the LIVE/DEAD BacLight Bacterial Viability kit (Molecular Probes).

Confocal scanning laser microscopy was performed with a Leica TCS-SP5 (Leica Microsystems, Heidelberg, Germany), with excitation wavelengths of 488 and 560 nm. To measure biofilm thickness, sections were scanned and Z-stacks were acquired at z step-size of 0.388 μm. Each field size was 455 μm by 455 μm at 20× magnification. Microscope images were acquired with the Leica Confocal Software LCS and further processed with ImageJ (National Institute of Health, USA) analysis software and COMSTAT 2 specific biofilm analysis software [24].

2.10. Statistical analysis

Values are expressed as mean ± standard deviation (SD). Statistical analyses were performed using GraphPad Prism 6.00 (GraphPad Software, San Diego, CA, USA) software package. Single comparisons were performed by unpaired *t*-test. A value of $p < 0.05$ was considered as statistically significant.

3. Results

3.1. Preparation and encapsulation of nanoparticles

NPs with spherical shape (Fig. 1A), average diameter between 200 and 300 nm, and narrow, monodisperse, size distribution (polydispersity index, PDI, value between 0.085 and 0.122) were fabricated. The physical properties of the NPs are summarized in Table 1. The Z-potential of the NPs varied accordingly to the type of surface coating applied. When PVA was the only additive in the coagulation bath, negatively charged NPs were obtained (approx. −13 mV), whereas the addition of PL generated positively charged particles (+30 mV). Functionalization with DNase I had no significant effect on the overall surface charge. The average CPX content in the carriers varied between 1.7 (for PLGA-PL-DNase I) and

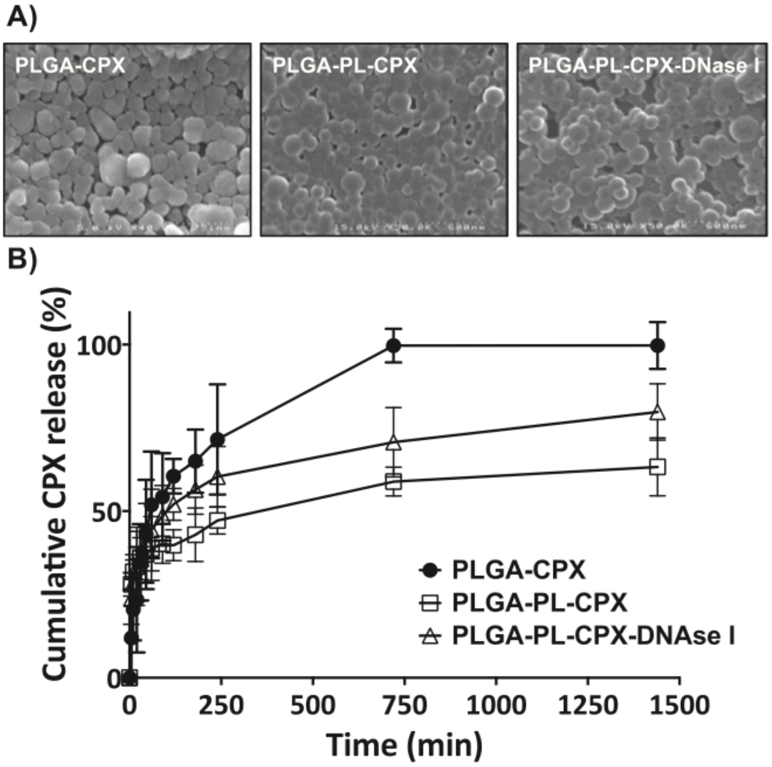

Fig. 1. Characterization of the NPs. A) SEM micrographs of PLGA–CPX (*left*), PLGA–PL–CPX (*center*) and PLGA–PL–CPX–DNase I (*right*) NPs. B) Ciprofloxacin release kinetics from the different NP formulations.

2.6 μg/mg of NPs (for PLGA–CPX). DNase I grafted on PL coated NPs retained its DNase I activity, as quantified by agarose gel electrophoresis, with 1 mg of functionalized NPs being able to degrade 26.2 or 32 μg of DNA in 1 h. Comparable DNase I activity was also found after submitting the NPs to a freeze–thaw-cycle (data not shown).

3.2. In-vitro release of ciprofloxacin

Negatively and positively charged (both PL and PL-DNase I coating) NPs presented a burst release in the first hour, upon suspension in PBS, when between 40 and 50% of the total CPX load is released (Fig. 1B). After this period, the drug release is slower, and negatively charged NPs end up depleting their drug amount within 12 h. Positively charged NPs showed a steady release of the remaining antibiotic, and after 12 h PL and PL-DNase coated NPs delivered respectively about 60 and 80% of the loaded CPX.

3.3. Cytotoxicity

The cytotoxicity results for J774 murine macrophages corresponding to 24 h and 48 h of incubation are shown in Fig. 2. The results clearly indicate the absence of cytotoxic effect of all the particles used in this study on the murine cell viability.

3.4. Determination of the antibacterial activity of ciprofloxacin loaded NPs

To characterize the antimicrobial activity of the different synthetized NPs, we first determined the in vitro susceptibilities of two common bacterial pathogens, *P. aeruginosa* and *S. aureus*, in the presence of different CPX–NP concentrations. The MICs of different CPX formulations (alone and encapsulated) are given in Table 2. Against *P. aeruginosa* PAO1, the MIC of control, free CPX, was 0.39 μg/ml and for CPX encapsulated (PLGA–CPX, PLGA–PL–CPX and PLGA–PL–CPX–DNase I) it was 0.0625, 0.5 and 0.5 μg/ml respectively. In the case of *S. aureus*, the representative MIC's were 0.0975, 0.125, 0.5 and 0.5 μg/ml.

3.5. Inhibition of biofilm formation by ciprofloxacin encapsulated NPs

Previous results suggested a good antibacterial activity of the NP for the inhibition of *P. aeruginosa* growth (Table 2), which is one of the main actors in chronic infections of the respiratory tract and found in cystic fibrosis patients. Therefore, capacity of the NPs to inhibit *P. aeruginosa* biofilm formation was studied. NPs were added at time 0 of biofilm formation and, as seen in Fig. 3, for concentrations as low as 0.0156 μg/ml, more than 80% of biofilm reduction was observed, and no biofilm production was seen at all with encapsulated CPX concentrations higher than 0.125 μg/ml, indicating the capacity of the NPs to avoid *P. aeruginosa* biofilm formation.

3.6. Antibiofilm activity of CPX loaded NPs

Established *P. aeruginosa* 48 h-old biofilm decreased in a dose-dependent manner when treated with highly active NPs containing DNase I (PLGA–PL–CPX + PLGA–PL–DNase I and PLGA–PL–CPX–DNAse I) and less active NPs without DNase I (PLGA–CPX and PLGA–PL–CPX) (Fig. 4). Any of the latest NP showed more than 50% inhibition at the highest CPX concentrations (0.5 μg/ml). With free soluble CPX (CPX free), a reduction of a formed biofilm around 50% was observed at 0.0156 μg/ml. Furthermore, in an additional control group, more than 90% biofilm decrease was observed at 0.0312 μg/ml when using a combination soluble free CPX and DNase I. Drastic reduction of formed biofilm (>95%) was observed at 0.0078 μg/ml CPX concentration with

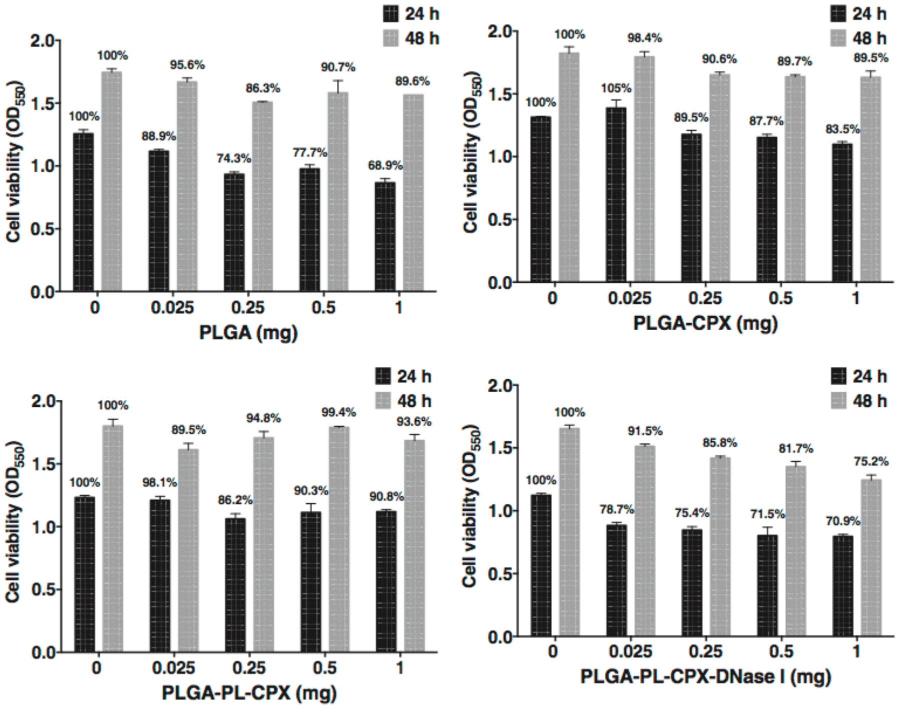

Fig. 2. Cytotoxicity assay. Murine J774 macrophage viability measured using the MTT assay. Values represent the mean ± standard deviation (SD) of triplicate culture wells. Results represent one out of two independent experiments. In each column, the viability percentage compared to the untreated samples is shown.

NPs that loaded simultaneously CPX and DNase I (PLGA–PL–CPX–DNase I), showing the best antibiofilm activity. No effect on removing formed biofilm of DNase I (free) or NP-linked (PLGA–PL–DNase I) was observed (see Supplementary Fig. 1). A limited effect was only observed at DNase I concentrations three times higher than the one used in this work.

To further evaluate and confirm the antibiofilm properties of DNase I-coated NPs, a more sophisticated biofilm model based on a flow cell system was employed. Flow chamber biofilms are close to the conditions found in vivo during infections. As shown in Fig. 5, when a four-day-old formed *P. aeruginosa* biofilm was treated with 0.5 μg/ml of free (CPX free) or encapsulated CPX in PLGA–PL–CPX and PLGA–PL–CPX–DNase I, the formed biofilm decreased simultaneously in biomass and average thickness (Fig. 5 and Table 3). Control biofilm without CPX treatment exhibited the highest value for total biomass and average thickness (Fig. 5A and Table 3). The addition of free CPX for 24 h reduces biomass and average thickness, reaching the highest reduction when the CPX is encapsulated in DNase I-coated NPs (Fig. 5F and Table 3).

3.7. Antibiofilm properties using repeated doses of treatment

As seen previously, NP with DNAse I (PLGA–PL–CPX–DNase I) resulted in higher activity to remove *P. aeruginosa* biofilm compared to control free CPX and the combination of free CPX and DNase I (Fig. 6A–B). Therefore, we evaluated the capacity of removing 48 h old biofilm (under static culture) with repeated administrations of encapsulated CPX (1 dose/day, for three consecutive days) (see Fig. 6). PLGA–CPX reduced formed biofilm around 80% at the second day of treatment only at the highest concentrations (Fig. 6C), while a lower concentration of encapsulated CPX (0.0156 μg/ml) was necessary to obtain a comparable result with PLGA–PL–CPX (Fig. 6D). The addition of DNase I to the formulation, improved the antibacterial effects. The highest antibiofilm activity was observed with PLGA–PL–CPX–DNase I NP (Fig. 6F) which eliminated more than 95% of the biofilm at the second day of application using a 0.0156 μg/ml CPX concentration, and even removed more than 99.8% of the pre-existing biofilm at 0.25 μg/ml already at the second day of treatment, performing better than PLGA–PL–CPX NPs separately combined with PLGA–PL–DNase I NPs (Fig. 6E). Repeated administrations of the combination of PLGA–PL–CPX and PLGA–PL–DNase I NPs at the highest concentrations tested (0.25 and 0.5 μg/ml CPX) were also able to eliminate established biofilms at the end of the treatment. However, the efficacy of PLGA–PL–CPX–DNase I particles alone was still higher, showing a significantly better reduction of the biofilm at the first day of treatment, at all the concentrations tested in the study ($p < 0.01$). Moreover, PLGA–PL–CPX–DNase I treatment showed better biofilm eradication ($p < 0.01$) for all the three time-points and at every concentration tested, against all the other experimental groups (PLGA–CPX, PLGA–PL–CPX) and controls (free CPX and the mixture of free CPX and DNase I).

Table 2
Minimal inhibitory concentrations (MICs) of soluble ciprofloxacin (CPX) and different encapsulation formulation (PLGA–CPX, PLGA–PL–CPS and PLGA–PL–CPX–DNase).

	Ciprofloxacin MIC (μg/ml)			
	CPX	PLGA–CPX	PLGA–PL–CPX	PLGA–PL–CPX–DNase I
P. aeruginosa PAO1 ATCC 4122	0.39	0.0625	0.5	0.5
S. aureus ATCC 12600	0.0975	0.125	0.5	0.5

4. Discussion

Due to the rising of multiresistant bacterial strains and to the intrinsic difficulty to deliver antibiotics to bacterial communities protected by biofilms, the development of clinically effective therapies and novel treatments against bacterial biofilm infections is one of the greatest challenges in modern infectious disease control. In this work, together

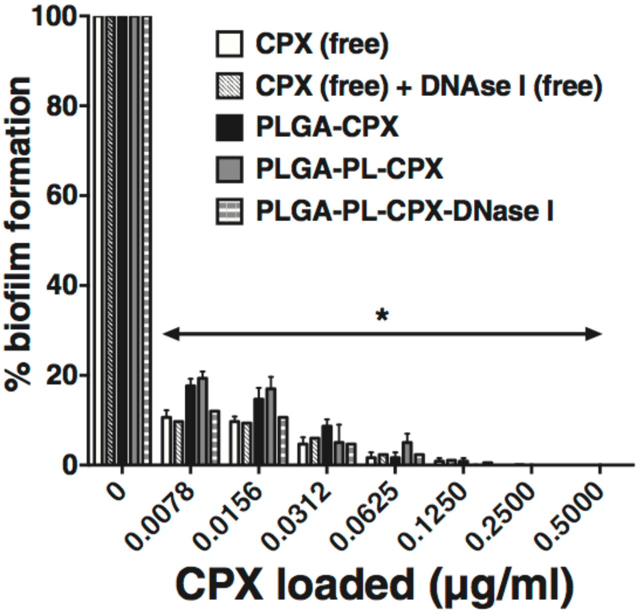

Fig. 3. Inhibition of PAO1 biofilm formation by different doses of free or encapsulated CPX. The values represent the percentages of biofilm form. The results are expressed as the mean ± standard deviations of six replicates from three independent experiments. A Student *t*-test was performed (*, $p < 0.01$; versus non-treated biofilms). The viable counts at control experiment without CPX were $1.9 \times 10^9 \pm 1.04 \times 10^8$ cfu/ml. DNase I free was used at 10 μg/ml concentration.

with the bacterial cells, the extracellular matrix that composes the biofilm is proposed as an additional and fundamental target to be attacked in order to combat bacterial chronic infections. For this purpose, DNase I-functionalized NPs capable of combining antibiotic controlled release while actively disassembling the biofilm matrix were developed. PLGA NPs encapsulating CPX were used as a carrier device and a platform for biofunctionalization. The size of the obtained particles (between 200 and 300 nm) falls in the range suitable for diffusion through the mucus pores in chronically infected lungs [25]. Untreated, polylysine, and polylysine–DNase I coated NPs were produced, characterized and tested in vitro for their capability to treat established *P. aeruginosa* biofilm.

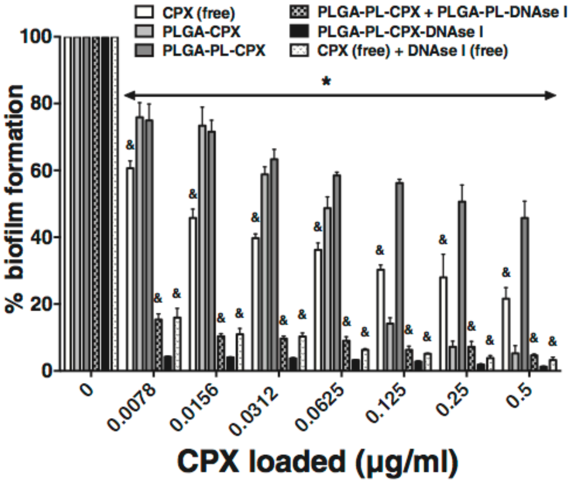

Fig. 4. Disassembling the existing *P. aeruginosa* biofilms by CPX and PLGA NPs. The values represent the percentages of biofilm formed. Control experiment with non-encapsulated DNase I (free) was included. The results are expressed as the mean ± standard deviations of six replicates from three independent experiments. A Student's *t*-test was performed (*, $p < 0.01$; versus non-treated biofilms) and (&, $p < 0.01$; versus treatment with PLGA–PL–CPX–DNase I NP). The viable counts at control experiment without CPX were $1.83 \times 10^9 \pm 1.5 \times 10^8$ cfu/ml. DNase I free was used at 10 μg/ml concentration and 0.125 mg PLGA–PL–DNase I was used.

The NPs were fabricated using a modification of the nanoprecipitation method, involving green non-toxic chemicals, such as ethyl lactate which benefits from a favorable regulatory status [26], and may facilitate different national authority approvals of the drug delivery device. Typically, NPs with monodisperse size distribution can be obtained with such method [27], as it is also confirmed by the DLS measurements presented in this study. As a downside, nano-precipitation is most suitable for the encapsulation of hydrophobic compounds [28] since hydrophilic molecules are easily dispersed into the water phase during the particle formation, and even though approaches to improve the encapsulation of hydrophilic drugs have been studied, they lead to limited improvement of encapsulation efficiencies [29]. This is confirmed by our results, despite of working at neutral pH, where CPX base displays its minimum solubility in water [30], and is also consistent with the data already reported in the literature in relation to encapsulation of fluoroquinolone antibiotics [31]. The addition of hydrophilic moieties to the NP formulations, such as lecithin or pluronic, has also been suggested to improve encapsulation efficiency [13,26], but preliminary tests performed in our work brought no improvement (data not shown). Hydrophilic molecules also tend to accumulate at the NP surface. This mode of entrapment usually leads to a burst release of the drug in the first hours, due to the compound being washed off the particle [32], as also seen in the CPX release profiles showed in Fig. 1. However, a fast burst release, followed by a sustained release is preferred, in the case of antibiotics in biofilms, since the quick delivery of high drug doses can help prevent the insurgence of antibiotic tolerance of the surviving biofilm [31,33]. PLGA–CPX NPs quickly depleted their antibiotic load; unlike PL- and PL–DNase I coated NPs. In the two positively charged NP types, the polycationic PL may have helped to stabilize the NPs and interact ionically with the antibiotic, reducing its rate of removal from the NPs [34]. Encapsulated antibiotics, especially those loaded in negatively charged PLGA–CPX NPs, are effective against planktonic bacteria, showing lower MIC values compared to positively charged NPs. While such

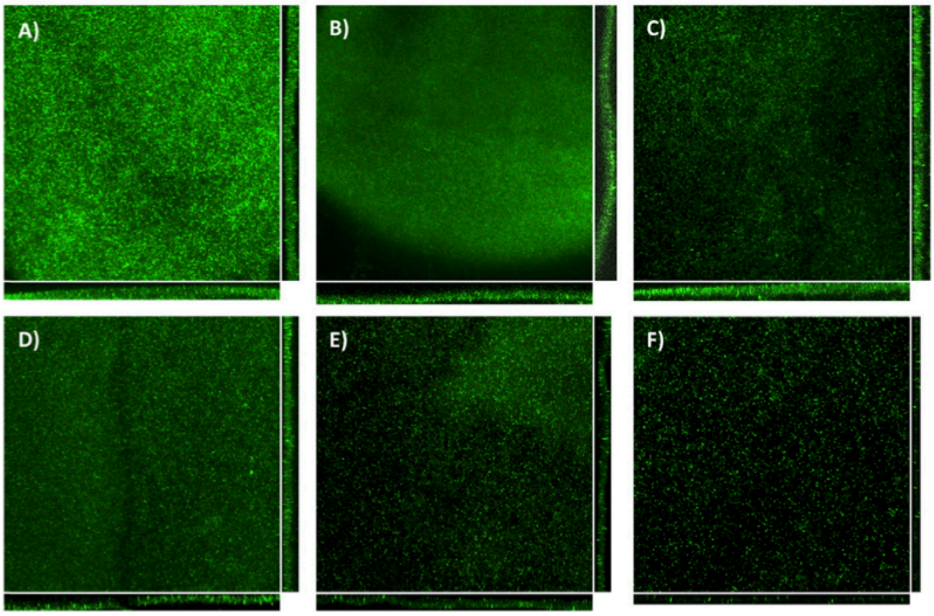

Fig. 5. Flow cell analysis of *P. aeruginosa* PAO1 biofilm formation in the absence and presence of PLGA NP. Living cells are stained in green. Each panel shows *xy*, *yz* and *xz* dimensions and is the representative of 5 different biofilm areas of two independent experiments. Each field size was 455 μm by 455 μm at 20× magnification. A) *P. aeruginosa* biofilm without treatment, B) treated with free CPX (0.5 μg/ml), C) treated with free CPX (0.5 μg/ml) + DNase I (10 μg/ml), D) treated with PLGA–PL–CPX NPs at 0.5 μg/ml, E) treated with PLGA–PL–CPX NPs at 0.5 μg/ml + PLGA–PL–DNase I (0.125 mg NP) and F) PLGA–PL–CPX–DNAse I NPs at 0.5 μg/ml.

difference could be determined by the different rates of release that affects the amount of drug released over time to the bacterial cells during the 12 h of the MIC determination assay, further studies have to be conducted to determine the mechanism behind this result. Furthermore, both free-soluble CPX and encapsulated CPX are capable to prevent biofilm formation. NP formulations were highly advantageous in treating established biofilms, as properly designed NPs can penetrate the biofilm porous matrix or at least be closer to the biofilm surface providing high local concentrations of antibiotics in the proximity of bacterial cells embedded into the biofilm matrix [35–37]. Ideally, NPs should be able to diffuse homogenously through the target biofilm, and their ability to penetrate the biofilm matrix depends on their size and surface chemistry. Forier et al. have demonstrated on model polystyrene NP systems that both positively and negatively charged NPs bind to biofilms, and suffer an equal reduction in diffusion velocity [38]. Positively charged NPs were found to be bound to wire-like components, possibly biofilm polymers and the negatively charged eDNA, while negatively charged NPs were bound to the proximity of bacterial cells, probably due to hydrophobic interactions [36].

Table 3
Flow cell biofilm parameters of wild-type *P. aeruginosa* treated with free CPX alone or encapsulated in NPs. Biomass values indicate the amount of living cells (stained in green in the assay) inside the biofilm. Values represent the mean ± SD of three independent experiments.

	Biomass ($\mu m^3/\mu m^2$)	Thickness (μm)
Non-treated	$29.6 \pm 3.1^{\#}$	$52.0 \pm 8.8^{\#}$
CPX (free)	$22.9 \pm 3.1^{*,\#}$	$33.8 \pm 1.6^{*,\#}$
CPX (free) + DNase I (free)	$21.9 \pm 1.1^{*,\#}$	$28.9 \pm 2.7^{*,\#}$
PLGA–PL–CPX	$22.5 \pm 1.6^{*,\#}$	$25.8 \pm 1.8^{*,\#}$
PLGA–PL–CPX–DNase I	$16.7 \pm 1.0^{*}$	$19.1 \pm 1.3^{*}$
PLGA–PL–CPX + PLGA–PL–DNase I	$20.9 \pm 2.1^{*,\#}$	$24.6 \pm 2.1^{*,\#}$

Asterisk (*) denotes significant differences compared to non-treated biofilm and number sign (#) denotes significant differences compared to PLGA–PL–CPX–DNase I ($p < 0.05$, Student's *t*-test).

Although some researchers have proposed non-fouling, PEG-coated particles in strategies to enhance carrier mobility [39], NPs functionalized with mucolytic agents hold the promise to improve the distribution of antibiotics into biofilms, while increasing biofilm eradication. While PLGA–CPX and PLGA–PL–CPX NPs alone showed a good extent of biofilm eradication, antibacterial activity of CPX was greatly improved in the presence of DNase I (Figs. 4, 5 and 6). Additionally, even though DNase I and PLGA–PL–DNase I (with no antibiotic) were ineffective at eliminating the biofilm, the mixture of free soluble CPX and DNase I, and that of PLGA–PL–CPX with PLGA–PL–DNase I, showed high antibiofilm capacity, indicating a synergistic effect. This could be due to an improved mobility of NPs, as the enzyme is actively degrading the eDNA of the biofilm matrix, as also indicated by Messiaen et al., who have found 10-times improved diffusional rates of charged polymeric NPs in biofilm, in the presence of DNase I [40]. Moreover, better results were obtained when NPs bearing both CPX and DNase I at the same time were used (PLGA–PL–CPX–DNase I), even at the lowest tested CPX concentrations and with a single application, both under static and dynamic conditions (in the flow cell system test). These results suggest that drug delivery-eDNA degrading NPs may penetrate better into the bacterial colony, and better harness its integrity. In fact, DNase I-mediated degradation of bacterial eDNA is known to disassemble the structure of the bacterial ECM, which in turn loosens up (but not necessarily dispersing the bacterial cells enclosed) and becomes more permeable, improving antibiotic efficacy [41]. This interpretation is strengthened by the flow cell biofilm assays, which clearly show that DNase I-coated NPs, apart from being more effective at eliminating bacterial cells (shown as a reduction in living biomass density), consistently reduced the thickness of the biofilm, indicating the ability of the NPs to disassemble the extracellular matrix and allowed increased efficacy of CPX to kill bacterial cells. The impact of this effect is even more important when considering a longer treatment of an established biofilm infection. With repeated daily administrations of this NP formulation, bacteria mass reduction was steadily improved with no sign of tolerance arising (Fig. 6). Moreover, at the highest concentrations, PLGA–PL–CPX–

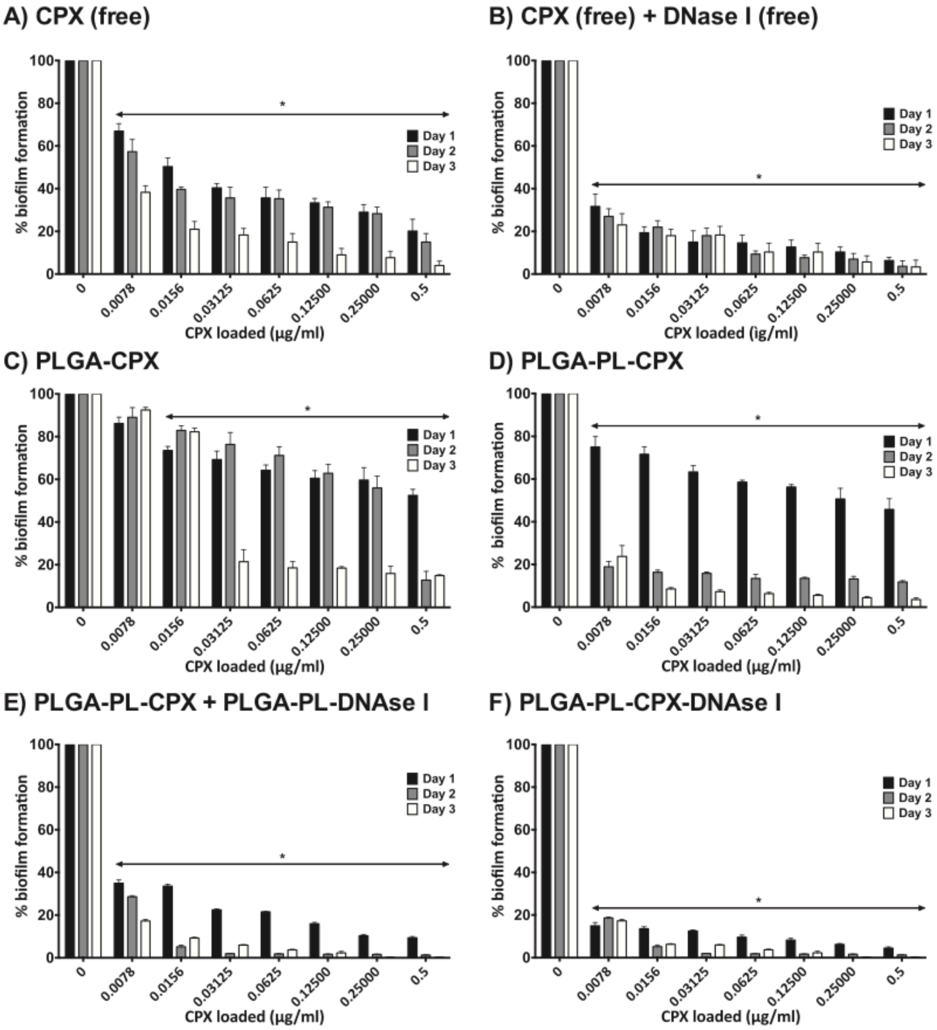

Fig. 6. Established *P. aeruginosa* biofilm response to three consecutive NP treatments. The values represent the percentages of biofilm formed and it is shown for each day independently (days 1, 2 and 3). The results are expressed as the mean ± standard deviations of six replicates from two independent experiments. A Student's *t*-test was performed (*, $p < 0.01$; versus non-treated biofilms). The viable counts at control experiment without CPX were $2.76 \times 10^9 \pm 5.12 \times 10^8$ cfu/ml. DNase I free was used at 10 µg/ml concentration and 0.125 mg PLGA–PL–DNase I was used.

DNase I NPs were even able to eradicate more than 99.8% of the established biofilm, outperforming the non-functionalized particles and the control groups. Further assessment of these NPs with animal models would be fundamental, also to evaluate DNase I stability in vivo. While aerosol formulations of DNase I have already been proven to be active to reduce airway mucus viscosity in vivo [17], it would be of interest to evaluate the degree activity of the enzyme-linked NPs against biofilm occurring in the respiratory tract. Cytoxicity of the NPs at the used doses was very low. The treatment of macrophages with all NP formulations did not disturb their metabolic activity, as indicated by increased proliferation rates during the second day of culture, which is a sign of cell health [42]. This data, together with other reassuring results regarding PLGA NP cytocompatibility [43,44], supports the feasibility of the proposed drug delivery approach.

5. Conclusions and future perspectives

In this work, DNase I functionalized NPs are proposed as drug carriers that can treat severe bacterial infections by attacking both the bacterial cell and their biofilm extracellular matrix. CPX-loaded PLGA NPs were successfully prepared using a method involving no harmful chemicals. These NPs have adequate size for antibiotic drug delivery to biofilms located in the airways, and also display a profitable drug release profile for this specific application. However, further refinement of the fabrication parameters would be required to improve the encapsulation efficiency of CPX. The proposed NPs were employed as a platform for chemical modification and to test the efficacy of functionalization with active DNase I. Coating the NPs with polylysine enriched the carriers with chemically reactive groups, enabling a simple way to functionalize them. Enzyme-linked NPs, able to degrade *P. aeruginosa* biofilm ECM, were successful at improving antibacterial potential of the encapsulated drug. Moreover, the DNase I-coated NPs showed the greatest extent of eradication of mature biofilms, a result that was not possible to achieve with the free-soluble drug, with a mixture of free soluble CPX and DNase I, and with the unmodified NPs. These results allow obtaining novel, antibiofilm-active drug delivery devices and paving the way for the application of the proposed approach to more type of carriers and antimicrobial compound combination, to treat persistent bacterial infections. After the necessary validation in in vivo models, DNase-coated NPs could represent a significant step forward in the pharmaceutical treatment of biofilm infections.

Supplementary data to this article can be found online at http://dx.doi.org/10.1016/j.jconrel.2015.04.028.

Acknowledgment

This work was supported by the Ministerio de Economia y Competitividad with grant BFU2011-24066, CSD2008-00013 and ERA-NET PathoGenoMics (BIO2008-04362-E) to ET. This work was also supported by the Generalitat de Catalunya SGR-2014-01260. ET was supported by the Ramón y Cajal and I3 program from the Ministerio de Ciencia e Innovación. RL and AB are thankful to the Ministerio de Educación, Cultura y Deporte for its financial support through the FPU Programme (grant reference AP2010-4827 and FPU13/08083).

References

[1] J.B. Lyczak, C.L. Cannon, G.B. Pier, Lung infections associated with cystic fibrosis, Clin. Microbiol. Rev. 15 (2002) 194–222.
[2] K. Ito, P.J. Barnes, COPD as a disease of accelerated lung aging, Chest 135 (2009) 173–180.
[3] J.W. Costerton, P.S. Stewart, E.P. Greenberg, Bacterial biofilms: a common cause of persistent infections, Science 284 (1999) 1318–1322.
[4] P.S. Stewart, M.J. Franklin, Physiological heterogeneity in biofilms, Nat. Rev. Microbiol. 6 (2008) 199–210.
[5] B. Spellberg, R. Guidos, D. Gilbert, J. Bradley, H.W. Boucher, W.M. Scheld, J.G. Bartlett, J. Edwards Jr., Infectious Diseases Society of America, The epidemic of antibiotic-resistant infections: a call to action for the medical community from the Infectious Diseases Society of America, Clin. Infect. Dis. 46 (2008) 155–164.
[6] M. May, Drug development: time for teamwork, Nature 509 (2014) S4–S5.
[7] R. Kalluru, F. Fenaroli, D. Westmoreland, L. Ulanova, A. Maleki, N. Roos, M. Paulsen Madsen, G. Koster, W. Egge-Jacobsen, S. Wilson, H. Roberg-Larsen, G.K. Khuller, A. Singh, B. Nystrom, G. Griffiths, Poly(lactide-co-glycolide)-rifampicin nanoparticles efficiently clear *Mycobacterium bovis* BCG infection in macrophages and remain membrane-bound in phago-lysosomes, J. Cell Sci. 126 (2013) 3043–3054.
[8] B. Khameneh, M. Iranshahy, M. Ghandadi, D. Ghoochi Atashbeyk, B.S. Fazly Bazzaz, M. Iranshahi, Investigation of the antibacterial activity and efflux pump inhibitory effect of co-loaded piperine and gentamicin nanoliposomes in methicillin-resistant *Staphylococcus aureus*, Drug Dev. Ind. Pharm. (2014) 1–6.
[9] Y. Zhao, X. Zhang, Y. Wang, Z. Wu, J. An, Z. Lu, L. Mei, C. Li, In situ cross-linked polysaccharide hydrogel as extracellular matrix mimics for antibiotics delivery, Carbohydr. Polym. 105 (2014) 63–69.
[10] V.T. Tran, J.P. Benoit, M.C. Venier-Julienne, Why and how to prepare biodegradable, monodispersed, polymeric microparticles in the field of pharmacy? Int. J. Pharm. 407 (2011) 1–11.
[11] F. Mohamed, C.F. van der Walle, Engineering biodegradable polyester particles with specific drug targeting and drug release properties, J. Pharm. Sci. 97 (2008) 71–87.
[12] R. Duncan, R. Gaspar, Nanomedicine(s) under the microscope, Mol. Pharm. 8 (2011) 2101–2141.
[13] F. Ungaro, I. d'Angelo, C. Coletta, R. d'Emmanuele di Villa Bianca, R. Sorrentino, B. Perfetto, M.A. Tufano, A. Miro, M.I. La Rotonda, F. Quaglia, Dry powders based on PLGA nanoparticles for pulmonary delivery of antibiotics: modulation of encapsulation efficiency, release rate and lung deposition pattern by hydrophilic polymers, J. Control. Release 157 (2012) 149–159.
[14] E.S. Gloag, L. Turnbull, A. Huang, P. Vallotton, H. Wang, L.M. Nolan, L. Mililli, C. Hunt, J. Lu, S.R. Osvath, L.G. Monahan, R. Cavaliere, I.G. Charles, M.P. Wand, M.L. Gee, R. Prabhakar, C.B. Whitchurch, Self-organization of bacterial biofilms is facilitated by extracellular DNA, Proc. Natl. Acad. Sci. U. S. A. 110 (2013) 11541–11546.
[15] B.W. Peterson, H.C. van der Mei, J. Sjollema, H.J. Busscher, P.K. Sharma, A distinguishable role of eDNA in the viscoelastic relaxation of biofilms, mBio 4 (2013) (e00497-00413).
[16] M. Okshevsky, R.L. Meyer, The role of extracellular DNA in the establishment, maintenance and perpetuation of bacterial biofilms, Crit. Rev. Microbiol. (2013), early online 1–11, http://dx.doi.org/10.3109/1040841X.2013.841639.
[17] P.I. Shah, A. Bush, G.J. Canny, A.A. Colin, H.J. Fuchs, D.M. Geddes, C.A. Johnson, M.C. Light, S.F. Scott, D.E. Tullis, et al., Recombinant human DNase I in cystic fibrosis patients with severe pulmonary disease: a short-term, double-blind study followed by six months open-label treatment, Eur. Respir. J. 8 (1995) 954–958.
[18] S.J. Shire, Stability characterization and formulation development of recombinant human deoxyribonuclease I [Pulmozyme®, (dornase alpha)], Formulation, Characterization, and Stability of Protein Drugs: Case Histories, 9 2002, pp. 393–426.
[19] M. Alipour, Z.E. Suntres, A. Omri, Importance of DNase and alginate lyase for enhancing free and liposome encapsulated aminoglycoside activity against *Pseudomonas aeruginosa*, J. Antimicrob. Chemother. 64 (2009) 317–325.
[20] H. Fessi, F. Puisieux, J.P. Devissaguet, N. Ammoury, S. Benita, Nanocapsule formation by interfacial polymer deposition following solvent displacement, Int. J. Pharm. 55 (1989) R1–R4.
[21] A.M. Cole, P. Weis, G. Diamond, Isolation and characterization of pleurocidin, an antimicrobial peptide in the skin secretions of winter flounder, J. Biol. Chem. 272 (1997) 12008–12013.
[22] N. Beckloff, D. Laube, T. Castro, D. Furgang, S. Park, D. Perlin, D. Clements, H. Tang, R.W. Scott, G.N. Tew, G. Diamond, Activity of an antimicrobial peptide mimetic against planktonic and biofilm cultures of oral pathogens, Antimicrob. Agents Chemother. 51 (2007) 4125–4132.
[23] T. Tolker-Nielsen, C. Sternberg, Growing and analyzing biofilms in flow chambers, Curr. Protoc. Microbiol. (2011) (Chapter 1, Unit 1B 2.1-1B 2.17).
[24] A. Heydorn, A.T. Nielsen, M. Hentzer, C. Sternberg, M. Givskov, B.K. Ersboll, S. Molin, Quantification of biofilm structures by the novel computer program COMSTAT, Microbiology 146 (Pt 10) (2000) 2395–2407.
[25] J.S. Suk, S.K. Lai, Y.Y. Wang, L.M. Ensign, P.L. Zeitlin, M.P. Boyle, J. Hanes, The penetration of fresh undiluted sputum expectorated by cystic fibrosis patients by non-adhesive polymer nanoparticles, Biomaterials 30 (2009) 2591–2597.
[26] R. Levato, M.A. Mateos-Timoneda, J.A. Planell, Preparation of biodegradable polylactide microparticles via a biocompatible procedure, Macromol. Biosci. 12 (2012) 557–566.
[27] M. Morales-Cruz, G.M. Flores-Fernandez, M. Morales-Cruz, E.A. Orellano, J.A. Rodriguez-Martinez, M. Ruiz, K. Griebenow, Two-step nanoprecipitation for the production of protein-loaded PLGA nanospheres, Results Pharma Sci. 2 (2012) 79–85.
[28] J.M. Barichello, M. Morishita, K. Takayama, T. Nagai, Encapsulation of hydrophilic and lipophilic drugs in PLGA nanoparticles by the nanoprecipitation method, Drug Dev. Ind. Pharm. 25 (1999) 471–476.
[29] U. Bilati, E. Allemann, E. Doelker, Development of a nanoprecipitation method intended for the entrapment of hydrophilic drugs into nanoparticles, Eur. J. Pharm. Sci. 24 (2005) 67–75.
[30] A.I. Caço, F. Varanda, M.J. Pratas de Melo, A.M.A. Dias, R. Dohrn, I.M. Marrucho, Solubility of antibiotics in different solvents. Part II. Non-hydrochloride forms of tetracycline and ciprofloxacin, Ind. Eng. Chem. Res. 47 (2008) 8083–8089.
[31] W.S. Cheow, M.W. Chang, K. Hadinoto, Antibacterial efficacy of inhalable levofloxacin-loaded polymeric nanoparticles against *E. coli* biofilm cells: the effect of antibiotic release profile, Pharm. Res. 27 (2010) 1597–1609.
[32] M. Enayati, E. Stride, M. Edirisinghe, W. Bonfield, Modification of the release characteristics of estradiol encapsulated in PLGA particles via surface coating, Ther. Deliv. 3 (2012) 209–226.
[33] K. Forier, K. Raemdonck, S.C. De Smedt, J. Demeester, T. Coenye, K. Braeckmans, Lipid and polymer nanoparticles for drug delivery to bacterial biofilms, J. Control. Release 190 (2014) 607–623.
[34] W.S. Cheow, K. Hadinoto, Green preparation of antibiotic nanoparticle complex as potential anti-biofilm therapeutics via self-assembly amphiphile–polyelectrolyte complexation with dextran sulfate, Colloids Surf. B Biointerfaces 92 (2012) 55–63.
[35] A. Henning, M. Schneider, N. Nafee, L. Muijs, E. Rytting, X. Wang, T. Kissel, D. Grafahrend, D. Klee, C.M. Lehr, Influence of particle size and material properties on mucociliary clearance from the airways, J. Aerosol Med. Pulm. Drug Deliv. 23 (2010) 233–241.
[36] N. Nafee, A. Husari, C.K. Maurer, C. Lu, C. de Rossi, A. Steinbach, R.W. Hartmann, C.M. Lehr, M. Schneider, Antibiotic-free nanotherapeutics: ultra-small, mucus-penetrating solid lipid nanoparticles enhance the pulmonary delivery and anti-virulence efficacy of novel quorum sensing inhibitors, J. Control. Release 192 (2014) 131–140.
[37] K.M. Jorgensen, T. Wassermann, P.O. Jensen, W. Hengzuang, S. Molin, N. Hoiby, O. Ciofu, Sublethal ciprofloxacin treatment leads to rapid development of high-level ciprofloxacin resistance during long-term experimental evolution of *Pseudomonas aeruginosa*, Antimicrob. Agents Chemother. 57 (2013) 4215–4221.
[38] K. Forier, A.S. Messiaen, K. Raemdonck, H. Deschout, J. Rejman, F. De Baets, H. Nelis, S.C. De Smedt, J. Demeester, T. Coenye, K. Braeckmans, Transport of nanoparticles in cystic fibrosis sputum and bacterial biofilms by single-particle tracking microscopy, Nanomedicine 8 (2013) 935–949.
[39] J.K. Miller, R. Neubig, C.B. Clemons, K.L. Kreider, J.P. Wilber, G.W. Young, A.J. Ditto, Y.H. Yun, A. Milsted, H.T. Badawy, M.J. Panzner, W.J. Youngs, C.L. Cannon, Nanoparticle deposition onto biofilms, Ann. Biomed. Eng. 41 (2013) 53–67.
[40] A.S. Messiaen, K. Forier, H. Nelis, K. Braeckmans, T. Coenye, Transport of nanoparticles and tobramycin-loaded liposomes in *Burkholderia cepacia* complex biofilms, PLoS One 8 (2013) e79220.
[41] M. Okshevsky, V.R. Regina, R.L. Meyer, Extracellular DNA as a target for biofilm control, Curr. Opin. Biotechnol. 33 (2015) 73–80.
[42] K. Xiang, Z. Dou, Y. Li, Y. Xu, J. Zhu, S. Yang, H. Sun, Y. Liu, Cytotoxicity and TNF-alpha secretion in RAW264.7 macrophages exposed to different fullerene derivatives, J. Nanosci. Nanotechnol. 12 (2012) 2169–2178.
[43] S. Xiong, S. George, H. Yu, R. Damoiseaux, B. France, K.W. Ng, J.S. Loo, Size influences the cytotoxicity of poly (lactic-co-glycolic acid) (PLGA) and titanium dioxide (TiO(2)) nanoparticles, Arch. Toxicol. 87 (2013) 1075–1086.
[44] I. Coowanitwong, V. Arya, P. Kulvanich, G. Hochhaus, Slow release formulations of inhaled rifampin, AAPS J. 10 (2008) 342–348.

Supplementary figure 1: Effect of DNase I (free) A) and NP-linked (PLGA-PL-DNase I) B) on formed *P. aeruginosa* biofilms. The values represent the percentages of biofilm formed. The results are expressed as the mean ± standard deviations of six replicates from three independent experiments as described in the material and methods. A student *t*-test was performed (*, $P < 0.01$; versus non-treated biofilms). The viable counts at control experiment was $1.63x10^{9}\pm8.5x10^{8}$ cfu/ml.

A) DNase I

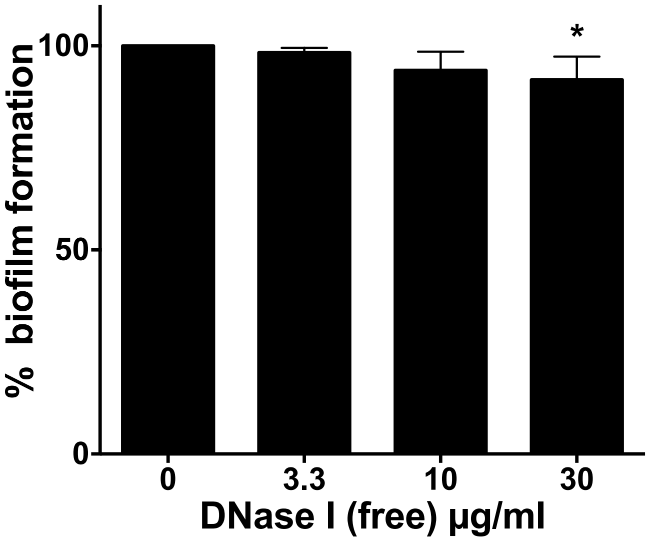

B) PLGA-PL-DNase I

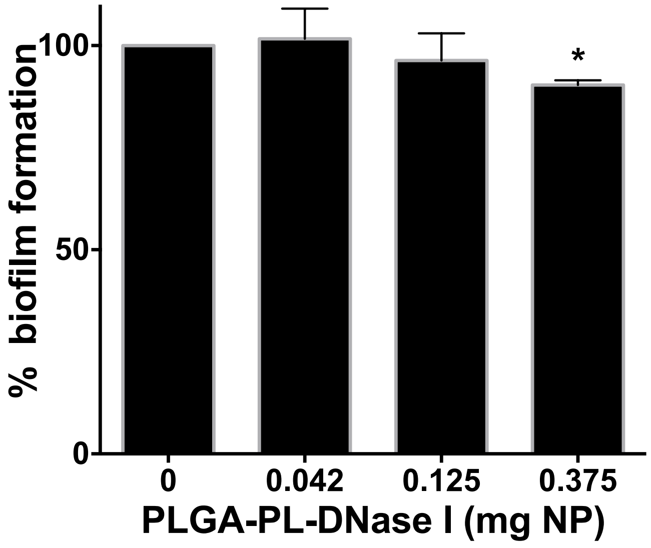

IV. ABSTRACT OF THE RESULTS AND DISCUSSION

Chapter 1: Radical scavengers as RNR inhibitors with antimicrobial properties

PUBLICATION 1

Bacterial infections are a major health concern worldwide due to the mortality and comorbidity associated levels. The frequent appearance and spreading of bacterial drug-resistant strains, together with the recalcitrance of infections caused by biofilms, has pointed out the urgent need to develop novel antibacterial agents that target essential bacterial processes. Since ribonucleotide reductase (RNR) performs critical functions in bacterial replication during infection conditions, it has been considered for long as an antibacterial target.

Amongst RNR inhibitors, some radical scavenger molecules have proved for long its inhibitory activity against the RNR enzyme, including some hydroxylamine derivatives such as hydroxyurea (HU). HU is a potent and well-known broad-spectrum RNR inhibitor that inhibits class I RNR in a wide variety of organisms from different domains of life, including bacteria but also complex eukaryotic organisms. It has been extensively used to treat several cancer types; however, since HU and other hydroxylamine radical scavengers lack specificity and inhibit eukaryotic cells replication, their use as antibacterial agents has been dismissed. Thus, the development of more specific radical scavenger hydroxylamines – with high antibacterial activity together with low eukaryotic cytotoxicity – has remained almost unexplored.

Here, we aimed to investigate the use of hydroxylamine derivative compounds as antibacterial candidates targeting the RNR enzyme. In previous investigations, two hydroxylamine radical scavengers similar to HU – hydroxylamine (HA) and *N*-methyl-hydroxylamine (M-HA) – (see **Fig. 13**) showed high antibacterial activity against the pathogenic bacteria *Bacillus anthracis* [242, 243]. Both molecules efficiently inhibit the activator subunit of *B. anthracis*

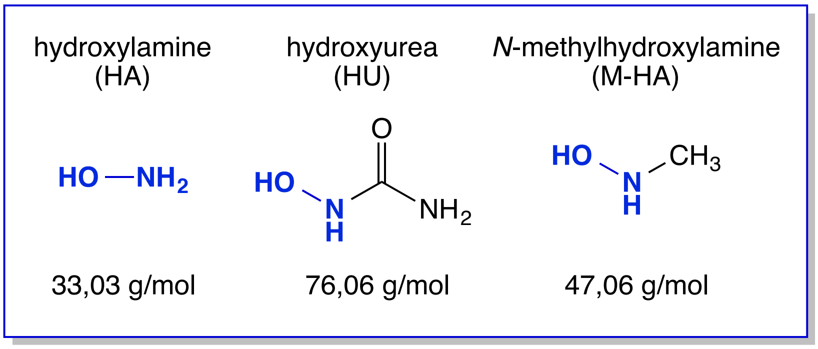

Figure 13. **Chemical structures of the radical scavangers HA, HU and M-HA.**

class Ib RNR by blocking the tyrosyl radical formation, similarly to HU. But whereas HU and HA clearly inhibit mouse class Ia at comparable levels than *B. anthracis* class Ib, M-HA only inhibits the bacterial enzyme. Indeed, other authors reported that M-HA delay senescence processes in human cells by acting as an antioxidant, demonstrating M-HA low toxicity in eukaryotic cells [310].

Since *N*-methyl-hydroxylamine shows as a specific drug candidate with antibacterial activity and potentially low cytotoxicity, by inhibiting bacterial RNRs but not eukaryotic RNRs, we explored in depth its antibacterial properties. These results are described in **Publication 1,** in which we evaluate both the growth inhibition of several pathogenic bacterial species by M-HA and its effect on eukaryotic cells, by comparing with HU and HA. Specifically, we assessed the 50% and 100% inhibitory concentrations of M-HA, HU, and HA on four Gram-positive bacteria (*S. aureus*, *Streptococcus mutans*, *Streptococcus sanguinis*, and *Mycobacterium bovis* BCG) and two Gram-negative bacteria (*P. aeruginosa* and *Burkholderia cenocepacia*) and determined the eukaryotic 50% cytotoxicity concentrations (CC_{50}) on murine macrophage cell cultures.

Both M-HA and HA globally inhibited bacterial growth better than the reference RNR inhibitor HU when testing the antibacterial properties of the radical scavengers in the different bacterial species (**Table** 1 from **Publication 1**), acting in both iron- and manganese-dependent class I RNRs. The direct inhibition that M-HA exerts in the bacterial RNR enzyme was previously determined to occur by quenching the radical formation, following a mechanism similar to HU and HA [243]. But while radical scavenging in RNR by HU and other radical scavengers with similar structures is presumed to occur somewhere in the electron transfer pathway between subunits [276], M-HA and HA may act directly in the radical generation site in the activator subunit in bacterial RNR due to their small size [311]. This may explain why both molecules are more effective at inhibiting the RNR enzyme than HU.

To complement the results and further confirm the antibacterial mode of action of M-HA, we analyzed *P. aeruginosa* cultures under the effect of M-HA, HA, and HU with a viability dye-based test by fluorescence microscopy imaging (**Figure 1** from **Publication 1**). As expected, bacterial cell integrity remained unaffected when using any of the three hydroxylamines, as radical scavengers inhibit bacterial growth by blocking DNA synthesis, but not directly destroying bacteria.

When determining eukaryotic cytotoxicity, M-HA affected at low levels eukaryotic cells proliferation, whereas both HU and HA showed highly cytotoxic. HU is used to inhibit eukaryotic cells in cancer chemotherapies, and both HU and HA previously showed to affect the eukaryotic RNR at significantly lower concentrations than M-HA, indicating better specificity of both HU and HA for the eukaryotic enzyme than M-HA [243]. Also, other authors had already demonstrated low cytotoxic effects when using M-HA on human fibroblasts [310], in concordance with our own results in murine macrophages.

Taking into account both antibacterial and cytotoxicity values, we calculated the therapeutic or selectivity indexes (SI) by using the ratio between CC_{50} and MIC_{50} values. Compared with HU and HA, M-HA resulted in high SI indexes (see **Table 1** from **Publication 1**), especially in *M.* bovis BCG and *P. aeruginosa*, which demonstrates the potential of such molecule as an antibacterial agent. However, the reason by which M-HA is more effective towards bacterial RNR than to the eukaryotic one has not been investigated. Bacterial and eukaryotic class I RNRs share low percentages of sequence identities [174, 312], and differences in the three-dimensional structure and in the activity of the redox centers may explain the differential inhibitory effects between bacteria and mammal cells. Apart from the role of radical scavenger molecules in inhibiting RNR, these molecules are unspecific and can also affect other cellular processes, either directly or indirectly. For instance, HU is known to mediate cell death by forming hydroxyl radicals induced by both superoxide production and increased iron uptake [313]. Whether M-HA could cause cell death due to similar mechanisms remains unknown.

Since the three radical scavengers, and particularly, M-HA, most affected *M. bovis* and *P. aeruginosa* bacteria, we determined their antimicrobial role to a greater extent during more realistic infection conditions: in *M. bovis* intracellular macrophage infection and in *P. aeruginosa* biofilm formation.

M. bovis BCG is a closer relative of the causative agent of tuberculosis, *M. tuberculosis*, and it has been validated as an *in vitro* model in mouse to study antimycobacterial agents to treat tuberculosis [314]. Also, *M. bovis* BCG shares 100 % of sequence identity of class I RNR protein to that of *M. tuberculosis* (**Fig.** S1 from **Publication 1**), indicating that results obtained with the testing of *M. bovis* BCG with M-HA can be extrapolated to *M. tuberculosis*. Whereas BCG cell number during mouse macrophage infection is indeed maintained in stable levels, it is known that mycobacteria inside macrophages are continuously growing and being killed, thus being a good model when studying inhibitors that act on DNA synthesis and cell replication processes [315].

Here, we demonstrated that *M. bovis* viability decreases during intracellular macrophage infection in the presence of the three radical scavengers. But whereas HU and HA inhibited bacterial cells at the same concentrations that inhibit macrophages growth, M-HA inhibited bacteria up to 85 % at very low concentrations without damaging macrophages (**Fig. 3** from **Publication 1**).

Since the antimycobacterial activity during intracellular macrophage infection was higher than expected, we wondered whether M-HA was inducing macrophage's own defense mechanisms and indirectly improved the global intracellular antibacterial activity. Different *in vivo* and *in vitro* studies have previously shown that both HU and HA induce the synthesis of different chemokines and cytokines, but with unknown mechanisms [316-318]. Here, we analyzed the ability of macrophages under the effect of the three radical scavengers to produce the immune factors TNF-α and NO, both known to have antibacterial activity against intracellular *M. bovis* BCG [319]. We showed that M-HA – but not HA neither HU – produces an increase in TNF-α levels on infected macrophages (**Fig. 4A** from **Publication 1**), which may amplify the antibacterial effect that M-HA exerts in *M. bovis* by inhibiting RNR. Mycobacterial infections in macrophages usually stimulate TNF-α production by increasing the synthesis of exosomes that contain mycobacterial antigens [320]. However, exosomes release is generally detected after 48 – 72 h post-infection [320] and we already detected an induction effect by M-HA at 24 h. For this reason, and together with the fact that uninfected macrophages under M-HA treatment also produced increased TNF-α, we believe that M-HA directly induces TNF-α production through other mechanisms, as described for other drugs [321, 322]. To go deepen in studying M-HA induced mycobacterial killing during intracellular infection, we also determined the levels of cytokines IL-10 and IL-12 during radical scavengers' treatment to determine if M-HA was affecting alternative cytokine routes. We detected an increase in IL-12 levels in infected macrophages under the effect of HA, but not under the effect of M-HA neither HU. Both TNF-α and IL-12 cytokines play critical roles in the control of mycobacterial infections by activating macrophages and favoring mycobacterial killing [323, 324]. Thus, both M-HA and HA radical scavengers could help macrophages in mycobacterial killing by inducing different cytokine induction.

Since *P. aeruginosa* is a pathogen causing severe infections mainly growing as biofilm (including infections in lungs, clinical devices, and wounds), we investigated the antibiofilm properties of M-HA. We analyzed the antibiofilm effect of M-HA, HA, and HU on *P. aeruginosa* biofilm formation by growing biofilm in the presence of the radical scavengers and demonstrated that M-HA completely prevents *P. aeruginosa in vitro* biofilm formation, with similar values for both HU and HA (**Fig. 5** from **Publication 1**). We also assessed the inhibition of *P. aeruginosa* already formed biofilm under both static (**Fig. 6** from **Publication 1**) and flow biofilm conditions (**Table 2** and **Fig. 7** from **Publication 1**). Despite HU and HA better inhibited *P. aeruginosa* biofilm, especially in biofilms formed under continuous flow, M-HA clearly reduced *P. aeruginosa* formed biofilm at significant levels, reducing approximately 60 % of biofilm mass after treating with repeated doses every 24 h for three days employing a concentration of 5.2 µg/mL (**Fig. 6** from **Publication 1**).

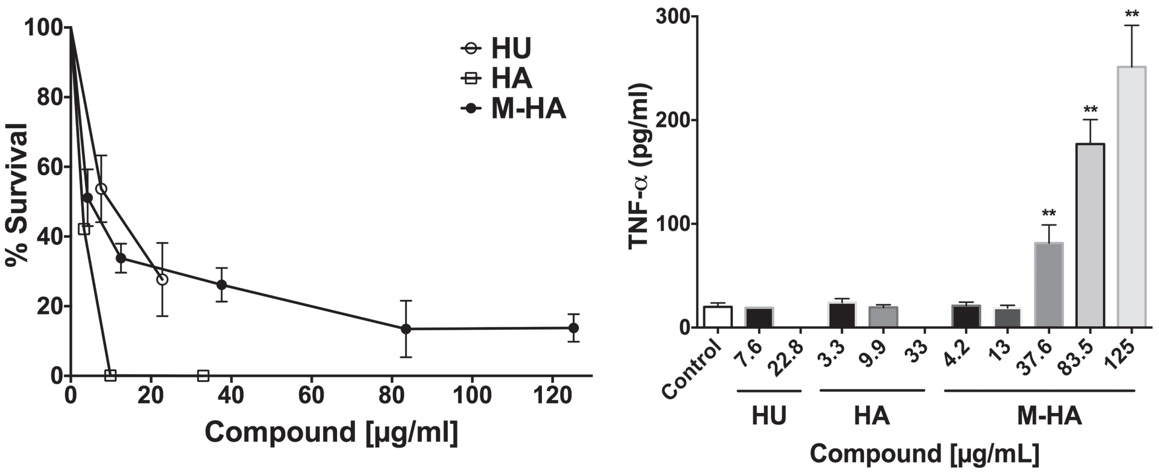

Figure 14. M-HA displays intracellular antimycobacterial activity in macrophages culture.

A) HU, HA, and M-HA radical scavengers reduce the viability of *M. bovis* BCG growing inside murine macrophages. Different concentrations of radical scavengers are added after 72 h of infection and renewed every 24 h.

B) M-HA induce infected macrophages to produce increased TNF-α levels after 24 h of infection.

Finally, we explored an antibacterial combined therapy by treating a *P. aeruginosa* formed biofilm with both M-HA and a well-known and clinically used antibiotic, ciprofloxacin. The use of antibiotic combination is frequently used in infections caused by multi-drug resistant Gram-negative bacteria as a strategy to prevent the appearance of genetic resistances [325]. We showed that ciprofloxacin in combination with M-HA removes biofilm more efficiently than using ciprofloxacin alone (**Fig. 8** from **Publication 1**).

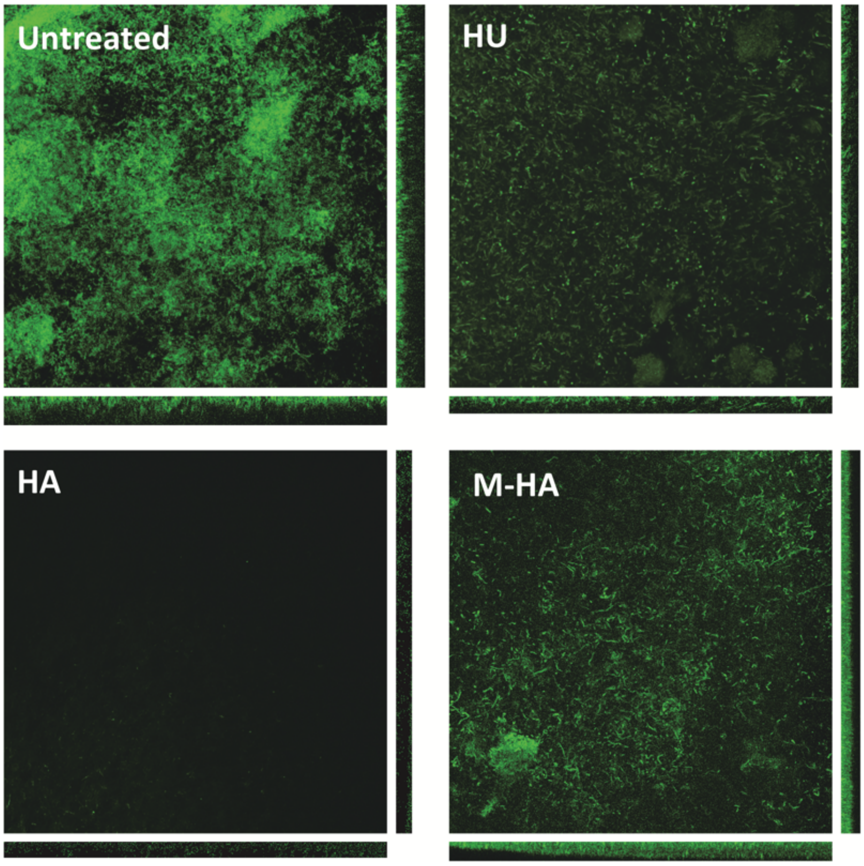

Figure 15. Reduction of *P. aeruginosa* biofilm by the radical scavengers HU, HA, and M-HA.

Radical scavengers HU, HA, and M-HA reduce *P. aeruginosa* biofilm cultured under flow conditions, which were imaged by Confocal Scanning Laser Microscopy.

PUBLICATION 2

To explore new RNR inhibitor radical scavengers with improved values of antibacterial activity and lower cytotoxicity than M-HA, we designed a small library of molecules with the *N*-hydroxylamine (-NH-OH) functional group, the radical scavenging active chemical moiety of HU, HA, and M-HA. These results are presented in **Publication 2**, where we evaluate the antibacterial and antibiofilm properties of the chemical library molecules on different bacterial pathogens and also their cytotoxic effect on eukaryotic cells.

Specifically, in **Publication 2**, in collaboration with a research group from the Department of Organic Chemistry from the University of Barcelona, we chemically synthesized 16 *N*-hydroxylamine molecules to get enhanced free-radical scavenging (FRS) activity against bacterial RNRs. The synthesis was carried on by reductive amination of different aldehydes to corresponding *N*-hydroxylamine molecules. We added six commercial *N*-hydroxylamine molecules, extending the library to a total of 22 molecules (**Fig. 16**) All the library molecules harbor a fixed -NH-OH moiety but with varied chemical structures that differently affect the global FRS activity: *N*-alkyl-hydroxylamines (compounds **1** to **6**), *N*-cycloalkyl-hydroxylamines (molecules **7** and **8**), *N*-aryl-hydroxylamines (molecules **9** and **10**), *N*-aryl-hydroxylamines with electron-withdrawing groups (fluorine and trifluoromethyl; molecules **11** to **15**), *N*-aryl-hydroxylamines with electron-donating groups (methyl and methoxy; molecules **16** to **19**), and *N*-hydroxylamines containing a heteroaryl group (molecule **20**) or being part of the heterocycle as secondary hydroxylamines (molecules **21** and **22**).

We screened the antibacterial activity of all the library *N*-hydroxylamines in six bacterial pathogens: four Gram-positive (*B. anthracis*, *S. aureus*, *S. epidermidis*, and *E. faecalis*) and two Gram-negative (*P. aeruginosa* and *E. coli*) bacteria. Minimum inhibitory concentrations of 50 % (MIC_{50}) were determined in liquid cultures of the six bacteria for all the 22 *N*-hydroxylamine molecules, for the reference radical scavengers HU and M-HA, and for the broad-spectrum antibiotic ciprofloxacin (**Table 1** from **Publication 2**).

The majority of the *N*-hydroxylamines (**1** to **5**, **7**, **9**, **13**, **16**, and **19** to **22**) showed inactive as antibacterial agents (MIC_{50} > 1000 µg/mL). The molecules that displayed antibacterial activity (**6**, **8**, **10**, **11**, **12**, **14**, **15**, **17**, and **18**) were mainly most effective in bacteria encoding for class Ib RNR (here, the Gram-positive) rather than in bacteria encoding for class Ia RNR (here, the Gram-negative), which were overall less affected.

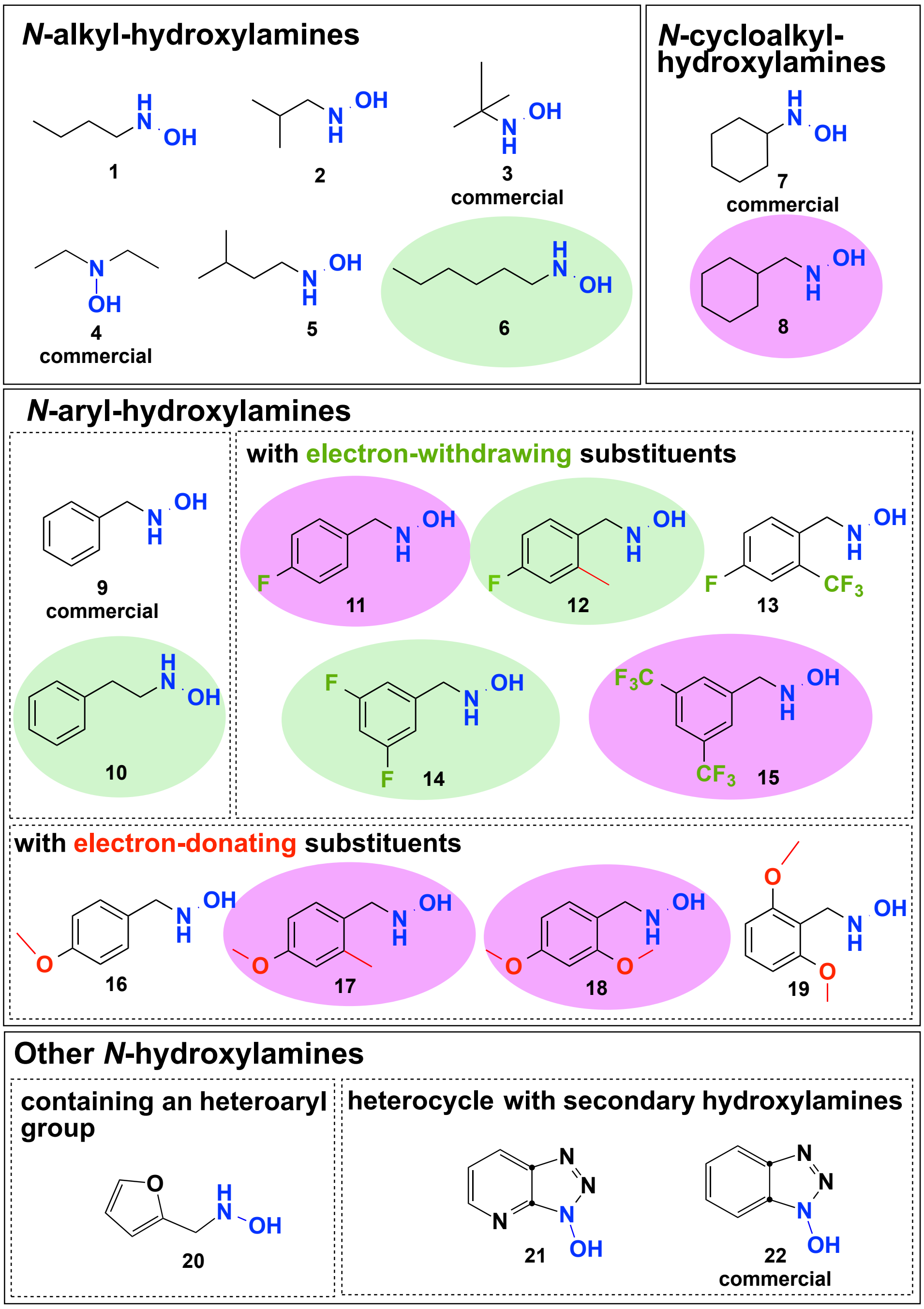
N-alkyl-hydroxylamines
1
2
3
commercial
4
commercial
5
6
N-cycloalkyl-hydroxylamines
7
commercial
8
N-aryl-hydroxylamines
9
commercial
10
with electron-withdrawing substituents
11
12
13
14
15
with electron-donating substituents
16
17
18
19
Other N-hydroxylamines
containing an heteroaryl group
20
heterocycle with secondary hydroxylamines
21
22
commercial

Figure 16. Chemical structures of the N-hydroxylamines library molecules from Publication 2.

The library contains 22 structurally diverse N-hydroxylamine molecules: six **linear** N-hydroxylamines (**1** to **6**), two **cyclic** N-hydroxylamines (**7** and **8**), two **aromatic** N-hydroxylamines (**9** and **10**), five aromatic N-hydroxylamines with **electron-withdrawing** groups (**11** to **15**), four aromatic N-hydroxylamines with **electron-donating** groups (**16** to **19**), one N-hydroxylamine containing a **heteroaryl group** (**22**), and two N-hydroxylamines formed by a **heterocycle with secondary hydroxylamines** (**21** and **22**). The N-hydroxylamine common moiety (-NH-OH) is colored in blue, electron-withdrawing groups in green, and electron-donating groups in red. Molecules with **antibacterial activity** are pictured inside a **green** or a **purple circle** (these last are selected molecules with **higher Selectivity Indexes**).

The fact that *N*-hydroxylamine molecules show more specific towards class Ib enzymes is consistent with previous investigations, as M-HA better inhibited bacterial class Ib RNR enzymes [243], resulting in higher antibacterial activity [326].

Molecules **8**, **10**, **12**, **14**, and **15** showed antibacterial activity against Gram-negative bacteria. Specifically, molecule **8** was the most active, inhibiting both *P. aeruginosa* and *E. coli* growth with slightly better results to those of M-HA.

Overall, the linear and cyclic aliphatic *N*-hydroxylamines with a small carbon number (**1** to **5**, and **7**), containing a heteroaryl group (**20**), or being part of the heterocycle as secondary hydroxylamines (**21** and **22**) were inactive as antibacterial agents. Only the linear and cyclic alkyl *N*-hydroxylamines with the bigger carbon number (molecules **6** and **8**, respectively) showed active, but the antibacterial activity of the linear *N*-hydroxylamine (**6**) was relatively low and it only inhibited *B. anthracis* growth. The aromatic *N*-hydroxylamines – with or without electron-donating or electron-withdrawing groups – were more effective against bacteria compared with the aliphatic ones, except some aromatic *N*-hydroxylamines that showed no antibacterial activity (molecules **9**, **13**, **16**, and **19**).

Since we designed the *N*- hydroxylamine library to identify molecules with improved FRS activity that could act on bacterial RNRs, we determined the radical scavenging of the active and two inactive molecules by calculating the *in vitro* scavenging of the free radical DPPH·. The most active molecules (**8**, **10**, **11**, **12, 14**, **15**, **17**, and **18**) displayed FRS activities similar to the reference radical scavenger RNR inhibitors, HU and M-HA, and to that of the well-known radical scavenger ascorbic acid (AA) (**Table 2** from **Publication 2**). However, and as expected, the FRS activities of the low- (**6**) or non-active (**2** and **3)** aliphatic *N*-hydroxylamines were several times lower (higher radical scavenger concentration needed) compared with the values of the active *N*-hydroxylamines.

	DPPH· scavenging activity (IC$_{50}$ (μM))^a	
compounds	8 h incubation time	12 h incubation time
2	>256	>256
3	>256	>256
6	171.4 ± 23.0	141.3 ± 17.4
8	9.3 ± 0.7	8.6 ± 0.5
10	14.3 ± 0.8	13.7 ± 0.9
11	6.4 ± 0.4	5.8 ± 0.3
12	4.2 ± 0.3	3.8 ± 0.3
14	23.1 ± 0.2	20.5 ± 0.3
15	8.1 ± 0.5	7.6 ± 0.5
17	4.8 ± 0.6	4.4 ± 0.8
18	6.5 ± 0.6	5.8 ± 0.6
AA	10.2 ± 1.8	10.1 ± 1.8
HU	8.6 ± 1.2	7.5 ± 0.9
M-HA	20.3 ± 2.0	18.1 ± 1.5

Figure 17. Free radical scavenging activities (FRS) of the *N*-hydroxylamine molecules.

FRS activity values of the radical scavenger N-HA molecules. The values represent the concentration of radical scavenger needed to reduce the 50 % of the stable DPPH· radical.

N-hydroxylamine free radical scavenging (FRS) activity depends on the ability to form stable and electron-rich N-oxyl species (-NH-O·), and their generation is mainly favored by resonance and electron-donating inductive effects [327]. Thus, we designed several molecules aiming to increase resonance and inductive effects of the *N*-hydroxylamines. To do so, we incorporated to the library *N*-alkyl-hydroxylamine molecules with increased chain length compared with M-HA to generate electron-donating inductive effects that could stabilize the radical (**1** to **5**), and molecules with increased resonance effects by adding *N*-benzyl-hydroxylamine analogues to the library (molecules **9** to **19**). The inductive effects generated by the different *N*-alkyl-hydroxylamines of the library, especially by the ones with the lowest carbon number (less than six) (**1** to **5**) were insufficient to stabilize N-oxyl species and exhibited both low FRS and antibacterial activities (being M-HA, with one carbon atom, an exception). Unlike inductive effects, increasing resonance effects resulted in increased FRS and antibacterial activities, with an IC_{50} at least to 13 times higher than linear molecules, thus being *N*-benzyl-hydroxylamine analogues the most active radical scavengers. When analyzing the addition of electron-withdrawing or with electron-donating groups to *N*-benzyl-hydroxylamine analogues to generate inductive effects, we did not observe any significant differences between the FRS and antibacterial activities, evidencing that resonance effects overlap the induction effects in these molecules. In consistency with our results, some authors have already described that aromatic molecules such as phenols possess high radical scavenging activities able to inhibit RNR [276, 328], probably because aromatic rings generate very stable spin delocalized systems that favor the free radical quenching. However, some of the library *N*-benzyl-hydrozylamine analogues showed as an exception, displaying no antibacterial activity (**9**, **13**, **16**, and **19**), and entailing a challenge for the discovery and the understanding of the structure-activity relationship of such molecules. We hypothesize that the different molecules could scavenge the free radical in several locations of the RNR long electron transfer pathway generated between the activator and catalytic subunits. Docking experiments in RNR with radical scavengers with similar molecular weight as our *N*-hydroxylamine library molecules already demonstrated that these molecules are unable to diffuse inside the radical generation site in the activator subunit and act in different parts of the electron transfer pathway, near the protein surface [276].

To investigate the potential of the active molecules (**6**, **8**, **10**, **11**, **12**, **14**, **15**, **17**, and **18**) as antibacterial drugs, we additionally determined the eukaryotic cytotoxicity in murine macrophages and calculated the selectivity indexes (SI; the ratio between cytotoxicity and antibacterial inhibitory concentrations) (**Table 1** from **Publication 2**). Taking into account both values we concluded that molecules **11**, **15**, **17**, and **18** possess a better balance between antibacterial activity and cytotoxicity in Gram-positive, and molecules **8** and **15** in Gram-negative bacteria. Several of the new *N*-hydroxylamine molecules exhibit significant toxicity levels to eukaryotic cells, but some of them have a high SI value (> 5) and should be taken into account as valuable antimicrobials. The lipophilicity values of representative active molecules (**8**, **10**, **12**, **13**, **14**, and **15**) were additionally determined as a measure of membrane permeability and solubility in physiologic conditions, obtaining moderate lipophilicity indexes in the majority of the molecules tested (**Fig. 1** from **Publication 2**).

To validate that the active *N*-hydroxylamines inhibited bacterial growth by inhibiting RNR, we further analyzed the direct effect on RNR activity by determining the amount of purine dNTPs in exponential growing cultures of *P. aeruginosa* in the presence of the most active molecules against this pathogen. Molecules **8** and **12**, and so HU, significantly reduced purine dNTPs levels in all the cases compared with a culture without any radical scavenger (**Figure 2 A)** from **Publication 2**). Besides, the induction of *P. aeruginosa* class Ia RNR enzyme under the effect of **8**, **12**, and HU was evaluated at the protein level, concluding that both **8** and **12** radical scavengers induced class Ia expression (**Figure 2 B)** from **Publication 2**), the same way as HU does [329]. This fact demonstrates the direct effect of such radical scavenger molecules in bacterial RNR.

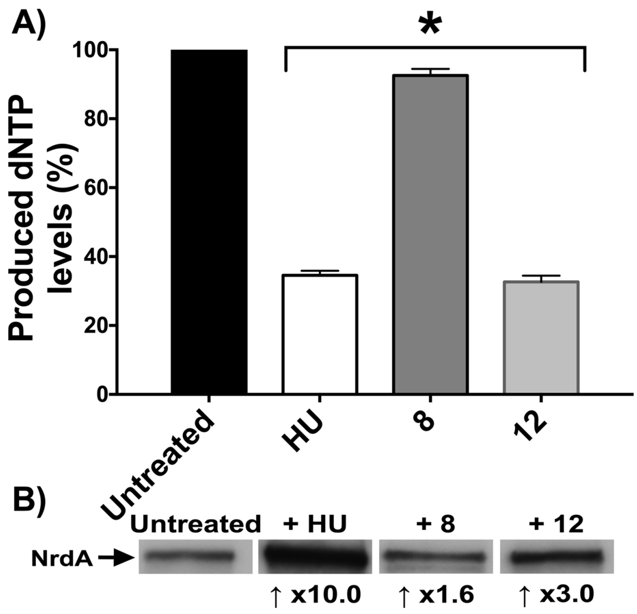

Figure 18. Effect of N-HA molecules on RNR.

A) Purine dNTP levels decrease in *P. aeruginosa* exponential cultures under the effect of HU and N-HA molecules **8** and **12**.

B) *P.* aeruginosa RNR catalytic subunit (NrdA) is overexpressed under the effect of HU and the N-HA molecules **8** and **12**.

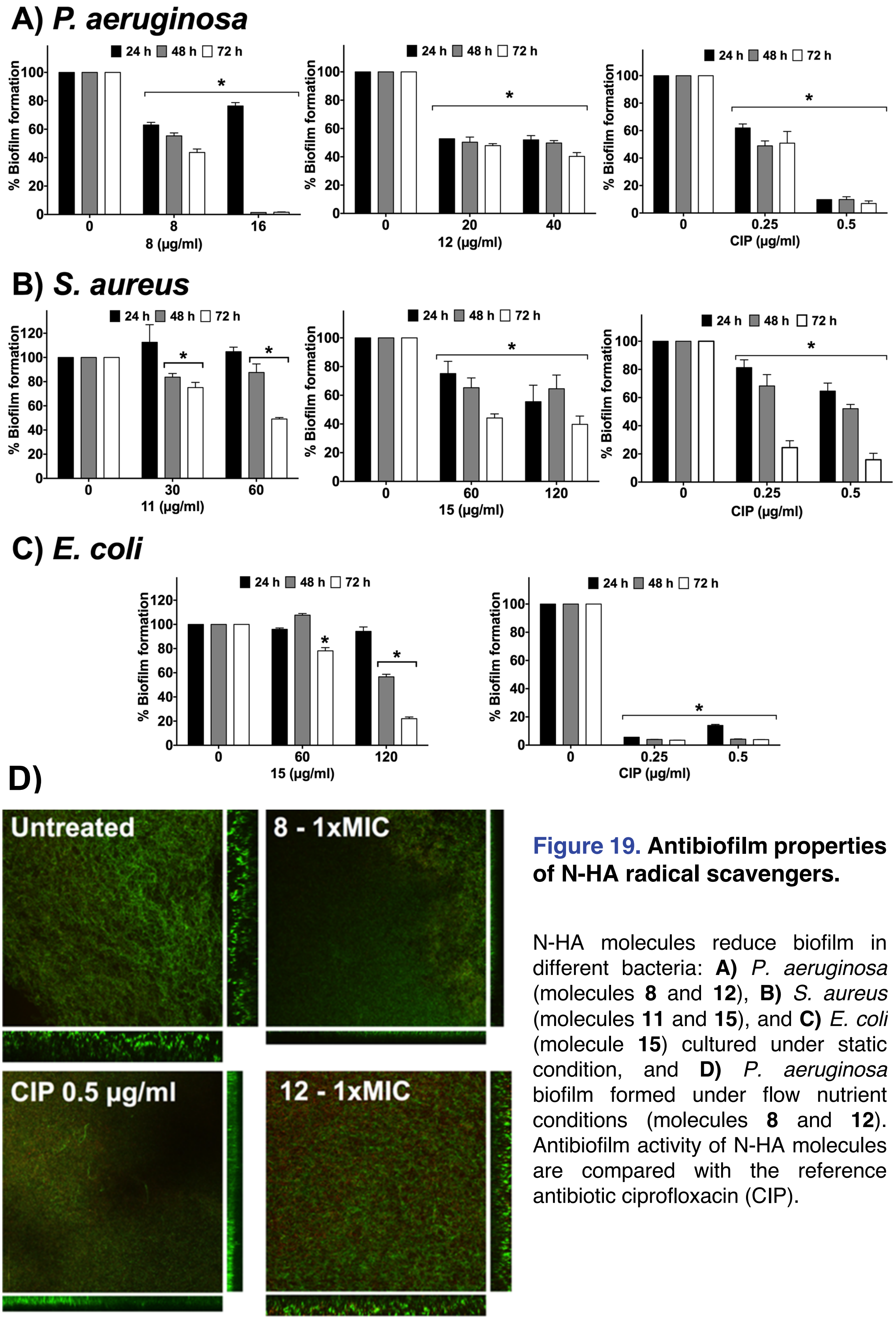

Figure 19. Antibiofilm properties of N-HA radical scavengers.

N-HA molecules reduce biofilm in different bacteria: **A)** *P. aeruginosa* (molecules **8** and **12**), **B)** *S. aureus* (molecules **11** and **15**), and **C)** *E. coli* (molecule **15**) cultured under static condition, and **D)** *P. aeruginosa* biofilm formed under flow nutrient conditions (molecules **8** and **12**). Antibiofilm activity of N-HA molecules are compared with the reference antibiotic ciprofloxacin (CIP).

Complementarily, we evaluated the antibacterial mode of action of the most active N-HA against *B. anthracis*, *S. aureus*, *E. coli*, and *P. aeruginosa* through fluorescence microscopy by using a dyed-based viability assay that measures bacterial membrane integrity (**Fig. 3** from **Publication 2**). As expected, the N-HA molecules tested behaved similar to the references HU, HA, and M-HA (see **Fig. 1** from **Publication 1**), by not destroying bacterial cells, but only inhibiting their growth in a bacteriostatic mode of action.

Finally, we analyzed the antibiofilm effect of the most promising N-HA molecules showing higher selectivity indexes in *P. aeruginosa* (**8** and **12**), *S. aureus* (**11** and **15**), and *E. coli* (**15**), together with the antibiotic ciprofloxacin as a reference, in static *in vitro* established biofilms (**Fig. 4** from **Publication 2**). Molecules **8** and **12** reduced *P. aeruginosa* biofilm mass with similar (**12**) or even better (**8**) results than ciprofloxacin, and **11** and **15** reduced *S. aureus* biofilm mass at similar levels than ciprofloxacin. However, despite **15** reduced *E. coli* biofilm biomass, ciprofloxacin reduction levels were greater. We analyzed the effects of both **8** and **12** in *P. aeruginosa* biofilm formed under continuous nutrient flow to evaluate their antibiofilm activities, determining both a biomass and thickness reduction in previously formed biofilms in both cases and with similar values to those under the effect of the reference antibiotic ciprofloxacin (**Fig. 5** from **Publication 2**).

Chapter 2: Improving the treatment of biofilm infections

PUBLICATION 3

Following our previous work centered on searching new antimicrobial therapies, we focused our attention on inhibiting bacteria growing in biofilms. Biofilms account for the vast majority of infections occurring in humans, being the cause of high rates of morbidity and mortality. Biofilm-forming bacteria fundamentally differ from their planktonic counterparts in the presence of an extracellular matrix that surround and bind together individual microorganisms, increasing tolerance and resistance to standard antimicrobial agents. Thus, many approaches to improve the treatment of biofilm infections aim to induce the dispersal of cells by dissociating matrix components with enzymes [16]. However, some authors have pointed out that matrix-hydrolytic enzymes should be combined with antibacterial agents to avoid bacteria to disperse through the bloodstream and lead to fatal septicemia [330].

Biofilm cell dispersal can be achieved by using degrading enzymes that target critical components of the matrix such as eDNA, which plays key roles in antimicrobial tolerance [122] and biofilm formation and stability [331]. DNaseI is a well-known DNA hydrolytic enzyme that possesses high antibiofilm activity since it prevents biofilm formation and disrupts already formed biofilms from different bacterial species, including the opportunist pathogen *P. aeruginosa* [121], which frequently establish severe chronic pulmonary biofilm infections in patients suffering diseases such CF and COPD. Aerosolized DNaseI has been employed as a treatment for the airway infections of cystic fibrosis patients, reducing biofilm mucus secretion [332].

Polymeric materials like poly(lactic-co-glycolic acid) (PLGA) can be assembled into nanoparticles (NPs) that encapsulate and deliver drugs in a sustained manner. This property makes them a useful tool to design new treatments for bacterial infections since they need a continuous drug supply in the infection site. PLGA is a biodegradable, biocompatible, and FDA-approved copolymer that can be used to fabricate NPs to load drugs with varied chemical composition and physical properties [333]. Also, NPs production can be carried out by a wide array of methods that are easy to scale-up, and the synthesis parameters can be modified to obtain specific particle size, desired drug kinetics release, and to hide specific drug chemical properties to both avoid unspecific interactions and favor solubility [334].

Here, we aimed to develop a drug delivery system that physically combines the use of the antibiotic ciprofloxacin with DNase I to: i) improve the antibiotic kinetics release and ii) enhance the diffusion of the antibiotic through the biofilm by disassembling the matrix eDNA. In **Publication 3**, in collaboration with the research group Biomaterials for Regenerative Therapies from the Institute for bioengineering for Catalonia, we describe the synthesis of biodegradable PLGA NPs containing ciprofloxacin with surface-coated DNase I by using a toxic-free fabrication method and assess its antimicrobial efficacy against *in vitro P. aeruginosa* biofilms. Since functionalization of PLGA NPs with DNase I requires surface chemical modification, we coated PLGA NPs with poly-(L-lysine) (PL). Additionally, we evaluate how the surface modification with PL coating affects the antibacterial and antibiofilm activity by producing NPs with and without PL coating (positively or negatively charged).

Specifically, we used a novel, non-toxic, modified nanoprecipitation method to synthesize four different types of PLGA NPs (see **Table 1** from **Publication 3**): containing ciprofloxacin (PLGA-CPX), containing ciprofloxacin and surface-coated with poly-(L-lysine) (PLGA-PL-CPX), surface-coated with poly-(L-lysine) and DNaseI (PLGA-PL-DNaseI), and containing ciprofloxacin and surface-coated with poly-(L-lysine) and DNaseI (PLGA-PL-CPX-DNaseI). Synthesized NPs were physically characterized in terms of shape, size, size distribution, charge, and ciprofloxacin and DNase I content. We obtained spherical, monodispersed PLGA NPs of approximately 200-300 nm (see **Fig. 1A** from **Publication 3**), a size that allows them to diffuse through mucus pores in pulmonary infections [335].

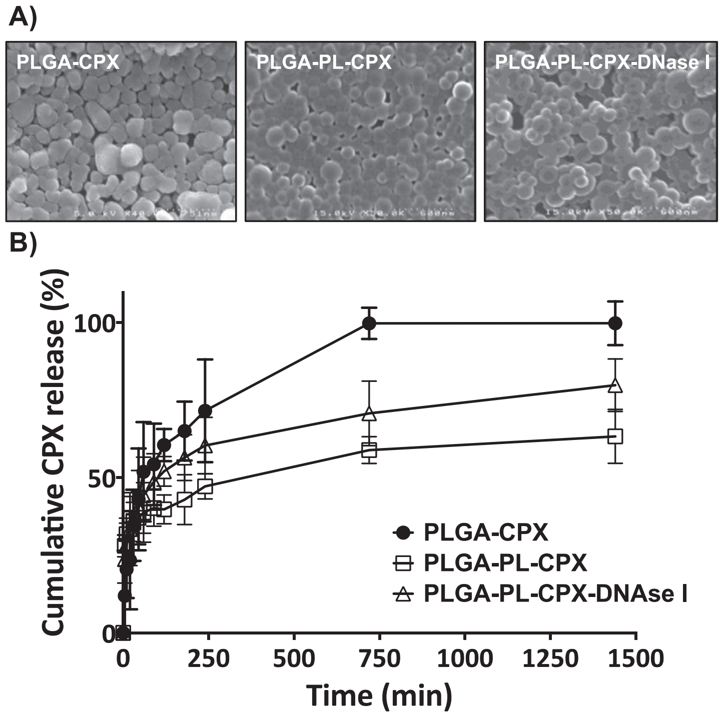

Figure 20. PLGA NPs characterization.

A) SEM images of synthesized PLGA NPs containing ciprofloxacin show spherical and monodispersed NPs in all the different formulations.

B) Ciprofloxacin-loaded PLGA NPs *in vitro* kinetics release present a biphasic profile consisting on a burst release followed by a slow sustained release.

NPs resulted positively charged (approximately +30 mV) when poly-(L-lysine) was used as a coating (PLGA-PL-CPX, PLGA-PL-DNaseI, and PLGA-PL-CPX-DNaseI) or negatively charged (approximately -13 mV) when poly-(L-lysine) was absent (PLGA-CPX). We obtained similar values of ciprofloxacin content (between 1.7 and 2.6 µg/mg of NPs) and DNaseI activity (26.2 and 32.0 µg/mg*h) (see **Table 1** from **Publication 3**).

This novel method for polymeric NPs synthesis seems promising since it makes use of ethyl-lactate as a green, non-toxic, and FDA-approved solvent [336], which should facilitate regulatory issues for drug commercialization approval. Also, NPs obtained by this method display a homogeneous size distribution, as we can corroborate with our own results (**Table 1** from **Publication 3**). However, hydrophobic molecules are better encapsulated than hydrophilic [337], and encapsulation yields for hydrophilic molecules such as ciprofloxacin are still low and should be improved.

To evaluate the ciprofloxacin *in vitro* kinetics release of the PLGA NPs, we measured by HPLC the released ciprofloxacin through time from a NPs suspension introduced in dialysis cassette. Between 40 and 50% of NP-loaded ciprofloxacin was quickly released at the first hour upon suspension for both negatively charged (PLGA-CPX) and positively charged (PLGA-PL-CPX and PLGA-PL-CPX-DNase I) NPs (see **Fig. 1B** from **Publication 3**). After the first hour, ciprofloxacin release slowed down in all the cases, but with small differences in their rates: at 12 h after preparing NPs suspension, negatively charged PLGA-CPX released all the antibiotic content, while positively charged PLGA-PL-CPX and PLGA-PL-CPX-DNase I released about 60 and 80 %, respectively. The first burst kinetics release may indicate that NP loaded-ciprofloxacin accumulates on the NPs surface, being quickly dissolved in the environment once suspended, a behavior reported by other hydrophilic molecules [338]. A desirable antibiotic kinetics release to treat bacterial biofilms should follow a biphasic profile consisting of a first burst release and a subsequent sustained release to avoid the appearance of antibiotic tolerance and resistance [339]. In our case, positively charged NPs (PLGA-PL-CPX and PLGA-PL-CPX-DNase I) displayed a prolonged and favorable late release than negatively-charged NPs (PLGA-CPX). We attribute these

Table 7. Minimal Inhibitory Concentrations of soluble ciprofloxacin and PLGA NPs loaded with ciprofloxacin.

	Ciprofloxacin MIC (µg/ml)			
	CPX	PLGA–CPX	PLGA–PL–CPX	PLGA–PL–CPX–DNase I
P. aeruginosa PAO1 ATCC 4122	0.39	0.0625	0.5	0.5
S. aureus ATCC 12600	0.0975	0.125	0.5	0.5

differences to the stabilization effects that cationic PL coating may provide on ciprofloxacin by direct interaction [340].

After PLGA NPs characterization, we proceeded by evaluating their cytotoxicity on murine macrophages together with their antimicrobial effect on both planktonic bacteria. Any of the different synthesized NPs did not interfere on murine macrophages viability, demonstrating no toxicity (see **Fig. 2** from **Publication 3**). Inhibition of *in vitro* planktonic cultures growth of the most co-occurring bacteria in lung infections, *P. aeruginosa* and *S. aureus*, demonstrated that negatively charged ciprofloxacin-loaded NPs (PLGA-CPX) displayed similar (*S. aureus*) or even higher (*P. aeruginosa*) antibacterial activity than free ciprofloxacin, but positively charged ciprofloxacin-loaded PLGA NPs (PLGA-PL-CPX and PLGA-PL-CPX-DNase I) presented reduced antibacterial efficiency (higher MIC values), compared with free ciprofloxacin (see **Table 2** from **Publication 3**). We hypothesize that the divergence between the antibacterial effect of negative- and positively charged NPs is due to the different releasing rates and to the total amount of ciprofloxacin released until the time of determination. More studies are still needed to understand such differences.

We evaluated the antibiofilm activity of the PLGA NPs in *P. aeruginosa* by determining the effect in two *in vitro* biofilm models: in static biofilms (on both during biofilm formation and on preformed biofilms) and in a continuous flow biofilm system. All of the synthesized NPs containing ciprofloxacin prevented biofilm formation at similar concentrations than soluble antibiotic (see **Fig. 3** from **Publication 3**). When determining the antibiofilm effect on static established biofilms, all the different PLGA NPs were able to decrease biofilm mass (see **Fig. 4** from **Publication 3**). We observed similar biofilm biomass levels between negatively and positively charged NPs loaded with ciprofloxacin (PLGA-CPX and PLGA-PL-CPX), indicating that surface charge was not a critical physicochemical parameter affecting NPs diffusion through biofilm matrix, similarly to what other authors have previously determined with polystyrene NPs [341]. As we hypothesized, the addition of the matrix-degrading agent DNase I, which lacks antibiofilm activity for itself (see **Supplementary Fig. 1** **Publication 3**), enhanced antibiofilm activity of soluble and encapsulated ciprofloxacin, demonstrating synergy between ciprofloxacin and DNase I (see **Fig. 4** and **Fig. 6** from **Publication 3**). Thus, NPs bearing both ciprofloxacin and DNase I (a mixture of positively charged NPs PLGA-PL-CPX and PLGA-PL-DNase I, and positively charged PLGA-PL-CPX-DNase I) showed significantly more active in degrading biofilm than NPs without DNase I (negatively charged PLGA-CPX and positively charged PLGA-PL-CPX NPs). In the same way, the combination of free ciprofloxacin with free

DNase I performed better than free ciprofloxacin. Interestingly, the synergy between ciprofloxacin and DNase I improved when using NPs that physically combined both ciprofloxacin and DNase I (PLGA-PL-CPX-DNase I), observing the highest biofilm mass reduction (> 95 %). This indicates that DNase I contained on NPs may facilitate NPs-contained ciprofloxacin diffusion through biofilm by disassembling eDNA, a critical stability component in *P.* aeruginosa biofilms. It is known that under the effect of DNase I, the biofilm matrix becomes more permeable to antibiotics, increasing their diffusion and efficacy [342].

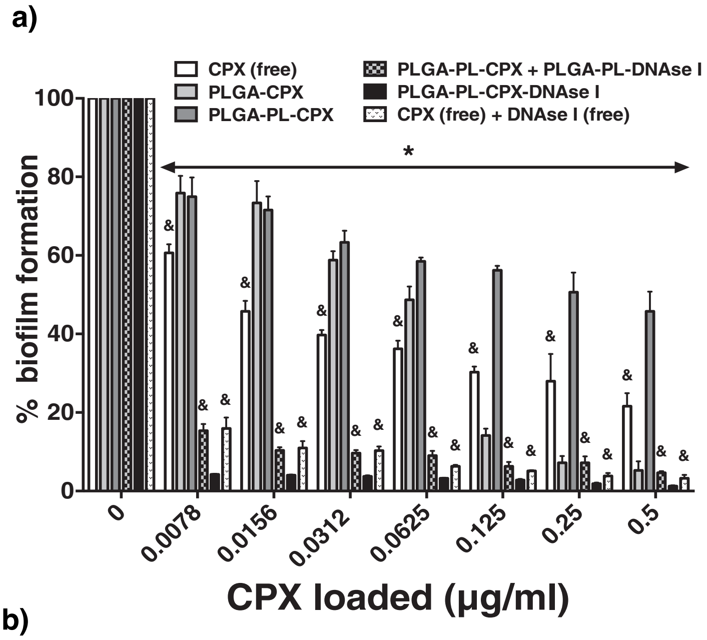

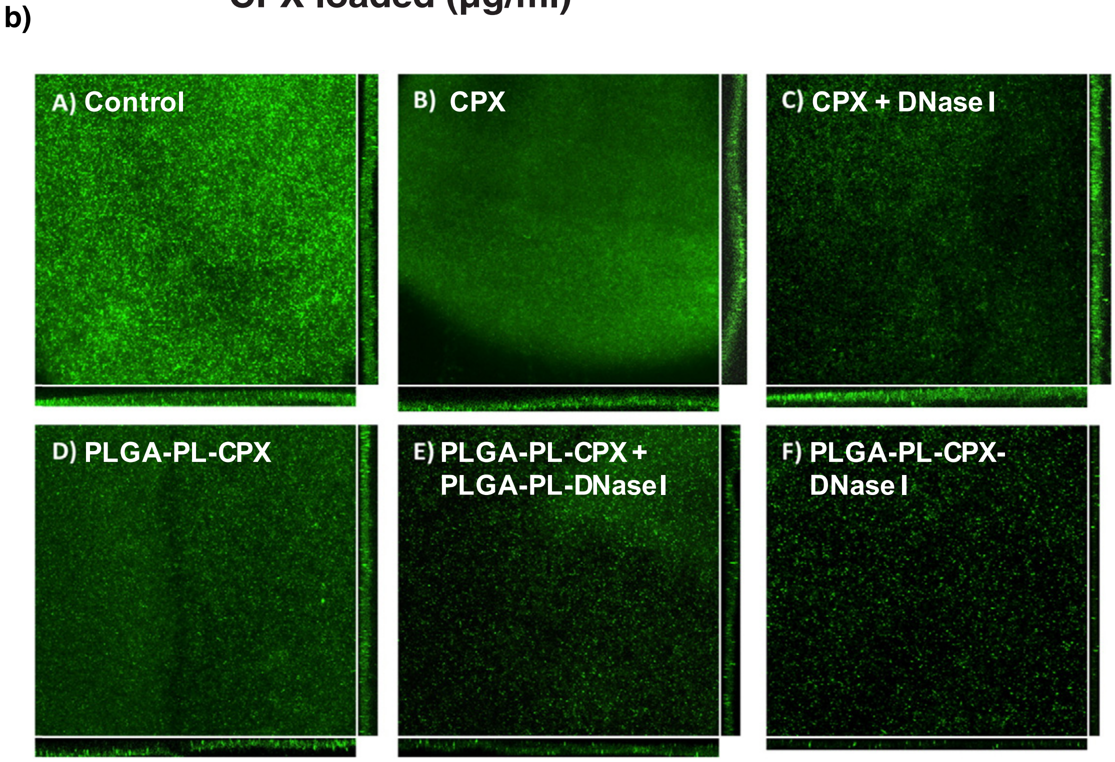

Figure 21. Eradication of mature biofilms by soluble ciprofloxacin and different formulations of PLGA NPs loaded with ciprofloxacin.

a) PLGA NPs containing ciprofloxacin and/or functionalized with DNase I show antibacterial activity against *P. aeruginosa* established static biofilms, being NPs combining ciprofloxacin and DNase I the most active.

b) Biomass and thickness of *P.* aeruginosa biofilms formed in flow cells decrease under the effect of NPs containing ciprofloxacin and/or functionalized with DNase I.

To further validate our results, repeated doses of the different NPs and soluble ciprofloxacin (every 24 h for three days) were administered to static preformed biofilms, improving the previous results, with no evidence of antibiotic tolerance, and observing similar differences between the formulations (see **Fig. 6** from **Publication 3**). Additionally, we show similar results when employing the different formulations in a biofilm formed under continuous nutrients flow (flow cells biofilm assay), an *in vitro* model that better resembles natural biofilms in infections. The results show that biofilm biomass, but also its thickness, decrease when applying both soluble and encapsulated ciprofloxacin, achieving the most significant reduction with NPs loaded with ciprofloxacin and coated with DNase I (PLGA-PL-CPX-DNase I) (see **Table 3** and **Fig. 5** from **Publication 3**), as seen with the previous experiments. The ability of DNase I – linked NPs to disassemble and destruct matrix biofilm seems obvious when analyzing flow cells biofilm because not only biomass, but biofilm thickness, significantly decreases in the presence of DNase I.

In conclusion, we demonstrate that PLGA-PL-CPX-DNase I NPs, combining the antibiotic ciprofloxacin and DNase I as a matrix-degrading enzyme, are promising drug-delivery systems to treat pulmonary biofilm infections caused by *P. aeruginosa*. Despite the antibiotic encapsulation method should be improved, the synthesized PLGA-PL-CPX-DNase I NPs show an enhanced antibiofilm activity, low cytotoxicity, together with material biocompatibility. Also, the NPs fall in the desired size range, and their kinetics drug release show an adequate biphasic profile. Further studies should be performed to evaluate the *in vivo* efficacy in animal models.

V. CONCLUSIONS

1. The radical scavenger M-HA, an inhibitor of the RNR enzyme, displays antibacterial activity against several Gram-positive and Gram-negative bacterial pathogens, with similar antibacterial levels to those of the radical scavengers HU and HA.

2. M-HA shows low cytotoxicity on murine macrophages, as compared with the high toxicity of hydroxyurea (HU) and hydroxylamine (HA).

3. M-HA decreases *M. bovis* BCG viability during intracellular macrophage infection and produces an increase in the synthesis of TNF-α.

4. M-HA possesses *in vitro* antibiofilm activity against *P. aeruginosa*, by preventing biofilm formation and by eradicating established biofilms under both static and flow conditions.

5. M-HA acts synergistically with ciprofloxacin to remove *P. aeruginosa* biofilms.

6. Some of the new N-HA derivative molecules (**6**, **8**, **10**, **11**, **12**, **14**, **15**, **17**, and **18**) show antibacterial activity against some relevant Gram-positive and Gram-negative bacteria. Overall, aromatic N-HA display higher antibacterial activities than lineal or cyclic aliphatic molecules.

7. Some of the active N-HA display high selectivity indexes in specific bacteria. N-HA **11**, **15**, **17**, and **18** display high selectivity indexes in the Gram-positives *B. anthracis* and *S. aureus*, N-HA **11**, **15**, and **18** display high selectivity indexes in the Gram-positive *S. epidermidis,* and N-HA **8** and **15** display high selectivity indexes in the Gram-negative bacteria *P. aeruginosa* and *E. coli*, respectively.

8. Selected N-HA show antibiofilm activity against *P. aeruginosa* (**8** and **12**), *S. aureus* (**11** and **15**), and *E. coli* (**15**). N-HA **12** and **8**, and N-HA **11** and **15** reduced biofilm mass at similar levels than ciprofloxacin in *P. aeruginosa*, and *S. aureus*, respectively.

9. N-HA scavenge free radicals *in vitro* at similar levels than M-HA and HU radical scavengers, and the FRS activity is correlated with the antibacterial activities' values.

10. N-HA inhibit bacterial RNR. N-HA **8** and **12** reduced *P. aeruginosa* purine dNTPs levels, and induce *P. aeruginosa* class Ia RNR in exponential growth, similarly to HU.

11. Four different types of PLGA nanoparticles containing CPX and/or functionalized with DNase I were synthesized using a novel toxic-free method, obtaining negatively-charged (PLGA-CPX) and positively-charged (PLGA-PL-CPX, PLGA-PL-DNase I, PLGA-PL-CPX-DNase I) nanoparticles.

12. The synthesized PLGA nanoparticles exhibits proper physical characteristics: spherical shape, monodispersed size between 200 – 300 nm, and a two-phase ciprofloxacin kinetics release appropriate for antibiotic delivery in biofilms.

13. Synthesized PLGA nanoparticles containing CPX (PLGA-CPX, PLGA-PL-CPX, PLGA-PL-CPX-DNase I) show antibacterial activity in planktonic cultures of *S. aureus* and *P aeruginosa*, together with no cytotoxicity on eukaryotic cells.

14. PLGA nanoparticles containing CPX (PLGA-CPX, PLGA-PL-CPX, PLGA-PL-CPX-DNase I) prevent *P. aeruginosa in vitro* biofilm formation, but at similar levels than soluble CPX, and without differences between negatively or positively charged PLGA nanoparticles.

15. Formulations combining CPX with DNase I, either soluble or in nanoparticles (soluble CPX + soluble DNase I, PLGA-PL-CPX + PLGA-PL-DNase I, PLGA-PL-CPX-DNase I) decrease *P. aeruginosa* biofilm mass at higher levels than formulations that only contain CPX (soluble CPX, PLGA-CPX, PLGA-PL-CPX).

16. PLGA nanoparticles physically combining CPX and DNase I (PLGA-PL-CPX-DNase I) show higher antibiofilm activity on *P. aeruginosa* formed biofilms that any formulation containing ciprofloxacin with DNase I (soluble CPX + soluble DNase I, and PLGA-PL-CPX + PLGA-PL-DNase I).

REFERENCES

1. Koo, H., et al., *Targeting microbial biofilms: current and prospective therapeutic strategies.* Nat Rev Microbiol, 2017. **15**(12): p. 740-755.
2. Pang, Z., et al., *Antibiotic resistance in Pseudomonas aeruginosa: mechanisms and alternative therapeutic strategies.* Biotechnol Adv, 2019. **37**(1): p. 177-192.
3. Torrents, E., *Ribonucleotide reductases: Essential Enzymes for bacterial life.* Front. Cell. Infect. Microbiol., 2014. **4**: p. 52.
4. Torrents, E., M. Sahlin, and B.M. Sjöberg, *The Ribonucleotide Reductase Family - Genetics and Genomics.* Ribonucleotide Reductases, 2008: p. pp. 17-77.
5. Logan, D.T., *Closing the circle on ribonucleotide reductases.* Nat Struct Mol Biol, 2011. **18**(3): p. 251-3.
6. Allen, H.K., et al., *Call of the wild: antibiotic resistance genes in natural environments.* Nat Rev Microbiol, 2010. **8**(4): p. 251-9.
7. Laxminarayan, R., et al., *Access to effective antimicrobials: a worldwide challenge.* Lancet, 2016. **387**(10014): p. 168-75.
8. Ventola, C.L., *The antibiotic resistance crisis: part 1: causes and threats.* P T, 2015. **40**(4): p. 277-83.
9. Laws, M., A. Shaaban, and K.M. Rahman, *Antibiotic resistance breakers: current approaches and future directions.* FEMS Microbiol Rev, 2019. **43**(5): p. 490-516.
10. Sengupta, S., M.K. Chattopadhyay, and H.P. Grossart, *The multifaceted roles of antibiotics and antibiotic resistance in nature.* Front Microbiol, 2013. **4**: p. 47.
11. Fair, R.J. and Y. Tor, *Antibiotics and bacterial resistance in the 21st century.* Perspect Medicin Chem, 2014. **6**: p. 25-64.
12. Michael, C.A., D. Dominey-Howes, and M. Labbate, *The antimicrobial resistance crisis: causes, consequences, and management.* Front Public Health, 2014. **2**: p. 145.
13. Tacconelli, E., Magrini, N., Carmeli, Y., Harbarth, S., Kahlmeter, G., Kluytmans, J., and M. Mendelson, Pulcini, C., Singh, N., Theuretzbacher, U., *Global Action Plan on Antimicrobial Resistance*. 2015, Geneva, Switzerland: World Health Organization Library Cataloguing-in-Publication.
14. Anderson, M., et al., in *Averting the AMR crisis: What are the avenues for policy action for countries in Europe?* 2019: Copenhagen (Denmark).
15. CDC, *Antibiotic Resistance Threats in the United States, 2019*. 2019, Department of Health and Human Services, CDC: Atlanta, GA: U.S.
16. Lebeaux, D., J.M. Ghigo, and C. Beloin, *Biofilm-related infections: bridging the gap between clinical management and fundamental aspects of recalcitrance toward antibiotics.* Microbiol Mol Biol Rev, 2014. **78**(3): p. 510-43.
17. Costerton, J.W., P.S. Stewart, and E.P. Greenberg, *Bacterial biofilms: a common cause of persistent infections.* Science, 1999. **284**(5418): p. 1318-22.
18. Burmolle, M., et al., *Enhanced biofilm formation and increased resistance to antimicrobial agents and bacterial invasion are caused by synergistic interactions in multispecies biofilms.* Appl Environ Microbiol, 2006. **72**(6): p. 3916-23.
19. Peters, B.M., et al., *Polymicrobial interactions: impact on pathogenesis and human disease.* Clin Microbiol Rev, 2012. **25**(1): p. 193-213.
20. Murray, J.L., et al., *Mechanisms of synergy in polymicrobial infections.* J Microbiol, 2014. **52**(3): p. 188-99.
21. Sanchez-Vizuete, P., et al., *Pathogens protection against the action of disinfectants in multispecies biofilms.* Front Microbiol, 2015. **6**: p. 705.

22. Baishya, J. and C.A. Wakeman, *Selective pressures during chronic infection drive microbial competition and cooperation.* NPJ Biofilms Microbiomes, 2019. **5**: p. 16.
23. Nogueira, F., et al., *Pathogenetic Impact of Bacterial-Fungal Interactions.* Microorganisms, 2019. **7**(10).
24. Joo, H.S. and M. Otto, *Molecular basis of in vivo biofilm formation by bacterial pathogens.* Chem Biol, 2012. **19**(12): p. 1503-13.
25. Bjarnsholt, T., *The role of bacterial biofilms in chronic infections.* APMIS Suppl, 2013(136): p. 1-51.
26. Tacconelli, E., Magrini, N., Carmeli, Y., Harbarth, S., Kahlmeter, G., Kluytmans, J., and M. Mendelson, Pulcini, C., Singh, N., Theuretzbacher, U. *Global priority list of antibiotic-resistant bacteria to guide research, discovery, and development of new antibiotics. World Health Organization 1–7*. 2017 [cited 2019 3 december]; Available from: **http://www.who.int/medicines/** publications/WHO-PPL-Short_Summary_25Feb-ET_NM_WHO.pdf.
27. WHO, *Prioritization of pathogens to guide discovery, research and development of new antibiotics for drug-resistant bacterial infections, including tuberculosis.* 2017, Geneva: World Health Organization.
28. Rice, L.B., *Federal funding for the study of antimicrobial resistance in nosocomial pathogens: no ESKAPE.* J Infect Dis, 2008. **197**(8): p. 1079-81.
29. Mulani, M.S., et al., *Emerging Strategies to Combat ESKAPE Pathogens in the Era of Antimicrobial Resistance: A Review.* Front Microbiol, 2019. **10**: p. 539.
30. Kimata, N., et al., *Pseudomonas aeruginosa isolated from marine environments in Tokyo Bay.* Microb Ecol, 2004. **47**(1): p. 41-7.
31. Green, S.K., et al., *Agricultural plants and soil as a reservoir for Pseudomonas aeruginosa.* Appl Microbiol, 1974. **28**(6): p. 987-91.
32. Rahme, L.G., et al., *Common virulence factors for bacterial pathogenicity in plants and animals.* Science, 1995. **268**(5219): p. 1899-902.
33. *Pseudomonas. Model Organism, Pathogen, Cell Factory.* 2008: WILEY-VCH.
34. Azam, M.W. and A.U. Khan, *Updates on the pathogenicity status of Pseudomonas aeruginosa.* Drug Discov Today, 2019. **24**(1): p. 350-359.
35. Bassetti, M., et al., *Rational approach in the management of Pseudomonas aeruginosa infections.* Curr Opin Infect Dis, 2018. **31**(6): p. 578-586.
36. Weiner-Lastinger, L.M., et al., *Antimicrobial-resistant pathogens associated with adult healthcare-associated infections: Summary of data reported to the National Healthcare Safety Network, 2015-2017.* Infect Control Hosp Epidemiol, 2019: p. 1-18.
37. Wagner, V.E. and B.H. Iglewski, *P. aeruginosa Biofilms in CF Infection.* Clin Rev Allergy Immunol, 2008. **35**(3): p. 124-34.
38. Aloush, V., et al., *Multidrug-resistant Pseudomonas aeruginosa: risk factors and clinical impact.* Antimicrob Agents Chemother, 2006. **50**(1): p. 43-8.
39. Stover, C.K., et al., *Complete genome sequence of Pseudomonas aeruginosa PA01, an opportunistic pathogen.* Nature, 2000. **406**(6799): p. 959-964.
40. Klockgether, J., et al., *Pseudomonas aeruginosa Genomic Structure and Diversity.* Front Microbiol, 2011. **2**: p. 150.
41. Igiri, B.E., et al., *Toxicity and Bioremediation of Heavy Metals Contaminated Ecosystem from Tannery Wastewater: A Review.* J Toxicol, 2018. **2018**: p. 2568038.
42. Pacwa-Plociniczak, M., et al., *Characterization of hydrocarbon-degrading and biosurfactant-producing Pseudomonas sp. P-1 strain as a potential tool for bioremediation of petroleum-contaminated soil.* Environ Sci Pollut Res Int, 2014. **21**(15): p. 9385-95.

43. Collier, D.N., P.W. Hager, and P.V. Phibbs, Jr., *Catabolite repression control in the Pseudomonads.* Res Microbiol, 1996. **147**(6-7): p. 551-61.
44. Rojo, F., *Carbon catabolite repression in Pseudomonas : optimizing metabolic versatility and interactions with the environment.* FEMS Microbiol Rev, 2010. **34**(5): p. 658-84.
45. Arai, H., *Regulation and Function of Versatile Aerobic and Anaerobic Respiratory Metabolism in Pseudomonas aeruginosa.* Front Microbiol, 2011. **2**: p. 103.
46. Zumft, W.G., *Cell biology and molecular basis of denitrification.* Microbiol Mol Biol Rev, 1997. **61**(4): p. 533-616.
47. Vander Wauven, C., et al., *Pseudomonas aeruginosa mutants affected in anaerobic growth on arginine: evidence for a four-gene cluster encoding the arginine deiminase pathway.* J Bacteriol, 1984. **160**(3): p. 928-34.
48. Eschbach, M., et al., *Long-term anaerobic survival of the opportunistic pathogen Pseudomonas aeruginosa via pyruvate fermentation.* J Bacteriol, 2004. **186**(14): p. 4596-604.
49. Costerton, J.W., *Anaerobic biofilm infections in cystic fibrosis.* Mol Cell, 2002. **10**(4): p. 699-700.
50. Schobert, M. and D. Jahn, *Anaerobic physiology of Pseudomonas aeruginosa in the cystic fibrosis lung.* Int J Med Microbiol, 2010. **300**(8): p. 549-56.
51. Lister, P.D., D.J. Wolter, and N.D. Hanson, *Antibacterial-resistant Pseudomonas aeruginosa: clinical impact and complex regulation of chromosomally encoded resistance mechanisms.* Clin Microbiol Rev, 2009. **22**(4): p. 582-610.
52. Breidenstein, E.B., C. de la Fuente-Nunez, and R.E. Hancock, *Pseudomonas aeruginosa: all roads lead to resistance.* Trends Microbiol, 2011. **19**(8): p. 419-26.
53. Taylor, P.K., A.T. Yeung, and R.E. Hancock, *Antibiotic resistance in Pseudomonas aeruginosa biofilms: towards the development of novel anti-biofilm therapies.* J Biotechnol, 2014. **191**: p. 121-30.
54. Jensen, P.O., et al., *The immune system vs. Pseudomonas aeruginosa biofilms.* FEMS Immunol Med Microbiol, 2010. **59**(3): p. 292-305.
55. Balaban, N.Q., et al., *A problem of persistence: still more questions than answers?* Nat Rev Microbiol, 2013. **11**(8): p. 587-91.
56. Harms, A., E. Maisonneuve, and K. Gerdes, *Mechanisms of bacterial persistence during stress and antibiotic exposure.* Science, 2016. **354**(6318).
57. Lee, J. and L. Zhang, *The hierarchy quorum sensing network in Pseudomonas aeruginosa.* Protein Cell, 2015. **6**(1): p. 26-41.
58. Wertheim, H.F., et al., *The role of nasal carriage in Staphylococcus aureus infections.* Lancet Infect Dis, 2005. **5**(12): p. 751-62.
59. van Belkum, A., et al., *Co-evolutionary aspects of human colonisation and infection by Staphylococcus aureus.* Infect Genet Evol, 2009. **9**(1): p. 32-47.
60. Archer, G.L., *Staphylococcus aureus: a well-armed pathogen.* Clin Infect Dis, 1998. **26**(5): p. 1179-81.
61. Thomer, L., O. Schneewind, and D. Missiakas, *Pathogenesis of Staphylococcus aureus Bloodstream Infections.* Annu Rev Pathol, 2016. **11**: p. 343-64.
62. Asgeirsson, H., A. Thalme, and O. Weiland, *Staphylococcus aureus bacteraemia and endocarditis - epidemiology and outcome: a review.* Infect Dis (Lond), 2018. **50**(3): p. 175-192.
63. Esposito, S., S. Noviello, and S. Leone, *Epidemiology and microbiology of skin and soft tissue infections.* Curr Opin Infect Dis, 2016. **29**(2): p. 109-15.
64. Kavanagh, N., et al., *Staphylococcal Osteomyelitis: Disease Progression, Treatment Challenges, and Future Directions.* Clin Microbiol Rev, 2018. **31**(2).
65. Mathews, C.J. and G. Coakley, *Septic arthritis: current diagnostic and therapeutic algorithm.* Curr Opin Rheumatol, 2008. **20**(4): p. 457-62.

66. Self, W.H., et al., *Staphylococcus aureus Community-acquired Pneumonia: Prevalence, Clinical Characteristics, and Outcomes.* Clin Infect Dis, 2016. **63**(3): p. 300-9.
67. Muder, R.R., et al., *Isolation of Staphylococcus aureus from the urinary tract: association of isolation with symptomatic urinary tract infection and subsequent staphylococcal bacteremia.* Clin Infect Dis, 2006. **42**(1): p. 46-50.
68. Le Loir, Y., F. Baron, and M. Gautier, *Staphylococcus aureus and food poisoning.* Genet Mol Res, 2003. **2**(1): p. 63-76.
69. Silversides, J.A., E. Lappin, and A.J. Ferguson, *Staphylococcal toxic shock syndrome: mechanisms and management.* Curr Infect Dis Rep, 2010. **12**(5): p. 392-400.
70. Tong, S.Y., et al., *Staphylococcus aureus infections: epidemiology, pathophysiology, clinical manifestations, and management.* Clin Microbiol Rev, 2015. **28**(3): p. 603-61.
71. Brooks, J.L. and K.K. Jefferson, *Staphylococcal biofilms: quest for the magic bullet.* Adv Appl Microbiol, 2012. **81**: p. 63-87.
72. Moormeier, D.E. and K.W. Bayles, *Staphylococcus aureus biofilm: a complex developmental organism.* Mol Microbiol, 2017. **104**(3): p. 365-376.
73. Haag, A.F., J.R. Fitzgerald, and J.R. Penades, *Staphylococcus aureus in Animals.* Microbiol Spectr, 2019. **7**(3).
74. Balasubramanian, D., et al., *Staphylococcus aureus pathogenesis in diverse host environments.* Pathog Dis, 2017. **75**(1).
75. Turner, N.A., et al., *Methicillin-resistant Staphylococcus aureus: an overview of basic and clinical research.* Nat Rev Microbiol, 2019. **17**(4): p. 203-218.
76. Ito, T., Y. Katayama, and K. Hiramatsu, *Cloning and nucleotide sequence determination of the entire mec DNA of pre-methicillin-resistant Staphylococcus aureus N315.* Antimicrob Agents Chemother, 1999. **43**(6): p. 1449-58.
77. Malachowa, N. and F.R. DeLeo, *Mobile genetic elements of Staphylococcus aureus.* Cellular and Molecular Life Sciences, 2010. **67**(18): p. 3057-3071.
78. de Jong, N.W.M., K.P.M. van Kessel, and J.A.G. van Strijp, *Immune Evasion by Staphylococcus aureus.* Microbiol Spectr, 2019. **7**(2).
79. Foster, T.J., *Surface Proteins of Staphylococcus aureus.* Microbiol Spectr, 2019. **7**(4).
80. Tam, K. and V.J. Torres, *Staphylococcus aureus Secreted Toxins and Extracellular Enzymes.* Microbiol Spectr, 2019. **7**(2).
81. Cheng, A.G., et al., *Contribution of coagulases towards Staphylococcus aureus disease and protective immunity.* PLoS Pathog, 2010. **6**(8): p. e1001036.
82. Oliveira, D., A. Borges, and M. Simoes, *Staphylococcus aureus Toxins and Their Molecular Activity in Infectious Diseases.* Toxins (Basel), 2018. **10**(6).
83. Jenul, C. and A.R. Horswill, *Regulation of Staphylococcus aureus Virulence.* Microbiol Spectr, 2018. **6**(1).
84. Davies, D., *Understanding biofilm resistance to antibacterial agents.* Nat Rev Drug Discov, 2003. **2**(2): p. 114-22.
85. Flemming, H.C., et al., *Biofilms: an emergent form of bacterial life.* Nat Rev Microbiol, 2016. **14**(9): p. 563-75.
86. Moradali, M.F., S. Ghods, and B.H. Rehm, *Pseudomonas aeruginosa Lifestyle: A Paradigm for Adaptation, Survival, and Persistence.* Front Cell Infect Microbiol, 2017. **7**: p. 39.
87. Harmsen, M., et al., *An update on Pseudomonas aeruginosa biofilm formation, tolerance, and dispersal.* FEMS Immunol Med Microbiol, 2010. **59**(3): p. 253-68.
88. Maisonneuve, E. and K. Gerdes, *Molecular mechanisms underlying bacterial persisters.* Cell, 2014. **157**(3): p. 539-48.

89. Percival, S.L., et al., *Healthcare-associated infections, medical devices and biofilms: risk, tolerance and control.* J Med Microbiol, 2015. **64**(Pt 4): p. 323-34.
90. Percival, S.L., S.M. McCarty, and B. Lipsky, *Biofilms and Wounds: An Overview of the Evidence.* Adv Wound Care (New Rochelle), 2015. **4**(7): p. 373-381.
91. Wu, Y.K., N.C. Cheng, and C.M. Cheng, *Biofilms in Chronic Wounds: Pathogenesis and Diagnosis.* Trends Biotechnol, 2019. **37**(5): p. 505-517.
92. Davies, J.C., E.W. Alton, and A. Bush, *Cystic fibrosis.* BMJ, 2007. **335**(7632): p. 1255-9.
93. Tolker-Nielsen, T., *Biofilm Development.* Microbiol Spectr, 2015. **3**(2): p. MB-0001-2014.
94. Stewart, P.S. and M.J. Franklin, *Physiological heterogeneity in biofilms.* Nat Rev Microbiol, 2008. **6**(3): p. 199-210.
95. Heacock-Kang, Y., et al., *Spatial transcriptomes within the Pseudomonas aeruginosa biofilm architecture.* Mol Microbiol, 2017. **106**(6): p. 976-985.
96. Boles, B.R., M. Thoendel, and P.K. Singh, *Self-generated diversity produces "insurance effects" in biofilm communities.* Proc Natl Acad Sci U S A, 2004. **101**(47): p. 16630-5.
97. Burmolle, M., et al., *Interactions in multispecies biofilms: do they actually matter?* Trends Microbiol, 2014. **22**(2): p. 84-91.
98. Rendueles, O. and J.M. Ghigo, *Mechanisms of Competition in Biofilm Communities.* Microbiol Spectr, 2015. **3**(3).
99. Ha, D.G. and G.A. O'Toole, *c-di-GMP and its Effects on Biofilm Formation and Dispersion: a Pseudomonas Aeruginosa Review.* Microbiol Spectr, 2015. **3**(2): p. MB-0003-2014.
100. Valentini, M. and A. Filloux, *Biofilms and Cyclic di-GMP (c-di-GMP) Signaling: Lessons from Pseudomonas aeruginosa and Other Bacteria.* J Biol Chem, 2016. **291**(24): p. 12547-55.
101. Su, T., et al., *The REC domain mediated dimerization is critical for FleQ from Pseudomonas aeruginosa to function as a c-di-GMP receptor and flagella gene regulator.* J Struct Biol, 2015. **192**(1): p. 1-13.
102. Jain, R., O. Sliusarenko, and B.I. Kazmierczak, *Interaction of the cyclic-di-GMP binding protein FimX and the Type 4 pilus assembly ATPase promotes pilus assembly.* PLoS Pathog, 2017. **13**(8): p. e1006594.
103. Merighi, M., et al., *The second messenger bis-(3'-5')-cyclic-GMP and its PilZ domain-containing receptor Alg44 are required for alginate biosynthesis in Pseudomonas aeruginosa.* Mol Microbiol, 2007. **65**(4): p. 876-95.
104. Baraquet, C., et al., *The FleQ protein from Pseudomonas aeruginosa functions as both a repressor and an activator to control gene expression from the pel operon promoter in response to c-di-GMP.* Nucleic Acids Res, 2012. **40**(15): p. 7207-18.
105. Borlee, B.R., et al., *Pseudomonas aeruginosa uses a cyclic-di-GMP-regulated adhesin to reinforce the biofilm extracellular matrix.* Mol Microbiol, 2010. **75**(4): p. 827-42.
106. An, S., J. Wu, and L.H. Zhang, *Modulation of Pseudomonas aeruginosa biofilm dispersal by a cyclic-Di-GMP phosphodiesterase with a putative hypoxia-sensing domain.* Appl Environ Microbiol, 2010. **76**(24): p. 8160-73.
107. Allesen-Holm, M., et al., *A characterization of DNA release in Pseudomonas aeruginosa cultures and biofilms.* Mol Microbiol, 2006. **59**(4): p. 1114-28.
108. Sakuragi, Y. and R. Kolter, *Quorum-sensing regulation of the biofilm matrix genes (pel) of Pseudomonas aeruginosa.* J Bacteriol, 2007. **189**(14): p. 5383-6.
109. Lin Chua, S., et al., *Reduced Intracellular c-di-GMP Content Increases Expression of Quorum Sensing-Regulated Genes in Pseudomonas aeruginosa.* Front Cell Infect Microbiol, 2017. **7**: p. 451.

110. Chambers, J.R. and K. Sauer, *Small RNAs and their role in biofilm formation.* Trends Microbiol, 2013. **21**(1): p. 39-49.
111. Flemming, H.C. and J. Wingender, *The biofilm matrix.* Nat Rev Microbiol, 2010. **8**(9): p. 623-33.
112. Mann, E.E. and D.J. Wozniak, *Pseudomonas biofilm matrix composition and niche biology.* FEMS Microbiol Rev, 2012. **36**(4): p. 893-916.
113. Lawrence, J.R., et al., *In situ evidence for metabolic and chemical microdomains in the structured polymer matrix of bacterial microcolonies.* FEMS Microbiol Ecol, 2016. **92**(11).
114. Chew, S.C., et al., *Dynamic remodeling of microbial biofilms by functionally distinct exopolysaccharides.* MBio, 2014. **5**(4): p. e01536-14.
115. Whitfield, G.B., L.S. Marmont, and P.L. Howell, *Enzymatic modifications of exopolysaccharides enhance bacterial persistence.* Front Microbiol, 2015. **6**: p. 471.
116. Nivens, D.E., et al., *Role of alginate and its O acetylation in formation of Pseudomonas aeruginosa microcolonies and biofilms.* J Bacteriol, 2001. **183**(3): p. 1047-57.
117. Jennings, L.K., et al., *Pel is a cationic exopolysaccharide that cross-links extracellular DNA in the Pseudomonas aeruginosa biofilm matrix.* Proc Natl Acad Sci U S A, 2015. **112**(36): p. 11353-8.
118. Zhao, K., et al., *Psl trails guide exploration and microcolony formation in Pseudomonas aeruginosa biofilms.* Nature, 2013. **497**(7449): p. 388-391.
119. Colvin, K.M., et al., *The pel polysaccharide can serve a structural and protective role in the biofilm matrix of Pseudomonas aeruginosa.* PLoS Pathog, 2011. **7**(1): p. e1001264.
120. Wang, S., et al., *The exopolysaccharide Psl-eDNA interaction enables the formation of a biofilm skeleton in Pseudomonas aeruginosa.* Environ Microbiol Rep, 2015. **7**(2): p. 330-40.
121. Whitchurch, C.B., et al., *Extracellular DNA required for bacterial biofilm formation.* Science, 2002. **295**(5559): p. 1487.
122. Wilton, M., et al., *Extracellular DNA Acidifies Biofilms and Induces Aminoglycoside Resistance in Pseudomonas aeruginosa.* Antimicrob Agents Chemother, 2016. **60**(1): p. 544-53.
123. Wilton, M., et al., *Chelation of Membrane-Bound Cations by Extracellular DNA Activates the Type VI Secretion System in Pseudomonas aeruginosa.* Infect Immun, 2016. **84**(8): p. 2355-2361.
124. Kadurugamuwa, J.L. and T.J. Beveridge, *Virulence factors are released from Pseudomonas aeruginosa in association with membrane vesicles during normal growth and exposure to gentamicin: a novel mechanism of enzyme secretion.* J Bacteriol, 1995. **177**(14): p. 3998-4008.
125. Reichhardt, C., et al., *CdrA Interactions within the Pseudomonas aeruginosa Biofilm Matrix Safeguard It from Proteolysis and Promote Cellular Packing.* MBio, 2018. **9**(5).
126. Tielker, D., et al., *Pseudomonas aeruginosa lectin LecB is located in the outer membrane and is involved in biofilm formation.* Microbiology, 2005. **151**(Pt 5): p. 1313-23.
127. Diggle, S.P., et al., *The galactophilic lectin, LecA, contributes to biofilm development in Pseudomonas aeruginosa.* Environ Microbiol, 2006. **8**(6): p. 1095-104.
128. Passos da Silva, D., et al., *The Pseudomonas aeruginosa lectin LecB binds to the exopolysaccharide Psl and stabilizes the biofilm matrix.* Nat Commun, 2019. **10**(1): p. 2183.

129. Fong, J.N.C. and F.H. Yildiz, *Biofilm Matrix Proteins.* Microbiol Spectr, 2015. **3**(2).
130. Chang, C.Y., *Surface Sensing for Biofilm Formation in Pseudomonas aeruginosa.* Front Microbiol, 2017. **8**: p. 2671.
131. Barken, K.B., et al., *Roles of type IV pili, flagellum-mediated motility and extracellular DNA in the formation of mature multicellular structures in Pseudomonas aeruginosa biofilms.* Environ Microbiol, 2008. **10**(9): p. 2331-43.
132. Schooling, S.R. and T.J. Beveridge, *Membrane vesicles: an overlooked component of the matrices of biofilms.* J Bacteriol, 2006. **188**(16): p. 5945-57.
133. Otto, M., *Staphylococcal Biofilms.* Microbiol Spectr, 2018. **6**(4).
134. Cramton, S.E., et al., *The intercellular adhesion (ica) locus is present in Staphylococcus aureus and is required for biofilm formation.* Infect Immun, 1999. **67**(10): p. 5427-33.
135. Dengler, V., et al., *An Electrostatic Net Model for the Role of Extracellular DNA in Biofilm Formation by Staphylococcus aureus.* J Bacteriol, 2015. **197**(24): p. 3779-87.
136. Fitzpatrick, F., H. Humphreys, and J.P. O'Gara, *Evidence for icaADBC-independent biofilm development mechanism in methicillin-resistant Staphylococcus aureus clinical isolates.* J Clin Microbiol, 2005. **43**(4): p. 1973-6.
137. O'Neill, E., et al., *A novel Staphylococcus aureus biofilm phenotype mediated by the fibronectin-binding proteins, FnBPA and FnBPB.* J Bacteriol, 2008. **190**(11): p. 3835-50.
138. Foulston, L., et al., *The extracellular matrix of Staphylococcus aureus biofilms comprises cytoplasmic proteins that associate with the cell surface in response to decreasing pH.* MBio, 2014. **5**(5): p. e01667-14.
139. Graf, A.C., et al., *Virulence Factors Produced by Staphylococcus aureus Biofilms Have a Moonlighting Function Contributing to Biofilm Integrity.* Mol Cell Proteomics, 2019. **18**(6): p. 1036-1053.
140. Sugimoto, S., et al., *Broad impact of extracellular DNA on biofilm formation by clinically isolated Methicillin-resistant and -sensitive strains of Staphylococcus aureus.* Sci Rep, 2018. **8**(1): p. 2254.
141. Rice, K.C., et al., *The cidA murein hydrolase regulator contributes to DNA release and biofilm development in Staphylococcus aureus.* Proc Natl Acad Sci U S A, 2007. **104**(19): p. 8113-8.
142. Mann, E.E., et al., *Modulation of eDNA release and degradation affects Staphylococcus aureus biofilm maturation.* PLoS One, 2009. **4**(6): p. e5822.
143. Izano, E.A., et al., *Differential roles of poly-N-acetylglucosamine surface polysaccharide and extracellular DNA in Staphylococcus aureus and Staphylococcus epidermidis biofilms.* Appl Environ Microbiol, 2008. **74**(2): p. 470-6.
144. Boles, B.R. and A.R. Horswill, *Agr-mediated dispersal of Staphylococcus aureus biofilms.* PLoS Pathog, 2008. **4**(4): p. e1000052.
145. Kiedrowski, M.R., et al., *Nuclease modulates biofilm formation in community-associated methicillin-resistant Staphylococcus aureus.* PLoS One, 2011. **6**(11): p. e26714.
146. Speziale, P., et al., *Protein-based biofilm matrices in Staphylococci.* Front Cell Infect Microbiol, 2014. **4**: p. 171.
147. Moormeier, D.E., et al., *Temporal and stochastic control of Staphylococcus aureus biofilm development.* mBio, 2014. **5**(5): p. e01341-14.
148. McCourt, J., et al., *Fibronectin-binding proteins are required for biofilm formation by community-associated methicillin-resistant Staphylococcus aureus strain LAC.* FEMS Microbiol Lett, 2014. **353**(2): p. 157-64.

149. Abraham, N.M. and K.K. Jefferson, *Staphylococcus aureus clumping factor B mediates biofilm formation in the absence of calcium.* Microbiology, 2012. **158**(Pt 6): p. 1504-1512.
150. Barbu, E.M., et al., *SdrC induces staphylococcal biofilm formation through a homophilic interaction.* Mol Microbiol, 2014. **94**(1): p. 172-85.
151. Schroeder, K., et al., *Molecular characterization of a novel Staphylococcus aureus surface protein (SasC) involved in cell aggregation and biofilm accumulation.* PLoS One, 2009. **4**(10): p. e7567.
152. Geoghegan, J.A., et al., *Role of surface protein SasG in biofilm formation by Staphylococcus aureus.* J Bacteriol, 2010. **192**(21): p. 5663-73.
153. Merino, N., et al., *Protein A-mediated multicellular behavior in Staphylococcus aureus.* J Bacteriol, 2009. **191**(3): p. 832-43.
154. Miajlovic, H., et al., *Direct interaction of iron-regulated surface determinant IsdB of Staphylococcus aureus with the GPIIb/IIIa receptor on platelets.* Microbiology, 2010. **156**(Pt 3): p. 920-8.
155. Yang, Y.H., et al., *Structural insights into SraP-mediated Staphylococcus aureus adhesion to host cells.* PLoS Pathog, 2014. **10**(6): p. e1004169.
156. Cucarella, C., et al., *Bap, a Staphylococcus aureus surface protein involved in biofilm formation.* J Bacteriol, 2001. **183**(9): p. 2888-96.
157. Taglialegna, A., et al., *Staphylococcal Bap Proteins Build Amyloid Scaffold Biofilm Matrices in Response to Environmental Signals.* PLoS Pathog, 2016. **12**(6): p. e1005711.
158. Houston, P., et al., *Essential role for the major autolysin in the fibronectin-binding protein-mediated Staphylococcus aureus biofilm phenotype.* Infect Immun, 2011. **79**(3): p. 1153-65.
159. Bose, J.L., et al., *Contribution of the Staphylococcus aureus Atl AM and GL murein hydrolase activities in cell division, autolysis, and biofilm formation.* PLoS One, 2012. **7**(7): p. e42244.
160. Gross, M., et al., *Key role of teichoic acid net charge in Staphylococcus aureus colonization of artificial surfaces.* Infect Immun, 2001. **69**(5): p. 3423-6.
161. Periasamy, S., et al., *How Staphylococcus aureus biofilms develop their characteristic structure.* Proc Natl Acad Sci U S A, 2012. **109**(4): p. 1281-6.
162. Le, K.Y., et al., *Molecular determinants of staphylococcal biofilm dispersal and structuring.* Front Cell Infect Microbiol, 2014. **4**: p. 167.
163. Schwartz, K., et al., *Functional amyloids composed of phenol soluble modulins stabilize Staphylococcus aureus biofilms.* PLoS Pathog, 2012. **8**(6): p. e1002744.
164. Marinelli, P., et al., *Dissecting the contribution of Staphylococcus aureus alpha-phenol-soluble modulins to biofilm amyloid structure.* Sci Rep, 2016. **6**: p. 34552.
165. Vanassche, T., et al., *The role of staphylothrombin-mediated fibrin deposition in catheter-related Staphylococcus aureus infections.* J Infect Dis, 2013. **208**(1): p. 92-100.
166. Zapotoczna, M., et al., *An Essential Role for Coagulase in Staphylococcus aureus Biofilm Development Reveals New Therapeutic Possibilities for Device-Related Infections.* J Infect Dis, 2015. **212**(12): p. 1883-93.
167. Jordan, A. and P. Reichard, *Ribonucleotide reductases.* Annu Rev Biochem, 1998. **67**: p. 71-98.
168. Nordlund, P. and P. Reichard, *Ribonucleotide reductases.* Annu Rev Biochem, 2006. **75**: p. 681-706.
169. Stubbe, J. and W.A. van der Donk, *Ribonucleotide reductases: radical enzymes with suicidal tendencies.* Chem Biol, 1995. **2**(12): p. 793-801.
170. Lundin, D., et al., *The origin and evolution of ribonucleotide reduction.* Life (Basel), 2015. **5**(1): p. 604-36.

171. Jordan, A., et al., *The ribonucleotide reductase system of Lactococcus lactis. Characterization of an NrdEF enzyme and a new electron transport protein.* J Biol Chem, 1996. **271**(15): p. 8779-85.
172. Mulliez, E., et al., *Formate is the hydrogen donor for the anaerobic ribonucleotide reductase from Escherichia coli.* Proc Natl Acad Sci U S A, 1995. **92**(19): p. 8759-62.
173. Hofer, A., et al., *DNA building blocks: keeping control of manufacture.* Crit Rev Biochem Mol Biol, 2012. **47**(1): p. 50-63.
174. Torrents, E., et al., *Ribonucleotide reductases: divergent evolution of an ancient enzyme.* J Mol Evol, 2002. **55**(2): p. 138-52.
175. Reichard, P., A. Baldesten, and L. Rutberg, *Formation of deoxycytidine phosphates from cytidine phosphates in extracts from Escherichia coli.* J Biol Chem, 1961. **236**: p. 1150-7.
176. Cotruvo, J.A. and J. Stubbe, *Class I ribonucleotide reductases: metallocofactor assembly and repair in vitro and in vivo.* Annu Rev Biochem, 2011. **80**: p. 733-67.
177. Minnihan, E.C., D.G. Nocera, and J. Stubbe, *Reversible, long-range radical transfer in E. coli class Ia ribonucleotide reductase.* Acc Chem Res, 2013. **46**(11): p. 2524-35.
178. Ando, N., et al., *Structural interconversions modulate activity of Escherichia coli ribonucleotide reductase.* Proc Natl Acad Sci U S A, 2011. **108**(52): p. 21046-51.
179. Kashlan, O.B., et al., *A comprehensive model for the allosteric regulation of mammalian ribonucleotide reductase. Functional consequences of ATP- and dATP-induced oligomerization of the large subunit.* Biochemistry, 2002. **41**(2): p. 462-74.
180. Rose, H.R., et al., *Structural Basis for Superoxide Activation of Flavobacterium johnsoniae Class I Ribonucleotide Reductase and for Radical Initiation by Its Dimanganese Cofactor.* Biochemistry, 2018. **57**(18): p. 2679-2693.
181. Rose, H.R., et al., *Structures of Class Id Ribonucleotide Reductase Catalytic Subunits Reveal a Minimal Architecture for Deoxynucleotide Biosynthesis.* Biochemistry, 2019. **58**(14): p. 1845-1860.
182. Blaesi, E.J., et al., *Metal-free class Ie ribonucleotide reductase from pathogens initiates catalysis with a tyrosine-derived dihydroxyphenylalanine radical.* Proc Natl Acad Sci U S A, 2018. **115**(40): p. 10022-10027.
183. Srinivas, V., et al., *Metal-free ribonucleotide reduction powered by a DOPA radical in Mycoplasma pathogens.* Nature, 2018. **563**(7731): p. 416-420.
184. Jordan, A., I. Gibert, and J. Barbe, *Two different operons for the same function: comparison of the Salmonella typhimurium nrdAB and nrdEF genes.* Gene, 1995. **167**(1-2): p. 75-9.
185. Jordan, A., et al., *Promoter identification and expression analysis of Salmonella typhimurium and Escherichia coli nrdEF operons encoding one of two class I ribonucleotide reductases present in both bacteria.* Mol Microbiol, 1996. **19**(4): p. 777-90.
186. Cotruvo, J.A., Jr. and J. Stubbe, *An active dimanganese(III)-tyrosyl radical cofactor in Escherichia coli class Ib ribonucleotide reductase.* Biochemistry, 2010. **49**(6): p. 1297-309.
187. Cotruvo, J.A. and J. Stubbe, *Escherichia coli class Ib ribonucleotide reductase contains a dimanganese(III)-tyrosyl radical cofactor in vivo.* Biochemistry, 2011. **50**(10): p. 1672-81.
188. Cotruvo, J.A., Jr., et al., *Mechanism of assembly of the dimanganese-tyrosyl radical cofactor of class Ib ribonucleotide reductase: enzymatic generation of superoxide is required for tyrosine oxidation via a Mn(III)Mn(IV) intermediate.* J Am Chem Soc, 2013. **135**(10): p. 4027-39.

189. Cotruvo, J.A., Jr. and J. Stubbe, *NrdI, a flavodoxin involved in maintenance of the diferric-tyrosyl radical cofactor in Escherichia coli class Ib ribonucleotide reductase.* Proc Natl Acad Sci U S A, 2008. **105**(38): p. 14383-8.

190. Roca, I., et al., *NrdI essentiality for class Ib ribonucleotide reduction in Streptococcus pyogenes.* J Bacteriol, 2008. **190**(14): p. 4849-58.

191. Jordan, A., et al., *Characterization of Escherichia coli NrdH. A glutaredoxin-like protein with a thioredoxin-like activity profile.* J Biol Chem, 1997. **272**(29): p. 18044-50.

192. Crona, M., et al., *NrdH-redoxin protein mediates high enzyme activity in manganese-reconstituted ribonucleotide reductase from Bacillus anthracis.* J Biol Chem, 2011. **286**(38): p. 33053-60.

193. Roshick, C., E.R. Iliffe-Lee, and G. McClarty, *Cloning and characterization of ribonucleotide reductase from Chlamydia trachomatis.* J Biol Chem, 2000. **275**(48): p. 38111-9.

194. Jiang, W., et al., *A manganese(IV)/iron(III) cofactor in Chlamydia trachomatis ribonucleotide reductase.* Science, 2007. **316**(5828): p. 1188-91.

195. Dassama, L.M., et al., *Evidence that the beta subunit of Chlamydia trachomatis ribonucleotide reductase is active with the manganese ion of its manganese(IV)/iron(III) cofactor in site 1.* J Am Chem Soc, 2012. **134**(5): p. 2520-3.

196. Stubbe, J. and M.R. Seyedsayamdost, *Discovery of a New Class I Ribonucleotide Reductase with an Essential DOPA Radical and NO Metal as an Initiator of Long-Range Radical Transfer.* Biochemistry, 2019. **58**(6): p. 435-437.

197. Blakley, R.L. and H.A. Barker, *Cobamide stimulation of the reduction of ribotides to deoxyribotides in Lactobacillus leichmannii.* Biochem Biophys Res Commun, 1964. **16**(5): p. 391-7.

198. Torrents, E., A. Poplawski, and B.M. Sjoberg, *Two proteins mediate class II ribonucleotide reductase activity in Pseudomonas aeruginosa: expression and transcriptional analysis of the aerobic enzymes.* J Biol Chem, 2005. **280**(17): p. 16571-8.

199. Eliasson, R., et al., *Allosteric control of three B12-dependent (class II) ribonucleotide reductases. Implications for the evolution of ribonucleotide reduction.* J Biol Chem, 1999. **274**(11): p. 7182-9.

200. Tamao, Y. and R.L. Blakley, *Direct spectrophotometric observation of an intermediate formed from deoxyadenosylcobalamin in ribonucleotide reduction.* Biochemistry, 1973. **12**(1): p. 24-34.

201. Licht, S., G.J. Gerfen, and J. Stubbe, *Thiyl radicals in ribonucleotide reductases.* Science, 1996. **271**(5248): p. 477-81.

202. Larsson, K.M., D.T. Logan, and P. Nordlund, *Structural basis for adenosylcobalamin activation in AdoCbl-dependent ribonucleotide reductases.* ACS Chem Biol, 2010. **5**(10): p. 933-42.

203. Fontecave, M., R. Eliasson, and P. Reichard, *Oxygen-sensitive ribonucleoside triphosphate reductase is present in anaerobic Escherichia coli.* Proc Natl Acad Sci U S A, 1989. **86**(7): p. 2147-51.

204. Sun, X., et al., *Generation of the glycyl radical of the anaerobic Escherichia coli ribonucleotide reductase requires a specific activating enzyme.* J Biol Chem, 1995. **270**(6): p. 2443-6.

205. Eliasson, R., et al., *The anaerobic ribonucleoside triphosphate reductase from Escherichia coli requires S-adenosylmethionine as a cofactor.* Proc Natl Acad Sci U S A, 1990. **87**(9): p. 3314-8.

206. Harder, J., et al., *Activation of the anaerobic ribonucleotide reductase from Escherichia coli by S-adenosylmethionine.* J Biol Chem, 1992. **267**(35): p. 25548-52.
207. King, D.S. and P. Reichard, *Mass spectrometric determination of the radical scission site in the anaerobic ribonucleotide reductase of Escherichia coli.* Biochem Biophys Res Commun, 1995. **206**(2): p. 731-5.
208. Sun, X., et al., *The free radical of the anaerobic ribonucleotide reductase from Escherichia coli is at glycine 681.* J Biol Chem, 1996. **271**(12): p. 6827-31.
209. Andersson, J., et al., *Cysteines involved in radical generation and catalysis of class III anaerobic ribonucleotide reductase. A protein engineering study of bacteriophage T4 NrdD.* J Biol Chem, 2000. **275**(26): p. 19449-55.
210. Wei, Y., et al., *The class III ribonucleotide reductase from Neisseria bacilliformis can utilize thioredoxin as a reductant.* Proc Natl Acad Sci U S A, 2014. **111**(36): p. E3756-65.
211. Kunz, B.A., et al., *International Commission for Protection Against Environmental Mutagens and Carcinogens. Deoxyribonucleoside triphosphate levels: a critical factor in the maintenance of genetic stability.* Mutat Res, 1994. **318**(1): p. 1-64.
212. Wheeler, L.J., I. Rajagopal, and C.K. Mathews, *Stimulation of mutagenesis by proportional deoxyribonucleoside triphosphate accumulation in Escherichia coli.* DNA Repair (Amst), 2005. **4**(12): p. 1450-6.
213. Mathews, C.K., *DNA precursor metabolism and genomic stability.* FASEB J, 2006. **20**(9): p. 1300-14.
214. Kumar, D., et al., *Mechanisms of mutagenesis in vivo due to imbalanced dNTP pools.* Nucleic Acids Res, 2011. **39**(4): p. 1360-71.
215. Pai, C.C. and S.E. Kearsey, *A Critical Balance: dNTPs and the Maintenance of Genome Stability.* Genes (Basel), 2017. **8**(2).
216. Brown, N.C. and P. Reichard, *Role of effector binding in allosteric control of ribonucleoside diphosphate reductase.* J Mol Biol, 1969. **46**(1): p. 39-55.
217. Rofougaran, R., M. Vodnala, and A. Hofer, *Enzymatically active mammalian ribonucleotide reductase exists primarily as an alpha6beta2 octamer.* J Biol Chem, 2006. **281**(38): p. 27705-11.
218. Rofougaran, R., et al., *Oligomerization status directs overall activity regulation of the Escherichia coli class Ia ribonucleotide reductase.* J Biol Chem, 2008. **283**(51): p. 35310-8.
219. Jonna, V.R., et al., *Diversity in Overall Activity Regulation of Ribonucleotide Reductase.* J Biol Chem, 2015. **290**(28): p. 17339-48.
220. Johansson, R., et al., *Structural Mechanism of Allosteric Activity Regulation in a Ribonucleotide Reductase with Double ATP Cones.* Structure, 2016. **24**(6): p. 906-17.
221. Rozman Grinberg, I., et al., *Novel ATP-cone-driven allosteric regulation of ribonucleotide reductase via the radical-generating subunit.* Elife, 2018. **7**.
222. Parker, M.J., et al., *An endogenous dAMP ligand in Bacillus subtilis class Ib RNR promotes assembly of a noncanonical dimer for regulation by dATP.* Proc Natl Acad Sci U S A, 2018. **115**(20): p. E4594-E4603.
223. Thomas, W.C., et al., *Convergent allostery in ribonucleotide reductase.* Nat Commun, 2019. **10**(1): p. 2653.
224. Torrents, E., et al., *Ribonucleotide reductase modularity: Atypical duplication of the ATP-cone domain in Pseudomonas aeruginosa.* J Biol Chem, 2006. **281**(35): p. 25287-96.
225. Aravind, L., Y.I. Wolf, and E.V. Koonin, *The ATP-cone: an evolutionarily mobile, ATP-binding regulatory domain.* J Mol Microbiol Biotechnol, 2000. **2**(2): p. 191-4.

226. Wang, J., G.J. Lohman, and J. Stubbe, *Mechanism of inactivation of human ribonucleotide reductase with p53R2 by gemcitabine 5'-diphosphate.* Biochemistry, 2009. **48**(49): p. 11612-21.

227. Artin, E., et al., *Insight into the mechanism of inactivation of ribonucleotide reductase by gemcitabine 5'-diphosphate in the presence or absence of reductant.* Biochemistry, 2009. **48**(49): p. 11622-9.

228. Fairman, J.W., et al., *Structural basis for allosteric regulation of human ribonucleotide reductase by nucleotide-induced oligomerization.* Nat Struct Mol Biol, 2011. **18**(3): p. 316-22.

229. Ando, N., et al., *Allosteric Inhibition of Human Ribonucleotide Reductase by dATP Entails the Stabilization of a Hexamer.* Biochemistry, 2016. **55**(2): p. 373-81.

230. Eriksson, M., et al., *Binding of allosteric effectors to ribonucleotide reductase protein R1: reduction of active-site cysteines promotes substrate binding.* Structure, 1997. **5**(8): p. 1077-92.

231. Herrick, J. and B. Sclavi, *Ribonucleotide reductase and the regulation of DNA replication: an old story and an ancient heritage.* Mol Microbiol, 2007. **63**(1): p. 22-34.

232. Aye, Y., et al., *Ribonucleotide reductase and cancer: biological mechanisms and targeted therapies.* Oncogene, 2015. **34**(16): p. 2011-21.

233. Wnuk, S.F. and M.J. Robins, *Ribonucleotide reductase inhibitors as anti-herpes agents.* Antiviral Res, 2006. **71**(2-3): p. 122-6.

234. Munro, J.B. and J.C. Silva, *Ribonucleotide reductase as a target to control apicomplexan diseases.* Curr Issues Mol Biol, 2012. **14**(1): p. 9-26.

235. Ingram, G.M. and J.H. Kinnaird, *Ribonucleotide reductase: A new target for antiparasite therapies.* Parasitol Today, 1999. **15**(8): p. 338-42.

236. Ahmad, M.F., et al., *Identification of Non-nucleoside Human Ribonucleotide Reductase Modulators.* J Med Chem, 2015. **58**(24): p. 9498-509.

237. Misko, T.A., et al., *Structure-guided design of anti-cancer ribonucleotide reductase inhibitors.* J Enzyme Inhib Med Chem, 2019. **34**(1): p. 438-450.

238. Malik, L., A. Zwiebel, and J. Cooper, *A phase I pharmacokinetic and pharmacodynamic study of GTI-2040 in combination with gemcitabine in patients with solid tumors.* Cancer Chemother Pharmacol, 2018. **82**(3): p. 533-539.

239. Crona, M., et al., *A ribonucleotide reductase inhibitor with deoxyribonucleoside-reversible cytotoxicity.* Mol Oncol, 2016. **10**(9): p. 1375-1386.

240. Tholander, F. and B.M. Sjoberg, *Discovery of antimicrobial ribonucleotide reductase inhibitors by screening in microwell format.* Proc Natl Acad Sci U S A, 2012. **109**(25): p. 9798-803.

241. Rawson, J.M., et al., *Synergistic reduction of HIV-1 infectivity by 5-azacytidine and inhibitors of ribonucleotide reductase.* Bioorg Med Chem, 2016. **24**(11): p. 2410-22.

242. Torrents, E. and B.M. Sjoberg, *Antibacterial activity of radical scavengers against class Ib ribonucleotide reductase from Bacillus anthracis.* Biol Chem, 2010. **391**(2-3): p. 229-34.

243. Torrents, E., et al., *Efficient growth inhibition of Bacillus anthracis by knocking out the ribonucleotide reductase tyrosyl radical.* Proc Natl Acad Sci U S A, 2005. **102**(50): p. 17946-51.

244. Berggren, G., et al., *Compounds with capacity to quench the tyrosyl radical in Pseudomonas aeruginosa ribonucleotide reductase.* J Biol Inorg Chem, 2019. **24**(6): p. 841-848.

245. Cerqueira, N.M., P.A. Fernandes, and M.J. Ramos, *Ribonucleotide reductase: a critical enzyme for cancer chemotherapy and antiviral agents.* Recent Pat Anticancer Drug Discov, 2007. **2**(1): p. 11-29.

246. Mannargudi, M.B. and S. Deb, *Clinical pharmacology and clinical trials of ribonucleotide reductase inhibitors: is it a viable cancer therapy?* J Cancer Res Clin Oncol, 2017. **143**(8): p. 1499-1529.
247. Shao, J., et al., *Ribonucleotide reductase inhibitors and future drug design.* Curr Cancer Drug Targets, 2006. **6**(5): p. 409-31.
248. Goan, Y.G., et al., *Overexpression of ribonucleotide reductase as a mechanism of resistance to 2,2-difluorodeoxycytidine in the human KB cancer cell line.* Cancer Res, 1999. **59**(17): p. 4204-7.
249. Davidson, J.D., et al., *An increase in the expression of ribonucleotide reductase large subunit 1 is associated with gemcitabine resistance in non-small cell lung cancer cell lines.* Cancer Res, 2004. **64**(11): p. 3761-6.
250. Ferrandina, G., et al., *Expression of nucleoside transporters, deoxycitidine kinase, ribonucleotide reductase regulatory subunits, and gemcitabine catabolic enzymes in primary ovarian cancer.* Cancer Chemother Pharmacol, 2010. **65**(4): p. 679-86.
251. Baker, C.H., et al., *2'-Deoxy-2'-methylenecytidine and 2'-deoxy-2',2'-difluorocytidine 5'-diphosphates: potent mechanism-based inhibitors of ribonucleotide reductase.* J Med Chem, 1991. **34**(6): p. 1879-84.
252. Manegold, C., et al., *Gemcitabine in non-small cell lung cancer (NSCLC).* Invest New Drugs, 2000. **18**(1): p. 29-42.
253. Kanazawa, J., et al., *The relationship between the antitumor activity and the ribonucleotide reductase inhibitory activity of (E)-2'-deoxy-2'-(fluoromethylene) cytidine, MDL 101,731.* Anticancer Drugs, 1998. **9**(7): p. 653-7.
254. Wisitpitthaya, S., et al., *Cladribine and Fludarabine Nucleotides Induce Distinct Hexamers Defining a Common Mode of Reversible RNR Inhibition.* ACS Chem Biol, 2016. **11**(7): p. 2021-32.
255. Aye, Y. and J. Stubbe, *Clofarabine 5'-di and -triphosphates inhibit human ribonucleotide reductase by altering the quaternary structure of its large subunit.* Proc Natl Acad Sci U S A, 2011. **108**(24): p. 9815-20.
256. Bonate, P.L., et al., *Discovery and development of clofarabine: a nucleoside analogue for treating cancer.* Nat Rev Drug Discov, 2006. **5**(10): p. 855-63.
257. Xie, K.C. and W. Plunkett, *Deoxynucleotide pool depletion and sustained inhibition of ribonucleotide reductase and DNA synthesis after treatment of human lymphoblastoid cells with 2-chloro-9-(2-deoxy-2-fluoro-beta-D-arabinofuranosyl) adenine.* Cancer Res, 1996. **56**(13): p. 3030-7.
258. Chiu, C.S., A.K. Chan, and J.A. Wright, *Inhibition of mammalian ribonucleotide reductase by cis-diamminedichloroplatinum(II).* Biochem Cell Biol, 1992. **70**(12): p. 1332-8.
259. Shao, J., et al., *Targeting ribonucleotide reductase for cancer therapy.* Expert Opin Ther Targets, 2013. **17**(12): p. 1423-37.
260. Larsen, I.K., et al., *Caracemide, a site-specific irreversible inhibitor of protein R1 of Escherichia coli ribonucleotide reductase.* J Biol Chem, 1992. **267**(18): p. 12627-31.
261. Stearns, B., K.A. Losee, and J. Bernstein, *Hydroxyurea. A New Type of Potential Antitumor Agent.* J Med Chem, 1963. **6**: p. 201.
262. Krakoff, I.H., N.C. Brown, and P. Reichard, *Inhibition of ribonucleoside diphosphate reductase by hydroxyurea.* Cancer Res, 1968. **28**(8): p. 1559-65.
263. Heo, S.H., Y. Cha, and K.S. Park, *Hydroxyurea induces a hypersensitive apoptotic response in mouse embryonic stem cells through p38-dependent acetylation of p53.* Stem Cells Dev, 2014. **23**(20): p. 2435-42.
264. Spivak, J.L. and H. Hasselbalch, *Hydroxycarbamide: a user's guide for chronic myeloproliferative disorders.* Expert Rev Anticancer Ther, 2011. **11**(3): p. 403-14.

265. Liew, L.P., et al., *Hydroxyurea-Mediated Cytotoxicity Without Inhibition of Ribonucleotide Reductase.* Cell Rep, 2016. **17**(6): p. 1657-1670.
266. Rosenkranz, H.S., B. Gutter, and Y. Becker, *Studies on the developmental cycle of Chlamydia trachomatis: selective inhibition by hydroxyurea.* J Bacteriol, 1973. **115**(2): p. 682-90.
267. Feiner, R.R., J.E. Coward, and H.S. Rosenkranz, *Effect of hydroxyurea on Staphylococcus epidermidis and Micrococcus lysodeikticus: thickening of the cell wall.* Antimicrob Agents Chemother, 1973. **3**(3): p. 432-5.
268. Gale, G.R., et al., *Effect of Hydroxyurea on Pseudomonas Aeruginosa.* Cancer Res, 1964. **24**: p. 1012-20.
269. Lori, F., et al., *Hydroxyurea as an inhibitor of human immunodeficiency virus-type 1 replication.* Science, 1994. **266**(5186): p. 801-5.
270. Epting, C.L., et al., *Cell Cycle Inhibition To Treat Sleeping Sickness.* MBio, 2017. **8**(5).
271. Holland, K.P., et al., *Antimalarial activities of polyhydroxyphenyl and hydroxamic acid derivatives.* Antimicrob Agents Chemother, 1998. **42**(9): p. 2456-8.
272. Asperti, M., et al., *The Antitumor Didox Acts as an Iron Chelator in Hepatocellular Carcinoma Cells.* Pharmaceuticals (Basel), 2019. **12**(3).
273. Elford, H.L., G.L. Wampler, and B. van't Riet, *New ribonucleotide reductase inhibitors with antineoplastic activity.* Cancer Res, 1979. **39**(3): p. 844-51.
274. Bhave, S., H. Elford, and M.A. McVoy, *Ribonucleotide reductase inhibitors hydroxyurea, didox, and trimidox inhibit human cytomegalovirus replication in vitro and synergize with ganciclovir.* Antiviral Res, 2013. **100**(1): p. 151-8.
275. Mayhew, C.N., et al., *Suppression of retrovirus-induced immunodeficiency disease (murine AIDS) by trimidox and didox: novel ribonucleotide reductase inhibitors with less bone marrow toxicity than hydroxyurea.* Antiviral Res, 2002. **56**(2): p. 167-81.
276. Luo, J. and A. Graslund, *Ribonucleotide reductase inhibition by p-alkoxyphenols studied by molecular docking and molecular dynamics simulations.* Arch Biochem Biophys, 2011. **516**(1): p. 29-34.
277. Lepoivre, M., et al., *Quenching of the tyrosyl free radical of ribonucleotide reductase by nitric oxide. Relationship to cytostasis induced in tumor cells by cytotoxic macrophages.* J Biol Chem, 1994. **269**(34): p. 21891-7.
278. Roy, B., et al., *Inhibition of ribonucleotide reductase by nitric oxide derived from thionitrites: reversible modifications of both subunits.* Biochemistry, 1995. **34**(16): p. 5411-8.
279. Fontecave, M., et al., *Resveratrol, a remarkable inhibitor of ribonucleotide reductase.* FEBS Lett, 1998. **421**(3): p. 277-9.
280. Finch, R.A., et al., *Triapine (3-aminopyridine-2-carboxaldehyde-thiosemicarbazone): A potent inhibitor of ribonucleotide reductase activity with broad spectrum antitumor activity.* Biochem Pharmacol, 2000. **59**(8): p. 983-91.
281. Aye, Y., M.J. Long, and J. Stubbe, *Mechanistic studies of semicarbazone triapine targeting human ribonucleotide reductase in vitro and in mammalian cells: tyrosyl radical quenching not involving reactive oxygen species.* J Biol Chem, 2012. **287**(42): p. 35768-78.
282. Kunos, C.A., et al., *Phase I trial of daily triapine in combination with cisplatin chemotherapy for advanced-stage malignancies.* Cancer Chemother Pharmacol, 2017. **79**(1): p. 201-207.
283. Kunos, C.A., et al., *Randomized Phase II Trial of Triapine-Cisplatin-Radiotherapy for Locally Advanced Stage Uterine Cervix or Vaginal Cancers.* Front Oncol, 2019. **9**: p. 1067.
284. Breidbach, T., et al., *Growth inhibition of bloodstream forms of Trypanosoma brucei by the iron chelator deferoxamine.* Int J Parasitol, 2002. **32**(4): p. 473-9.

285. Amisigo, C.M., et al., *In vitro anti-trypanosomal effects of selected phenolic acids on Trypanosoma brucei.* PLoS One, 2019. **14**(5): p. e0216078.
286. Sen, G., et al., *Quercetin interferes with iron metabolism in Leishmania donovani and targets ribonucleotide reductase to exert leishmanicidal activity.* J Antimicrob Chemother, 2008. **61**(5): p. 1066-75.
287. Zahedi Avval, F., et al., *Mechanism of inhibition of ribonucleotide reductase with motexafin gadolinium (MGd).* Biochem Biophys Res Commun, 2009. **379**(3): p. 775-9.
288. Chitambar, C.R., et al., *Inhibition of ribonucleotide reductase by gallium in murine leukemic L1210 cells.* Cancer Res, 1991. **51**(22): p. 6199-201.
289. Climent, I., B.M. Sjoberg, and C.Y. Huang, *Carboxyl-terminal peptides as probes for Escherichia coli ribonucleotide reductase subunit interaction: kinetic analysis of inhibition studies.* Biochemistry, 1991. **30**(21): p. 5164-71.
290. Cooperman, B.S., *Oligopeptide inhibition of class I ribonucleotide reductases.* Biopolymers, 2003. **71**(2): p. 117-31.
291. Cohen, E.A., et al., *Specific inhibition of herpesvirus ribonucleotide reductase by a nonapeptide derived from the carboxy terminus of subunit 2.* Nature, 1986. **321**(6068): p. 441-3.
292. Liuzzi, M., et al., *A potent peptidomimetic inhibitor of HSV ribonucleotide reductase with antiviral activity in vivo.* Nature, 1994. **372**(6507): p. 695-8.
293. Moss, N., et al., *Peptidomimetic inhibitors of herpes simplex virus ribonucleotide reductase: a new class of antiviral agents.* J Med Chem, 1995. **38**(18): p. 3617-23.
294. Nurbo, J., et al., *Novel pseudopeptides incorporating a benzodiazepine-based turn mimetic--targeting Mycobacterium tuberculosis ribonucleotide reductase.* Bioorg Med Chem, 2013. **21**(7): p. 1992-2000.
295. Ericsson, D.J., et al., *Identification of small peptides mimicking the R2 C-terminus of Mycobacterium tuberculosis ribonucleotide reductase.* J Pept Sci, 2010. **16**(3): p. 159-64.
296. Nurbo, J., et al., *Design, synthesis and evaluation of peptide inhibitors of Mycobacterium tuberculosis ribonucleotide reductase.* J Pept Sci, 2007. **13**(12): p. 822-32.
297. Yang, F.D., et al., *The carboxyl terminus heptapeptide of the R2 subunit of mammalian ribonucleotide reductase inhibits enzyme activity and can be used to purify the R1 subunit.* FEBS Lett, 1990. **272**(1-2): p. 61-4.
298. Fisher, A., et al., *R2 C-terminal peptide inhibition of mammalian and yeast ribonucleotide reductase.* J Med Chem, 1993. **36**(24): p. 3859-62.
299. Aye, Y., et al., *Clofarabine targets the large subunit (alpha) of human ribonucleotide reductase in live cells by assembly into persistent hexamers.* Chem Biol, 2012. **19**(7): p. 799-805.
300. Chen, S., et al., *Inhibition of human cancer cell growth by inducible expression of human ribonucleotide reductase antisense cDNA.* Antisense Nucleic Acid Drug Dev, 2000. **10**(2): p. 111-6.
301. Aurelian, L. and C.C. Smith, *Herpes simplex virus type 2 growth and latency reactivation by cocultivation are inhibited with antisense oligonucleotides complementary to the translation initiation site of the large subunit of ribonucleotide reductase (RR1).* Antisense Nucleic Acid Drug Dev, 2000. **10**(2): p. 77-85.
302. Chakrabarti, D., S.M. Schuster, and R. Chakrabarti, *Cloning and characterization of subunit genes of ribonucleotide reductase, a cell-cycle-regulated enzyme, from Plasmodium falciparum.* Proc Natl Acad Sci U S A, 1993. **90**(24): p. 12020-4.
303. Lee, Y., et al., *GTI-2040, an antisense agent targeting the small subunit component (R2) of human ribonucleotide reductase, shows potent antitumor activity against a variety of tumors.* Cancer Res, 2003. **63**(11): p. 2802-11.

304. Orr, R.M., *GTI-2040. Lorus Therapeutics.* Curr Opin Investig Drugs, 2001. **2**(10): p. 1462-6.

305. Kirschbaum, M.H., et al., *A phase I pharmacodynamic study of GTI-2040, an antisense oligonucleotide against ribonuclotide reductase, in acute leukemias: a California Cancer Consortium study.* Leuk Lymphoma, 2016. **57**(10): p. 2307-14.

306. Heidel, J.D., et al., *Administration in non-human primates of escalating intravenous doses of targeted nanoparticles containing ribonucleotide reductase subunit M2 siRNA.* Proc Natl Acad Sci U S A, 2007. **104**(14): p. 5715-21.

307. Rahman, M.A., et al., *Systemic delivery of siRNA nanoparticles targeting RRM2 suppresses head and neck tumor growth.* J Control Release, 2012. **159**(3): p. 384-92.

308. Zuckerman, J.E., et al., *Correlating animal and human phase Ia/Ib clinical data with CALAA-01, a targeted, polymer-based nanoparticle containing siRNA.* Proc Natl Acad Sci U S A, 2014. **111**(31): p. 11449-54.

309. Davis, M.E., *The first targeted delivery of siRNA in humans via a self-assembling, cyclodextrin polymer-based nanoparticle: from concept to clinic.* Mol Pharm, 2009. **6**(3): p. 659-68.

310. Atamna, H., A. Paler-Martinez, and B.N. Ames, *N-t-butyl hydroxylamine, a hydrolysis product of alpha-phenyl-N-t-butyl nitrone, is more potent in delaying senescence in human lung fibroblasts.* J Biol Chem, 2000. **275**(10): p. 6741-8.

311. Gerez, C. and M. Fontecave, *Reduction of the small subunit of Escherichia coli ribonucleotide reductase by hydrazines and hydroxylamines.* Biochemistry, 1992. **31**(3): p. 780-6.

312. Lundin, D., et al., *Ribonucleotide reduction - horizontal transfer of a required function spans all three domains.* BMC Evol Biol, 2010. **10**: p. 383.

313. Davies, B.W., et al., *Hydroxyurea induces hydroxyl radical-mediated cell death in Escherichia coli.* Mol Cell, 2009. **36**(5): p. 845-60.

314. Altaf, M., et al., *Evaluation of the Mycobacterium smegmatis and BCG models for the discovery of Mycobacterium tuberculosis inhibitors.* Tuberculosis (Edinb), 2010. **90**(6): p. 333-7.

315. Jordao, L., et al., *On the killing of mycobacteria by macrophages.* Cell Microbiol, 2008. **10**(2): p. 529-48.

316. Navarra, P., et al., *Hydroxyurea induces the gene expression and synthesis of proinflammatory cytokines in vivo.* J Pharmacol Exp Ther, 1997. **280**(1): p. 477-82.

317. Trifilieff, A., et al., *Inducible nitric oxide synthase inhibitors suppress airway inflammation in mice through down-regulation of chemokine expression.* J Immunol, 2000. **165**(3): p. 1526-33.

318. Lanaro, C., et al., *Altered levels of cytokines and inflammatory mediators in plasma and leukocytes of sickle cell anemia patients and effects of hydroxyurea therapy.* J Leukoc Biol, 2009. **85**(2): p. 235-42.

319. Arko-Mensah, J., et al., *TLR2 but not TLR4 signalling is critically involved in the inhibition of IFN-gamma-induced killing of mycobacteria by murine macrophages.* Scand J Immunol, 2007. **65**(2): p. 148-57.

320. Bhatnagar, S., et al., *Exosomes released from macrophages infected with intracellular pathogens stimulate a proinflammatory response in vitro and in vivo.* Blood, 2007. **110**(9): p. 3234-44.

321. Cui, W., et al., *Differential modulation of the induction of inflammatory mediators by antibiotics in mouse macrophages in response to viable Gram-positive and Gram-negative bacteria.* J Endotoxin Res, 2003. **9**(4): p. 225-36.

322. Mendez, S., et al., *The antituberculosis drug pyrazinamide affects the course of cutaneous leishmaniasis in vivo and increases activation of macrophages and dendritic cells.* Antimicrob Agents Chemother, 2009. **53**(12): p. 5114-21.

323. Dorhoi, A. and S.H. Kaufmann, *Tumor necrosis factor alpha in mycobacterial infection.* Semin Immunol, 2014. **26**(3): p. 203-9.
324. Wang, J., et al., *Macrophages are a significant source of type 1 cytokines during mycobacterial infection.* J Clin Invest, 1999. **103**(7): p. 1023-9.
325. Tamma, P.D., S.E. Cosgrove, and L.L. Maragakis, *Combination therapy for treatment of infections with gram-negative bacteria.* Clin Microbiol Rev, 2012. **25**(3): p. 450-70.
326. Julian, E., et al., *Methyl-hydroxylamine as an efficacious antibacterial agent that targets the ribonucleotide reductase enzyme.* PLoS One, 2015. **10**(3): p. e0122049.
327. Dao, R., et al., *Landscape of the structure-O-H bond dissociation energy relationship of oximes and hydroxylamines.* Phys Chem Chem Phys, 2017. **19**(33): p. 22309-22320.
328. Saban, N. and M. Bujak, *Hydroxyurea and hydroxamic acid derivatives as antitumor drugs.* Cancer Chemother Pharmacol, 2009. **64**(2): p. 213-21.
329. Crespo, A., N. Blanco-Cabra, and E. Torrents, *Aerobic Vitamin B12 Biosynthesis Is Essential for Pseudomonas aeruginosa Class II Ribonucleotide Reductase Activity During Planktonic and Biofilm Growth.* Front Microbiol, 2018. **9**: p. 986.
330. Fleming, D. and K. Rumbaugh, *The Consequences of Biofilm Dispersal on the Host.* Sci Rep, 2018. **8**(1): p. 10738.
331. Okshevsky, M. and R.L. Meyer, *The role of extracellular DNA in the establishment, maintenance and perpetuation of bacterial biofilms.* Crit Rev Microbiol, 2015. **41**(3): p. 341-52.
332. Shire, S.J., *Stability characterization and formulation development of recombinant human deoxyribonuclease I [Pulmozyme, (dornase alpha)].* Pharm Biotechnol, 1996. **9**: p. 393-426.
333. Tran, V.T., J.P. Benoit, and M.C. Venier-Julienne, *Why and how to prepare biodegradable, monodispersed, polymeric microparticles in the field of pharmacy?* Int J Pharm, 2011. **407**(1-2): p. 1-11.
334. Ungaro, F., et al., *Dry powders based on PLGA nanoparticles for pulmonary delivery of antibiotics: modulation of encapsulation efficiency, release rate and lung deposition pattern by hydrophilic polymers.* J Control Release, 2012. **157**(1): p. 149-59.
335. Suk, J.S., et al., *The penetration of fresh undiluted sputum expectorated by cystic fibrosis patients by non-adhesive polymer nanoparticles.* Biomaterials, 2009. **30**(13): p. 2591-7.
336. Levato, R., M.A. Mateos-Timoneda, and J.A. Planell, *Preparation of biodegradable polylactide microparticles via a biocompatible procedure.* Macromol Biosci, 2012. **12**(4): p. 557-66.
337. Barichello, J.M., et al., *Encapsulation of hydrophilic and lipophilic drugs in PLGA nanoparticles by the nanoprecipitation method.* Drug Dev Ind Pharm, 1999. **25**(4): p. 471-6.
338. Enayati, M., et al., *Modification of the release characteristics of estradiol encapsulated in PLGA particles via surface coating.* Ther Deliv, 2012. **3**(2): p. 209-26.
339. Cheow, W.S., M.W. Chang, and K. Hadinoto, *Antibacterial efficacy of inhalable levofloxacin-loaded polymeric nanoparticles against E. coli biofilm cells: the effect of antibiotic release profile.* Pharm Res, 2010. **27**(8): p. 1597-609.
340. Cheow, W.S. and K. Hadinoto, *Green preparation of antibiotic nanoparticle complex as potential anti-biofilm therapeutics via self-assembly amphiphile-polyelectrolyte complexation with dextran sulfate.* Colloids Surf B Biointerfaces, 2012. **92**: p. 55-63.

341. Forier, K., et al., *Transport of nanoparticles in cystic fibrosis sputum and bacterial biofilms by single-particle tracking microscopy.* Nanomedicine (Lond), 2013. **8**(6): p. 935-49.
342. Messiaen, A.S., et al., *Transport of nanoparticles and tobramycin-loaded liposomes in Burkholderia cepacia complex biofilms.* PLoS One, 2013. **8**(11): p. e79220.

ANNEXES

Report of the impact factor of the presented scientific papers

I declare that the impact factor of the published scientific papers that constitute the present doctoral thesis is as follows:

Publication 1:

“Methyl-Hydroxylamine as an Efficacious Antibacterial Agent That Targets the Ribonucleotide Reductase Enzyme”. DOI: 10.1371/journal.pone.0122049

Published in ***PLoS ONE*** in 2015 with an impact factor of **3.057**

Publication 2:

“Hydroxylamine Derivatives as a New Paradigm in the Search of Antibacterial Agents”. DOI: 10.1021/acsomega.8b01384

Published in ***ACS Omega*** in 2018 with an impact factor of **2.584**

Publication 3:

“Disassembling bacterial extracellular matrix with Dnase-coated nanoparticles to enhance antibiotic delivery in biofilm infections”

Published in ***Journal of Controlled Release*** in 2015 with an impact factor of **7.441**

Barcelona, October 2020

Dr. Eduard Torrents Serra
Thesis supervisor

Report of participation in the presented scientific papers

I declare that the participation of Aida Baelo Álvarez in the published scientific papers that constitute the present doctoral thesis is the following:

In Publication 1, "**Methyl-Hydroxylamine as an Efficacious Antibacterial Agent That Targets the Ribonucleotide Reductase Enzyme**", Aida Baelo Álvarez is the second author and contributed to the research by designing and performing the experiments, analyzing the data, and by writing the manuscript.

In Publication 2**,** "**Hydroxylamine Derivatives as a New Paradigm in the Search of Antibacterial Agents**", Aida Baelo Álvarez shares first authorship with Laia Miret-Casals, contributing equally to the work. Aida Baelo Álvarez designed and performed all the biological experiments and wrote the manuscript.

In Publication 3, "**Disassembling bacterial extracellular matrix with Dnase-coated nanoparticles to enhance antibiotic delivery in biofilm infections**". Aida Baelo shares first authorship with Ricardo Levato, contributing equally to the work. She was involved in the biological experiments and in the manuscript writing.

Barcelona, October 2020

Dr. Eduard Torrents Serra
Thesis supervisor